UNIVERSITY OF BIRMINGHAM

THE RESPONSE OF STONE COLUMNS UNDER CYCLIC LOADING

By

SAMIR ASHOUR

A Thesis submitted to

The University of Birmingham

For the degree of

DOCTOR OF PHILOSOPHY

School of CIVIL ENGINEERING

College of ENGINEERING AND PHYSICAL SCIENCE

The University of Birmingham

September 2015

ABSTRACT

Soft clay soils in railway track can be problematic as, unless they are treated, they can result in increased deformation of track. This will inheritably mean lower track speed. A number of techniques including stone columns are available for improving strength of weak soils.

The use of stone columns, for improving both bearing capacity and settlement is well rehearsed for static loading; little is understood about their response, when subjected to cyclic loading. This study is focused on investigating the behaviour of stone columns when subjected to cyclic loading as in railway tracks based on a laboratory scale investigation.

A series of monotonic and cyclic loading conditions were undertaken on two laboratory models undrained triaxial (diameter 100 mm, and 200 mm height) and large scale model (diameter 300 mm, and 300 mm height). Tests were conducted on both soft soils (no column) and soil/ stone column composite. All tests were performed on normally consolidated specimens of soft clay (undrained shear strength of ≈ 12 kPa) and for treated soils they were reinforced with 28 mm diameter stone columns. Three cyclic stress (50, 60 and 70 kPa) on subgrade level and three loading frequencies (0.5, 1 and 3 Hz) simulating different train speeds (35, 70 and 225 km/hr) were used to study the performance of both soft soils (with and without column). The effect of both cyclic stresses and loading frequency on the permanent deformation, soils stiffness and pore water pressure generation were investigated.

Generally, soft clay bed reinforced with stone column showed a significant improvement in terms of load/deformation characteristics; in monotonic loading condition, there was approximately 30% increase in failure load of soil with the stone column compared to that soil only.

It was found that threshold dynamic stress of soil for cyclic loading increased from 50 kPa for soil only to 60 kPa for soil with stone column. This is equivalent to CSR of 0.7.

Changes in frequencies from 0.5 to 3 Hz did not significantly influence the permanent strain of reinforced soil, but these changes do affect the stiffness. Stiffness of the soil with the stone column was about 25% higher at 3.0 Hz compared to that at 0.5 Hz.

Stone columns also helped reduce pore water pressure build up under cyclic loading by providing a drainage path. This resulted in an increase in cyclic stress ratio from 0.6 to 0.7. It also decreases the permanent deformation by about 70% in most tests, when compared to situation without stone column.

DEDICATION

This thesis work is dedicated to my parents, who have always loved me unconditionally and whose good examples have taught me to work hard for the things that I aspire to achieve. Also to my brother who always has been there for me.

This work is also dedicated to my wife and children, who have been a constant source of support and encouragement during the challenges of life. I am truly thankful for having you in my life.

And above all

This thesis is dedicated to the sake of Allah, my Creator and my Master, My great teacher and messenger, Mohammed (May Allah bless and grant him)

ACKNOWLEDGMENTS

I would like to acknowledge gratefully for the assistance received from supervisors Dr Gurmel Ghataora and Professor Ian Jefferson for their constant supervision, guidance and encouragement throughout the research.

I would also express my sincere thanks to Lap technicians Mr Sebastian Ballard and Mr Jim White for their help and support.

I am very much grateful to Libyan Ministry of Higher Education for granting the scholarship for this research.

Finally, I thank my family for their patience and understanding to make this piece work possible.

TABLE OF CONTENTS

LIST OF FIGURES

LIST OF TABLES

LIST OF ABBREVIATION

A_s	*Area replacement ratio*
C_c	*Compression index*
c_g	*Constant dependent upon the pattern of stone columns*
CSR	*Cyclic stress ratio*
c_u	*Undrained shear strength of the soil*
c_v	*Coefficient of consolidation*
d_c	*Column diameter*
D_e	*Equivalent diameter*
d_g	*Average particle diameter of stone column material*
E	*Deformation modulus of soil*
e_0	*Initial void ratio*
f	*Frequency*
F_c *and* F_q	*Cavity expansion factors*
G_c	*Elastic shear modulus of the clay*
G_s	*Specific gravity*
G_s	*Elastic shear modulus of the column material*
h	*Depth of ballast*
I_r	*Rigidity index*
K_{ac}	*Coefficient of active pressure of the column*
K_P	*Coefficient of the passive pressure of the column*
K_s	*The modulus of subgrade reaction*

L	*Column length*
Lc	*Critical column length*
$L.L$	*Liquid limit*
LI	*Liquidity index*
M_r	*Resilient modulus*
m_v	*Coefficient of compressibility*
n	*Stress concentration factor*
N	*Number of cycles*
N_c	*Bearing capacity factor*
p	*Mean stress*
P_C	*Subgrade pressure*
P_m	*Applied stress on ballast*
P_{ult}	*Ultimate column load*
q	*Deviator stress*
S	*Spacing between the columns*
T_v	*Time factor of 90% consolidation*
u	*Pore water pressure*
Δu	*Change in pore water pressure*
w	*Water content*
Δe	*Change in void ratio*
σ_3'	*Effective confining pressure*
σ_c	*Stress in the surrounding soil*
σ_v	*Vertical stress*

σ_r	*Lateral confining pressure*
σ_s	*Stress in the stone column.*
Υ_c	*Unit weight of the clay*
Υ_s	*Unit weight of the column material*
μc	*Stress ratios in the soil*
μs	*Stress ratios stone column*
φ	*Angle of internal friction*
$\bar{C}$	*Average shaft cohesion*
ε_p	*Permanent strain*

CHAPTER 1

INTRODUCTION

1.1 Background

Soil improvement methods have received much attention over the last few decades, as a result of shortage of good quality land for development, together with the need to develop transport infrastructure in areas which were previously regarded as being unsuitable. These often included soft soil deposits. In many instances, the proposed structures on improved/ stabilised soft soils are considered to be viable on economic grounds due to the high cost of virgin land and the environmental need to site infrastructure away from developed areas.

Soft soil deposits are characterised as having low bearing capacity, and high compressibility leading to potential instability and large settlement. Therefore, in order to reduce these problems, either the structure or the underlying soils or both needs to be modified. Most often, it is cheaper to undertake ground improvement than to modify the structure. Although in some cases, this is a possible solution.

A range of ground improvement methods can be used. They can be categorised as: densification, consolidation, reinforcement, chemical stabilization, thermal stabilization, and biotechnical stabilization. Sometimes it may be more efficient to use more than one type of treatment.

Stone columns are constructed by using the same equipment as vibro-compaction. They are considered as a densification method and also can act as a vertical drain that can lead to speedier the consolidation progress of the soil. It is also considered as a ground reinforcement

technique due to the granular nature of the column material. Granular columns are installed into the soft soil by means of compacting gravel or crushed rock into the cylindrical void created by a vibrating poker. This technique has been used extensively over the last few decades in many parts of the world. The design and construction techniques have been improved to an extent that stone columns could be used in some cases as an alternative to the traditional foundations such as piling (McCabe et al., 2009; Barksdale & Bachus, 1983; Greenwood & Kirsch, 1984; Mitchell and Huber 1985; Priebe, 1995; Sivakumar et al., 2010).

Many full-scale, laboratory experimental and analytical investigations have been undertaken, which have led to improvement of the stone column technique and methods of analysis, providing better prediction for both bearing capacity and settlement (Bergado and Lam, 1987; Greenwood, 1991). These studies demonstrate that the behaviour of the stone columns was affected considerably by a number of parameters, including: column length to diameter ratio; the area replacement ratio; column spacing; column and surrounding soil stiffness; the stress ratio of both the column and surrounding soil; and the method of installation. Also they have shown that columns can fail by bulging, bending, punching and shearing, depending on the length of the column and the method of applying the loads on top of the column.

Despite of the fact that, the previous investigations have provided a wide understanding on using stone columns to improve the properties of soft soils, these investigations were focused the behaviour of stone columns under the application of static and monotonic loading and there was very limited information on their behaviour when subjected to cyclic loading. The key difference in this study and the previous ones is the mode of loading, where the applied loads will vary with time. Thus this research will provide a better understanding of the behaviour of stabilised stone columns under static and dynamic loading conditions. This

includes evaluation of deformation under loading and mechanisms of stress transfer in both treated and untreated soil.

1.2 Research problem

There is increasing need for higher performance track substructure systems (ballast, sub-ballast and subgrade) in order to provide constant and uniform support for the sleepers and the rail allowing them to cope with increased demand for high speed trains. Without any upgrades, tracks built over soft ground can be problematic, leading to increase in maintenance in order to maintain line and level (Raju, 2003).

Many researchers (Seed et al., 1955; Brown et al., 1975; Li and Selig, 1996; Miller et al., 2000; Li-Zhong Wang et al., 2011) have studied the effect of cyclic loading on the compressibility and strength characterisation of soft soil. They demonstrated that such soils have high compressibility and low bearing capacity. Therefore, under cyclic stresses above the threshold stress ratio (i.e. ratio between the dynamic stresses to the soils static strength, which is typically between 0.4 and 0.65 depending on the soil type and conditions), it is expected to have a high residual settlement resulting in a reduction in strength. Hence leading to a reduction in track speed limit.

In order to overcome this problem, it is generally better (i.e cost-effective) to improve the ground rather than import materials of suitable quality to replace poor soils. This has additional environmental benefits. A number of treatment options including the construction of vibro stone columns can be considered for improving subgrade soil (Raju, 2003; Fatahi et al., 2012).

Vibro stone columns have been widely used to reinforce and stabilise railway tracks built on soft soils to control the permanent deformation and the generation of excess pore pressure

(Abdullah et al., 2009; Fatahi et al., 2012). However, studies on the dynamic performance of stone columns are mostly limited to liquefaction mitigation potential in silty soils (Munfakh, 1984; Priebe, 1995; Munfakh, 2003; Rollins et al., 2009). Additionally, very limited research has been carried out on the performance of stone columns subjected to repeated vertical loading. Therefore, aspects such as identifying failure mechanisms and quantifying the amount of settlement, especially at low replacement ratio (under 10%) require investigation.

For this study, vibro stone column were modelled in both triaxial tests and small scale tank tests. Stone columns were constructed in soft soils (c_u <15 kPa) and loaded to failure under both monotonic and dynamic loading. The main objective of the testing program was to examine the effect of loading rate, loading frequency, and cyclic stress ratio on the behaviour of both soft soils and stone column reinforced soil. Thus, allowing for a better understanding of the response of stone column under dynamic loading application can be achieved.

1.3 Research Aim and Objectives

This research aim is to ***assess the behaviour of stone column subjected to cyclic loading as a precursor to their application as a railway subgrade improvement technique***. This can be approached by developing the appropriate loading frequency and dynamic stresses on both treated and untreated soft soils in order to investigate the stiffness, permanent deformation and pore water pressures. In order to achieve the above aim, the following objectives were set:

i. Develop a suitable physical, laboratory scale model
ii. Examine the effect of loading strain rate during the monotonic conditions on the degree of improvement of soft ground;
iii. Examine the effect of relative density of the column material on column bearing capacity;

iv. Investigate the effect of loading frequency on the behaviour of stone column;

v. Investigate the effect of dynamic stress level on the behaviour of stone column.

1.4 Outline of Thesis

Brief descriptions of the remaining chapters of this thesis are outlined below:

Chapter 2 provides a brief background of stone column foundations and reviews previous research work relevant to the subject.

The properties of the materials used; the design and manufacture of testing apparatus and instrumentation used in this laboratory base study; and the specimen preparation and general procedures used for the model testing are presented in Chapter 3.

The monotonic testing programme and results of the effect of varying strain rate and column density are described in Chapter 4. Results from current study are analysed and compared with other research findings from both laboratory tests and field studies. In addition to this, the failure mechanisms for a single stone column reinforced foundation in both models (triaxial and large scale) are discussed.

Chapter 5 shows results and discussion of tests on stone columns, subjected to cyclic loading. (i.e the effect of both frequency and cyclic stress level) in order to provide a further understanding to the behaviour of stone columns.

Finally, both conclusions and recommendations are presented in Chapter 6.

CHAPTER 2

LITERATURE REVIEW

2.1 Introduction

Vibro stone column method has been widely used to improve soft soils over the last four decades. This chapter reviews and the design concepts, installation methods, failure mechanisms, current practice, and relevant experimental procedures.

2.2 Introduction to Ground Improvement

Geotechnical engineers are often faced with the challenges of building on poor ground and have to match the level of ground improvement with project requirements. Apart from abandoning the project, Mitchell and Jardine, (2002) suggested four alternatives:

- replace poor ground with more suitable material;
- bypass the area of poor ground laterally by relocating the facility, or vertically by using piles or deep foundations;
- redesign the structure to meet the ground limitations; or
- modify the natural condition of the poor ground to meet the project requirements.

The rising cost of land and increasing awareness of the impact that construction has on the environment have been major contributors to the increasing use of ground improvement techniques.

Ground improvement techniques generally aim to modify some of the soil characteristics in order to meet the requirements of a construction project. These improvements include increasing the density and shear strength in order to: improve bearing capacity; reduce soil

compressibility; influence permeability in order to control ground water flow or to increase the rate of consolidation; and improve the homogeneity of soil. Therefore, ground improvement can be defined as "the controlled alteration of the state, nature or mass behaviour of ground materials in order to achieve an intended satisfactory response to existing or projected environmental and engineering actions" (Mitchell and Jardine, 2002).

A wide range of ground treatments are available. Different classifications are proposed depending on: equipment used; required period of treatment (temporary or permanent), or the purpose of use (Munfakh, 1997; Van Impe et al., 1997; Mitchell and Jardine, 2002; Munfakh, 2003). Munfakh (1997) divides ground improvement methods into the following categories:

- **Densification methods include vibro-compaction; dynamic compaction; blasting; and compaction grouting.**
- **Consolidation method: preloading and vertical drains.**
- **Reinforcement methods include mechanically stabilised backfill; soil nailing; element wall; micro-piles; and stone columns.**
- **Chemical stabilization: permeation grouting; jet grouting; deep soil mixing; and lime/ cement columns.**

Vibro stone columns can be considered one of the most effective methods to improve performance of the soft ground. stone columns have the advantages of accelerating consolidation, increasing the bearing capacity of poor ground, and improving the slope stability and mitigate liquefaction by providing a sufficient reinforcement and providing a drainage path allowing the pore water pressure to dissipate. Therefore, they have been used in a verity of applications, such as road and railway embankments, tanks and marine structures (Unnikrishnan et al., 2002; Fatahi et al., 2012).

2.3 Stone Column Technique: Historical Development

In 1937 there was the first reported application of vibro compaction used to densify a loose sand deposit under a building in Berlin by penetrating a vibrating poker to the ground (Slocombe et al., 2000).

In the 1950's this technique was adopted in the UK, however, its application was limited due to the geological nature of the ground (soft soil; shear strength < 15 kPa). This led to the development of vibro compaction technique to cover the treatment of fine grained and cohesive soils by introducing a coarse granular backfill into a vertical void in soft ground formed using a vibratory poker. This early method of stone column construction received further improvement in Europe and the United State of America until it became a well-established technique (Greenwood, 1975; Mitchell, 1981).

Over the last three decades this technique has been widely used for both compaction of cohesion-less soils and for reinforcing soft soils with granular columns. The method has been shown to be an effective and reliable ground improvement method, especially, in cases, where high sensitivity to settlement is not critical. It has proven to be a good alternative to the traditional deep foundation methods such as piles (Serridge, 2006; McCabe et al., 2009).

2.4 Stone Column Construction Methods

Soil type and condition are the key factors that govern the method of installation of stone columns to ensure the required quality of improvement (McCabe et al., 2009). The commonly applicable installation techniques for soft soils (and the equipment used) are discussed below. A brief summary of the installation methods are shown in Table 2.1.

Table 2.1 Summary of stone column installation methods

Installation method	c_u (kPa)	L (m)	d_c (mm)	Commentary
Replacement (wet top feed) Section 2.4.2.1	15 to 35	5-20	600-1200	- Suitable for very soft soil, and deep treatments; - Applicable blow ground water level - Has an environmental issue.
Displacement (dry top feed) Section 2.4.3.1	> 30	10	400-800	- Suitable only for stable and stiff soils; - Shallow and medium treatment depth.
Displacement (dry bottom feed) Section 2.4.3.2	15 to50	15	400-800	- Suitable for very soft soil; - Applicable below ground water level; - Borehole stability is insured - Clean stone, column diameter and column length are assured.

c_u: undrained shear strength of the soil;
L: column length;
d_c: column diameter.

2.4.1 Vibro Equipment (Vibro-float)

Stone columns are constructed first by creating a vertical void in soft ground using a vibratory poker (Figure 2.1). As the poker is slowly withdrawn, stone is inserted in the void in typical

stages of 300 to 500 mm thickness and then compacted by the vibrating poker for 30 to 60 seconds. This process is continued upward to form a column (Watts, 2000).

The equipment used to form the stone column typically comprises a hollow cylindrical steel pipe with diameter ranging between 300 mm and 450 mm, and length ranges from 2.00 to 3.50 meter. The vibrator body unit consists of two main parts: the upper part known as the extension or follower tube as shown in Figure 2.1. The main function of the follower tube is to allow deep penetration into the ground (Watts, 2000; Moseley and Kirsch, 2004).

The lower section of the vibrating unit contains an eccentric weight which is powered by a motor at the top of an axial shaft (typical motor power capacity ranges between 50 to 150 kW and operating frequency ranging from 10 to 30Hz). This eccentric weight typically ranges between 15 and 40 kN depending on the level of improvement and the condition of the ground. There is a vibratory force of 150 to 700 kN can be transmitted from the vibrator casing to the surrounding soil. (Greenwood and Kirsch, 1984; Raju and Sondermann, 2005).

In order to improve the installation process with a high level of quality control, the equipment was modified by including useful features such as bottom feed delivery system, and computerised monitoring system that could transfer data from site (Slocombe et al., 2000).

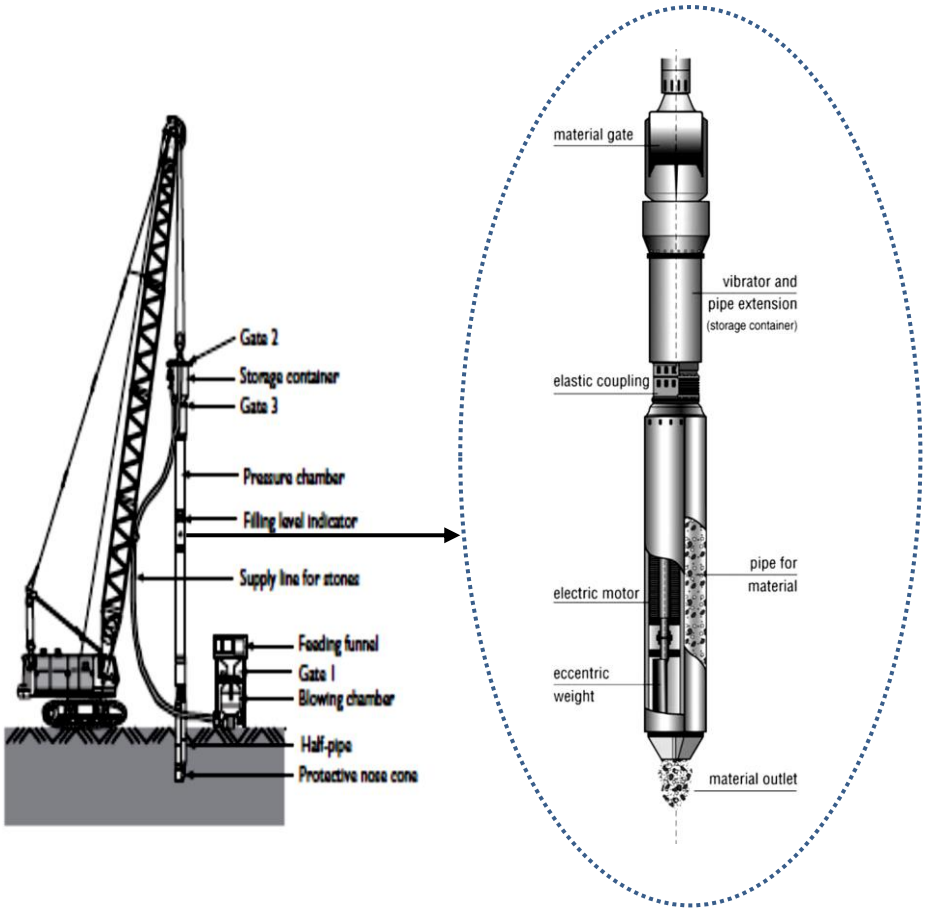

Figure 2.1 Deep vibrator details (Moseley and Kirsch, 2004)

2.4.2 Vibro Replacement (Wet Method)

2.4.2.1 Wet top feed

This technique has been used successfully in soft soils (fines content over 20 %; and undrained shear strength of soil, c_u, in range of 15 to 35 kPa), it can also be used for deep ground treatments below water level (Moseley and Kirsch, 2004; McCabe et al., 2009).

In order to increase the bearing capacity and the stiffness of soft soil, a 10 to 35 % of the soil may need to be replaced with uniformly graded stone, column diameters ranging between 0.6

and 1.2 meter and column depths between 5 and 15 meters. In this method it is preferable to build columns that extend to end bearing stratum (Barksdale and Bachus, 1983).

The installation sequence of this technique is illustrated in Figure 2.2. The vibrator is inserted into the soil with the assistance of jetted water. Both the flow of flushing water and the vibration can reduce soil resistance and allow the vibrator to penetrate the soil under its own weight. Once the required depth is achieved, granular backfill is placed from the bottom of the hole to the top where gravel falls against a continuous upward flow of water. As the gravel is accumulated at the bottom of the column, the vibrator is withdrawn gradually in approximately 0.50 meter intervals. A continuous water flow protects the bore from the collapsing. As the vibrational energy is dissipated in radial waves through the backfill materials into the surrounding soil and additional expansion of the column is prevented by the passive resistance of the cohesive soil. (Greenwood and Kirsch, 1984; Watts, 2000).

However, due to environmental issues relating to disposal of flush arising, application of this method is limited currently to developments where large bearing capacity is required (McCabe et al., 2009).

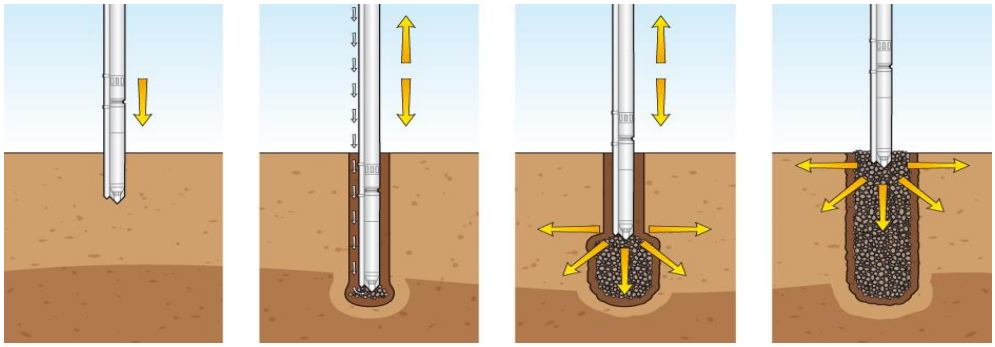

Figure 2.2 Vibro-replacement method (Keller GmbH, 2005)

2.4.3 Vibro Displacement (Dry Method)

2.4.3.1 Dry top feed

Dry top feed method is considered to be the simplest installation method, and most preferred in the case of shallow to medium treatment depths of stable soils with undraind shear strength larger than 30 kPa. This method is not applicable for treatment of soft clay soils due to the fact that the borehole will collapse when the poker withdrawn due to lack of lateral support (McKelvey, 2002; McCabe et al., 2009).

In this method, (Figure 2.3), once the required depth is reached the poker is lifted and the granular backfill of material introduced from the ground surface into the hole. The vibro-float is reinserted and stone in the column is compacted. Typical geometries of formed stone columns are usually 400 to 800 mm diameter and 10 to 15 meters in length (Munfakh, 1984; McKelvey, 2002).

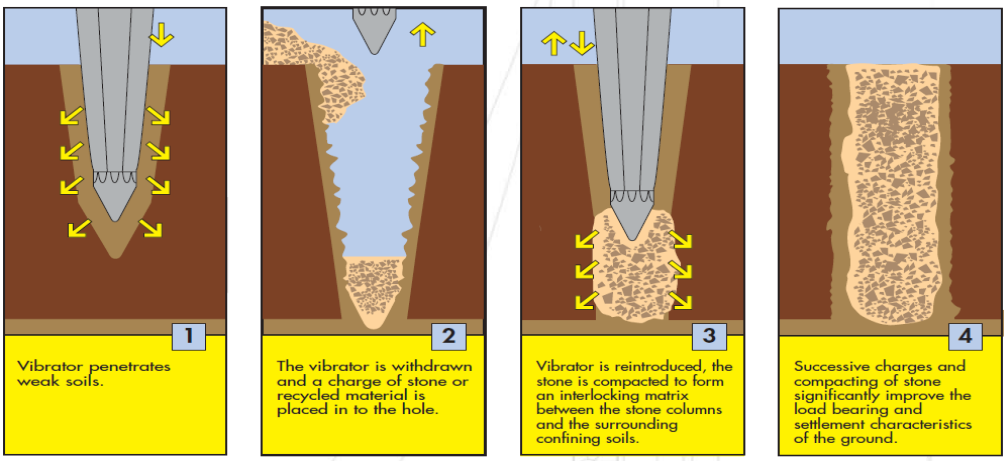

Figure 2.3 Vibro-displacement (Keller GmbH, 2005)

2.4.3.2 Dry bottom feed

This method was introduced into the UK in the 1980's and currently considered the most commonly adopted installation method for stone column (McCabe et al., 2009). In terms of application it is used in soils (c_u ranges between 15 and 50 kPa), and unaffected by the presence of ground water. During the backfill process the vibro-float remains inside the bore providing more stability and preventing unwanted inclusion. The stone material is supplied using a hopper to a pipe fixed to the side of the vibro-float shown in Figure 2.4. This can allow the column to be constructed clean with the same back fill material. As with the top feed method the stone is then compacted by repeated withdrawal and insertion of the poker (McCabe et al., 2009). The average treatment depth achieved by this method is 15 meter (Watts, 2000).

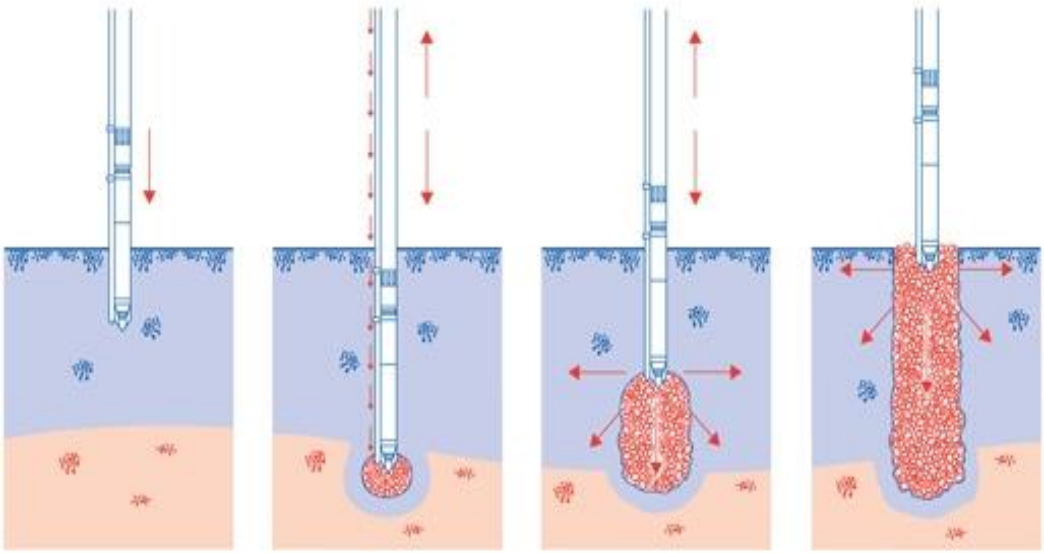

Figure 2.4 Dry bottom feed (Keller GmbH, 2005)

2.4.4 Monitoring, Quality Control and Assessment of Stone Columns Performance

As a result of the variety of equipment and construction methodologies and due to the lack of availability of a fixed procedure to design vibro replacement method, construction of the stone column is controlled by recording a range of parameters, including penetration depth, energy consumption of the vibrator, and air/water pressure (Moseley and Kirsch, 2004). Continuous recording of parameters as a function of time can provide reliable data that can be used to control stone column construction and help prevent problems. This includes the possibility of having to alter the design of columns and ensures column uniformity over entire length.

In addition to the above, cone penetration test (CPT) and standard penetration test (SPT) are generally used to confirm the achievement of a satisfactory level of vibro compaction (Bell, 2004; McCabe et al., 2009). However, it should be noted that, whilst the data collected during column construction are for quality control, the penetration tests are used to ensure the degree of improvement achieved post-construction.

In order to evaluate the compressibility of treated soil, it is better to conduct compaction tests within at least one week of the compaction work to prevent the effect of ageing factor, which influences the soil properties and causes an increase to its strength ranging from 50 to 100%. This increase in strength occurs as a result of the reduction in water pressure, and also could be due to the rearrangement of the physical and chemical bonding forces between the soil particles within the column.

Stone columns are primarily used to reduce settlement. Therefore, large-scale loading tests, which can be carried out by loading a rigid plate on top of one or more columns are used to assess the degree of improvement in terms of settlement. However, as this test is costly and

time-consuming, it cannot be used as a control of workmanship, so it is only used in case of large projects (Greenwood and Kirsch, 1984; Greenwood, 1991).

Recently, geophysical methods including continuous surface wave have been used to assess settlement improvement (Madun et al., 2012). Although there is no large database to validate the data collected by geophysical investigation, this method has an advantage of covering large areas and could be used for both short and long term investigations, which could make it cost effective (Redgers et al., 2008; Madun, 2012; Madun et al., 2012).

2.4.5 Material Used for Stone Columns Constructions

The key parameter in stone column design is the angle of shearing resistance, which is a function of several parameters such as degree of compaction, grading and material strength (McKelvey and Sivakumar, 2000; Jefferson et al., 2010). Most of the design methods developed for predicting the bearing capacity of soils improved by stone column reinforcement (Hughes and Withers, 1974; Greenwood and Kirsch, 1984) are related to the undrained shear strength of surrounding soil and the internal angle of friction of the stone materials; a reduction of 10^o in the internal angle of friction can reduce the bearing capacity by 50% (McKelvey et al., 2002).

In general, 45^o can considered to be the maximum friction angle, while in the UK 40^o considered to be the most typical value used in the design (Serridge, 2006). Therefore, it is important that the stone aggregate within the column have sufficient shear resistance whereby the particles are strong enough to withstand local stress concentrations which occur during construction. In addition aggregate used must be durable in the long-term (Watts, 2000).

There are three main sources of aggregate, which can be used in stone column construction. Until recently natural or primary stone aggregate was the main source. However, increasing demands for sustainable construction has led to the use of recycled aggregate as a second source (e.g. construction demolitions and recycled railway ballast) and when possible the secondary aggregates (i.e. industrial processed products such as steel slag, rock waste, and china clay waste) (Jefferson et al., 2010).

Stone columns were installed in closely spaced groups beneath pad and strip foundations to provide bearing pressures of 100 kN/m2 (associated with the main portal frame structure) and on a square grid pattern beneath ground-bearing floor slab areas to provide bearing pressures in the range 30–50 kN/m2

Serridge (2005), provides a detailed case history of a project in Coatbridge, Scotland, where recycled (crushed concrete) aggregate was used successfully for stone column construction. Columns with diameter of 600 mm and varied in lengths from 2.5 to 6 meters were installed in a square pattern beneath pad and strip foundations to provide bearing pressure of 100 kN/m^2 (for the main frame structure) and 30 kN/m^2 under floor slab areas. The average deformation modulus of 48 MN/m^2 was achieved when assessed using plate load tests. He suggested that, this value was comparable with typical results if natural aggregate was used in similar ground condition.

McKelvey et al. (2002) examined the shear strength of different recycled aggregates (i.e. quarry waste, crushed concrete, and building debris). The performance of these materials were compared with the performance of crushed rock primary aggregate, in terms of the influence of dry and wet conditions and the effect of the fines content. They found that the primary aggregate performed better than the other recycled aggregate in all test conditions.

For example, in the dry condition, the angle of internal friction for the primary aggregate was 51^o, whereas for the secondary aggregate was ranging from (46^o to 37^o). These values were decreased by about 6 % in the wet condition and by about 30 % when 20 % of Kaolin slurry was add to the aggregate. This study indicated that the internal angle of friction of natural aggregate had been influenced by all the tested conditions while the quarry waste showed independency toward the slurry content and affected by the water content, where it showed different trend in case of crushed concrete aggregate, where it was influenced by the slurry content but not with the water content.

This could indicate that, regardless of the stone source used, the achievable quality of the stone column is mostly dependent on the quality of aggregate adopted. The ICE (1987) and BSI (2005) suggested that in order to achieve a good interlock between the stone particles and to allow an adequate level of drainage through the column, the grading of aggregates should range between 20 to 75 mm, also the percentage of fine content should not exceed 10 %.

2.5 Application and Limitation of Stone Column

Stone column technique has been used successfully in many projects around the world for ground improvement purposes (e.g. reduce differential settlement, accelerate the consolidation process; increase the bearing capacity and to mitigate liquefaction) in various types of soil from coarse gravel to fine sand, silt and clay (Woodward, 2004). The same benefits have been found when this technique was also applied to improve the characterisation of soft marine clay, non-engineering fills and layered soils (McKelvey, 2002; Raju and Sondermann, 2005; Han, 2015).

2.5.1 Limitations

Although stone columns have been installed successfully in soils with undrained shear strengths ranging between 10 kPa and 50 kPa (Hu, 1995; McKelvey, 2002), they are not suitable for soils with very low undrained shear strength and in soils with thick layers of peat. This is due to insufficient lateral support that these materials provide and excessive settlement that could occur due to the loss of water content during consolidation (Greenwood and Kirsch, 1984). Barksdale and Bachus (1983) suggest that stone columns can be more effective when used for soil stabilisation rather than structural foundations. Most recommended treatment depths are in the range of 6 to 15 m although columns have been constructed to a depth greater than 30 m (Watts, 2000). Floating columns are not recommended to be used in weak soils and therefore, a competent end bearing for stone columns is generally specified (Killeen and McCabe, 2014).

2.6 Design Approaches of Stone Column

As the column and the surrounding soils work together and share the stresses subjected to them, the bearing response of the soil/ column system is influenced by the properties of both materials and their interaction between each other. In order to theoretically solve this complex problem a certain level of idealisation (unit cell idealisation) is used. Most existing theories consider stone and clay as perfect elastic or elastic-plastic materials (Hughes and Withers, 1974; Barksdale and Bachus, 1983; Priebe, 1995). Therefore the design of stone columns requires cognisance of parameters such as used grid pattern, area replacement ratio and stress concentration factor (Sections 2.6.1.1 to 2.6.1.3). The typical design procedure suggested by Watts (2000) can be summarised as follow:

1. Predict the ultimate bearing capacity of the single column using the undrained shear strength of the soil and the internal angle of friction,
2. Determine the column diameter and the allowable spacing between the column,
3. Predict the level of settlement.

2.6.1 Basic Design Parameters

2.6.1.1 Unit Cell Idealization

Balaam et al. (1977) stated that the unit cell idealises for the behaviour of single column and the soil around it, and the behaviour of one unit cells within a group is the same. This concept is used to determine the area within which vertical stresses are considered to be distributed (Barksdale and Bachus, 1983). Stone columns can be installed in three main patterns: triangle, square and rectangular patterns. The equilateral triangle pattern is considered the most usable and efficient arrangement with regards to large areas and uniform rate of densification, while the square and rectangular pattern is applied in condition of isolated spread footing (Watts, 2000; BSI, 2005).

Typical layouts of stone columns in different patterns are shown in Figure 2.5. It is convenient to associate the tributary area of soil surrounding each stone column. The tributary area can be closely approximated as an equivalent circle (unit cell) with equivalent diameter (D_e) having approximately similar total area.

The spacing (S) between the columns is a critical factor since it influences the degree of improvement. The spacing is generally determined in order to provide an overlapping zone to cover a wide area of treated soils. Greenwood (1970) stated that, in practice, a narrow spacing is preferential under isolated foundation compared to beneath large raft foundations.

However, the spacing is generally ranges from 2 to 3 times the column diameter (Hughes and Withers, 1974).

Depending on the stone column arrangements, spacing and the equivalent diameter can be related to each other as shown in Table 2.2

Table 2.2 Equivalent unit cell diameter (adopted from Balaam & Booker, (1981))

Arrangement	Equivalent unit cell diameter (D_e); (S) centre-to-centre spacing
Triangular	$\left(\frac{12}{\pi^2}\right)^{0.25} S \cong 1.05\, S$
Square	$\left(\frac{16}{\pi^2}\right)^{0.25} S \cong 1.13\, S$

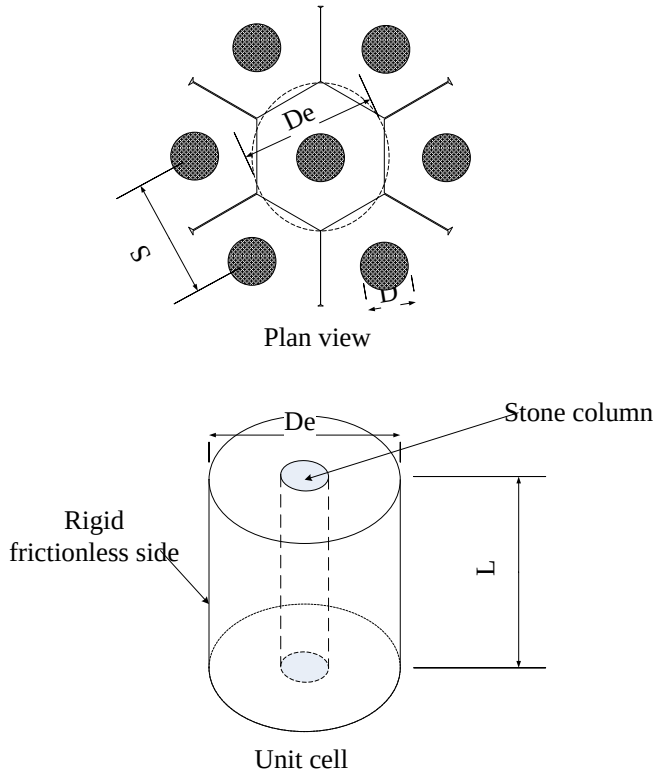

Figure 2.5 Unit cell concept (Barksdale and Bachus, 1983)

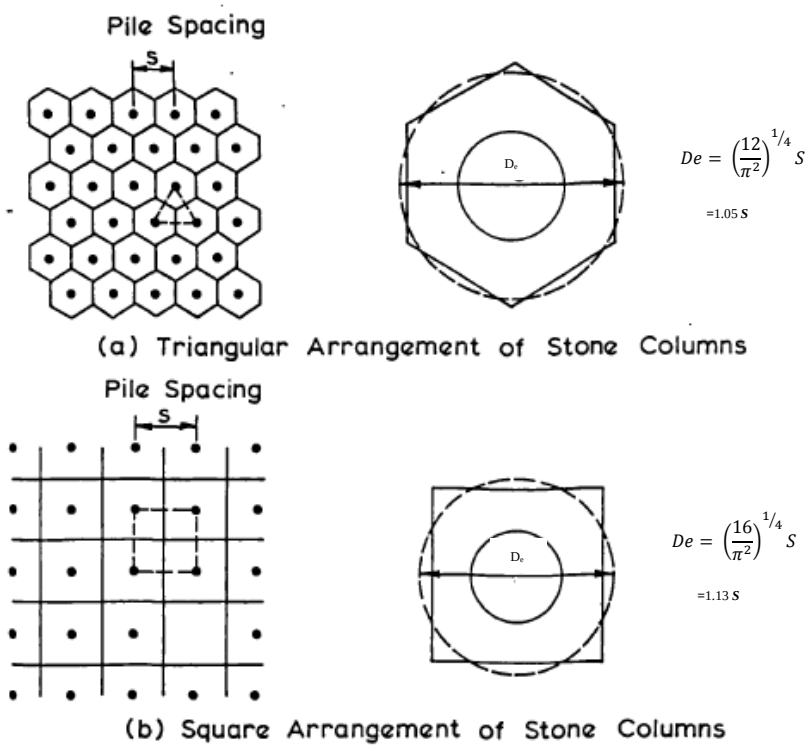

Figure 2.6 Stone Column arrangements in (a) Triangular (b) Square (Balaam & Booker, 1981)

2.6.1.2 Area Replacement Ratio

Based on the concept of unit cell, it is possible to use the geometry of a mesh of stone columns in order to determine the amount of soil replaced and the area replacement ratio A_s, which is defined as the ratio between the area of each column A_c and soil area A (Barksdale and Bachus, 1983):

$$A_s = {}^{A_c}/_{A} = \left[{}^{D_c}/_{D_e}\right]^2 \qquad 2.1$$

Where: D_c is the compacted stone column diameter; and D_e is the equivalent unit cell diameter.

The area replacement ratio, also can be presented in terms of the diameter and spacing of the stone column as follows:

$$A_s = c_g \langle \frac{D_c}{S} \rangle^2 \qquad 2.2$$

Where: D_c is the diameter of the compacted stone column; S is centre-to-centre spacing; c_g is a constant dependent upon the pattern of stone columns used.

In general, increasing the area replacement ratio leads to improved behaviour of the composite soil (i.e. increased bearing capacity and reduced settlement). For improvement in bearing capacity larger than 30 %, Wood et al. (2000) indicated that the area replacement ratio should be 25% or above.

2.6.1.3 Stress Concentration Factor (*n*)

A large portion of the stress concentration is transferred from the loaded foundation to the stone column. The remaining stresses are transferred to the soil as it is weaker than the column material. The vertical stress distribution within the unit cell (concentration factor) is defined as the ratio of the stress on the stone column to that on the surrounding soil within a unit cell (Han & Ye, 1991). The magnitude of the concentration factor generally ranges from 2 to 6 (Aboshi et al., 1979; Barksdale and Bachus, 1983).

$$n = {}^{\sigma_s}/_{\sigma_c} \qquad 2.3$$

Where: σ_s is stress in the stone column; and σ_c is the stress in the surrounding soil.

There are several factors that could influence the magnitude of stress concentration such as type of foundation, length of the column and time of consolidation. Juran and Guermazi (1988) stated that the magnitude of (n) increases with time of consolidation and decreases with the length of the column. in addition, loading the soil/column system through a rigid

foundation would lead to larger stress concentration than if flexible a foundation was used (Barksdale and Bachus, 1983).

Ambily and Gandhi (2007) indicated that the modular ratio had a direct impact on the stress concentration, they found that the n factor increased with any increase in modular ratio; and reduced with any increase in the strength of the surrounding soil.

The total vertical stresses σ in stone columns and the surrounding soil over the unit cell area and corresponding to a given area replacement ratio, can be expressed as:

$$\sigma = \sigma_s . A_s + \sigma_c (1 - A_s) \qquad 2.4$$

Where the terms have been previously defined.

Thus the stress concentration factor can be estimated (as follow) assuming equal vertical displacement would occur and using the elastic theory as a function of the modular ratio of the column and the soil (Barksdale and Bachus, 1983; Babu et al., 2013).

$$\sigma_c \leq \mu_c \sigma = \mu_c \left({}^{\sigma_s}/_{\mu_s}\right) 2 \qquad 2.5$$

Where: $\mu_c \; and \; \mu_s$ are the stress ratios in the clay and the stone column respectively.

$$\mu_s = {}^{n}/_{[1 + (n-1)A_s]} \qquad 2.6$$

$$\mu_c = {}^{1}/_{[1 + (n-1)A_s]} \qquad 2.7$$

2.6.2 Consolidation and Settlement

One of the main purposes of using stone columns is to reduce the overall settlement of the treated soil. This reduction is governed by the magnitude of applied load distribution that occurs between the column and surrounding soil.

In order to satisfy the unit cell concept condition (Figure 2.7), most of the design approaches for predicting settlement of soil/column system assume an infinitely wide loaded area reinforced with granular column with a constant diameter and spacing. The column is assumed to be loaded via a rigid plate and ending in an undeformable bearing layer (Van Impe et al., 1997; Babu et al., 2013).

There are various methods for estimating the settlement of the stone column/ soil system. These are summarised in Table 2.3.

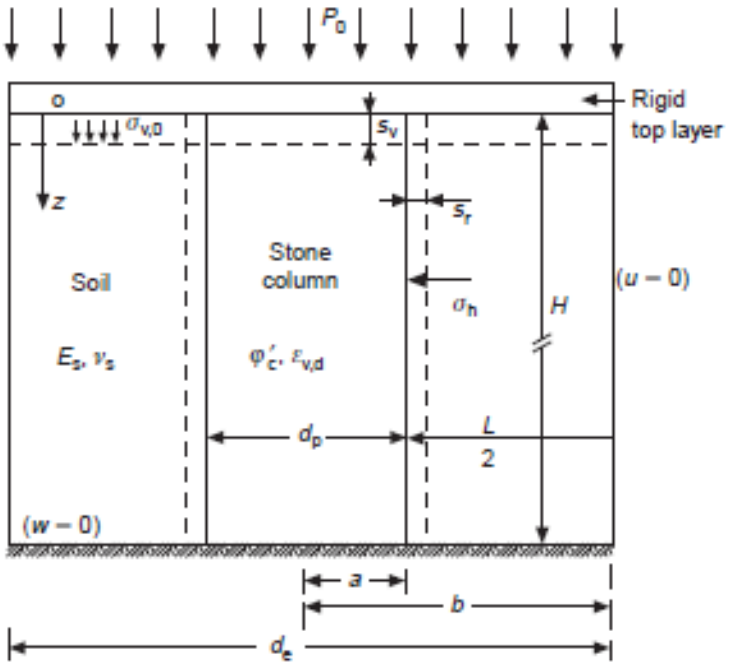

Figure 2.7 Settlement estimation conditions

Table 2.3 Methods of estimation of settlement

Method	Reference	Equation	comment
Greenwood's method (2.6.2.1)	Greenwood (1970)	Empirical design curve (Figure 2.8)	Limited to c_u between 20 and 40kPa ; underestimate settlement when S>2.5m
Equilibrium method (2.6.2.2)	Aboshi et al. (1979)	$S_t = m_v(\mu_c\sigma)H$ $R = \mu_c = \frac{1}{1+(n-1)A_s}$	Dependent on the *n* and A_s; Might be sufficient for preliminary design;
Priebe method (2.6.2.3)	Priebe (1976, 1995)	$\frac{1}{R} = 1 + A_s\left[\frac{0.5 + f(\mu, A_s)}{(k_A)_s f(\mu, A_s)} - 1\right]$ $f(\mu, A_s) = \left[\frac{1-\mu^2}{1-\mu-2\mu^2}\right]\left[\frac{(1-2\mu)(1-A_s)}{1-2\mu+A_s}\right](k_A)_s$ $= \tan^2\left(45 - \frac{\emptyset}{2}\right)$	Overestimated results
Finite element method	Balaam et al. (1977)	$[K_E]\{\Delta\sigma^{(m-1)}\} = \left\{\{\Delta F_E\} + \left\{K_c^{(m)}\right\}\{\Delta\sigma^{(m)}\} + \left\{\Delta F_{DN}^{(m)}\right\}\right\}$	Its accuracy dependent on the input parameters

2.6.2.1 Greenwood Method.

Greenwood (1970) was one of the first to introduce empirical design curves to estimate the settlement of stone column/ soil systems under widespread loading. The empirical curves showed in Figure 2.8, represents the settlement reduction as a function of column spacing and the undrained shear strength of the surrounding soil, which was limited between 20 and 40 kPa. The shaded zone in the curve represents the expected settlement reductions when applying a wet process of construction. Greenwood (1970) suggested that these charts should be used with caution within the indicated range. Although Balaam and Booker (1985) indicated that these curves showed a close agreement with their finite element analysis

approach for settlement estimation, they suggested that at column spacing of over 2.5 m, the Greenwood's method might underestimate the degree of improvement.

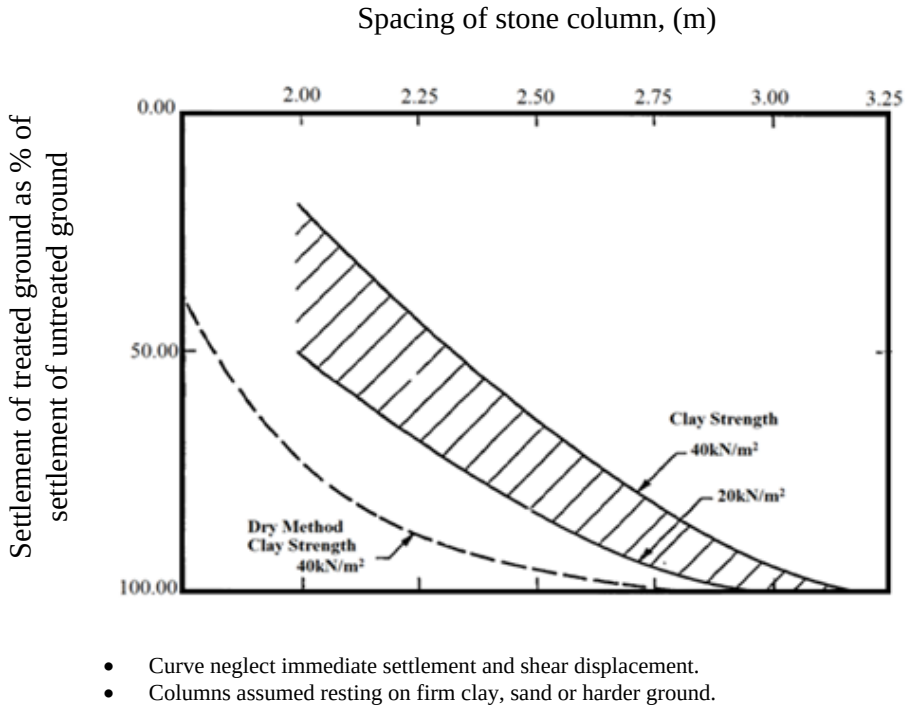

Figure 2.8 Settlement diagram for stone column in uniform soft clay (Greenwood, 1970)

2.6.2.2 The equilibrium method

This method has been used (mainly in Japan) to estimate the settlement of sand compaction piles (Barksdale and Bachus, 1983). Aboshi et al. (1979) presented this simple approach for estimating the reduction in settlement of ground reinforced by stone columns based on the unit cell assumptions and the one dimensional consolidation theory. This approach require estimation of stress concentration factor *n* using previous work experience and the past results from field measurements of stresses.

The variation of the vertical stress in the clay (σ_c) due to the applied external stress can be expressed by:

$$\sigma_c = \mu_c \sigma \qquad 2.8$$

Where: σ is the average external applied stress; and μ_c is the ratio of stresses in the clay (Eq. 2.7).

By applying the one dimensional consolidation theory the primary consolidation settlement can be estimated using the following equation.

$$S_t = \left(\frac{C_c}{1+e_0}\right).\log_{10}\left(\frac{\sigma_0' + \sigma_c}{\sigma_0'}\right) . H \qquad 2.9$$

Where: S_t is the primary consolidation settlement over distance H of stone column treated ground; H is the height of stone column; e_0 is the initial void ratio; C_c is the compression index; σ_0 is the average initial effective stress; and σ_c is the changing in stress in the clay layer.

Additionally, the following equation may be used to estimate the settlement of unreinforced and reinforced soils.

$$S = m_v.\sigma.H \qquad 2.10$$

$$S_t = m_v(\mu_c \sigma)H \qquad 2.11$$

Where, S and S_t, as defined previously, are the consolidation settlements of unreinforced and reinforced soils respectively; m_v if the coefficient of compressibility; and H is the thickness of the soil layer.

The ratio of the settlement of the stone column (i.e. improved soil to the unimproved soils) can be expressed as:

$$R = {}^{S_t}/_{S} = \frac{1}{[1 + (n-1)A_s]} \qquad 2.12$$

Where *n* is the stress concentration factor and A_s is the area replacement ratio.

The above equation showed that the settlement ratio is a function of the area replacement ratio and the stress concentration factor, and the settlement of the treated soil decreases as those parameters increases. Therefore, as suggested by Barksdale and Bachus (1983) the equilibrium method would be sufficient for preliminary design if the stress concentration factor was reasonably estimated.

2.6.2.3 Priebe method

Priebe method is considered one of the most widely adopted semi-empirical methods used to obtain the improvement factor (estimating settlement reduction due to soil treatment with stone column). This method has undergone a series of improvements and modifications to its current version proposed (Priebe, 1995). These modifications considered a number of additional factors such as the effect of compressibility of the column material and confinement from overburden, which considers the effect of unit weight of both column and soil materials by adding the depth factor to the design calculation (Barksdale and Bachus, 1983; Ellouze et al., 2010; Babu et al., 2013).

The original solution proposed contained a number of simplifying assumptions that are listed below:

- equal vertical settlement of the stone and soil;
- uniform stresses in the column/soil system;
- stone column is overlying a rigid soil layer;
- incompressible stone column, so changing in volume within the soil associated to the axial reduction of the cylindrical column;
- long elastic hollow cylinder solution is assumed in order to find out the radial deformation of the soil and;
- a uniform internal pressure within the unit cell boundary.

According to these assumptions it can be concluded that the column is designed to only fail in a bulging mode and the settlement can be controlled.

Based on these assumptions, Priebe (1995) presented in Figure 2.9 the ratio of settlement of untreated to treated ground S/S_t as a function of the area replacement ratio A_s and internal angle of friction of the stone column φ_s.

Therefore, the radial deformation of the column/soil system can be determined from the solution of expanding cylindrical cavity in half elastic. This expression gives the radial deformation of the column based on vertical stress acting on it and on the ground (Priebe, 1995). Establishing equality of vertical deformations in the soil and the column and by the equilibrium condition of vertical stresses, the following improvement factor n_0 expression can be obtained:

$$n_0 = 1 + \frac{A_c}{A} \cdot \left(\frac{{}^1/_2 + f(\mu_s, A_c/A)}{K_{ac} \cdot f(\mu_s, A_c/A)} - 1 \right) \quad 2.13$$

Where: $$f(\mu_s, A_c/A) = \frac{(1-\mu_s) \cdot \left(1 - {}^{A_c}/_A\right)}{1 - 2\mu_s + {}^{A_c}/_A}; \quad 2.14$$

μ_s is the Poisson's ratio; and (K_{ac}) coefficient of active pressure of the column is defined as:

$$(K_{ac}) = tan^2\left(45^o - {\emptyset_c}/{2}\right) \quad 2.15$$

Although this method has been widely used in ground improvement industry, it has limitations in settlement prediction, such as not being suitable for estimating the behaviour of floating columns (Babu et al., 2013).

Ellouze et al. (2010) reported that some of the assumptions in Preibe's method, such as that the unit weights of column material and initial soil are neglected, are questionable and not well defined. Additionally, they highlight that the design procedure is not connected mathematically and inconsistence. For example, in the first step of the design, Priebe (1995) considers a cylindrical cavity subjected to lateral expansion during which zero vertical deformation is assumed in order to give a solution expressed in plane stress condition. In a second step, this solution is incorporated in the soil/column model for which there is a distribution of vertical stress generating non-null vertical deformation, and, consequently, the settlement is assumed constant.

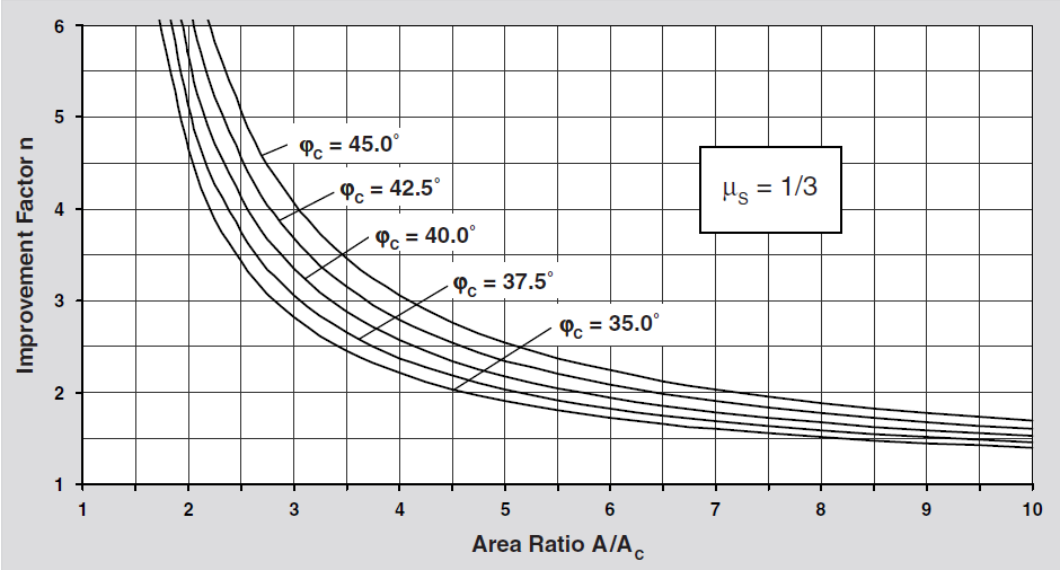

Figure 2.9 Improvement factor (Priebe, 1995)

Using a case study of 54 m diameter tank built on reclaimed ground reinforced by stone columns to ensure the stability of the tank at Zarzis terminal (Tunisia), Ellouze et al. (2010) demonstrated that Priebe's method was overestimated the settlement of reinforced soil by stone columns comparing with other linear elastic models (Balaam and Booker (1981); Chow (1996) Bouassida et al. (2003) and the French recommendations (Françaises, 2005)).

Working load of the tank was approximated as a quasi-uniform stress of 120 kPa. The reinforcement was performed along an average depth of 7 meters with a columns diameter of 1.2 meter installed in a triangular pattern. The soil was improved on a circular area with a diameter of 62 meters, which implies an improved area ratio of about 32 %.

The settlement of unreinforced soil was estimated to be about 230 mm underneath the centre-line of the tank, whereas the settlement at the edge of tank was estimated to be about 60 mm.

The settlement predictions of the reinforced soil at the centre-line of the tank and its edge that were obtained using the software columns (Bouassida et al., 2009) and Priebe's method are presented in Table 2.4.

Table 2.4 Comparison between predictions of tank's settlement (Ellouze et al., 2010)

Method	**Settlement of reinforced soil at the centre line of the tank, (mm)**	**Settlement of reinforced soil at the edge of the tank, (mm)**	**Settlement reduction factor at the centre line of the tank**	**Settlement reduction factor at the edge of the tank**
Recorded	-	30	-	2.00
Bouassida et al. (2003)	58	28	3.96	2.14
French recommendation (Françaises, 2005)	55	26	4.18	2.30
Balaam and Booker (1981)	51	24	4.50	2.50
Priebe (1995)	61	21	3.77	2.85

2.6.2.4 Finite Element Method

The finite element method could provide an appropriate theoretically approach to model stone column reinforced ground, where nonlinear material properties, the column/ soil interface and the boundary conditions can all be sufficiently modelled (Gniel and Bouazza, 2007; Killeen, 2012; Babu et al., 2013; Killeen and McCabe, 2014; Mohanty and Samanta, 2015). Most of the finite elements studies have utilized the axisymmetric unit cell model to analyse the conditions of either a uniform load on a large group of stone columns or a single stone column. Balaam et al. (1977) used finite element method to investigate the behaviour of stone column, and developed a design curves for predicting settlement reduction. Figure 2.10 showed an example of these curves. Balaam et al. (1977) highlited that column diameter and

ratio of column length to depth of the soil layer had significant influence on settlement amount, whereas modular ratio of column to soil was less important.

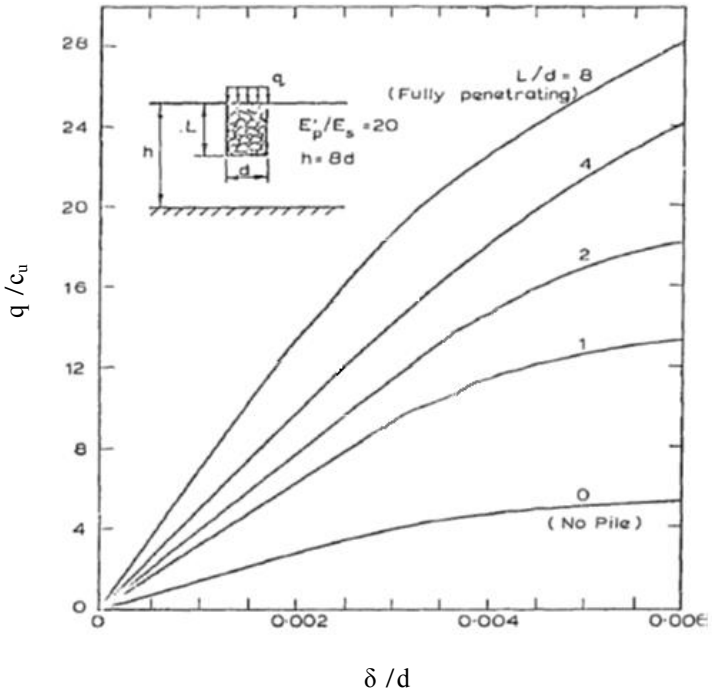

Figure 2.10 Load – settlement curves for stone column (Balaam et al., 1977)

Barksdale and Bachus (1983) developed a design curves for estimating settlement in both low compressibility and compressible soils using a nonlinear finite element method combined with the idealisation of unit cell to predict the primary consolidation settlement of column/soil system. In this approach the soil modulus of elasticity was assumed to be constant with the depth of the soil. In addition to this, different area replacement ratios (10, 20, 25, and 35 %) at different L/D ratios (5, 10, and 20) were considered and each case has a different design chart.

Poorooshasb and Meyerhof (1997) introduced an elastic soil model to predict the settlement reduction of raft foundation resting on end bearing stone column reinforced soft soils. This model indicated that the design pattern, spacing and the degree of compaction of the column material were the most viable parameters to control the level of settlement.

Generally, finite element solution claimed by authors (Ambily and Gandhi, 2007; Killeen, 2012; Killeen and McCabe, 2014) to provide a good agreement with the full scale and site investigation results; however, their utility is governed by the accuracy of the input parameters.

2.6.3 Bearing Capacity Prediction Methods

Stone columns are often constructed penetrating through soft soil to end bearing layers with a critical length of 4 to 6 times the column diameter. Thus the most possible mode of failure that might develop for an isolated stone column over a depth of 2 to 3 diameters from the surface is bulging failure (Barksdale and Bachus, 1983; Bergado et al., 1991). Several approaches have been developed to predict the ultimate capacity of an isolated stone column surrounded by soft soils. Table 2.5 summaries the most common of these corresponding to the mode of failure as presented by Bergado et al. (1991).

These approaches were developed on the basis that the lateral confining stress supporting the column is usually considered as the ultimate passive resistance which the surrounding soil can mobilize as the column bulges. Since then the ultimate vertical stress(σ_v) can be predicted as the coefficient of the passive pressure of the column (k_p) times the lateral confining pressure (σ_r).

$$\sigma_v = \sigma_r * k_p$$

$$= \sigma_r \left(\frac{1+\sin\phi'}{1-\sin\phi'} \right) \qquad 2.16$$

Table 2.5 Estimation of ultimate bearing capacity (Bergado et al., 1991)

Mode of failure	Design equation	Reference
Bulging	$q_{ult} = \left(\gamma_c z k_{pc} + 2c_o z\sqrt{k_{pc}}\right)\frac{1+\sin\emptyset_s}{1-\sin\emptyset_s}$	Greenwood (1970)
	$q_{ult} = \left(F_c' C_o + F_q' Q_o\right)\frac{1+\sin\emptyset_s}{1-\sin\emptyset_s}$	Vesic (1972)
	$q_{ult} = (\sigma_{ro} + 4C_u)\frac{1+\sin\emptyset_s}{1-\sin\emptyset_s}$	Hughes and Withers (1974)
	$q_{ult} = (N_c C_u)$	Barksdale and Bachus (1984)
General shear	$q_{ult} = C_u N_c + 0.5\gamma_c N_\gamma B + \gamma_c D_f N_q$	Madhav and Vitkar (1978)
	$q_{ult} = 0.5\gamma_c B tan_\psi^3 + 2C_o tan_\psi^2 + 2\,(1-a_s)C_o tan_\psi$ $\psi = 45^o + \frac{\tan(\mu_s a_s \tan\emptyset_s)}{2}$	Barksdale and Bachus (1983)

Greenwood (1970) noted that there was no exact mathematical method to estimate the bearing capacity of cohesive soils treated by stone columns, because of the dilation that occurs within the column and the resulting lateral stress to the surrounding soil which can be resisted by passive pressure; (Greenwood, 1970) hypothesed that the column will behave as if it was in a triaxial chamber, and the degree of improvement in the bearing capacity would be governed by the lateral support from the surrounded clay to the column and the internal angle of friction. In addition, Greenwood (1970) highlighted that the carrying capacity of the column increases until either a local shear failure in the clay or end bearing failure at the bottom of the column accords.

Hughes and Withers (1974) used a laboratory based model and radiography device, to study the behaviour of both sand columns and surrounding clay by tracking the deformations occurred within and outside the column. They concluded that the cylindrical cavity expansion theory can be used to define the column behaviour. They proposed the following equation for estimating the ultimate vertical stress (σ_v) in a stone column:

$$\sigma_v = \frac{1+\sin\emptyset'}{1-\sin\emptyset'}(\sigma'_{ro} + 4c) \qquad 2.16$$

Vesic (1972), based on the theory of cylindrical cavity expansion, developed an expression for estimating lateral resistance where the ultimate lateral resistance is:

$$\sigma_3 = c\, F_c + q\, F_q \qquad 2.17$$

where: c is the cohesion of the soil, q is the mean stress at the equivalent failure depth and F_c, F_q are cavity expansion factors which determine from Figure 2.11 using the rigidity index, I_r,:

$$I_r = \frac{E}{2(1+v)(c+q\tan\phi')} \qquad 2.18$$

Where: E is the modulus of elasticity of the soil in which cavity expansion occur, c is the cohesion of the soil, v is the Poisson's ratio of the soil, ϕ' is the effective angle of friction of the soil and q is the mean stress within the zone of failure.

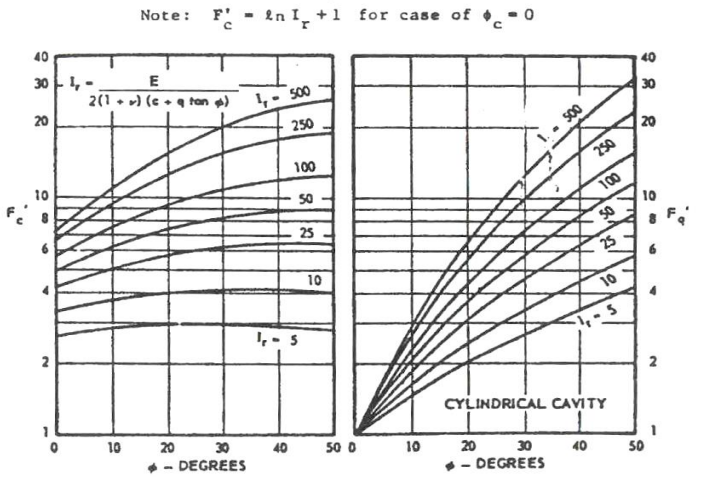

Figure 2.11 Vesic's cylindrical cavity expansion factors (Barksdale and Bachus 1983).

Therefore assuming $(\sigma_3 = \sigma_r)$ substituting (2.18) in (2.16) the ultimate stress that can be applied to a stone column is:

$$\sigma_v = [c\ F_c + q\ F_q] \left(\frac{1+\sin\phi'}{1-\sin\phi'} \right) \quad 2.19$$

The mean stress q used in the above equations should be taken as stress at the average depth of the bulge taking into account the initial and the final stresses in the ground. Vesic (1972) expressions can be used both for short and long term calculation.

Barksdale and Bachus (1983) developed a simple approach for estimating the bearing capacity of a single column. (Equation 2.21) based on authors 'past experience and utilising good engineering judgment'.

$$q_{ult} = c_u * N_c \quad 2.20$$

Where, q_{ult} is the ultimate bearing capacity of the stone column; c_u is the undrained shear strength of the surrounding soil; and N_c is the bearing capacity factor for the stone column usually ranging between 18 and 22, and 5 for estimating the bearing cabacity of the untreated soil. The value of N_c is highly dependent on the compressibility of the soil surrounding the column, where it is increased with the increase of soil stiffness (Barksdale and Bachus, 1983; McKelvey, 2002).

To conclude, determination of load bearing capacity of a single stone column is complex and there is no exact mathematical solution to predict it. This is due to the uncertainty of the interaction behaviour between the stone column and the surrounding soils. However, the relationship based on the laboratory model tests proposed by Hughes and Withers (1974) is

widely considered realistic for vibro stone columns design (Greenwood, 1991; Babu et al., 2013; Najjar, 2013).

2.7 Mechanism and Performance of Stone Columns

2.7.1 Stone Columns Investigation under Monotonic Loading Condition

2.7.1.1 Failure mechanism

Generally, stone columns are created using high friction granular material where the stiffness of the column is dependent on the lateral support given by the surrounded soil. If this support is not sufficient the column will fail (Barksdale and Bachus, 1983; Bergado et al., 1991).

The failure mechanism of a single column can be a function of two main factors in addition to its length whether it is considered to be long or short (i.e. the length of the column is greater or shorter than the critical length($\frac{L}{D} \approx 6$)).

The first one is the method of column construction as either end bearing on a firm competent layer of soil, or as floating columns.

The second factor is the load application on the column, which could be either directly to the top of the column or through a rigid cap over an area larger than the diameter of the stone column (Barksdale and Bachus, 1983; Sivakumar et al., 2004a). Figures 2.12 shows the expected mod of failures, which can be summarised as:

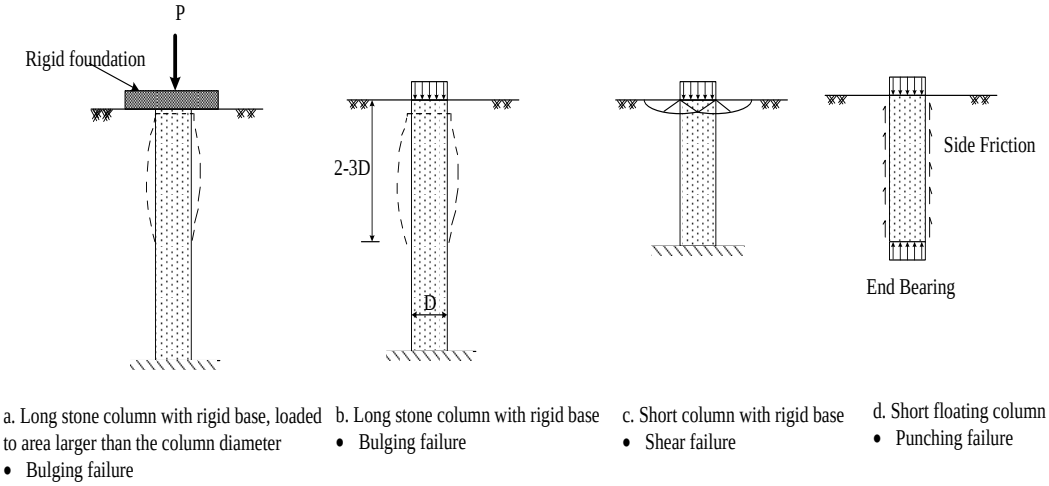

Figure 2.12 Failure mechanism of single stone column (Barksdale and Bachus, 1983)

- Bulging failure: for columns overlying on rigid base, having length over their critical length and loaded directly over the column area, a bulging failure would occur over 2 to 3 diameter of the depth. However, if the load was applied over larger area, then there would be an increase in the vertical and lateral stresses as in the surrounding soft soil, which would then affect the response of the column to loading. Normally this leads to smaller bulging and higher ultimate bearing capacity (Barksdale and Bachus, 1983).

- Shear and punching failure: columns shorter than the critical length ($\frac{L}{D} \approx 6$) were likely to fail in shear failure if they were end bearing on rigid base, or in punching failure if they were floating columns (Barksdale and Bachus, 1983).

Bulging of the column is more noticeable in the upper portion of the column as indicated by Greenwood (1970), Hughes and Withers (1974), Barksdale and Bachus (1983), Charles and Watts (1983), Greenwood (1991), and Sivakumar et al. (2004a). Barksdale and Bachus (1983) suggested that bulging would occur within 2 to 3 times the column diameter whereas Hughes and Withers (1974) and Sivakumar et al. (2004a) observed that the column bulged at depth of approximately four times the diameter of the column. Bae et al. (2002), suggested that the column diameter could be the main parameter affecting the depth of this bulging zone, while

other factors such as soil strength and the depth ratio could be considered to have less influence. on the other hand Sivakumar et al. (2007) noted that the degree of bulging is largely dependent on in situ shear strength of the surrounding soil.

The mode of failure of stone columns in group has been investigated by a number of researchers (e.g. Barksdale and Bachus (1983); Hu (1995); McKelvey (2002); Sivakumar et al. (2004a)). In general they indicated that stone columns constructed in groups showed different failure behaviour than the isolated columns; in groups, each column can interact and restrain the expansion of the neighbouring column leading to increase the bearing capacity.

Hu (1995) studied the behaviour of stone column groups and suggested that there are three different modes of failures (bulging, shearing and lateral deflection) which depend on the geometric configuration of the columns. Different geometry parameters (L/r_0 = 2, 3.2 and 3.4; r_c = 5.5 and 8.75 mm; A_s = 24 and 30 %) were tested in group of 5 and 7 sand column reinforced by a footing with a radius (r_0) of 50 mm. Hu (1995) showed that the shear planes through the columns would occur towards the edge of the footing, while bulging could be seen deep directly under the foundation. The depth of the bulging was found to increase as the area replacement ratio A_s increases. Additionally he observed that short columns tend to penetrate underlying clay, however, as column length increases penetration decreases.

Sivakumar et al. (2004a) noted that the central columns beneath the foundation bulge uniformly, whereas the others at the edge they bulge away toward the surrounding soils.

A range of methods can be used to examine the deformation and failure patterns of stone columns. For example, Hughes and Withers (1974) used an X ray technique to monitor the deformation of isolated stone column. Whereas (Hu (1995), Wood et al. (2000), Ambily and

Gandhi (2007)) successfully formed a plaster-cast of the vacuumed holes after exhuming the columns material.

McKelvey (2002) and Sivakumar et al. (2004a) used a transparent medium as can be seen in Figure 2.13 (with shear strength properties similar to the soft clay) allowing constant monitoring to the column deformation.

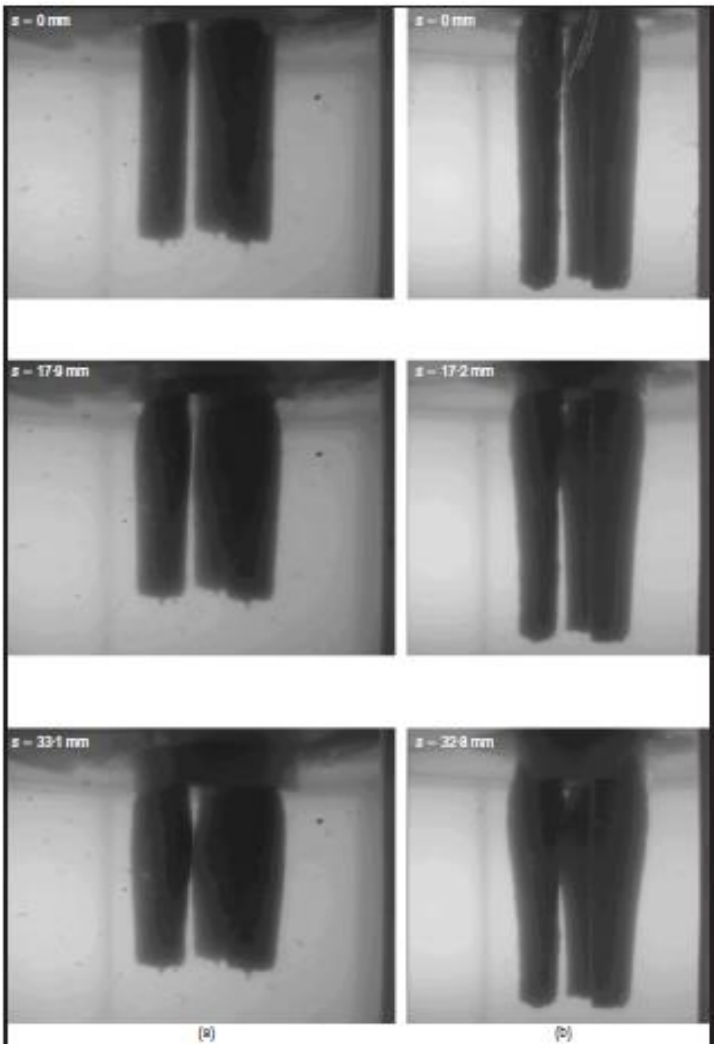

Figure 2.13 Photographs of sand columns beneath circular footing at beginning, middle and end of foundation loading process: (a) TS-01, 150 mm; (b) TS-02, 250 mm

(Sivakumar et al., 2004a)

Sivakumar et al. (2004b) investigated the behaviour of single stone column under the condition of undrained triaxial, they examined the mode of failure by splitting the specimen (100 mm diameter X 200 mm length) vertically along its centre axis.

Another method that can be used for this purpose by grouting the stone column by pouring the concentrated cement slurry after testing and allowing it to set for some time depending on the concentration of the slurry and then carefully removing the surrounding soils (Sivakumar et al., 2010).

2.7.1.2 Critical length

Hughes et al. (1976) defined the critical length of the column as the shortest length that allows the column to carry the designed ultimate load regardless of the deformation that would occur.

$$P_{ult} = \bar{c}(\pi D L_c) + N_c c\, A_c \qquad 2.21$$

Where, P_{ult} is the ultimate column load; $\bar{c}\ and\ c$ are respectively the average shaft cohesion and the cohesion of the soil at the bottom of the critical length; A_c is the column area with diameter *D*; and $(\pi D L_c)$ representing the surface area of the side of the column with critical length L_c.

Hughes and Withers (1974) introduced the L/D ratio and they found that there is no improvement in the bearing capacity of the column beyond (L/D = 4.1). Samadhiya et al. (2008) studied the effect of the column length on the column bearing capacity, they identified that the critical length was at 4.5D and found that any increase of the bearing capacity was marginal after this length. Black et al. (2011) presented results obtained from a large physical triaxial model, they investigated the influence of L/D ratio and the area replacement ratio on the settlement improvement factor. Black et al. (2011) suggested that the L/D ratio greater

than 6 is required to provide the full limiting axial stress on the column. in addition they found that an L/D ratio beyond 8 offers insignificant improvement in terms of settlement control (i.e less than 5%). They also suggested that settlement can be controlled in short columns (L/D < 6) using a relatively high area replacement ratio (> 30 %).

In conclusion, column length larger than the critical length may not provide further improvement in the column bearing capacity, but it may be used to control the level of settlement

2.7.1.3 Undrained shear strength of the surrounding soil

As explained in previous sections (2.7.2 and 2.7.3), surrounding soils provide the lateral confinement to stone columns, therefore when designing stone column it is important to have an appropriate knowledge of the soils undrained shear strength. Figure 2.14 shows the influence of this factor on the ultimate carrying capacity of the stone column according to both an empirical design relation presented in Equation 2.16 and different laboratory investigation results carried out by Hughes and Withers (1974), Ambily and Gandhi (2004), Kim and Lee (2005), Ambily and Gandhi (2007), Zahmatkesh and Choobbasti (2010) , Black et al. (2011), and Ali et al. (2014). Although the obtained results did not show a perfect fit with the prediction lines, they show that the column bearing capacity increases with the increase of the soil shear strength. However, the degree of improvement at similar soil strength is dependent on other factors such as the area replacement ratio and the internal angle of friction. For example, Ambily and Gandhi (2007) investigated the effect of the soil shear strength c_u= 7, 14, and 30 kPa) and the area replacement ratio (A_s = 5, 10, and 19 %) on the behaviour of single stone column, they noted that the ultimate bearing capacity of the

improved soil increased in linearly from 175 kPa to 740 kPa when increasing the undrained shear strength from 7 to 30 kPa.

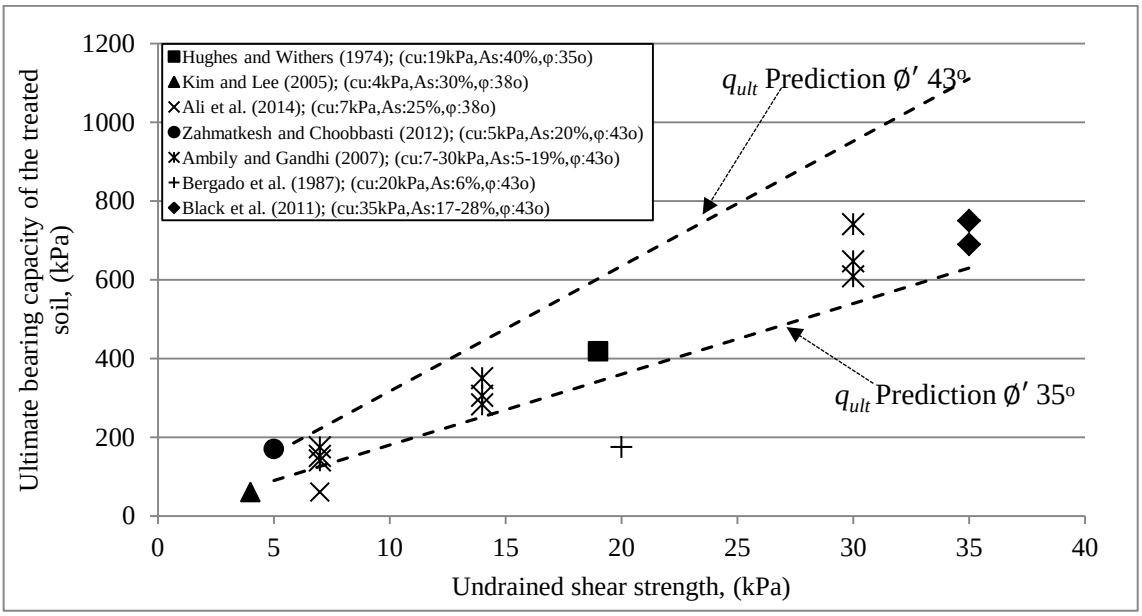

Figure 2.14 Effect of undrained shear strength of the surrounding soil on the ultimate bearing capacity of the treated ground

2.7.1.4 Area replacement ratio

Data from previous research studies Wood et al. (2000), Kim and Lee (2005), Ambily and Gandhi (2007), Najjar et al. (2010), Zahmatkesh and Choobbasti (2010), Black et al. (2011), were collected and plotted together in Figure 2.15 in order to observe the impact of the area replacement factor on the bearing capacity of the improved ground. From Figure 2.15 it can be seen that as spacing between the columns increases, the area replacement ratio decreases, leading to a decrease in the axial capacity of the column which may lead to increase degree of settlement. An area replacement ratio from 5 to 25 % could improve the column capacity by about 30 to 45 % depending on the surrounding soil characterisation; significant improvement

occurs when the area replacement ratio between 0 and 20 % and beyond A_s of 20 % the increment became very small.

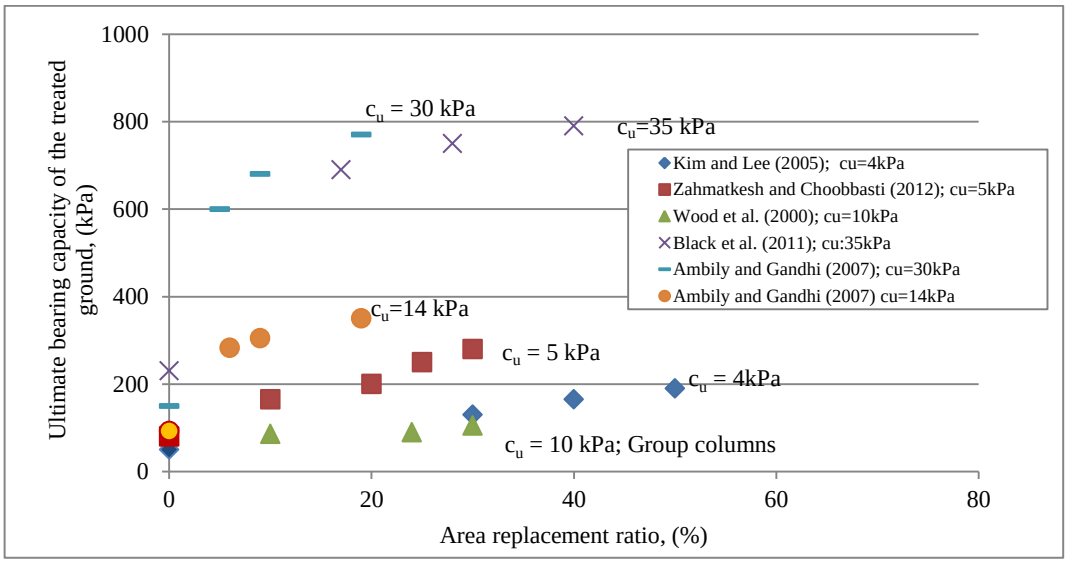

Figure 2.15 Effect area replacement ratio on the ultimate bearing capacity of the treated ground

The shear strength of the surrounding soil has a large impact on the improved ground bearing capacity, where at A_s of 20 %, for example, the column capacity was increased from 170 to 770 kPa by increasing the undrained shear strength from 5 to 30 kPa.

For significant improvement in bearing capacity, Wood et al. (2000) indicated that the area replacement ratio should be 25% or above, and Ambily and Gandhi (2007) suggested that the improvement beyond S/D = 3 (i.e. As < 7 %) is negligible.

Black et al. (2011) examined the influence of area replacement ratio and the column length on the performance of a footing supported on stone column using a developed large triaxial cell. The cell accommodated a consolidated specimen (c_u =35 kPa) of 300 mm diameter by 400 mm height. Granular columns with different diameters of 25, 32, and 38 mm and various lengths 125, 250, and 400 mm were tested. Results indicated that the settlement improvement factor any increased with the increase in the area replacement ratio; however, the

improvement appeared to have a threshold of about 30–40 % area replacement ratio. For foundations supported on column groups, the pressure-settlement response was found to be similar to the individual columns at the same area replacement ratio. Therein settlement improvement factors for the area replacement ratios of 28 and 40 % were 3.2 and 3.8 respectively. The settlement improvement factors for the corresponding single columns were about 6.5–7.5 indicating that the performance of the group is not as good as that of the single columns. Limited results for pressures recorded in the column and in the clay in the group indicate a stress concentration factor of 1.5.

Bergado et al. (1987) conducted a full scale investigation on six footings by applying load on single rammed aggregate piers (crushed gravel) with a diameter of 0.3 m and installed to a depth of 8 m in a site characterized by a 2 m thick layer of overconsolidated clay overlying a layer of very soft clay with 6 meter thickness. The undrained shear strength ranged from 30 to 40 kPa for the upper clay layer, and from 15 to 25 kPa for the soft clay. Columns were loaded in maintained stress increments with footings with diameters of 0.3, 0.45, 0.60, 0.75, 0.9, and 1.2 m, representing replacement ratios of 100, 44, 25, 16, 11, and 6 %, respectively. Results indicated that the settlement improvement factor decreased from 8 to 1.5 as the area replacement ratio decreased from 100 to 6 %.

2.7.2 Dynamic Loading Condition

2.7.2.1 General soil behaviour under cyclic loading

Dynamic loading applications on the subsurface of soft soil layers induced by vibration sources (e.g. earthquakes, traffic loads, or offshore waves) can cause a complex stress field, in which these stresses vary with time (Gu et al., 2012). The stress strain behaviour of clay soils

under cyclic loading is dependent on factors such as stress level, drainage condition, type and rate of loading (Brown, 1996).

Undrained long-term cyclic loading for normally consolidated clays may lead to cyclic failure. This failure can be identified by number of loading applications in which an arbitrary predetermined double amplitude failure axial strain is reached (Andersen et al., 1980; Jianhua Wang et al., 2006; Li-Zhong Wang et al., 2011). Yasuhara et al. (1992) considered residual pore pressure as an indication of cyclic failure.

Loading frequency is also considered an important issue in cyclic loading. For example, Ishihara (1996) classified the dynamic problems according to the time of loading as shown in Figure 2.16. in other wards instances where a load application stays for more than tens of seconds are considered as static whereas those with a shorter time of loading are considered as dynamic loading. For example, a shaking wave during earthquakes involves 10 to 20 times repetition of loads with different amplitudes, and the period of each impulse ranges between 0.1 and 3.0 seconds, which gives a time of loading of 0.02 to 1.0 seconds. On the other hand, in case of repetitive loads induced by traffic, the soils in the subgrade underneath railways or road embankments are subjected to a large number of load cycles during the life span. The time of loading may be deemed on the order of 0.1 second to a few seconds.

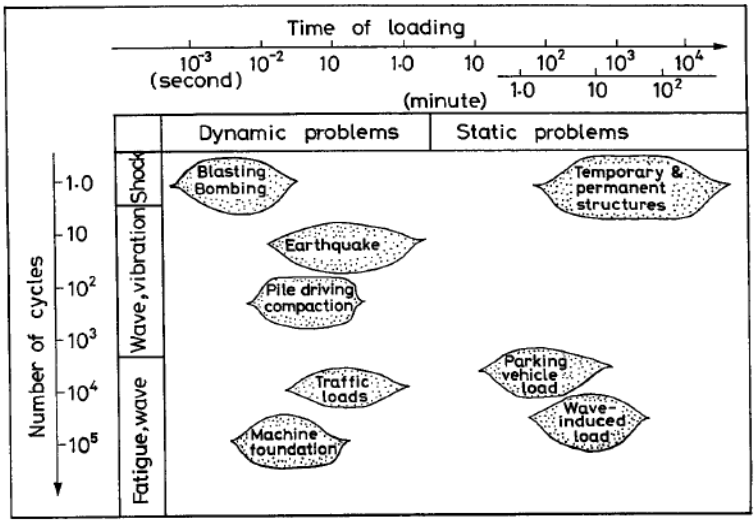

Figure 2.16 Classification of dynamic problems (Ishihara; 1996)

The influence of loading frequency on soft clay behaviour is not well understood. Some published studies show that both the accumulated pore pressure and shear strain induced by cyclic loading increases with the reduction in loading frequency (Matsui et al., 1980; Procter and Khaffaf, 1984; Wang et al., 1998). However, Ansal and Erken, (1989) and Hyde et al., (1993) reported different results, indicating that frequency has negligible influence on cyclic strength and deformation of soils.

2.7.2.2 Stone column studies under dynamic loading

Stone columns have been used to provide the efficient support for different type of foundations in different soils. They have been used to support infrastructure projects, where dynamic loading is imposed such as railway and road embankments. Stone columns also have been used to mitigate liquefaction induced by earthquakes, by increasing the density of the surrounding soil, allowing drainage, which controls the level of pore water pressure under the foundation. Also the presents of the stone column will increase the total load carrying

capacity and at the same time the stress level on the surrounding soil will decrease (Munfakh, 1984; 1997; Van Impe et al., 1997; Raju, 2003; Adalier and Elgamal, 2004).

Liquefaction mitigation

Liquefaction occurs in loose to medium dense, saturated soils with fairly uniform grain size distribution, covering the silty sandy range. In this soil condition, the dynamic forces imposed by earthquake lead to a rearrangement of the grain structure to a denser state. Therefore, if the drainage is insufficient, pore water pressure will increase and shear resistance of the soil will reduce (Seed and Booker, 1977; Salahi et al., 2015).

Priebe (1998) presented a method for evaluating the potential impact of liquefaction with stone columns. This method is similar to some extent to the design of vibro replacement in static condition which was reported by him in 1976 and 1995.

In the dynamic condition, in order to be more realistic and to simplify the problem, Priebe (1998) considers deformation of soil with the constant volume to calculate with Poisson's ratio μ_s = 0.5. In this method, the improvement factor n_0 is determined using some simplifications and approximations shown in Figure 2.17

$$n_0 = 1 + \frac{A_c}{A} * \left[\frac{1}{K_{ac} * \left(1 - {}^{A_c}/_{A}\right)} - 1 \right] \qquad 3.14$$

$$K_{ac} = tan^2 \left(45^o - {}^{\emptyset'_c}/_{2} \right) \qquad 3.15$$

Where: A is the area within the compaction grid; A_c is cross section of stone column; and $\emptyset'_c$ is friction angle of column material.

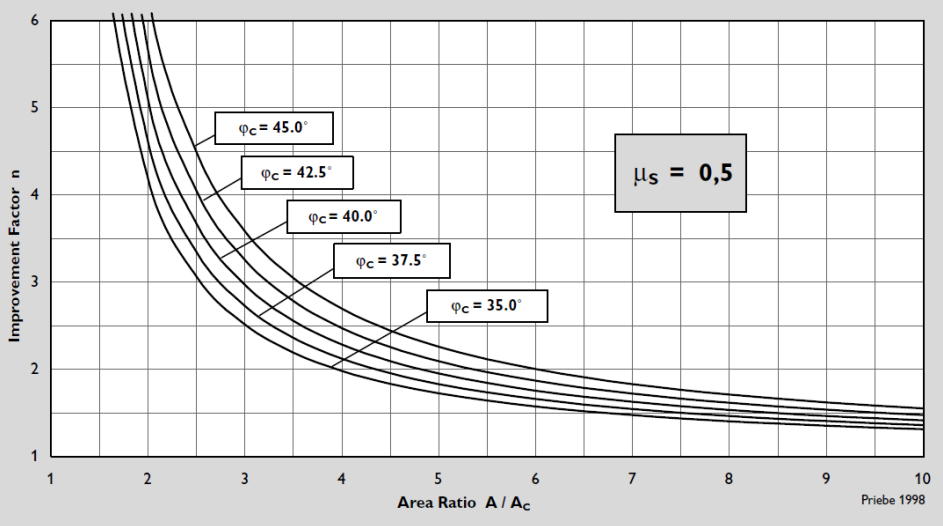

Figure 2.17 Design chart for vibro replacement (Priebe; 1998)

Baez and Martin (1992) reviewed experimental data on the use of stone column for earthquake liquefaction mitigation and indicated that a linear mechanism of consolidation is valid only if the pore pressure ratio remains below 0.5. In addition, they noted that pore pressure within the gravel drain is not constant, contrary to the assumption that they remain essentially unchanged.

A case study presented by Rudolph et al. (2011) looked at the effectiveness of using rammed aggregate piers (RAP) in mitigating the liquefaction potential in a site containing artificial fills over liquefiable sandy clay soils; and a groundwater level was approximately 3.4 meters below ground surface. RAP used had a 0.40 meter diameter, 8.5 meters depth and spaced at 2.1 meters centre to centre. The study focused on the densification of the soil surrounding the RAPs. pre- and post-RAP CPTs measurements were used to calculate the Liquefaction Potential Index (LPI) of the matrix soil and residual liquefaction and seismic settlement potential, as it relates to tolerable settlement of the constructed project.

Their results indicated that using rammed aggregate piers improved the soil properties of the site and has been effective at mitigating liquefaction potential to acceptable levels, for example, within the spread footing area, the reduction in LPI from the pre-RAP CPT versus post-RAP CPT shows a reduction from very high risk (LPI of approximately 17.8) to low risk (LPI of approximately 3.2).

Rollins et al. (2006) presented a case history in which prefabricated vertical drains and stone columns were used in combination to provide treatment for a 4 meters thick layer of liquefiable silty and sandy silt. They suggested that this method can only be suitable for the soils with fines percentage lower than 20%, otherwise less effectiveness of this method will be achieved. Also they reported that using stone column together with wick drain will significantly improve the penetration resistance by an average of 94 %, where the average $(N_1)_{60\text{-}cs}$ increased from a pre-treatment value of 17 to an average post-treatment value of 33.

Embankments:

Building embankments on soft clay soils is usually a very challenging geotechnical task due to the potential of bearing failure, excessive settlement, and local and global instability under dynamic load (Mitchell and Jardine, 2002). Vibro stone column is one of the most commonly adopted soil improvement method, it has been utilized to increase the bearing capacity and reduce the settlement of superstructures (Raju, 2003).

Kempfert et al., (1999) investigated the bearing and deformation behaviours of a geotextile encased sand column foundation at area ratios of 4; 12 and 16 % under static and cyclic using both small scale models with scales of 1:6.5; 1:11.5 and 1:13 and full scale models with scale of 1 : 1. The cyclic loading was divided into two stages as shown in Figure 2.18, the first sequence was simulating an embankment with low height (i.e low preloading pressure (25

kPa) and high cyclic stresses expected on the soil (62.4 kPa)), whereas in the second cyclic loading sequence a deep embankment was simulated by applying a low cyclic stresses with an amplitude of 30.5 kPa and high preloading pressure 100 kPa). At the end of the cyclic loading stages, the sample was subjected to increment of static loads to failure.

Results showed that at the same level of stresses the system developed a higher settlement during the cyclic loading compared with the static; also they indicated that during the first loading sequence the settlement was developed very quickly in comparison with the second loading sequence. They showed that at a constant Area ratio of 12 %, 100 kN/m^2 of loading stress and a scale model of 1:6.5, using a geotextile coated sand columns can reduce settlement by more than 30 % compared with a non-coated columns.

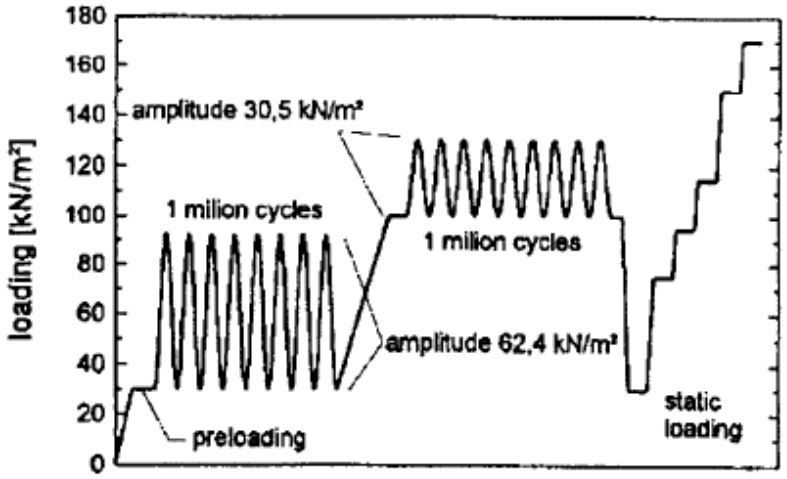

Figure 2.18 Cyclic loading sequences for railway embankment (Kempfert et al., 1990).

Kolekar et al. (2011) presented results from an experimental study investigating the behaviour of stone columns under repeated loading. The cyclic test consists of two stages, in stage one 35 % of the static load failure was applied in a form of sinusoidal wave at a frequency of 0.1 Hz for a number of cycles of 500, whereas in the second stage the load was increased to about

100 % of the load at the static failure. The study was focused on the vertical stiffness ratio. Kolekar et al. (2011) claimed that the stiffness ratio was increased dramatically (from 7 to 80 kPa/mm) by moving from stage one to stage two loading condition and suggest that the first loading stage compacted the column making it more dense, however, they defined the stiffness ratio as the ratio between the change in the vertical stress to the average vertical settlement and as the deformation is much smaller in stage one compared with that in stage two the material stiffness should be larger than that in the second stage.

Fatahi et al. (2012) employed a finite element model using PLAXIS to assess the relation between the column position beneath the train track and overall settlement of the ballast rail formation. The study also includes the effect of using geogrid reinforcement (where two layers of geogrid were placed at the interface between the subgrade and sub-ballast; and sub-ballast and ballast). The model geometry considers the typical track cross section with concrete sleepers as recommended on the NSW rail network (i.e. layers depth from top to bottom including sleeper, ballast, sub-ballast, are 150, 300 and 150 mm). The subgrade layer depth was assumed to be 10 m and the gauge length of the track was 1.4 m. Also train load was considered as 125 kN/m. Stone columns (1 m diameter) were arranged in rectangular grid pattern at with a spacing of 1.5 m along the rail track.

Results indicated that the overall settlement was reduced by the presence of stone columns spaced more closely at the centre of the track and not just under the rail (i.e. when the offset distance of the columns from the track centreline increases, the maximum horizontal displacement of the improved sub-grade also increases). Also indicated that the optimum column pattern will occur, when stone columns just overlap in the cross section and located right in the centreline of the track.

In addition, Fatahi et al. (2012) showed that the use of stone columns (no geogrids reinforcement) was less effective in reducing vertical settlements than geogrids only (no column), when distance of columns from the centre line exceeds 1 m. Furthermore, the use of two stone columns with geogrids

has limited benefits over the use of just geogrids when the distance of columns from the track centreline is greater than 1.6 m

2.8 Concluding Remarks

Soft clay deposits usually have a low bearing capacity, low permeability, and high compressibility. Thus it is important that these soils receive sufficient improvement before construction activities commence. Whilst there are a range of ground improvement techniques available, the use of stone columns is still regarded as one of the most popular and effective techniques. Stone columns provide an adequate level of improvement to soft soils by increasing its shear strength, reducing excessive and differential settlement whilst speeding up the consolidation progress by shortening horizontal drainage paths. Thus, it has been successfully adopted for projects such as highway embankment, industrial and residential structures.

Over the last three decades a considerable amount of research has been conducted to investigate the behaviour of stone column in soft soils. This chapter reviewed different aspects (i.e. critical column length, area replacement ratio, surrounding soil strength, internal angle of friction of the column material, different column material, and column mode of failure) that have been examined by authors to identify their influence on the behaviour of the stone column. In addition, this chapter discussed design approaches and construction methods that are commonly adopted. Almost all the previous study parameters mentioned above were based on the assumptions that the external loading is applied monotonically with a constant strain rate during the whole duration of the test. However, in many engineering projects, such as tank filling and discharging, highway embankments, ocean banks, etc., the surcharge loading is not applied instantaneously, but changes with time. Therefore, it must be

acknowledge that the exact behaviour of foundation on unimproved soft soil and on stone column/ soft soil composite is not fully understood.

high demands for high speed railway upgrade became a topic of discussion. Modern railway infrastructure demands have increased not only to provide a high level of performance in terms of settlements and stability of the railway track but also to reduce maintenance cost. In areas where loose or soft cohesive deposits are found, ground improvement methods are often required to ensure the required level of performance. Therefore, is it still viable to consider stone column as one of these methods?

Bulging or stone column expanding under applied load is important to understand the general behaviour of vibro stone column foundation, whilst some researchers have studied this topic under the application of static loading, the question here is would a column bulge in the same way if the loading sequence was changed (i.e. cyclic loading)? In addition to this, what are the implications for the threshold stress such improved soils can carry when compared to the static stress failure? And what is the influence of the loading frequency on the overall behaviour of improved soils?

The current research was undertaken in an attempt to investigate the above questions and to provide a better understanding to the behaviour of stone column under cyclic loading application.

CHAPTER 3

METHODOLOGY

3.1 Introduction

As noted in the previous chapter, laboratory investigations have played an important part in development of vibro-stone column technique. Findings of laboratory studies were advanced trough full scale trials. Thus, mindful of the cost of full scale trials; and in order to further advance the development of stone columns for cyclic loading a laboratory investigation was undertaken. This study includes investigation of behaviour of stone columns under both static and cyclic loading.

Properties of material used together with both the description of apparatus used and procedure are described in this chapter. It also includes a programme of the laboratory investigation undertaken.

3.2 Materials

This laboratory scale investigation focused mainly on the fundamental mechanical behaviour of stone column foundations subjected to cyclic loading. Twenty two laboratory based studies (see Table 3.1) were reviewed in order to identify best practice and to identify suitable materials for both the stone column construction and that for the surrounding soil. It was found that over 50% of the studies were based on Kaolin clay bed because of its high rate of consolidation compared to that of other fine soils derived from natural deposits. It could also be used to produce high quality repeatable samples as Kaolin is a processed clay. In terms of stone column construction, crushed rocks were found to give the highest angle of internal

friction (over 40^o) and were used by about 50 % of the researchers. Others used sand and river gravel. Therefore a crushed basalt and kaolin clay were chosen to simulate the column and the clay bed materials.

Table 3.1 Materials used in previous studies

	Column material	Surrounding material	φ' (^{o})	c_u (kPa)	Reference
1	Leighton buzzard sand	Kaolin clay	35	19	Hughes and Withers (1974)
2	River gravel	Grey silty clay	38	22	Hughes et al. (1975)
3	Gravel	Boulder clay	-	4.4	Greenwood (1975)
4	Uniform gravel	Boulder clay	47, 51, 53	30	Charles and Watts (1983)
5	Quartz	Kaolin clay	-	14.4-19.1	Barksdal and Bachus (1984)
6	Sand/gravel	Bangkok marine clay	35, 43	20-45	Bergado and Lam (1987)
7	River sand	Silt	38	-	Juran and Guermazi (1988)
8	Loch Aline fine sand	Kaolin clay	30	-	Hu (1995).
9	River sand	-	40.5	-	Rajagopal et al. (1999)
10	Stone	Ash/ clay	45	40	Watts et al. (2000)
11	-	Kaolin clay	35	28	Sivakumar et al. (2004)
12	Crushed rock, Quarry waste, Crushed concrete	Transparent clay-type material, Kaolin clay	51, 46, 39	17.5-21.5, 32	McKelvey (2002)
13	Coarse sand	Sand/clay	44	-	Ayadat and Hanna (2005)
14	Sand/gravel	CH	38, 49	12	Kim and Lee (2005)
15	Crushed basalt	Kaolin clay		35	Black et al. (2006)
16	Crushed limestone	CL clay	43	30	White et al. (2007)
17	stones	CH	43	7, 14, 30	Ambily and Gandhi (2007)
18	Granite chips	Lake clay	41	2.5	Murugesan and Rajagopal (2008)
19	Commercial sand	Kaolin clay	35	5	Gniel and Bouazza (2009)
20	Quartz	Kaolin clay	33	-	Najjar et al. (2010)
21	Crushed basalt	Kaolin clay	35	-	Black et al. (2011)
22	Crushed basalt	Kaolin clay	35	-	Sivakumar et al. (2011)
23	Gravel	Kaolin clay	-	41	Cimentada et al. (2011)
24	Gravely sand	Oxford clay	-	16	Madun et al. (2012)
25	Aggregate	Soft clay	41	5	Vekli et al. (2012)
26	Sand	Clay	38-45	10.5-16.5	Hanna et al. (2013)
27	Hostun sand and Gravel	Kaolin clay	-	-	Frikha et al. (2014)
28	Stone chips	Kaolin clay	-	6-6.8	Ali et al. (2014)
29	Aggregate	Pulverized clay	45	54, 15	Mohanty and Samanta (2015)

Physical properties of Kaolin clay were determined in accordance with British Standard BS 1377 (1990) (The tests data available in Appendix A). These properties are summarised in Table 3.2.

Table 3.2 Physical properties of Kaolin clay

Material	Property	Value
Kaolin clay	Specific gravity	2.63
	Liquid limit (%)	56
	Plastic limit (%)	27
	Plasticity index (%)	29
	Undrained shear strength (kPa)	12
Crushed basalt aggregate	Particle size: (mm)	1.18-2.0
	The peak internal angle of shearing, ϕ (degree)	48
	Specific gravity	2.70

3.3 Physical Properties of the Model Stone Column and Surrounding Soil Material

3.3.1 Index Properties

Both the Liquid and Plastic limits for the Kaolin clay were determined according to the procedures in Clauses 4.3 and 5.0 of BS1377: Part 2 (1990) (BSI, 1990). Liquid Limit of Kaolin was 56%, and the Plastic Limit was 27%. These values are considered typical for Kaolin clay (John, 2011).

3.3.2 Particle Size Distribution

The particle size distribution of the Kaolin clay material was determined, using a hydrometer in accordance with Clause 9.5 of BS1377: Part 2 (1990) (BSI, 1990). Results showed that about of 50 % of the material was in the fine silt range and 50 % was clay (sub 0.002 mm).

The particle size distribution of the crushed rock was determined by using a dry sieve analysis method in accordance with Clause 9.3 of BS1377: Part 2 (1990) (BSI, 1990), all the material

used was between 1.18 and 2 mm. Typical grading curves for both the Kaolin clay and the crushed basalt are shown in Figure 3.1.

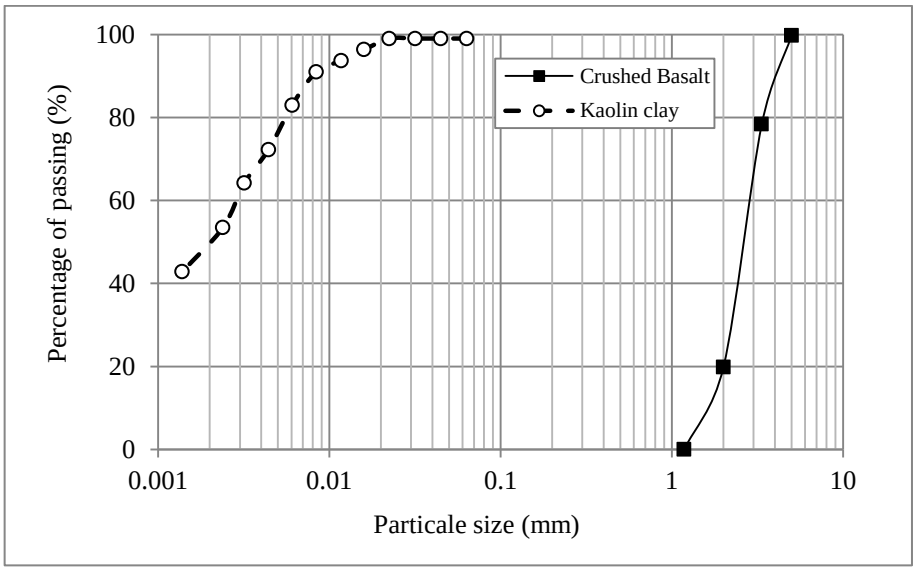

Figure 3.1 Typical particle size distribution of Kaolin clay and crushed basalt

3.3.3 Specific Gravity

Specific gravity was determined in accordance with Clause 8.3 of BS1377: Part 2 (1990) (BSI, 1990). The specific gravity of the Kaolin clay ranged from 2.61 to 2.65 with an average of 2.63, and the values for crushed rock used to form the column, ranged from 2.70 to 2.73 with an average of 2.71. These values fall within the range typical of these material types.

3.3.4 Dry Density/Moisture Content Relationship of Kaolin Clay and Crushed Aggregate

The compaction test for Kaolin clay was conducted using a 2.5 kg rammer compaction falling from 300mm (light compaction method). The test was carried according to BS 1377: Part 4 (BSI, 1990). The dry - moisture content relationship is given in Figure 3.2. The maximum dry density was estimated as 1410 kg/m^3 which occurred at an optimum moisture content of 29%.

The maximum density of the crushed aggregate was determined in accordance with the procedure explained in BS 1377: Part 4. 3 kg of saturated crushed materials were compacted in a mould under a controlled water level using a vibrating hammer. This procedure was repeated three times to ensure the results repeatability. The maximum density was found to be 1892 kg/m^3 with variation of ± 1% which considered acceptable.

The minimum density was determined by pouring the material from 0.5 m height into the mould without disturbing the soil (BSI, 1990). The minimum density for the crushed basalt was 1494.5 kg/m^3 with less than 0.01kg/m^3 variation.

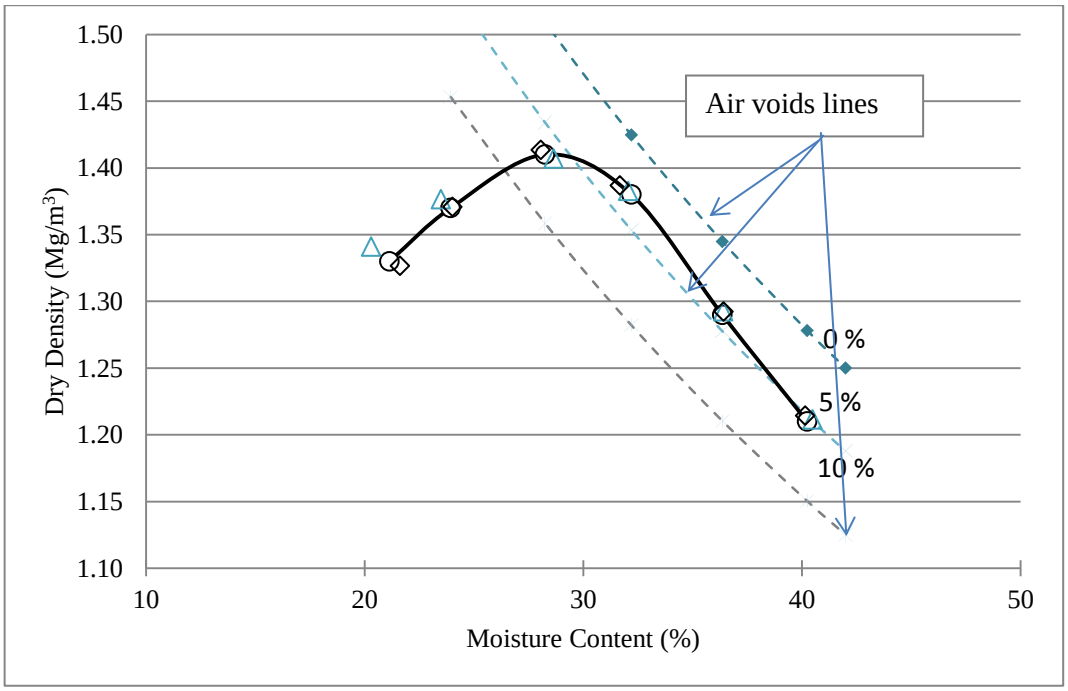

Figure 3.2 Dry density-water content relationship for Kaolin clay

3.3.5 Shear Strength

In order to simulate very soft ground that has shear strength below 15 kPa, a series of quick undrained triaxial tests and hand vane shear tests were conducted on compacted Kaolin clay, at different water contents ranging from 30 % to 48 %. Shear strength of soil ranged between

53 kPa and 5 kPa for moisture content of 33 % to 48 % respectively. Correlation between the water content and undrained shear strength is shown in Figure 3.3. From these test result, it can be concluded that soil shear strength of 15 kPa can be achieved with a water content of 42%.

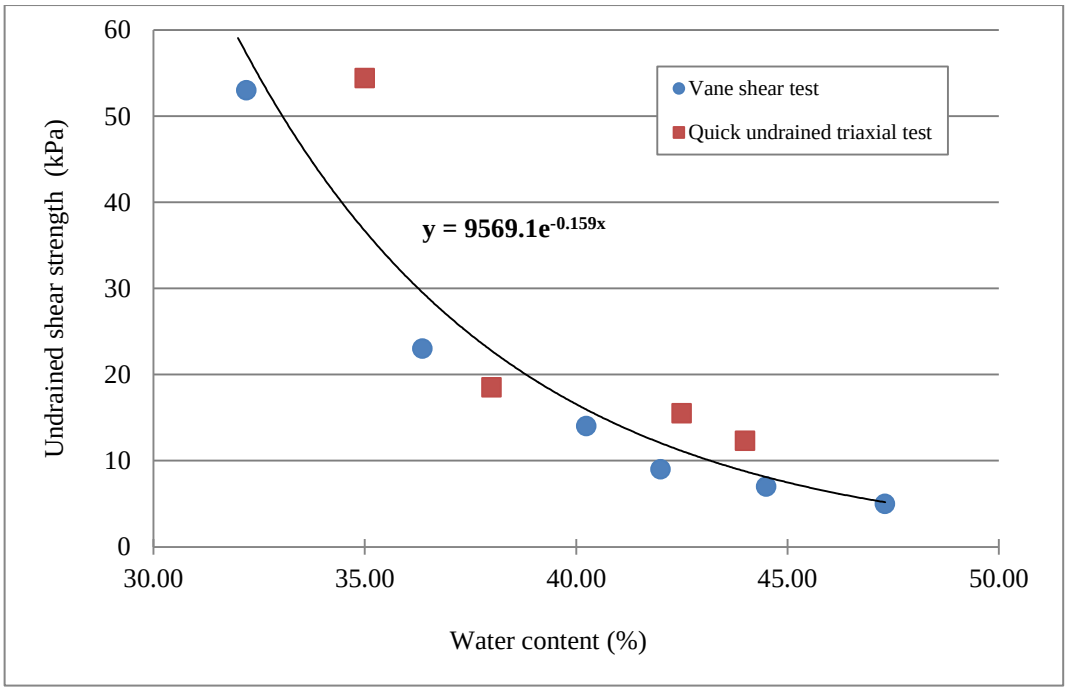

Figure 3.3 Relationship between undrained shear strength and water content for Kaolin clay

Undrained shear strength can be related to liquidity index of soil (Skempton, 1957), as shown in Figure 3.4, this relationship generally follows the following trend.

$$LI \cong 1 - 0.192 \ln c_u \qquad 3.1$$

Vardanega and Haigh (2014) examined a database of 641 fall cone tests in different soil types in order to determine a statistical relationship between the undrained shear strength and the liquidity index. Although they used a different method (fall cone tests) to carry out the undrained shear strength of the soil, a considerable agreement between their statistical model (Eq. 3.2) and the one presented in the current study was found.

$$LI \cong 1.12 - 0.226 \ln c_u \quad 3.2$$

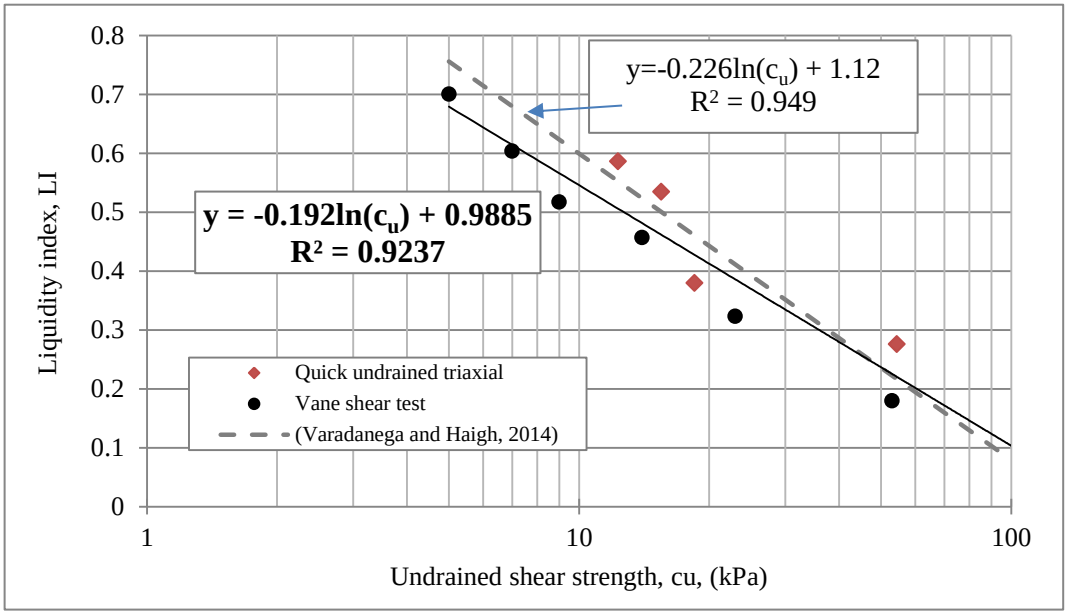

Figure 3.4 The undrained shear strength – liquidity index relationship

A series of direct shear tests were carried out on dry and wet samples of crushed basalt. In order to simulate the condition where stone columns are installed in wet ground, the crushed basalt was left to soak in water for 24 hr before testing. Each test was repeated three times to ensure result repeatability. All tests were performed in a 100 mm x 100 mm direct shear box, under vertical stresses of 25 kPa, 50 kPa, 100 kPa and 200 kPa. These normal stresses were chosen to represent the typical application in the field. The material was placed into the shear box in three layers; each one was compacted using a small wooden block. The average density of the compacted material was 1540.6 kg/m^3, with variation of about ± 20 kg/m^3. Shearing rate of 1 mm/min was used for all the tests, as suggested in the BS 1377: Part 7 (BSI, 1990), for the aggregate material. During the test, horizontal; vertical displacements and the shear force measurements were recorded. Typical test results are presented in Figure 3.5.

The general behaviour of the crushed basalt was followed a typical pattern for dense granular material where by a small initial contraction occurs and is followed by dilation.

The peak value of the shear stress was plotted against the corresponding normal stress in order to determine the failure envelop (see Figure 3.6). for example at 100 kPa effective pressure, under dry condition, the angle of internal friction was found to be 50^{o}, whilst in wet condition the internal angle of friction reduced to 48^{o}.

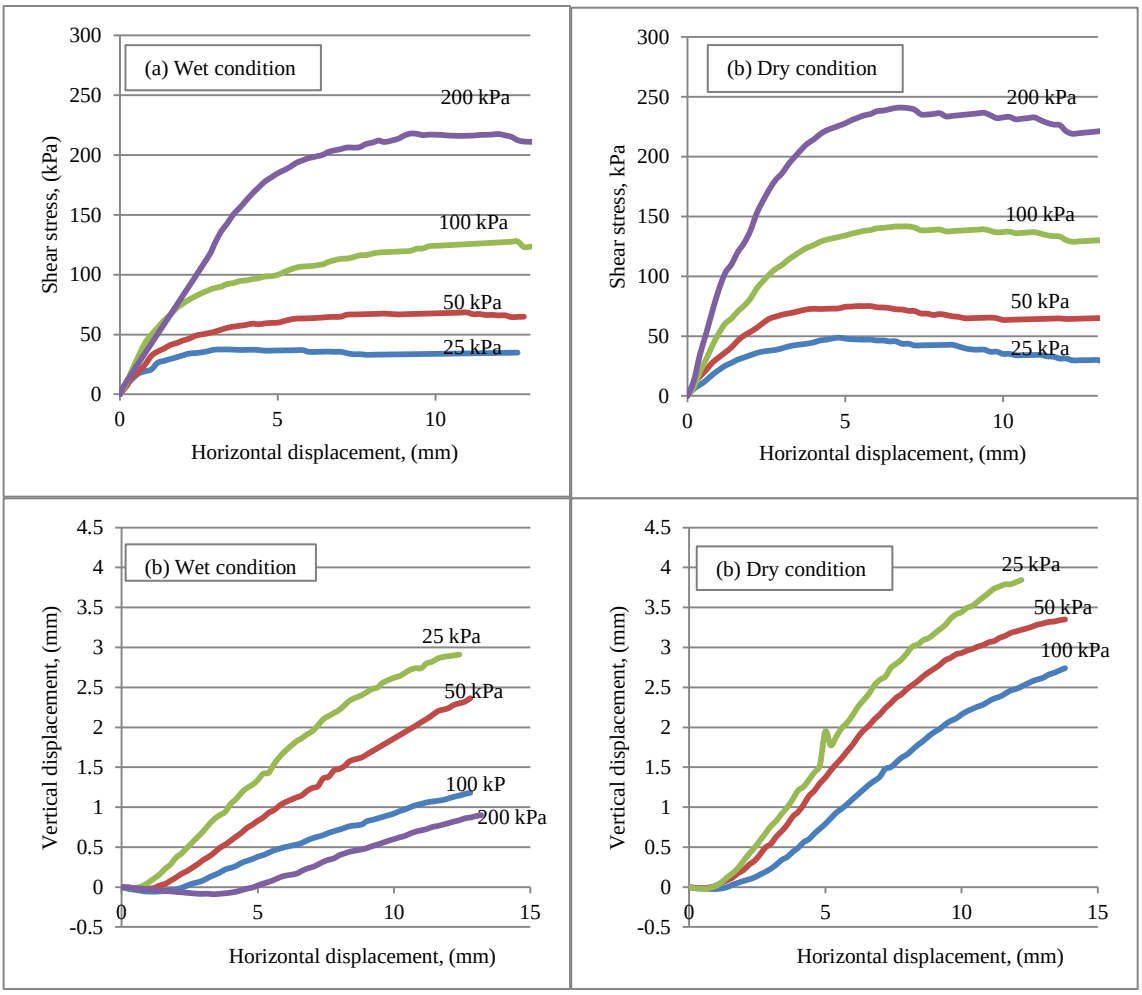

Figure 3.5 Typical stress-strain, direct shear box test (a) wet condition and (b) dry condition

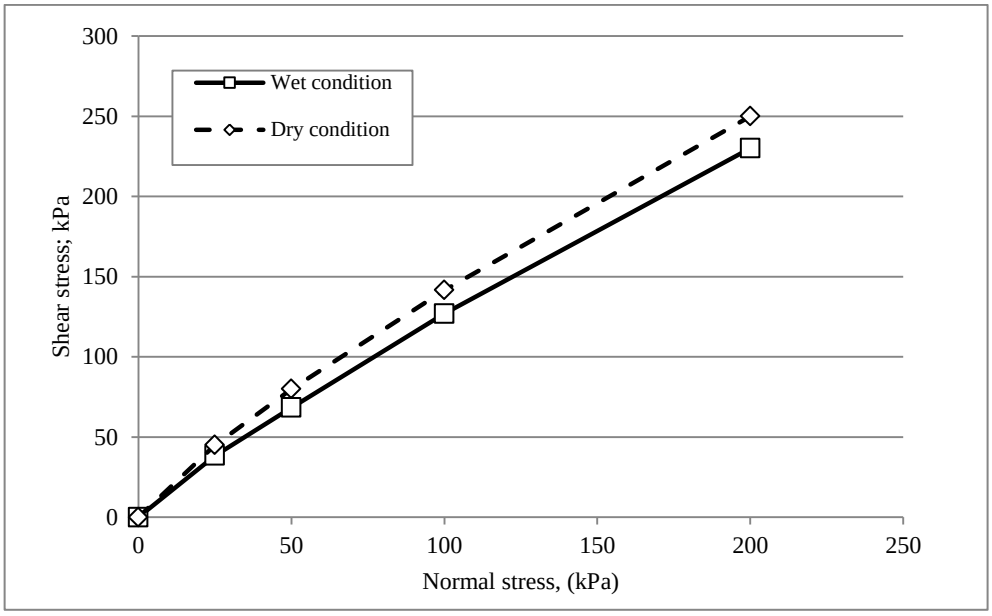

Figure 3.6 Shear stress verses normal stress at peak

3.3.6 Compressibility Properties

In order to determine the primary consolidation behaviour of Kaolin clay within tests, the consolidation time, settlement and required load were needed. One dimensional consolidation tests were carried out using the oedometer apparatus. A small quantity of slurry (1.5 * L.L water content (Head, 1996; Sivakumar et al., 2004b)) was prepared then placed in the 75 mm diameter consolidation ring. Considering the condition of the soil (slurry), the specimens were firstly consolidated under the load of the apparatus hunger only for 24 hour, and then they were monotonically loaded to pressures of 25 kPa, 50 kPa, 100 kPa, 200 kPa and 400 kPa. At this stage the samples were unloaded to 50 kPa then reloaded to 800 kPa. Each pressure maintained for a period of 24 h. During the increment loading period, the settlement of the sample was carefully measured and the coefficient of consolidation, c_v, was determined using Equation 3.3:

$$c_v = \frac{T_v d^2}{t_{90}} \qquad 3.3$$

Where: T_v is time factor of 90% consolidation and equals 0.848;

D is the drainage path length;

t_{90} is the time taken for 90% consolidation.

The square root time method was used to determine t_{90} (Head, 1998). A typical result for the pressure increment 50 kPa to 100 kPa is presented in Figure 3.7.

The relationship between the void ratio and applied consolidation stresses is presented in Figure 3.8. The void ratio, e, at the end of each increment period was calculated using Equation 3.4:

$$\frac{\Delta e}{\Delta H} = \frac{1 + e_0}{H_0} \qquad 3.4$$

where: H_0 is the initial thickness of the specimen;

ΔH is the change in thickness during each loading increment (H_0 - H_1);

Δe is the change in void ratio during each loading increment (e_0-e_1).

e_0 is initial void ratio and can be found using the relationship between the water content and void ratio in the condition of saturated soils,

$$\text{Thus:} \quad e_0 = wG_s \qquad 3.5$$

Where, w is the water content, and G_s is the specific gravity of the clay.

The coefficient of compressibility, m_v, at each pressure increment was determined using the following equation:

$$m_v = \frac{1}{1+e_0}\left(\frac{e_0 - e_1}{\sigma_1 - \sigma_0}\right) \qquad 3.6$$

In Equation 3.6, e_0 and e_1 are the initial and final void ratio respectively; and σ_0, and σ_1 are the initial and final applied stresses.

The coefficient of consolidation, c_v, ranged from 7.8 to 27.2 m^2/minute, whereas the coefficient of compressibility, m_v, ranged between 0.51 and 3.62 (m^2/MN). Both of these coefficient values are comparable with other typical values of normally consolidated clays (Head, 1998). The compressibility and consolidation coefficients for each loading increment are presented in Figure 3.9.

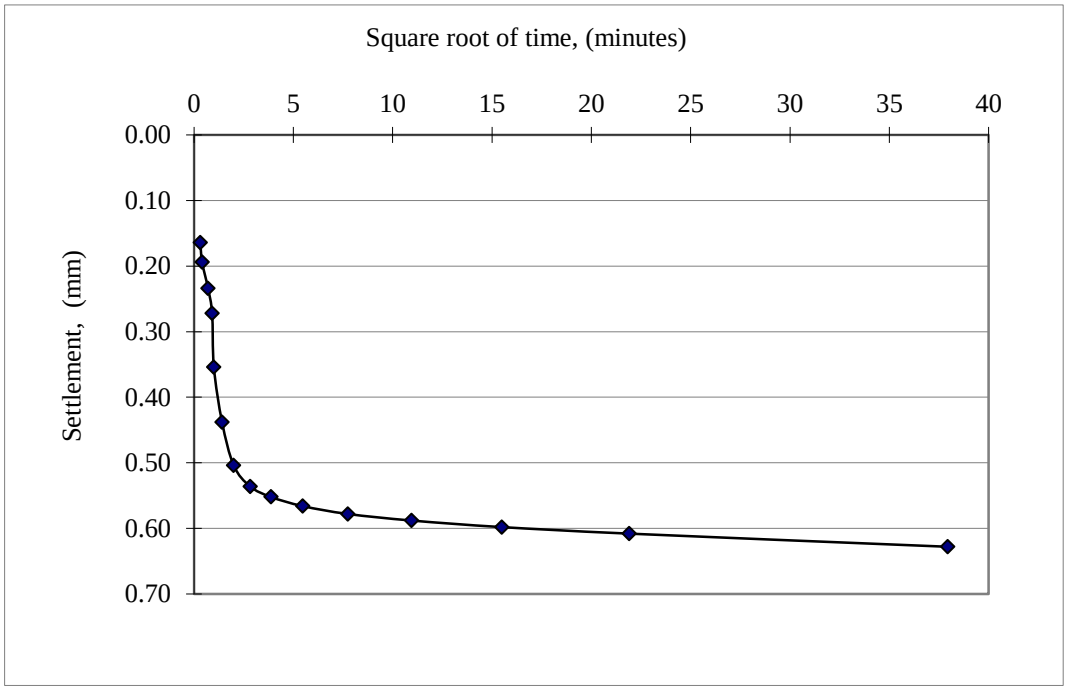

Figure 3.7 Consolidation curve square root of time step 50 to 100 kPa

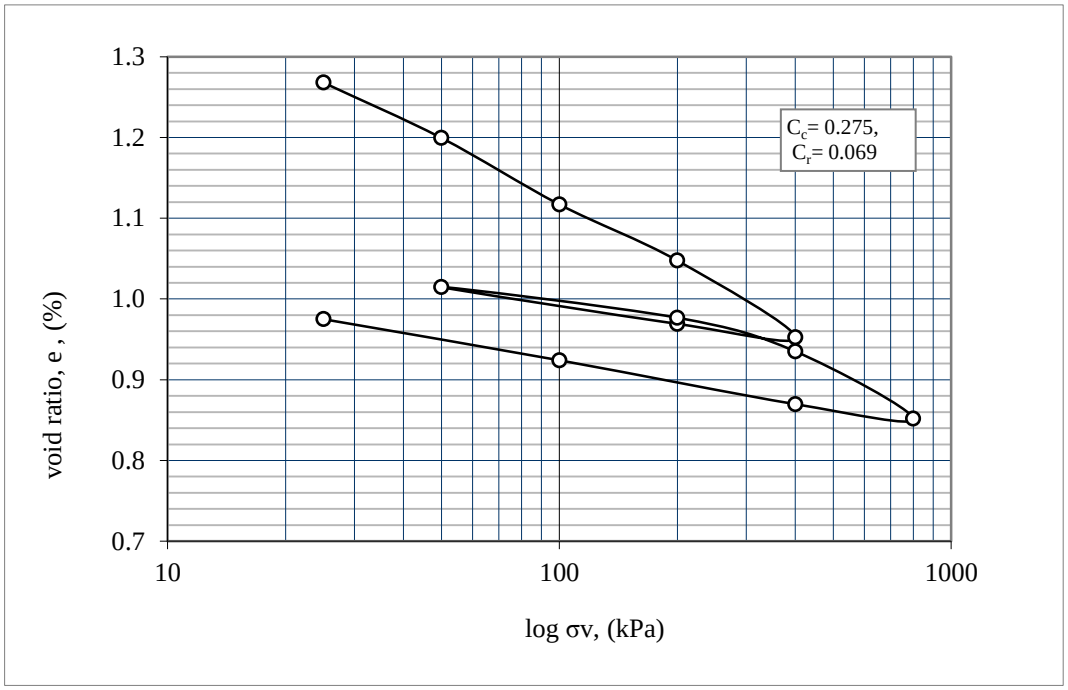

Figure 3.8 Void ratio / pressure increment relationship

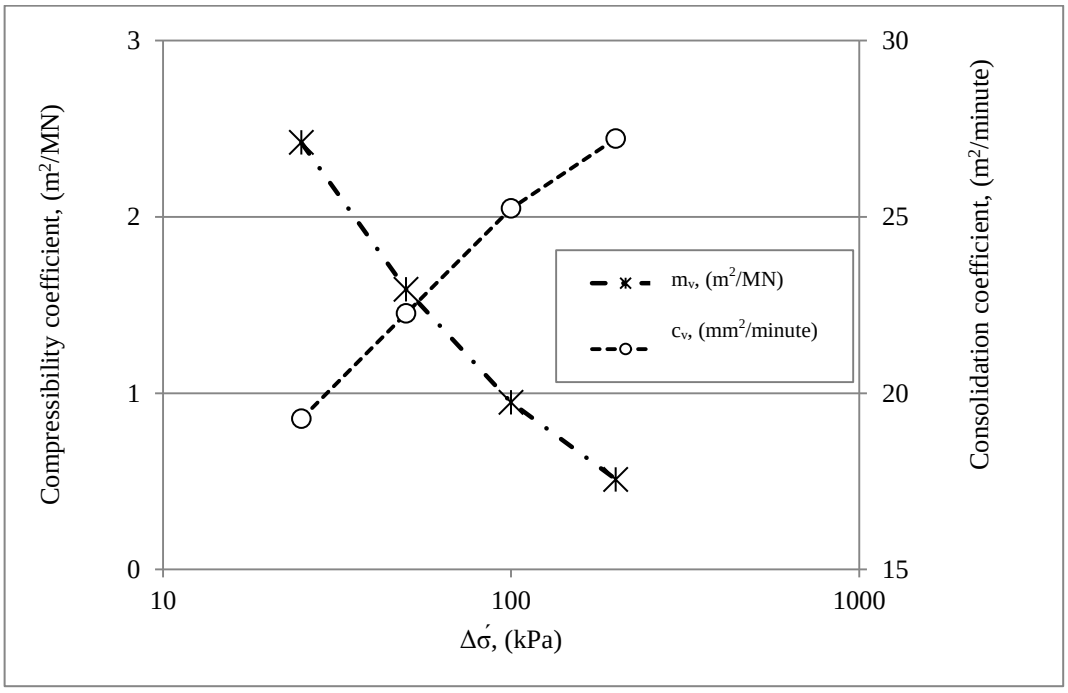

Figure 3.9 Cofficients of consolidation and compressibilty and stress relationship

3.4 Test Requirement and Apparatus Design

3.4.1 Scale Effect

An appropriate scale factor should be selected in order to simulate field situations in laboratory scale test. However, it was not possible in physical model tests undertaken to maintain a suitable scale factor that satisfies completely all the parameter that governs the prototype response. In spite of this, using a geotechnical centrifuge, it may be possible to maintain the prototype stress level (Wood, 2004); however, this approach was unavailable for this current study due to laboratory limitation.

Hu (1995) noted that parameters affecting response of soil-stone column systems and influencing the load and settlement relationship can be divided into two categories of major and minor influence as representing in equation 3.7.

$$q_{ult}/c_u = f_1\left(S/D, L/D, L/d, G_c/G_s, A_s, \emptyset'\right).f_2\left(G_s/c_u, \gamma_s/\gamma_c, d_g/d_c, D_B, \gamma_c/c_u\right) \quad 3.7$$

Where:

S: the spacing between the column and represented by the area replacement ratio A_s

$$A_s = \left(\frac{d}{mS}\right)^2 \quad 3.8$$

c_u: the undrained shear strength of soil

d: the diameter of the footing

L: the length of the column

d: the diameter of the column

d_g: the average particle diameter of stone column material

D: diameter of the unit cell

Ø': the angle of the internal friction of the stone column materials

G_s: elastic shear modulus of the column material

G_c: elastic shear modulus of the clay

Υ_s: unit weight of the column material

Υ_c: unit weight of the clay
m: shape factor which depends on the pattern of columns arrangements.

According to this, some of the main aspects of the field situation such as L/D, L/d, As, and ϕ' were maintained in the laboratory scale testing. It was considered that this could provide an adequate response and would generate high enough quality data so that it can be compared with other studies of similar conditions and would suggest expected behaviour from full scale columns.

On the other hand, adopting the unit cell concept, and using the relationship between area of the column to the area of the treated soil then refer it to the diameter ratio (N) as in equation 3.9.

$$A_s = {}^{A_{col}}/_{A} = \left[{}^{d_c}/_{d_e}\right]^2 = {}^{1}/_{N^2} \qquad 3.9$$

Where: A_{col} and A is the area of the column and the soft soil area, respectively. Typical value of this ratio is 5 to 30%. This range results in approximate values of diameter ratio (N) between 2 and 5. This shows an agreement with (Hughes and Withers, 1974) indicated that the column can improve the strength of the surrounding soil that falls within a diameter of 2.5 times the diameter of the column. Also Bowels (1988) identified the failure zone extended radially to a distance of 1.5 times the diameter of the foundation and over a depth of approximately 2 times the diameter of the column.

To satisfy the above conditions and taking account of the facilities available, the maximum size of 100 mm diameter foundation could be used. Therefore, N could be used as 3.5. This leads to the diameter of the column of 28 mm. In terms of area replacement, these values

correspond to replacement rates of 7%. With this, assumption the horizontal scale of the model from reality was about 1 / 20.

3.4.2 Geometrical Dimension of Column

The diameter of the stone column (28 mm) and the spacing (100 mm) were selected on the basis of a pre-selected area replacement ratio of 7 % as explained before.

The length of sample was determined by taking account of the typical value of length/ column diameter ratio (L/d), which is generally between 6 and 20. This ratio may reduce to 4 in case of an isolated stone column (Hughes and Withers, 1974) .

After selecting the diameter and length of stone column, it is important to select an appropriate particle size of material to be used. Typical ratios of column diameter to average particle diameter range from 20 to 40, thus granular materials of 2 mm particle sizes were adopted. The stone column was subsequently tested in two sizes of clay beds as described below.

Model I: A single 28 mm diameter stone column was installed in a clay specimen of 100 mm diameter and 200 mm height and subjected to triaxial loading. This set simulated of constant pressure surrounding the clay. This approach was first used by Hughes and Withers (1974) and later by Sivakumar et.al. (2004).

Model II: The test is conducted on a single column of 28 mm diameter constructed in clay bed of 300 mm diameter and 300 mm height. The column was loaded through a 70 mm diameter steel plate which was 2.5 times the diameter of a single column. The lateral dimension of the tank (300 mm) was chosen according to the minimum free distance between the side-line of the column and the wall of the tank.

The values of the main parameters relating to columns used in the field and those used in this study are summarised in Table 3.4. Comparing the typical stone column diameter to the model diameter implies the scale factor of the model column was about 1/20.

Table 3.4 Typical and model values of stone column parameters

Parameter **Unit**	**As** **(%)**	**L** **(m)**	**d** **(mm)**	**L/d**	**dg** **(mm)**
Typical values	5-35	Up to 20	600-1200	6-20	20-50
Model I	7	0.2	28	7.14	2
Model II	16	0.3	28	10.7	2

3.4.3 General Test Requirements

The test programme involved application of both static and cyclic loading application, in two models (3.4.2). Investigating the behaviour of soft soil /stone column system under cyclic loading requires examining the influence of loading frequencies, in addition to the effect of the cyclic stress ratios. Therefore, in order to fulfil this aim, the test apparatus and procedures was developed and described below:

- The clay bed for all tests was prepared by consolidating slurry with an initial moisture content of 84 %. This allowed for a uniform and homogenous soil sample in which stone columns were constructed.
- Target strength of the clay bed was 12 kPa.
- In order to eliminate the boundary effect of the tank walls on the specimen, a tank diameter of 300 mm was used (i.e. 4.25 times the model footing diameter (70 mm).

3.5 Sample Preparation

The clay bed was prepared by placing kaolin slurry into five plastic tanks. Two tanks were designed to prepare 100 mm triaxial specimens. The containers were 100 mm in diameter and 400 mm height and the set up was shown in Figure 3.10. Pressures were applied by adding weights to a load hanger connected to a piston in top of the slurry in four stages giving pressures equivalent to 12, 25, 50, and 100 kPa. The piston was perforated to allow water to escape from the specimen.

Three tanks measuring 300 mm in diameter with 550 mm depth were used to create the larger specimens of 300 mm diameter by 300 mm height and the set up was shown in Figure 3.11.

For safety reasons the large quantity of weights that would be necessary in order to generate the required pressure could not be used. Therefore, loading was applied via hydraulic jack attached to a pump connected to air compressor. Proving rings were fitted between the hydraulic jack and the perforated plate placed on top of the slurry sample to monitor and control the amount of loading. Two dial gauges were placed on top of each sample to monitor and record the settlement of the sample as consolidation progressed, also to recognise a possible plate tilting at an early stage.

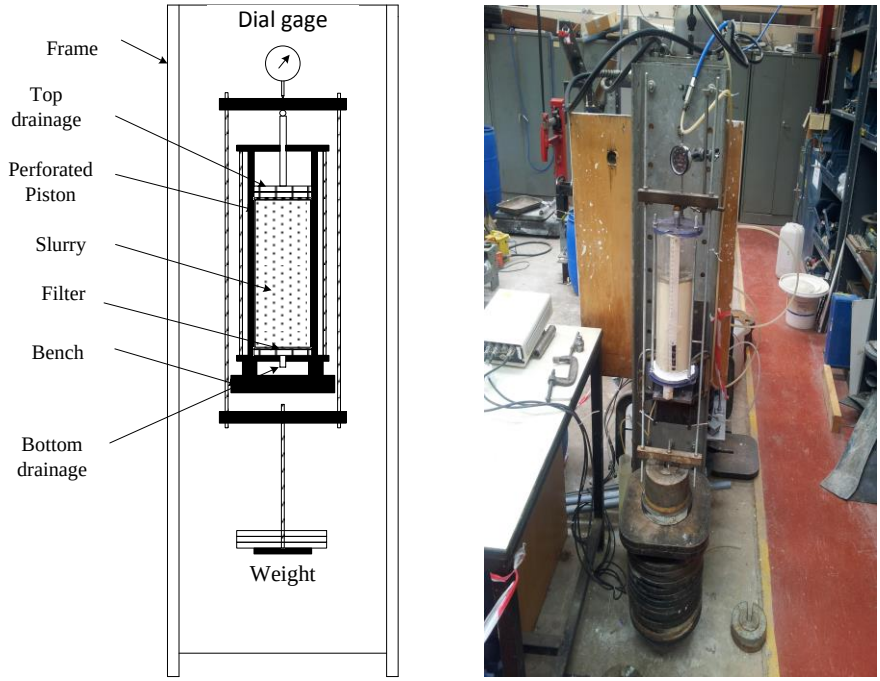

Figure 3.10 Model I consolidation process for 100 mm dia. Samples

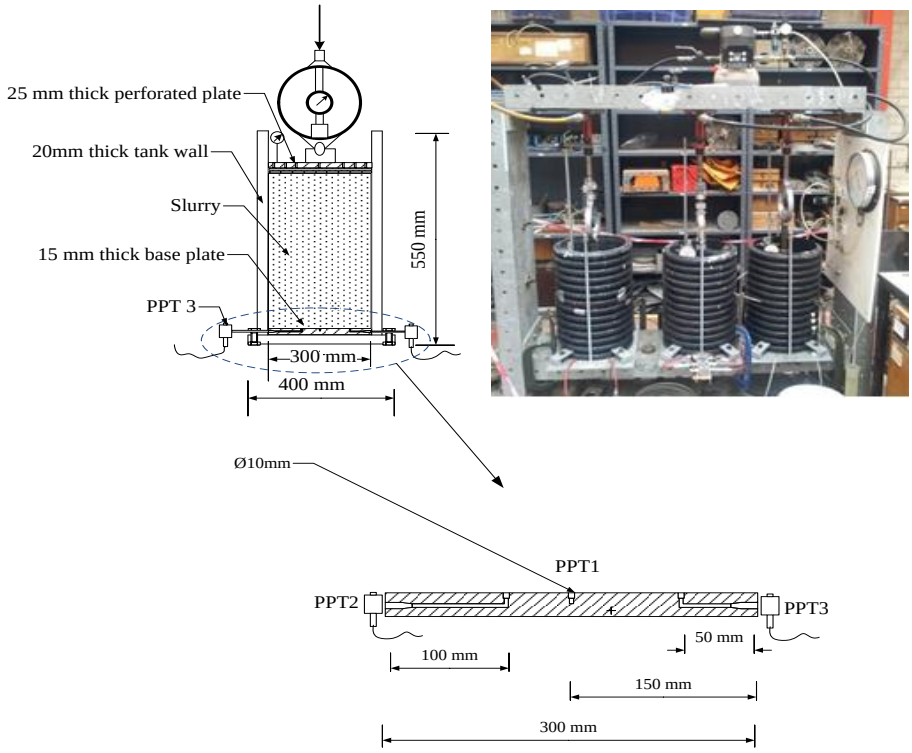

Figure 3.11 Model II consolidation chamber for preparing 300 mm dia. Samples

3.6 Test Apparatus

3.6.1 Cyclic Load Frame

A 50 kN capacity load frame (Figure 3.12) was used to apply both static and cyclic loading. Although it is specified that this machine can provide a range of cyclic loading frequency between 10 Hz and 0.0001 Hz, several trials were conducted to check capacity of the load frame. Loading frequencies adopted ranged from 0.5 Hz to 3 Hz. The minimum applied load that was 0.25 kN with minimum amplitude of 0.1 kN.

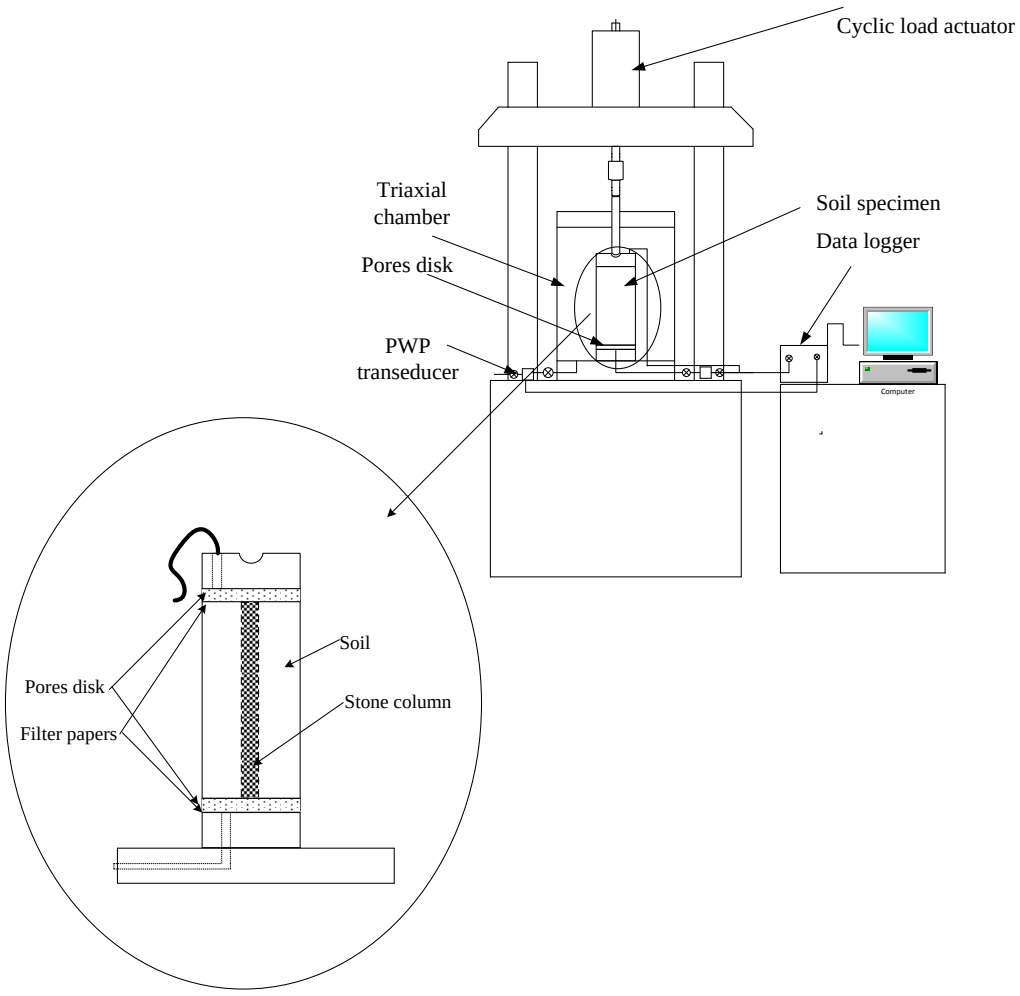

Figure 3.12 Testing equipment

3.6.2 Instrumentation

- Load cell: A 10 kN capacity load cell was used for this study. It was calibrated using SANS electromechanical universal testing machine (CMT 5000 series). A dynamic test was run in this cell three times for both compression and tension, in order to ascertain margins of error, which was found to be less than 1 %.

- Pore water pressure transducers: Three WF17060 (Wykeham Farrance) pressure transducers with 1000 kPa capacity were fitted to the base of the tank for measuring the pore pressures. These transducers were calibrated before each test using a cylindrical triaxial chamber full of water. Compressed air was used to pressurise the water.

- Data acquisition: A logging system supplied by Servocon Digital Control Ltd was used. to control and monitor the load and pressure transducers. The signals were read up to 0.001 accuracy, which was considered acceptable for this research. A logging interval of 0.1 second was used. This leads to a very large number of data, especially for the static loading test which lasted up to 10 hours at 0.03 mm/min. For cyclic loading test of data can was recorded every 10 cycles. The large quantity of data was considered important as it would help to better define the behaviour of specimen under loading.

3.7 Test Variables

Several factors affect the behaviour of soft subgrade soil subjected to train induced cyclic loading. these include load frequency, level of applied cyclic stress and stress condition, and the physical condition of the soil (Brown et al., 1975; Li and Selig, 1998). These are discussed below.

3.7.1 Loading Frequency (*f*)

It has been suggested that loading frequencies and number of loading application have a small influence on the deformation behaviour of the granular materials (Peacock and Bolton, 1968;

Brown and Hyde, 1975). However, effect can be significant in case of soft cohesive soils (Brown et al., 1975; Yasuhara et al., 1982; Zhou and Gong, 2001).

Table 3.5 shows the type of soil and test loading frequency applied by other researchers. This shows that all the cyclic tests were conducted under triaxial conditions with loading frequencies ranging between of 0.1 to 5 Hz to simulate the loading condition of traffic and passing trains. The number of load applications ranged between 500 and 1,000,000 depending on the material.

Table 3.5 Cyclic load testing conditions for previous laboratory investigation

	Material	Test condition					Application	Reference
		Sample size (mm) D X L	Sample preparation	σ_3' (kPa)	Frequency *f*, (Hz)	Number of cycles		
1	clay	100X100	OCR=(2-20)	38-380	10	$1x10^6$	-	(Brown et al., 1975)
2	marine clays	35X87.5	CSR=1		0.1-1		-	(Yasuhara et al., 1982)
3	marine clays	35X87.5	CSR=1	σ_a = 200 σ_a = 75-120	0.1-3	3600-538200	-	(Yasuhara et al., 1992)
4	clay	39.1X80	OCR=(1-4)	110-240	0.01- 1	200-3000	-	(Zhou and Gong, 2001)
5	Ballast	300X600	compaction	1-240	20	500000	High-speed trains	(Lackenby et al., 2007)
6	Kaolin clay	300X600	anisotropic K_0 = 0.6	-	5	3500	PVD installation beneath rail tracks	(Indraratna et al., 2009)
7	Marine clay	-	CSR=1	41	0.01, 0.1, 1	1000	-	(Li-Zhong Wang et al., 2011)
8	Clay	50X100	-	100, 200	0.1, 0.5	400	Traffic loading	(Gu et al., 2012)
9	Silt (ML)	76X152	-	100-250	1	100	Traffic loading	(Ng et al., 2013)
	(25% Kaolin + 75% Kansas River sand)	(2 m × 2.2 m × 2m)	-	-	0.77	100	Subgrade stabilisation	(Sun et al., 2014)
10	Nanjing fine sand	50X200	-	50-150	0.1	10000	Traffic loading	(Cai et al., 2015)

Load frequency of a train, at the subgrade level is related to train speed (v), and carriage length (L), Sekine (1996) developed a relationship to estimate the loading frequency at the subgrade level:

$$f = \frac{V}{3.6L} \tag{3.10}$$

In this study, a sinusoidal loading wave form was used to simulate train movement with loading frequencies of 0.5, 1.0 and 3.0 Hz representing train speed of 35, 70 and 225 km/hr for a typical carriage length of 20 metres.

3.7.2 Amplitude and Dynamic Stress

Based on the depth of ballast and the axle load, there are several theoretical relationships for determining the pressure at the subgrade level. Perhaps the most well-known is the Talbot equation (Selig and Waters, 1994).

$$P_C = \frac{16.8P_m}{h^{1.25}} \tag{3.11}$$

where P_C is subgrade pressure in psi, P_m is the applied stress on ballast in (psi) and h is the depth of ballast in (inches).

Japanese National Railway also used similar formula to estimate the stresses at the subgrade level.

$$P_C = \frac{50P_m}{10+h^{1.35}} \tag{3.12}$$

where P_C and P_m are as defined in equation 3.11 and h is the depth of ballast in cm.

Field observation of dynamic stresses conducted by Yoo and Selig (1979) using a four axle hopper cars each weighing 131 tons, with ballast layer thickness of 300 mm, showed that the maximum stress on the subgrade level ranged between 80 and 110 kPa (Figure 3.13).

Figure 3.13 Dynamic measurement of subgrade stress (Yoo and Selig, 1979)

However, there are other empirical equations where the speed of the train is also taken it account together with axle load. Zhou, (1996) derived an empirical formula to predict the dynamic stress at the subgrade level:

$$\sigma_d = 0.26\,P(1 + \alpha V) \qquad 3.13$$

where σ_d =dynamic vertical stress on the subgrade surface (kPa); P is the axel load of the train (kN); V is the train speed (km/hr) and α is speed coefficient and equals to 0.005, 0.004 and 0.003 for ordinary grade railways speed, quasi-high speed and high speed railway respectively.

Furthermore, field measurements in existing railways in China indicates that the average magnitude of the vertical dynamic stress on the subgrade level for passenger trains is about 46 kPa (Chinese Academy of Railway Science, CARS., 2006). Therefore, for a 225 km/hr train speed and 100 kN axle load the cyclic stress will be about 43 kPa.

A large scale test at the University of Birmingham (unpublished work) included application of 125 kN wheel load applied at 2 Hz for 2 million cycles on rail across three sleepers (moor information include in Appendix G) indicated that the stresses subgrade level were approximately 80 kPa (Figure 3.14) showing good agreement with Yoo and Selig (1979) study.

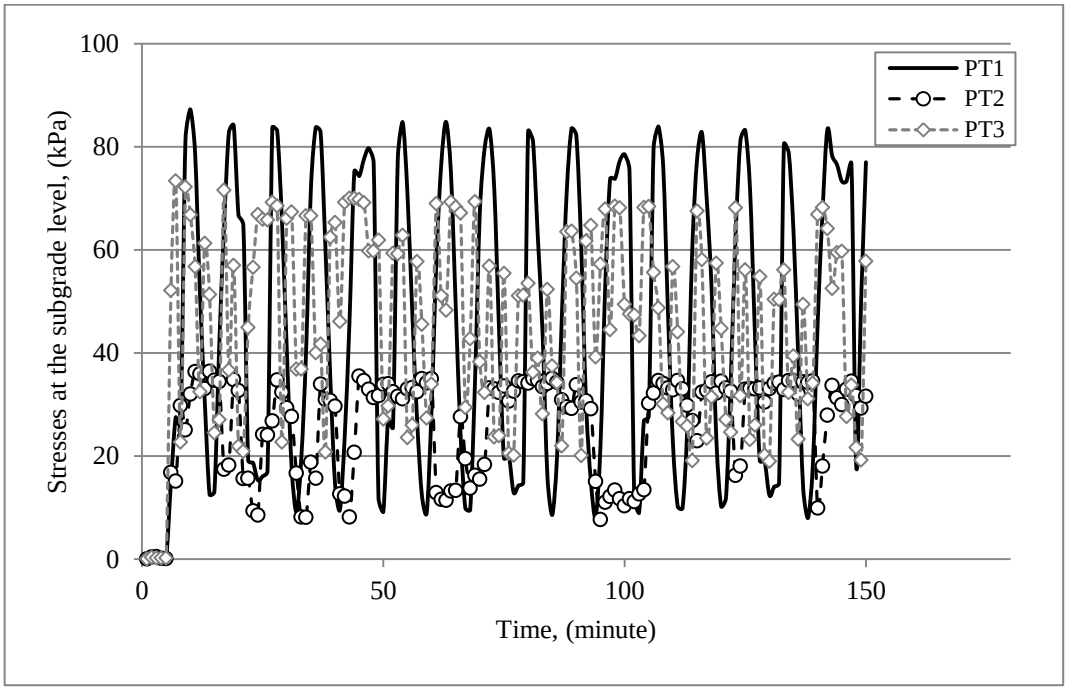

Figure 3.14 Dynamic stresses mesurments at subgrade level (under 300mm of ballast)

Based on the above, cyclic stresses of 50 kPa, 60 kPa and 70 kPa were used in this study. These values are equivalent to a cyclic stress ratio (CSR) of 0.6, 0.7 and 0.8 (CSR = the cyclic deviator stress (q_{cyclic})/ the static deviator stress of reinforced soil at failure ($q_{failure}$)).

3.8 Experimental Procedure

3.8.1 Clay Bed Preparation

3.8.1.1 Mixing process

In order to create homogenous bed of soft clay, Kaolin clay was mixed with water content of 1.5 times the Liquid Limit (i.e. water content of 84 %). A Hobart A-120 mixer with capacity of 12 litres was used for mixing 5 kg of Kaolin with 4.2 litre of de-aired water for each required batch. Soil and water was mixed a constant speed of 60 rpm for 60 minutes. At the middle of the mixing process, in order to check the quality of mixing, the mixer was stopped and the slurry was checked by hand and freed from any created masses (lumps). Once fully mixed the slurry mixture was stored in sealed plastic containers for 24 hours before using it to insure saturation. Each batch was just enough to prepare two samples for triaxial testing. For the large sample five more batches were required to prepare one sample.

3.8.1.2 Consolidation

A one directional consolidation method is considered to be the most commonly adopted approach by many researchers to create homogeneous clay bed (Juran and Guermazi, 1988; Sivakumar et al., 2004b; Maakaroun et al., 2009). However, whilst this technique can provide satisfactory results in short consolidation chambers (< 200 mm) such as the Rowe consolidation cell (Rowe and Barden, 1966), some difficulties have been reported by a number of researcher (Anderson et al., 1991; McKelvey, 2002; Ahmadi and Robertson, 2004; Black et al., 2011) when using this method for preparing larger depth samples. This because friction occurs between the soil and the walls of the consolidation chamber which could lead clay particles to arrange themselves into an internal concave structure. In addition, there might be a loss in consolidation pressure with the depth of the samples. (Valls-Marquez, 2009;

Black et al., 2011). To mitigate these problem, as proposed by the previous researchers inner walls were carefully lubricated with silicon grease which also aids sample extrusion after consolidation. A hydraulic pump was adopted in order to keep the consolidation pressure constant when preparing the larger samples.

Preparation of specimens for Model I (triaxial test):

Approximately 4000 g of the prepared slurry was poured into each consolidation chamber to an initial height of 294 mm in three stages. The cell was vibrated for 30 seconds to eliminate trapped air.

According to BS 1377-5:1990, under the fully saturation conditions the initial void ratio (e_0) and the initial height (H_0) were calculated using equations 3.2 and 3.3, they were 2.209 and 294 mm respectively. Before and after placing the soil, a 100 mm diameter saturated porous plastic filter (Vyon sheet) with 1.2 mm thickness was placed on top of the slurry surface to ensure that only water could drain out.

Every load step was held for a minimum of 24 hours and a maximum of 72 hours to ensure that primary consolidation was complete. Typical consolidation plots are shown in Figures 3.15 and 3.16 (see Appendix A for more information).

The void ratio, e, at the end of each increment period was calculated using equation 3.2. The relationship between void ratio and applied consolidation stresses is presented in Figure 3.17.

After completion of consolidation, the sample was either directly extruded from the consolidation chamber (no column installed) or the stone column was first installed and then extruded. A 100 mm diameter Piston extruder was used to remove the samples in the same direction as consolidation loading. A steel ruler was used to trim the surface of the specimen to ensure the flatness and height of 200 mm. In each test samples were taken to measure water

content. Filter papers were fitted around the sample and then a rubber membrane was placed around the sample, before being mounted in the triaxial apparatus.

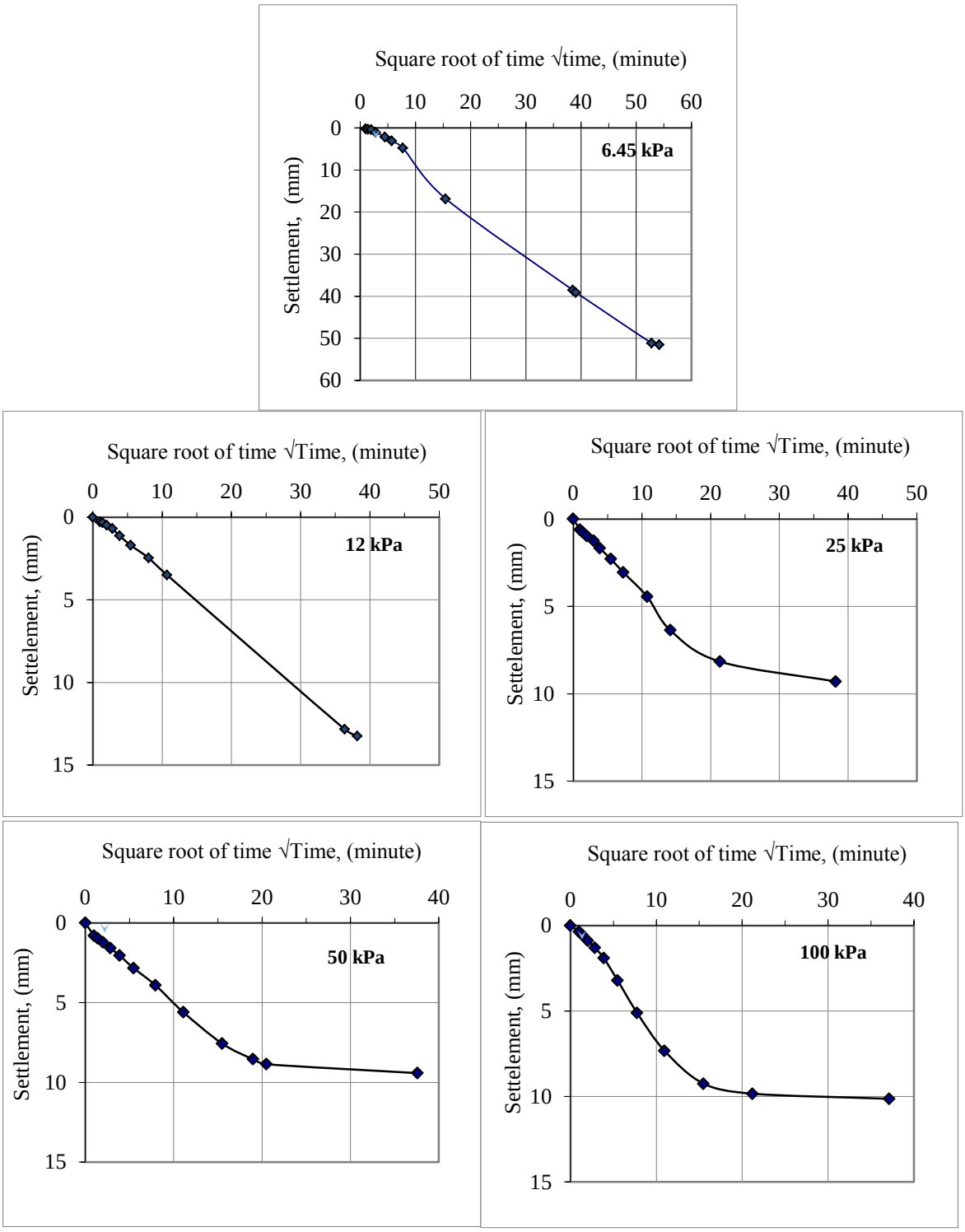

Figure 3.15 Typical settlement /√time relationship for 100 mm dia. triaxial sample

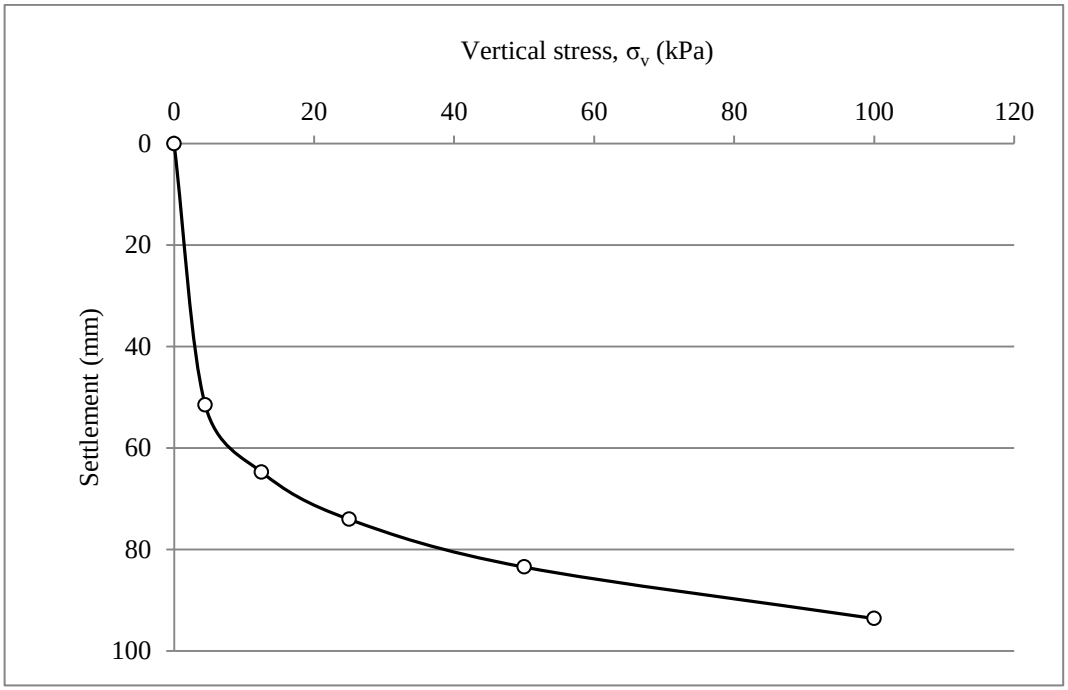

Figure 3.16 Settlement and total vertical stress relationship for 100 mm dia. triaxial sample

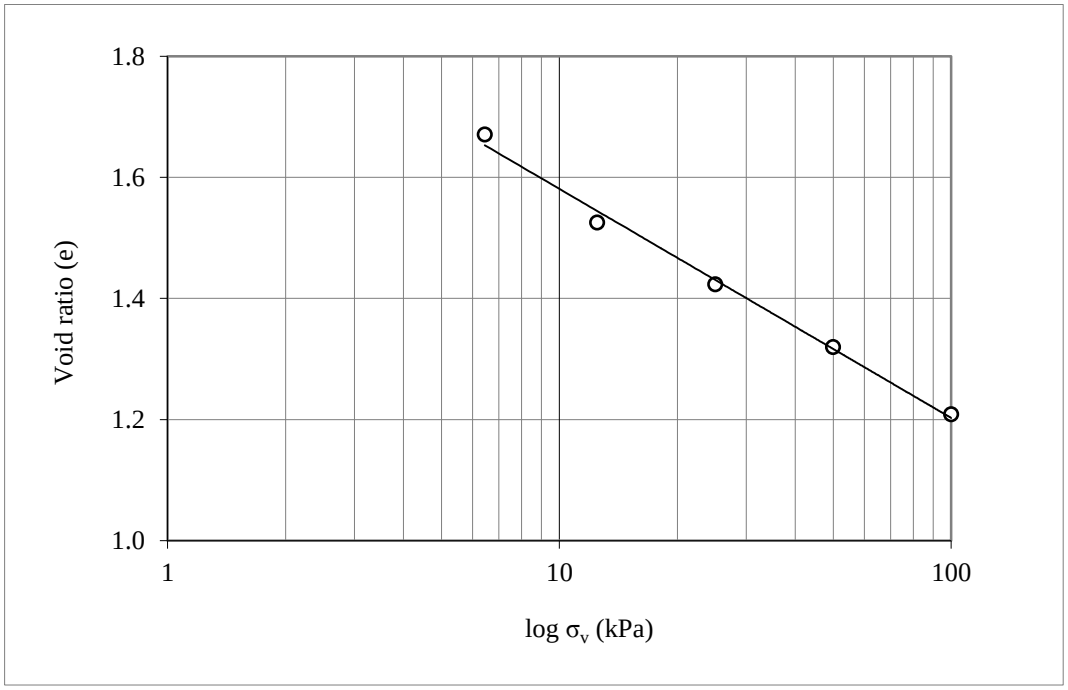

Figure 3.17 Void ratio/ log σ_v relationship for 100 mm dia. triaxial sample

Preparation of Model II (300 mm specimens):

A similar procedure was followed when preparing larger specimens, with the exception of drainage which was allowed only from the top in order to measure pore water pressure from the bottom of the sample at different positions (PPT1, PPT2, and PPT3) as shown in Figure 3.11. As mentioned in Section 3.5 three samples were consolidated simultaneously, approximately 45 kg of slurry to be poured into each tank giving an initial slurry height of 448 mm. A saturated plastic porous filter was placed on top surface of the slurry. A perforated 25 mm thickness plate was placed at the top of the filter, and used as a consolidation loading plate. A similar loading sequence was used then adopted to give pressures of 6, 12, 25, 50, and 100 kPa. After the completion of the consolidation stage, the specimens surface was flattened using metal ruler with 298 mm length, samples were taken for determining water content. Stone column was installed in the clay bed (as explained in the following section 3.8.2), and the tank was moved to the loading frame for testing.

Figure 3.18 shows typical consolidation curves for each loading sequence. Accumulated settlement against the associated loading stress is presented in Figure 3.19.

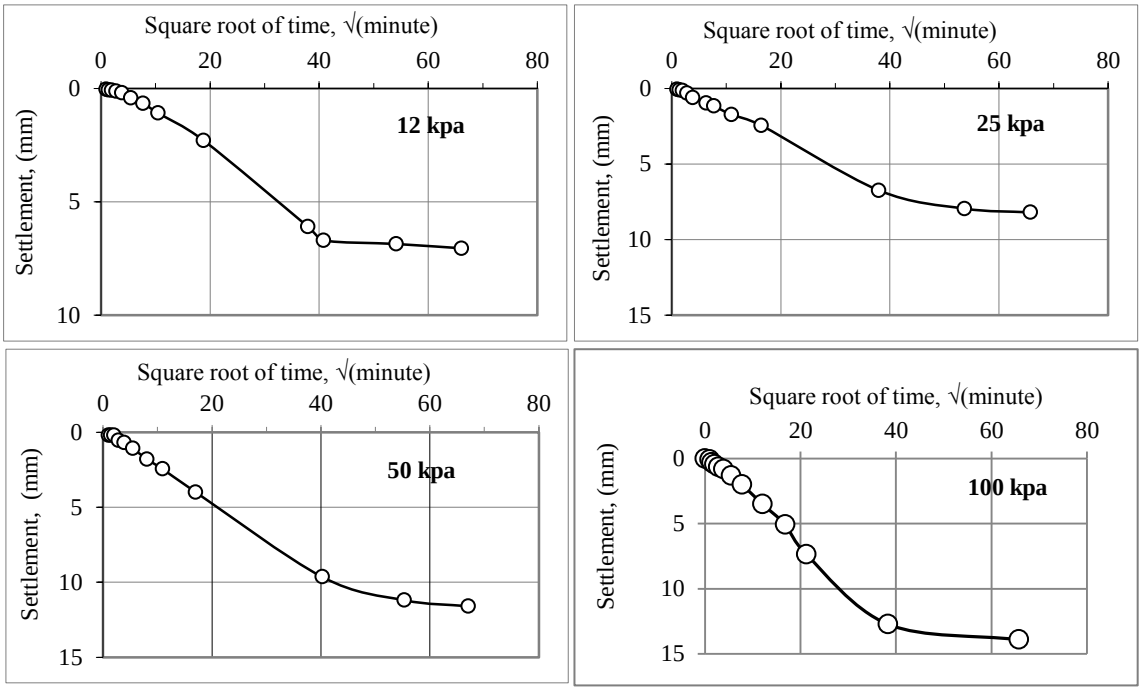

Figure 3.18 Typical settlement / time relationship for 300 mm specimens

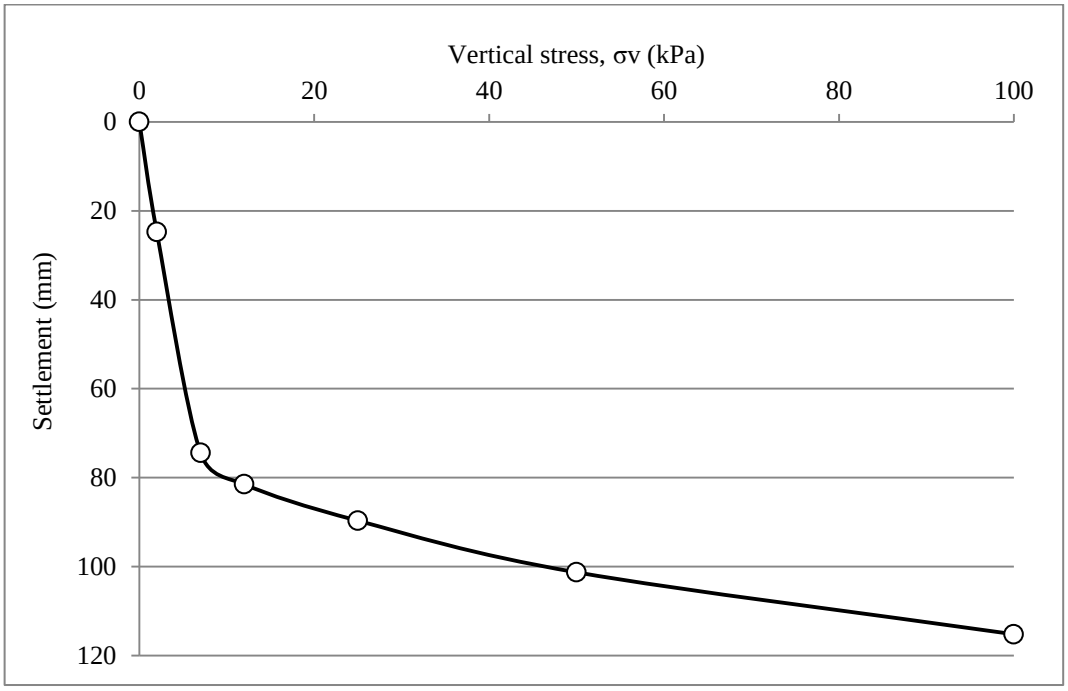

Figure 3.19 Settlement and total vertical stress relationship for 300 mm specimes

In the case of 300 mm diameter specimens, settlement during the consolidation stage was measured together with change in pore water pressure. Load was only increased when pore pressure had reached an equilibrium value as there was a minimal increase in settlement beyond this value as can be observed in Figures 3.18. Figure 3.20 shows typical response of pore water pressure during loading stages during consolidation of slurry. It was difficult to take measurements in the initial loading stage (7 kPa) where the data logger was showing un-stabilised readings, this was probably as a result of trapped air in the system. During the subsequent loading stages, pore water pressure increased to approximately the increment in pressure. Pore water pressure dissipated and stabilised at about 3 kPa.

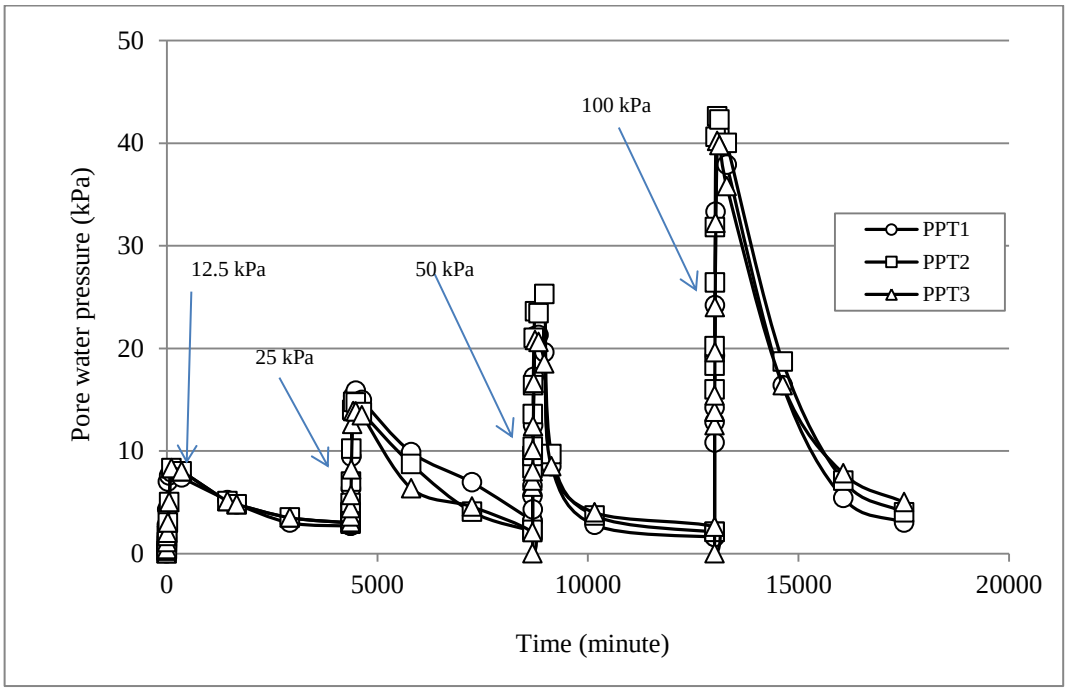

Figure 3.20 Variation of excess pore water pressure at PPT1, PPT2, and PPT 3 positions during consolidation

3.8.2 Column Installation

As stated in the literature review (section 2.4) stone columns can be constructed in the field either by replacement or displacement method. Wood et al. (2000) and Sivakumar et al. (2004b) investigated various methods for installing model stone columns in laboratory. They used methods such as forming the column by freezing the stone material in a mould of the same size of the required columns, another method was by displacing the soil using a rod with the same size of the column and then filling the formed cavity by the column material, and also the most common used method which was done by replacing a part of the soil and compacting the stones in the cavity. A reduction in the density of the column upon thawing was found in case of preformed frozen columns, while it was difficult to implement the displacement technique in a small scale model due to the generated suction that may occur during the removal of used rod.

In this study the replacement method was adopted because it proved to be repeatable. Thus a 28 mm diameter cavity at the centre of the sample was created by inserting a pipe with this diameter to the clay bed and removing the soil included in the tube (Figures 3.21 and 3.22).

After creating the cavity, the granular aggregate was introduced in four stages and compacted using a 1.5 Kg metal rod free falling through a fixed distance of 50 mm. 15 bowls were applied to each layer. Aggregate between 1.18 mm and 2.1 mm in the size was used to form the stone column.

The average bulk density of the column was calculated in each test. It was 1900 ± 45 kg/m^3. It is suggested that some of the variation in density may have been due to small increases in diameter of the column as it was formed.

Making a cavity in the soil Introdusing aggregate Extroding the sample

Figure 3.21 Sample preparation for Model I

Making cavity and colum Installation

Figure 3.22 Sample prepartion for Model II

3.8.3 Loading Test

3.8.3.1 Triaxial model test

The prepared sample was located in the triaxial cell, and saturated using increments of cell pressure and back pressure. A Skempton $\bar{B}$ parameter of over 0.95 was achieved. The sample was then consolidated at an effective confining pressure of 100 kPa with a back pressure of 300 kPa.

Two loading conditions were examined:

i) Static loading: where the specimens were sheared at a constant axial strain rate of 0.03 mm/ minute.

ii) Cyclic loading: load was applied at different cyclic stress ratios (CSR) 0.6, 0.7, and 0.8, each at three frequencies 0.5, 1 and 3 Hz. The cyclic stress was applied in sine wave form as shown in Figure 3.23.

In both loading conditions, pore water pressure was measured at the bottom of the specimen.

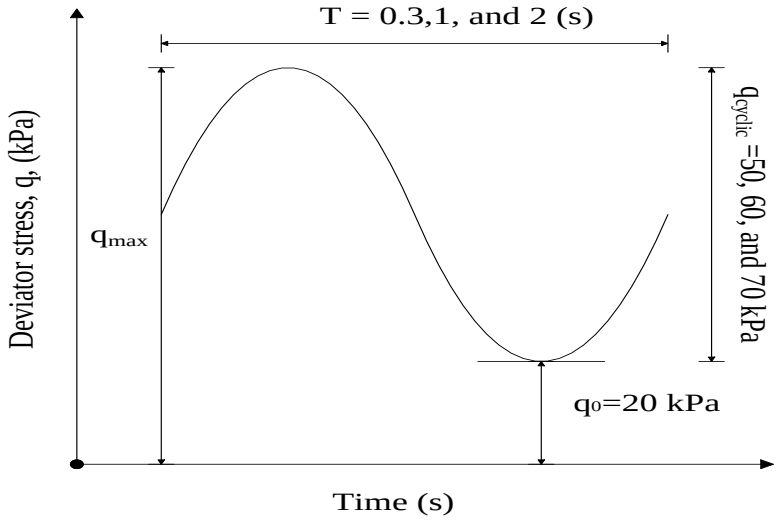

Figure 3.23 Cyclic stress state

3.8.3.2 Large scale model test

Following installation of the column, the specimen was saturated slowly from bottom to top using piezometer. This process took about 4 hours, in order to ensure that the stone column was saturated and the air trapped between the particles was forced out, so as not to affect the quality of pore water pressure measurement beneath the column. Then a sand blanket of 3 mm thickness was placed covering the entire top surface of both soil and column to ensure that the stress imposed from the surcharge load will be uniformly distributed to cover the entire area. The footing was then located at the centre using a guide plate (see Figure 3.24). the sample was then reconsolidated for 48 hours using a slightly higher pressure (120 kPa) than that used to create samples (100 kPa), the extra pressure simulated the surcharge pressure on top of the footing. Following this, in similar manner to the triaxial model, both static and cyclic loading condition was applied.

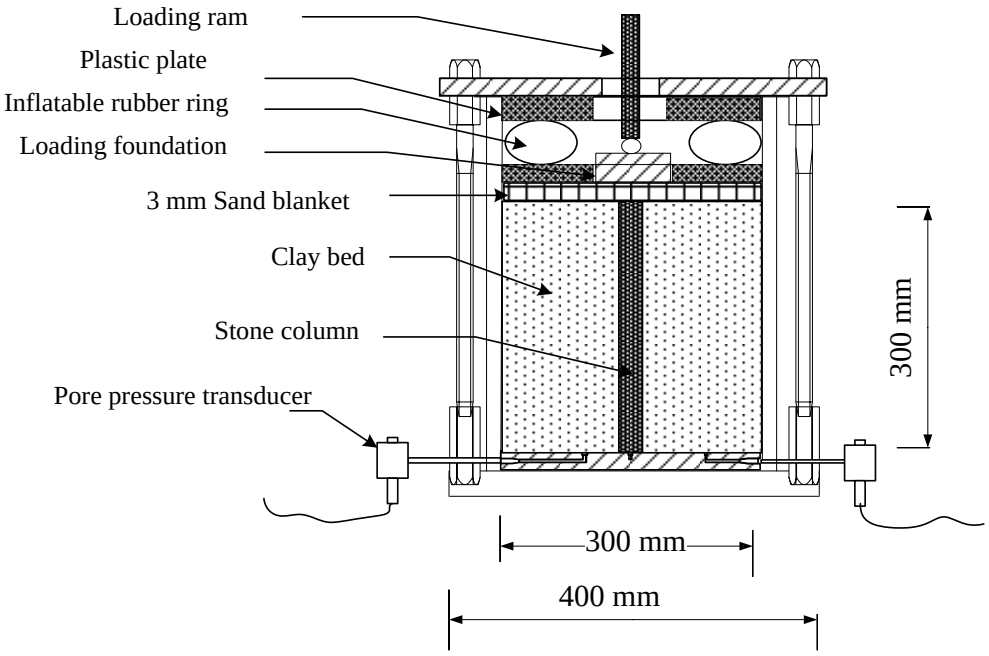

Figure 3.24 Large test set up

3.8.4 Preloading Investigation

3.8.4.1 Water content

Water content in the clay bed can provide a good indication of its strength and uniformity. This was carried before testing (Figure 3.25) in order to ensure the quality and the general undrained shear strength of the soil.

A plastic pipe (similar to the one used to install the column) with 28 mm diameter and 45 mm height was used to take the soil samples for water content test. Soil within the pipe was loosened and a vacuum was used to lift out the soil from within. This technique can provide samples along the depth of the clay bed and can be applied in different locations.

As observed in Figure 3.25 the water contents through the clay bed were consistent and ranged between about 43 and 42.5 %. This range of water content was very close to that estimated using the relationship of undrained strength and liquidity index (3.3.5). At about 43 % water content, strength was estimated to be around 12 kPa.

Results showed that in most of the tests the variation in water content was comparatively larger at the middle height of the specimen (± 0.5 %); this could be related to length of the drainage path.

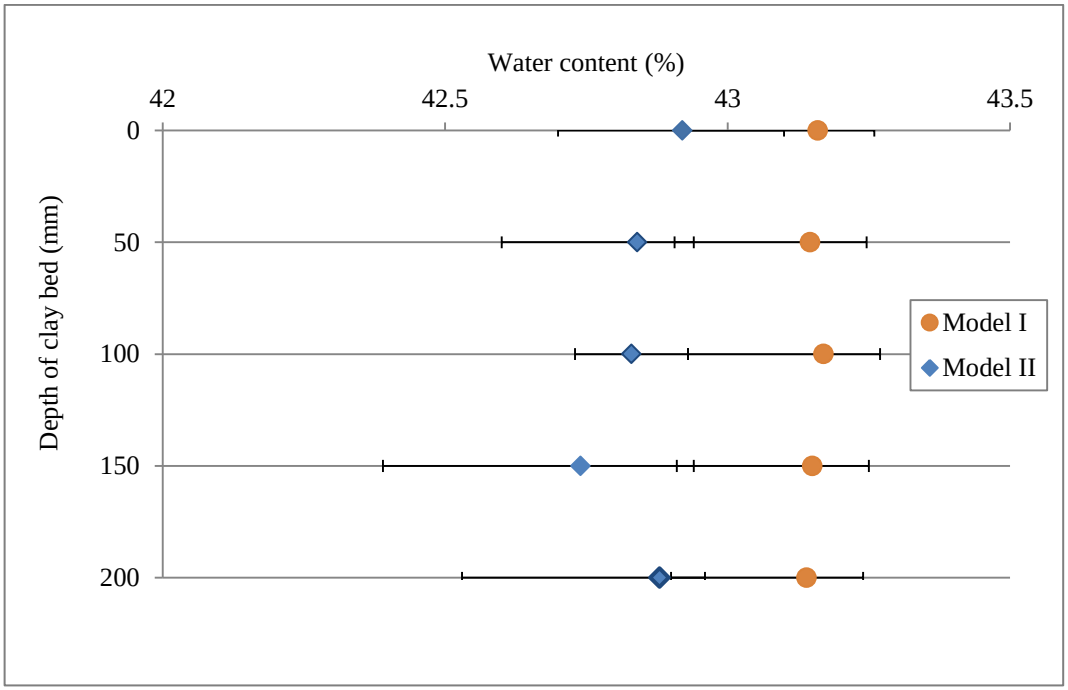

Figure 3.25 Variation in water content before testing for both Models (I and II)

3.8.4.2 Shear strength of clay bed

In order to investigate the quality of the prepared clay bed, a hand vane was used to determine the variation in shear strength by testing clay at a range of positions near where samples were taken for water content determinations. Hand vane tests were conducted in accordance with BS 1377:1990. A 12.7 mm hand vane was used to limit clay disturbance to minimum. For the 100 mm diameter specimens, due to size of the specimen it was difficult to perform the hand vane test at more than one location; however, three pilot tests in three specimens were carried at different depth. In the large sample, the undrained shear strength was determined at four (50, 100, 150, and 200 mm) depth and four horizontal positions (80 mm around the centre). This procedure was carried out in three pilot tests only. After that the shear vane test was taken in each sample before testing only in the centre and after testing in various locations to collect as much data as possible to observe the changes that occurred before and after testing.

Figure 3.26 shows the undrained shear strength values obtained from these tests including estimated values using Equation 3.2 (3.3.5). The average undrained shear strength was 11.5 kPa with a variation of ± 0.5 kPa. This result was less than the estimated values with a difference of less than 2 kPa.

The results from both water content and undrained shear strength demonstrated excellent repeatability of both the mixing and consolidation process.

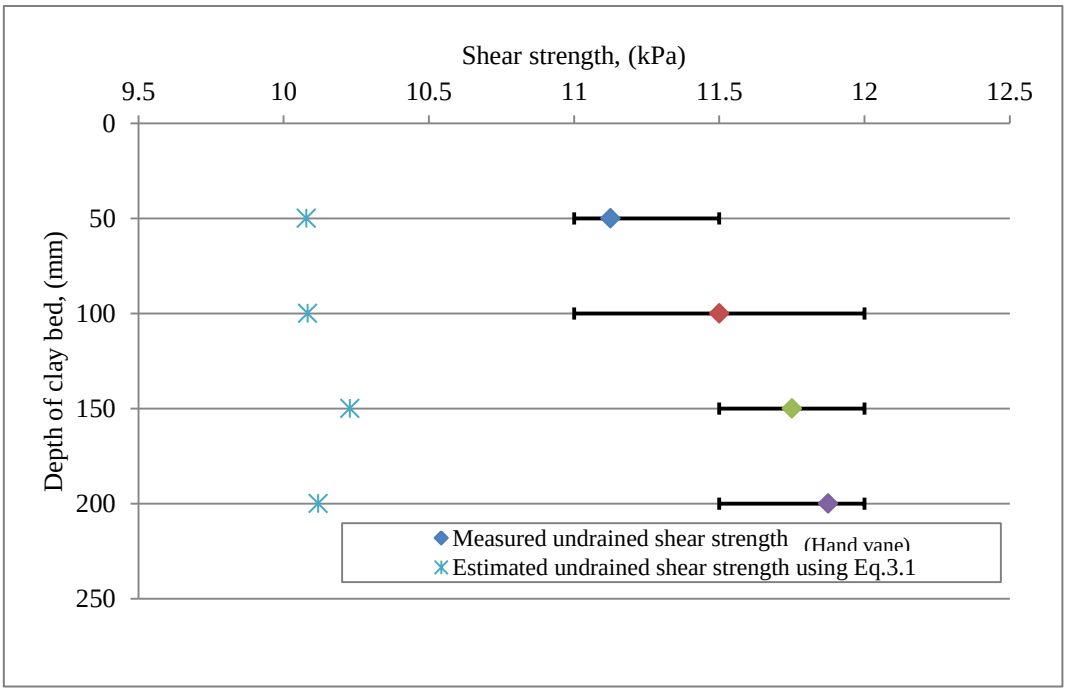

Figure 3.26 Shear strength determinations in test bed (pilot stage)

3.8.4.3 Column deformation

Investigating the shape of the column after testing can provide a good indication of the failure mechanisms and the interaction between the soil and the stone column. As it is not easy to monitor changes during the test, observation at the end of the test is the only available guide about the behaviour of the materials. Several techniques were investigated to assess condition and shape of the column at the end of the test. These included grouting the column material,

freezing, using both wax and resin to hold the aggregate material together and section slicing method.

The simplest was slicing the specimen in half vertically through a selected section. This method appeared to be a very effective, quick and showed the shape of the column. It was adopted in this study.

CHAPTER 4

MONOTONIC LOADING RESULTS AND DISCUSSION

4.1 Introduction

This chapter presents the results of both 100 mm diameter triaxial specimens and foundation loading tests on 300 mm diameter specimens according to the methodology described in Sections 3.6. The general behaviour of both soft clay (no column) and clay/stone column composite system are discussed together with the influence of loading rate, and column stone density on the bearing capacity. The discussion includes results from previous studies with similar testing conditions in order to validate the current study work. The test programme adopted for this study is shown in Table 4.1

Table 4.1 Test programme

Test type	Test No.	P_c (kPa)	C_u (kPa)	σ'_3 (kPa)	A_s (%)	H_c/H_s	Strain rate (mm/min)	Column density (kg/m^3)	comment
Triaxial Model	TRI-C-01	100	12	100	-	0	0.003	-	
	TRI-C-02						0.03		
	TRI-C-03						0.3		
	TRI-C.C-04				7	1	0.003	1805	
	TRI-C.C-05						0.03		
	TRI-C.C-06						0.3		
	TRI-C.C-07								
	TRI-C.C-08						0.03	1805	
	TRI-C.C-09							1640	
	TRI-C.C-10							1500	
Large Model	LM-C-01	100	12	100	-	0	0.03	-	70 mm Footing
	LM-C-02				-	0			
	LM-C.C-03				16	1		1805	70 mm Footing
	LM-C.C-04				16	1			

4.2 Model I (Triaxial)

Two types of samples were prepared one representing the soft soil (no column) and another representing soil/ stone column composite. These two types of specimens were tested under the same testing conditions. After extruding the specimen from the consolidation chamber, they were installed in a triaxial cell for loading. Each sample was first saturated and then isotopically consolidated under effective confining pressure of 100 kPa, with back pressure of 300 kPa. At this stage drainage was allowed from the bottom of the specimen, as such a volume change device was connected, allowing volume changes to be recorded during consolidation. After consolidation, the entire top of the sample was loaded under undrained condition.

4.2.1 Saturation

The specimen was saturated by increasing the pore water pressure so that any air in the void space can be eliminated. This allows for reasonable, reliable and repeatable readings of pore water pressure changes during loading stage (Head, 1998). As described on BS1377: Part 8(1990), there are several established methods for saturation of samples, the one applied in this study is saturating samples by using the application of back pressures, so that air in the system is forced into solution. To achieve over 95 % of saturation, the process were carried out by raising the confining pressure and back pressure in alternate increments as shown in Table 4.2.

As the tested material is characterized by its low permeability and the size of the sample is considered large, therefore the time required to reach 95 % of saturation was quite long between 3 and 5 hours. The stone column reinforced samples took a shorter time to saturate

.

Table 4.2 Typical triaxial saturation data

Soil only					**Soil/ column composite**				
Cell pressure (kPa)	Back pressure (kPa)	PWP (kPa)	PWP difference (kPa)	B value	Cell pressure (kPa)	Back pressure (kPa)	PWP (kPa)	PWP difference (kPa)	B value
0	-	-1.2	-	-	0	-	-2.5	-	-
50	-	27	28.2	0.56	50	-	35	37.5	0.75
50	40	38	-	-	50	40	39.6	-	-
100	-	69	31	0.62	100	-	80	40.4	0.81
100	90	89	-	-	100	90	89.7	-	-
200	-	170	81	0.81	200	-	178.5	88.8	0.9
200	190	188	-	-	200	190	188	-	-
300	-	283	95	0.95	300	-	284	96	0.96
300	290	288	-	-	300	290	289	-	-
400	-	384	96	0.96	400	-	387	98	0.98

4.2.2 Consolidation

After the saturation stage was complete the cell and back pressures were adjusted to allow the sample to be isotopically consolidated under effective confining pressure of 100 kPa and back pressure of 300 kPa. By allowing the water to drain from the sample to the back pressure system, the pore water pressure was gradually decreased until it reached approximately the value of the back pressure. 95% dissipation of pore water pressure was achieved after 24 hours.

The degree of consolidation was determined by expressing volume change at a given time as a function of the final volume change. As expected consolidation took place quicker when stone columns were installed compared to soil only (without stone column), where 90% consolidation was achieved seven times faster, see results presented in terms of degree of consolidation versus the square root of time in Figure 4.1. This result showed similar

behaviour to previous research by Sivakumar et al. (2004b) under similar test conditions. However, as shown in Figure 4.1, there was a difference in approaching 100 % of consolidation between this current study and the one conducted by Sivakumar et al. (2004b), this difference could be due to using the filter papers around specimens used in this current study as there was no indication that they used such method in their study. In addition to this, in case of reinforced specimens, the size of the column material particles used and the resulting void ratio could have a significant influence on rate of consolidation.

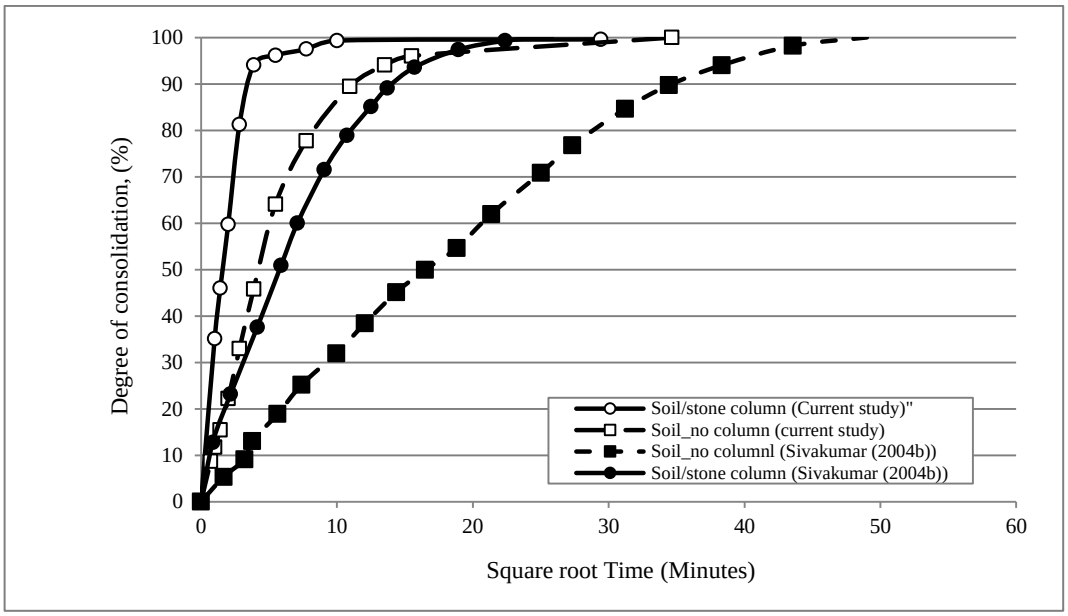

Figure 4.1 Consolidation characteristics

4.2.3 Stress - Strain Behaviour

The unit cell approach was used to analyse the load – deformation data, where the column and the surrounding soil were assumed to act as a single element with a homogeneous distribution of stresses and strains as proposed by Balaam et al. (1977). Whilst this assumes that the sample is homogeneous, this approach has proved satisfactory for many practical design

applications (Lee and Pande, 1998; Maakaroun et al., 2009; Shahu et al., 2000; Sivakumar et al., 2010, 2004b).

The influence of the inclusion of stone column in soft clay bed was observed in all tests curried out. A typical stress – strain relationship is presented in Figure 4.2. The results from reinforced clay tests are compared with tests carried out on soft clay specimens only. It was observed that the reinforced samples developed higher bearing capacity than the soil only samples. The deviator stress at failure for soil samples was approximately 60 kPa, while with the presence of full length stone column this increased to about 90 kPa. This is an increase of about 30 % for an area ratio of 7 %. This can considered to be as a substantial improvement, especially; when many previous researches have reported that the area over 15 % is required to show significant improvement in the bearing capacity. This significant improvement can be attributed to higher internal angle of friction of the material used in this study for building the stone column (48^o in wet condition) compared to other studies.

Figure 4.3 shows results of tests conducted by Sivakumar et al. (2004b); Black et al. (2006); Andreou et al. (2008); Najjar et al. (2010) at similar testing condition (undrained triaxial condition at the same effective confining pressure) are shown together with results determined in the current study. In terms of the degree of improvement of bearing capacity, results show that a higher angle of internal friction would provide a greater improvement ratio at a lower area replacement ratio. For example, using material with an angle of friction at 48^o in this study (comparing with 35^o at the other studies) enhanced the degree of improvement by about 35 % at the same area replacement ratio (7 %).

Despite of the limited number of studies on stone columns using undrained triaxial conditions, it is possible to obtain a relationship between the improvement ratio and the area replacement ratio as presented in Equation 4.1.

$$Improvement\ ratio = 4.003A_s - 10.831\ A_s^2 \qquad 4.1$$

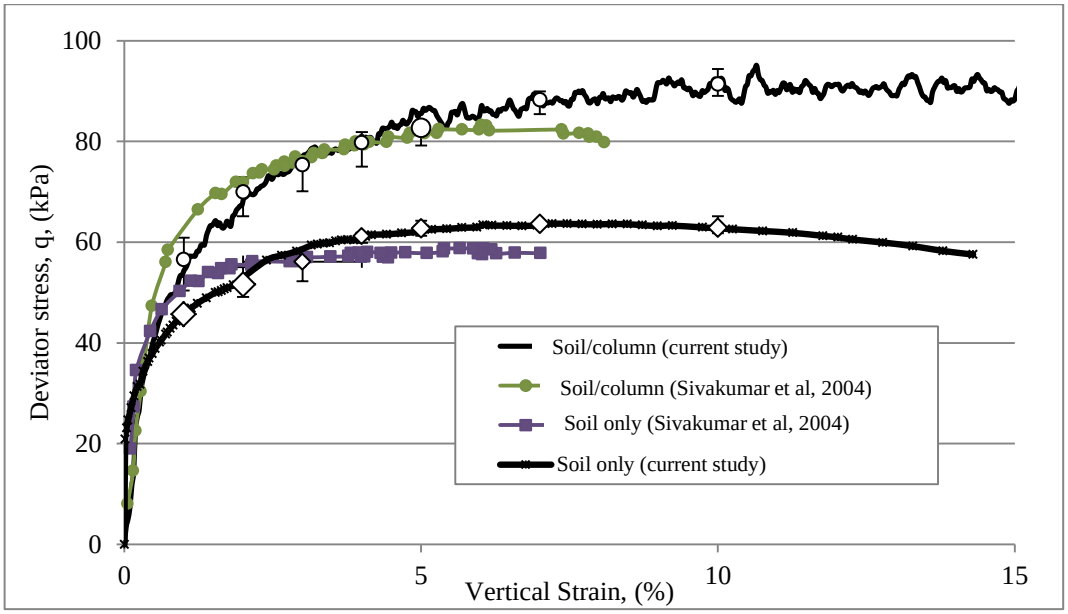

Figure 4.2 Stress strain behaviour of soft soil (no column) and soil/stone column composite.

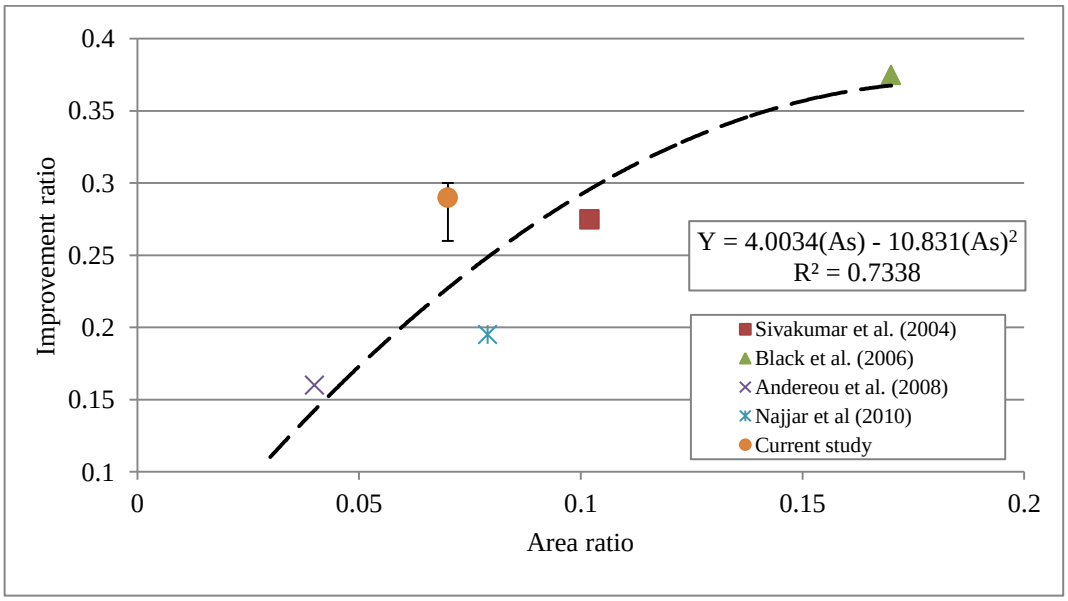

Figure 4.3 Improvement ratio versus area replacement ratio

In all tests, pore water pressures were measured, and expected application of stress on low permeability soils induces excess pore water pressure. Through the process of consolidation, pore water is reduced resulting in a gradual increase in effective stress. The speed of consolidation amongst other factors depends on drainage path. Installation of stone column leads to a reduction in drainage path resulting in faster consolidation.

Figure 4.4 shows that the pore water pressure in all cases increased tending towards their highest value as the deviator stresses reaches their maximum value at axial strain of about 5 %. There was a reduction in pore water pressure at about 15 % in case of the reinforced soils. This reduction during the undrained loading stage is possibly due to the dilation of the stone column.

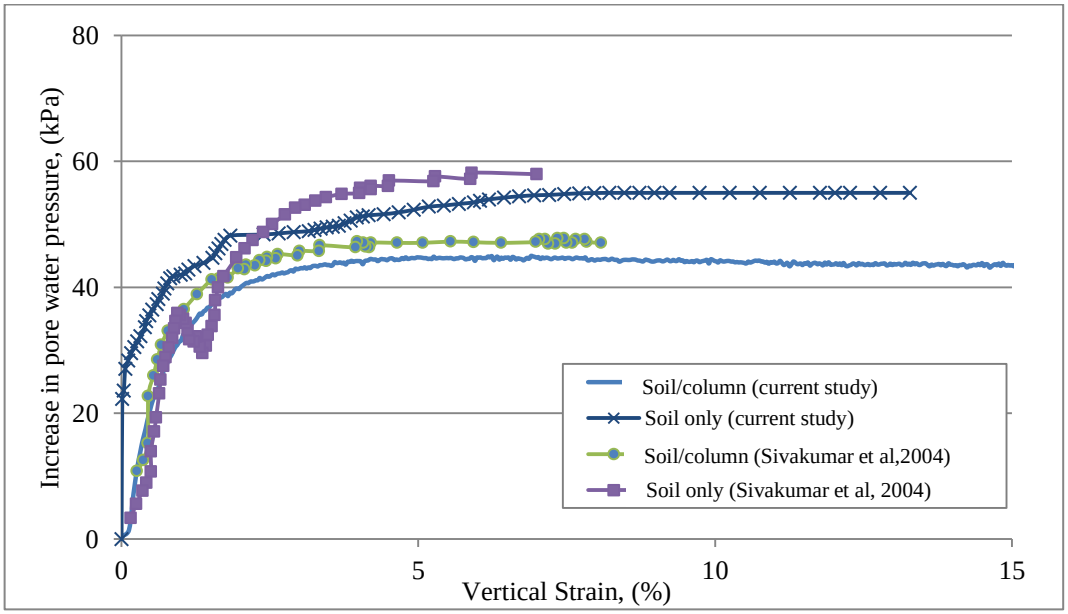

Figure 4.4: Excess pore water pressure of soil (no column) and soil/ stone column composite.

The vertical deviator stresses at failure for both unreinforced and reinforced specimens under undrained conditions are presented in Table 4.3, for tests under similar condition to this study. The improvement occurred in terms of bearing capacity, which ranged between 27 and 56 %,

and was mainly dependent on the area ratio and the internal angle of friction of the column materials.

The estimation of vertical stress at failure of a single column is included in Table 4.3. using the expression proposed by Hughes and Withers (1974):

$$\sigma_v = \left(\frac{1+\sin\emptyset'}{1-\sin\emptyset'}\right)\left(4c + \sigma_{r_0'}\right) \qquad 4.2$$

In the above equation $\sigma_{r_0'}$ was considered firstly equivalent to $2c_u$ as suggested by Hughes and Withers (1974), and secondly was considered to be equivalent to the effective confining stress in the test (100 kPa). These calculated values are presented in Table 4.3 as $\sigma_{v(calculated)}$ (1) and (2) respectively. Whilst both assumption provide an over estimation of values for all tests, it shows that the first assumption ($\sigma_{r_0'}$ $=2c_u$) would provide a closer prediction (within an average of 25 %) than considering the amount of the effective stress.

Table 4.3 Measured and calculated vertical stress obtained from different studies

Reference	$\Phi^{(o)}$	A_s (%)	σ_3 kPa	σ_3' kPa	$q_{untreated}$ kPa	$q_{treated}$ kPa	$u_{untraeted}$ kPa	$u_{tratead}$ kPa	q_{ratio}	$\sigma_{v(measured)}$ kPa	$\sigma_{v\ (calculated)}$, (kPa)		
											(1)	(2)	Using Eq 4.1
Sivakumar et al. (2004)	35	0.10	400	100	60	83	56	47	1.38	483	664	812	478
Black et al. (2006)	35	0.17	400	100	160	254	-	-	1.59	654	775	1550	619
Andereou et al. (2008)	35	0.04	300	100	51	65	65	51	1.27	368	554	738	357
Najjar et al (2010)	33	0.08	410	100	64	74	61	50	1.16	484	651	773	490
Current study	48	0.07	400	100	60	88	53	44	1.46	488	529	1004	474

After each test, the specimens were removed from the cell and split vertically along their diameter to examine the mode of failure. It was expected that the columns would bulge at a depth of 2 to 3 times the column diameter as suggested by Hughes and Withers, (1974). In all cases the column bulging was found to be relatively uniform with the depth of the sample as shown in Figure 4.5. This probably was due to the constant confining pressure along the depth

of the specimen (triaxial test condition), whereas in the field condition the confining stress increases as the depth of the soil increases.

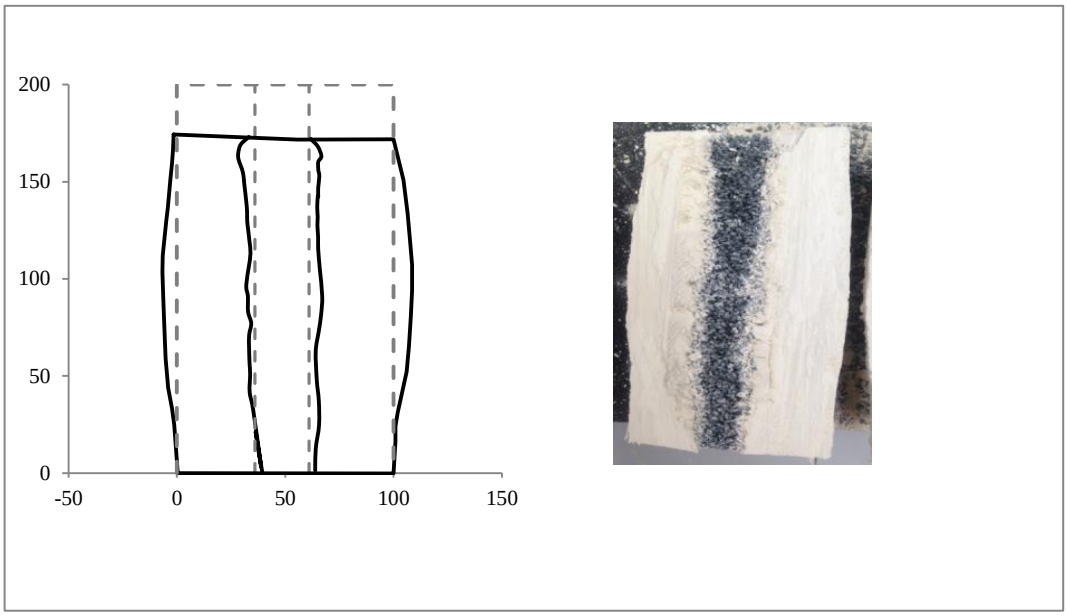

Figure 4.5 Shape of failure under static loading condition

4.2.4 Effect of Strain Rate

4.2.4.1 Stress-strain characteristics

Strain rate has been recognised as having a significant influence on the undrained shear strength of saturated soils (Kimura and Saitoh, 1983; Nakase and Kamei, 1986). Skempton and Bishop (1954) summarised that the strength of cohesive soil are generally sensitive to the change in strain rate and any reduction in the strain rate would decrease the strength of the soil, whereas the granular soils are generally independent of this factor.

The strain rate for shearing saturated soils under undrained condition can be determined using the following expression:

$$Rate\ of\ strain\ \left({}^{mm}/_{minute}\right) = \frac{\varepsilon_f L}{100 t_f} \qquad 4.3$$

Where: ε_f is the strain at failure and typically ranging from 15 to 20 % for normally consolidated clay; and L is the specimen length (mm); and finally t_f (minute) is the time to failure which is calculated from t_{100} which is the time required to ensure at least 95 % equalisation of pore water pressure in the specimen (Head, 1996).

The axial strain rate for consolidated undrained triaxial test with pore water pressure measurement was carried out using the above expression and it was found to be 0.03 mm/ minute. This study included investigation of the influence of the strain rate on the undrained shear strength of both soft soils and stone column reinforced soft soil.

Three strain rate values were applied to cover the range recommended for cohesive soils (0.3, 0.03, and 0.003 mm/minutes). Each test was repeated at least two times to ensure repeatability in results.

Figure 4.6 (a) and (b) show the typical stress-strain curves of both treated and untreated soils.

Considering the load capacity of the both soils to be at 5 % of the specimen strain (equivalent to 10 % of the foundation width) as suggested by Bowles (1996). Results show that there is about increase of about 10 % change in deviator stress associated with increasing the magnitude of rate of strain from 0.003 to 0.3 mm/minute in unreinforced specimens. In case of reinforced specimens the trend was in reverse order where the deviator stress showed an increase by 8 % with the reduction of the strain rate.

Conversely, if failure zone was considering to be at 8 % of the deformation (i.e. 58% of stone column diameter (Hughes and Withers, 1974)), the deviator stress in the reinforced specimens was almost fall toward same point, this could be due to the drainage path provided by the presents of the stone column which results in reduction in the effect of pore water

pressures. Whereas in case of unreinforced soils the deviator stress was continued to increase with the increase of strain rate.

This suggests that with or without stone column results are not very sensitive to rate of strain. This may be due to the fact that the soil examined is kaolin clay which has a high percentage of silt content (about 50%). In addition to this it is worth noting that the soil with stone column is less sensitive to change in rate of strain.

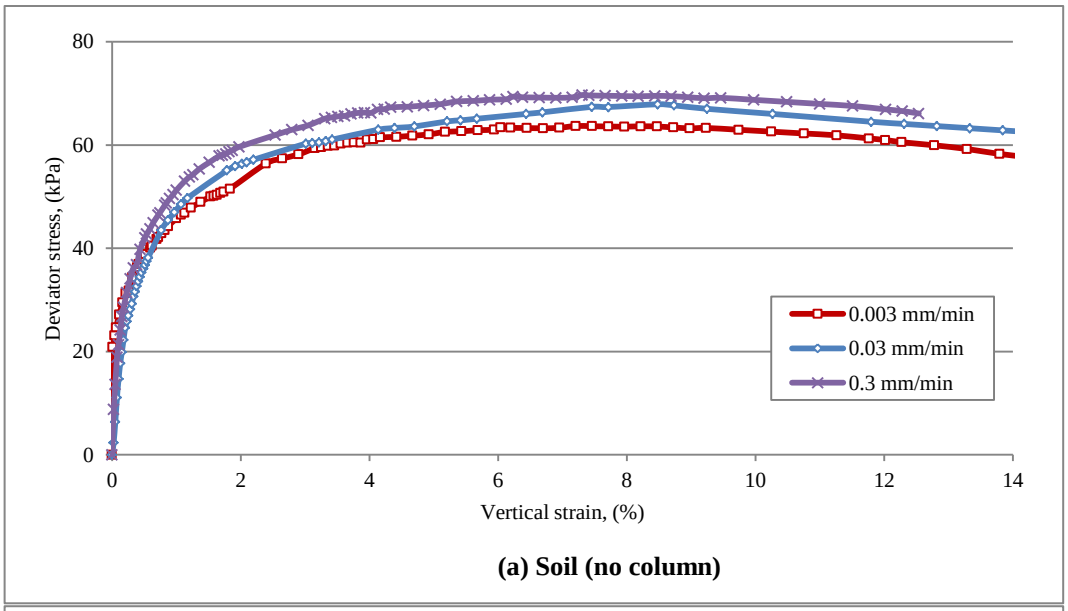

(a) Soil (no column)

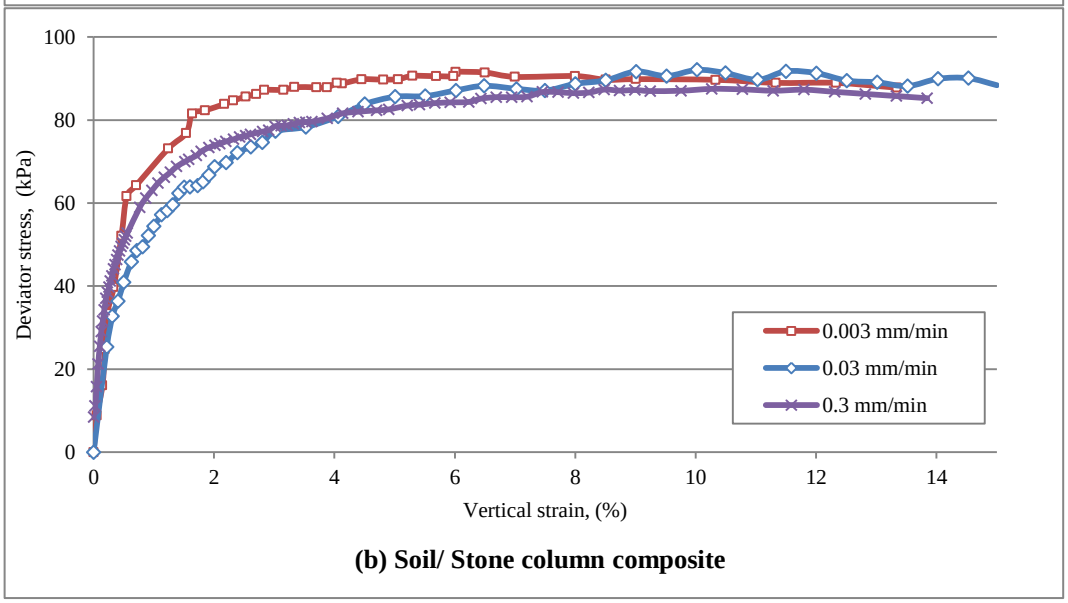

(b) Soil/ Stone column composite

Figure 4.6 Typical stress-strain curves: (a) soil (no column); (b) soil/stone column composite

4.2.4.2 Excess Pore Water Pressure-Strain Characteristics

The typical observed relationships of the change in pore water pressures and the axial strains for both soil only and stone column/soil specimens for strain rates of 0.3 to 0.003 mm/minute are given in Figure 4.7 (a) and (b). Results show that there is an approximate 20 % increase in pore water pressure for reduction in speed of second order of magnitude for clay only specimens. For the case of stone column reinforced soil, change in pore water pressure was about 8 %. This was most likely due to shorter drainage path. Thus, the effect of rate of testing stone column reinforced soil can be discounted when assessing their behaviour in case of silty soil such as kaolin.

Figure 4.8 shows the change in pore water pressure- strain rate at the peak deviator stress level. The pore water pressure was normalised in terms of the effective confining pressure (σ_3'). Findings tend to confirm that reduction in pore water pressure at tested strain rate as observed in this study. It also showed the difference in pore water pressure between treated and untreated soils.

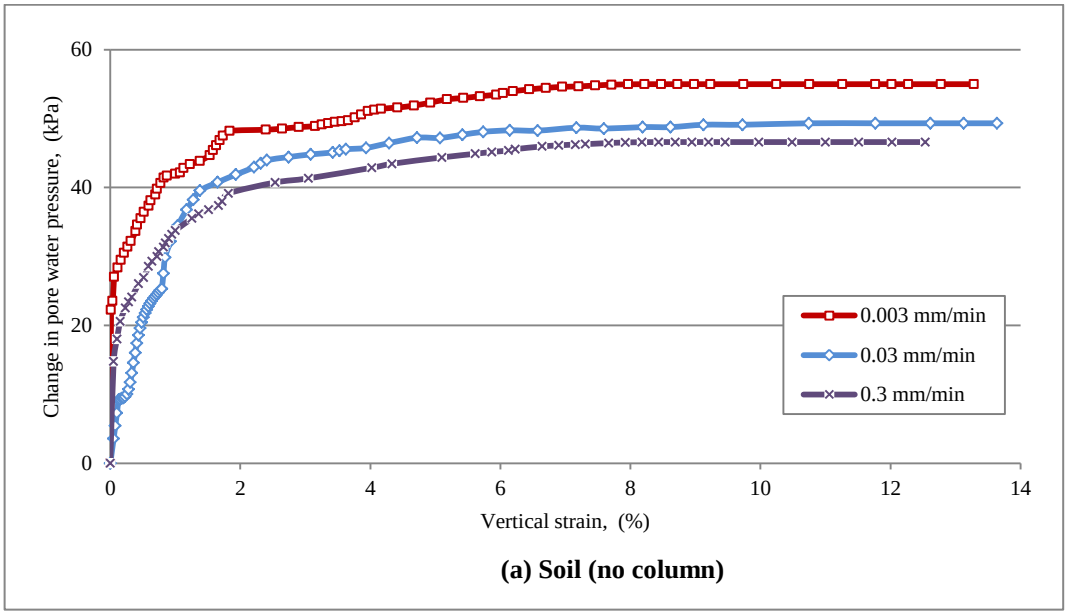

Figure 4.7(a) Typical change in pore water pressures-strain curves for soil only

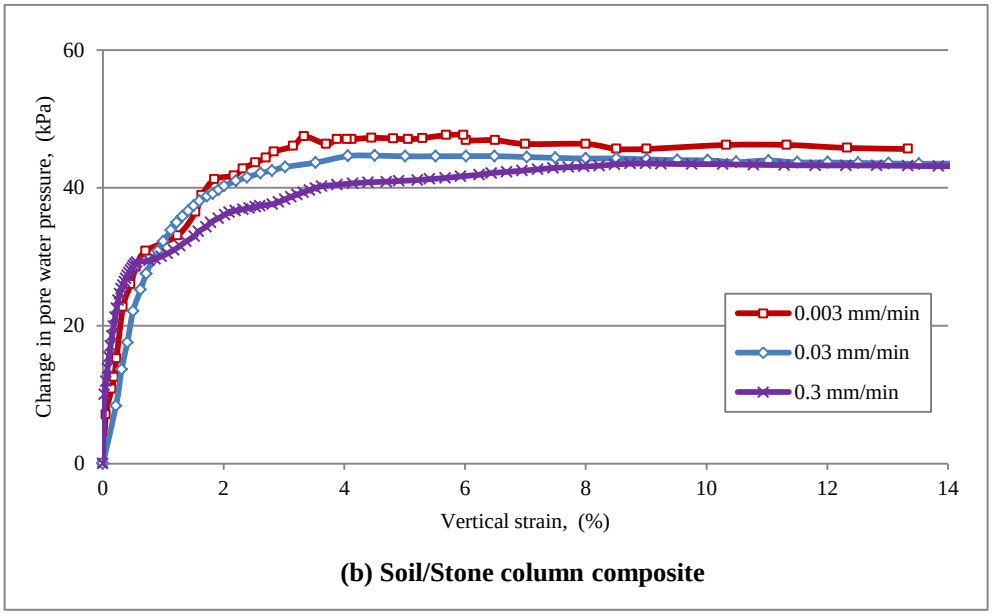

Figure 4.7(b) Typical change in pore water presures-strain curves for soil/ stone column composit

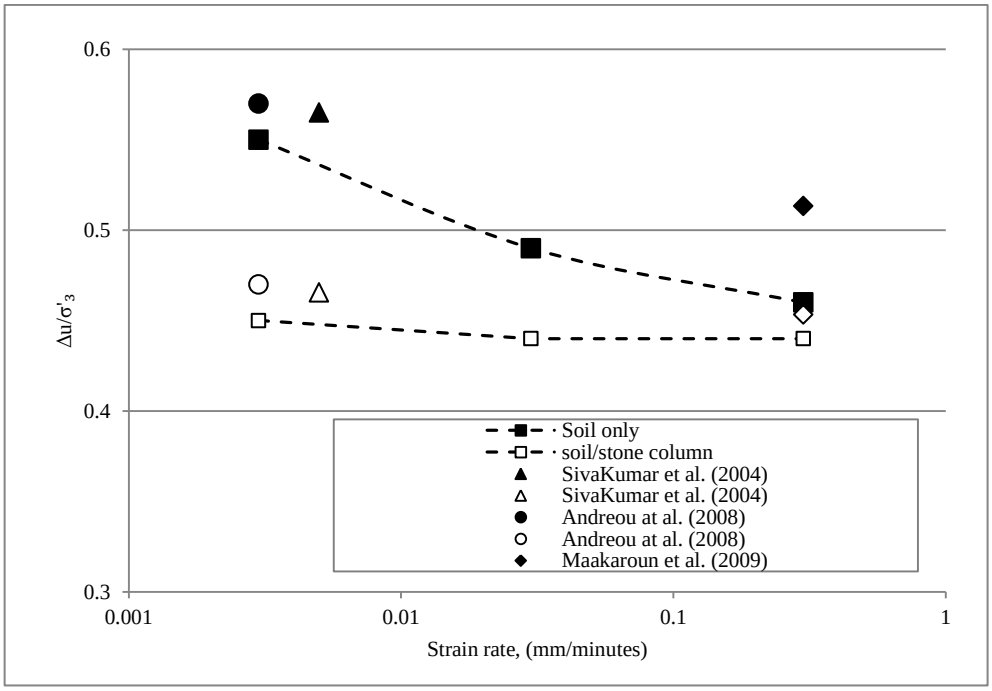

Figure 4.8 Normalised excess pore water pressure – strain rate relasionship

4.2.4.3 Rate Effect on Soil Modulus

Young's modulus of soil (E) is the proportion between the changes in deviator stress to change in axial strain (Powrie, 2013).

$$E = \frac{\Delta\sigma}{\Delta\varepsilon} \qquad 4.4$$

Secant modulus, which is defined as the slope of the secant drawn from the origin to a particular point on the stress-strain curve (Schanz et al., 1999), can provide a convenient measure of soil stiffness. This modulus is an important parameter for the design of projects such as roads and railways, where it is used to predict settlement (Selig and Waters, 1994).

During this study the effect of rate of strain and inclusion of stone column on soil stiffness were investigated by tracking the secant modulus behaviour of both reinforced and unreinforced soils at different stress between 50 and 100% of the soils shear strength.

Figure 4.9 shows the relationship between the secant modulus of both soil only and soil reinforced by stone column and the strain at different strain rates. Other data from different studies are also included in this graph. Generally the deformation modulus of soil showed a independency on the tested strain range for both treated and untreated soils specimens. In addition to this, there is a trend of reduction in deformation modulus with increase in strain to about 4 %. After that a very small reduction was noted for both soil and soil with column.

In case of soil/stone column composite, the secant modulus was increased by about 30% compared to soil (no column). This improvement was higher between 1 and 3 % strain. For strains higher than about 4 % the secant modulus decreases and the degree of improvement in modulus decreased by about 17%. These trends showed a very close agreement with results

conducted by Sivakumar et al. (2004b) and Andreou et al. (2008) in terms of percentage of improvement in the deformation modulus, but in lower modulus value.

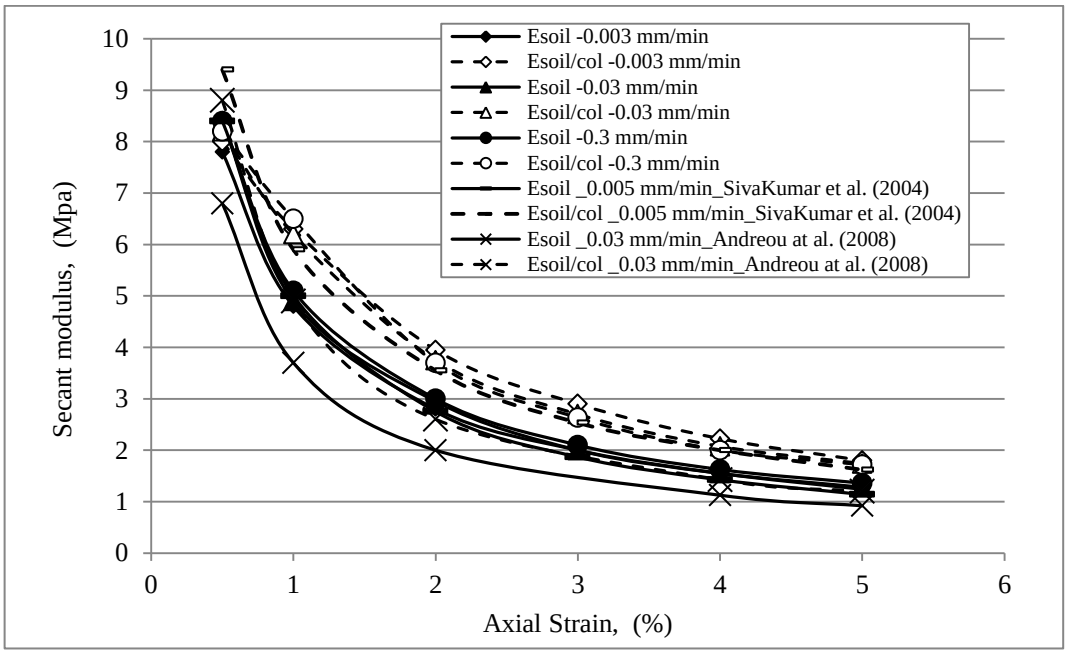

Figure 4.9 Soil modulus of both soils only and soil/ stone column composit

In order to relate soil stiffness to road and railway applications results were used for evaluation of subgrade reaction, which is used mainly in the design of foundation under wheel and concentrated loads. The modulus of subgrade reaction (k_s) can be defined as the relation between soil pressure (q) and deflection(δ) (Bowles, 1996).

$$k_s = \frac{q}{\delta} \qquad 4.5$$

Bowles (1996) provided an empirical equation to estimate the modulus of subgrade reaction using the allowable bearing capacity q_a.

$$k_s = (40, 50, 83, or\ 160) * (SF) * q_a \qquad 4.6$$

Where: Factors (40, 50, 83, and 160) are dependent on the settlement(ΔH) at 25, 20, 12 and 6 mm respectively; and

$$q_a = {}^{q_{ult}}/_{SF} \qquad 4.7$$

Therefore, the subgrade modulus of reaction for both soil (with no column) and soil/ stone column composit were compared for a settlement of 1.25 mm as suggested by the UK Department of Transport (as for pavement foundations the modulus should be limited to small strains in the elastic range) and at 6 mm and 10 mm as suggested by Bowles (1996) for foundation design. Results illustrated in Figure 4.10 (a, b, and c) show that the strain rate has no significant effect on modulus of subgrade reaction for both soils (with and with no column) for each level of modulus deformation. However, the installation of the stone column increased k_s by about 30 % compared with the soil only specimens; this improvement was observed in all deformation levels. It was also observed that the subgrade modulus of reaction was decreased with the increase of deformation level.

A comparison between test results and the calculated modulus of subgrade reaction using equation (4.3) can be seen in Table 4.4 which shows good agreement as the empirical equation is dependent only on the ultimate stresses.

Table 4.4 Modulus of subgrade reaction

Settlement (mm)	$q_{ult-soil}$ **(kPa)**	**Calculated** $(k_s)_{soil}$ **(kN/m^2/m)**	**Lab result** $(k_s)_{soil}$ **(kN/m^2/m)**	$q_{ult-soil/col}$ **(kPa)**	**Calculated** $(k_s)_{soil/col}$ **(kN/m^2/m)**	**Lab. Result** $(k_s)_{soil/col}$ **(kN/m^2/m)**
6	61	9760	10000	90	14400	14500
10	61	5063	6200	90	7470	9000

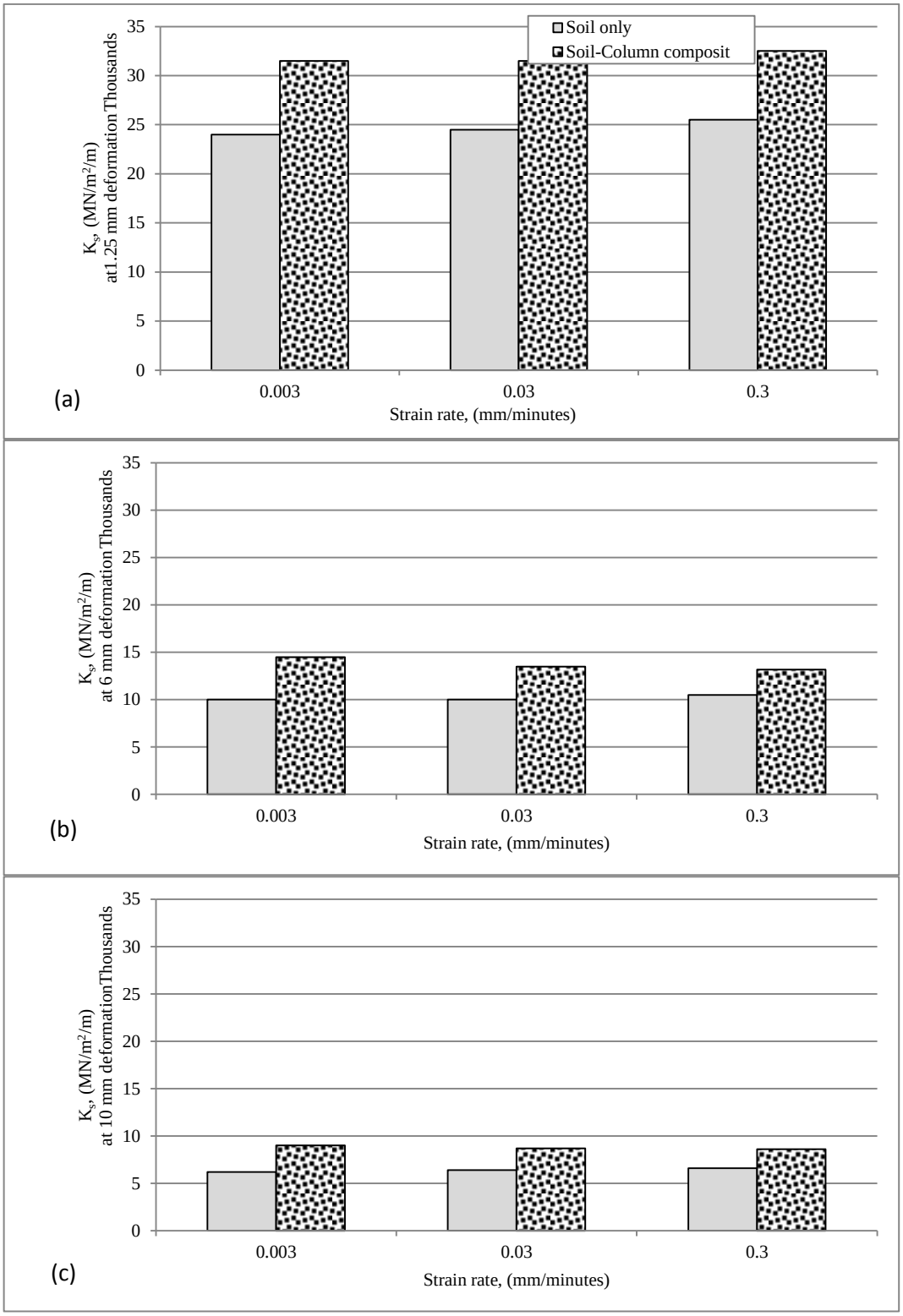

Figure 4.10 The subgrade modulus of reaction (k_s) for both soils (with no column and soil/ stone column composit) at a) at settlement of 1.25 mm; b) at settlement of 6 mm; and c) at settlement of 10 mm

4.2.5 Effect of Column Density

Most of the widely adopted design methods used for predicting bearing capacity of stone columns are mainly dependent on two factors, shear strength of the surrounding soil and the internal angle of friction of the column material (as discussed in Section 2.6). In the specific case of constant surrounding soil properties, the friction angle of a fill material (i.e. granular soil) plays a crucial role in estimating stresses that the soil/ stone column composite can carry. This friction angle is dependent on many factors such as the magnitude of stresses; relative density; and on the size and shape of soil particles (Bolton, 1991).

The impact of density on the shear strength of granular material has been widely investigated, however, very limited information on the influence of this factor on the stone column application is available. This might be due to that the final diameter of the column is only roughly known which makes the estimation of density unreliable.

Generally, for a given material, the internal angle of friction decreases with the reduction in density, which in itself is substantially influenced by the particle size distribution.

In this study, columns were constructed with three different densities 1805, 1642, and 1500 kg/m^3 representing relative densities of 80, 42, and 2% respectively. All tests were conducted at the same effective confining pressure of 100 kPa and same strain rate of 0.03 mm/minute. The stress-strain results are shown in Figure 4.11. These results show that the degree of improvement was influenced by the increase column density.

Firstly, for columns made at the loose density (1500 kg/m^3) (columns were installed by pouring the aggregate from 500 mm height with no compaction was applied (simulating a condition close to the minimum dry density of 1490 kg/m^3, (maximum void ratio))) there was about 25 % improvement.

At the second test where the density was increased by applying compaction to the column (the material was filled in two layers and 10 tamps were applied each time by 1.5 kg rod) the improvement was increased to 28 %.

At the final test the column material was compacted to achieve the a density close to the maximum density, the deviator stress reach its maximum at about 90 kPa which is about 31 % improvement in bearing capacity.

The variation of bearing improvement ratio q_t/q_{unt} versus the relative density D_r is shown in Figure 4.12. This indicates that the relative density may have a significant influence in increasing the strength of soil/column system and accordingly the bearing capacity of the ground.

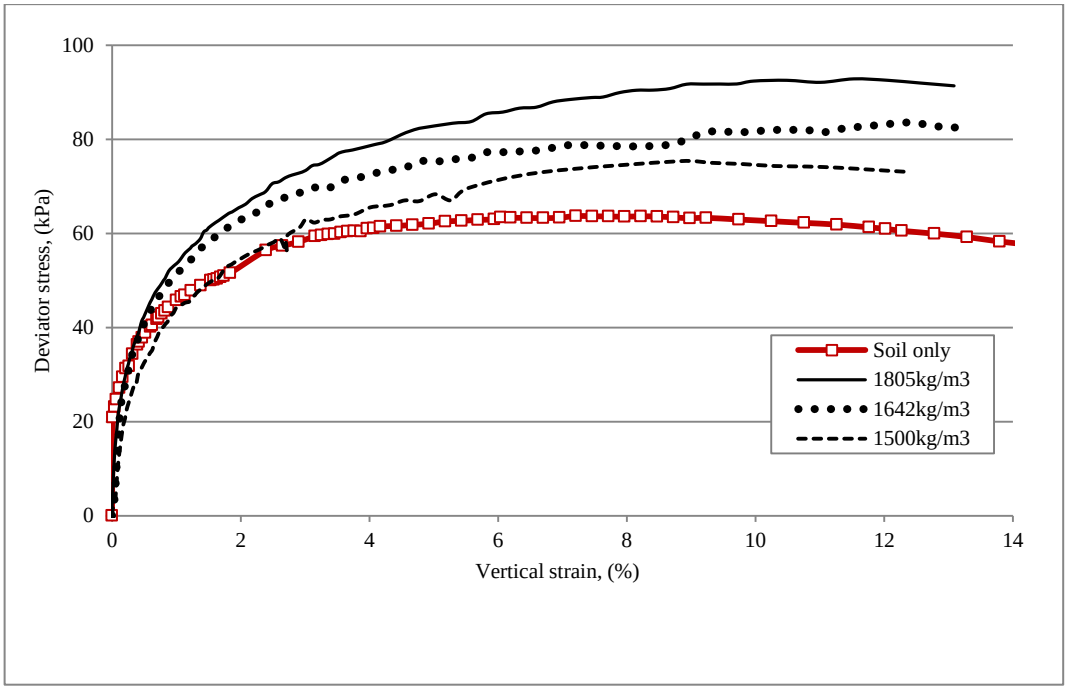

Figure 4.11 The stress-strain for different column densities

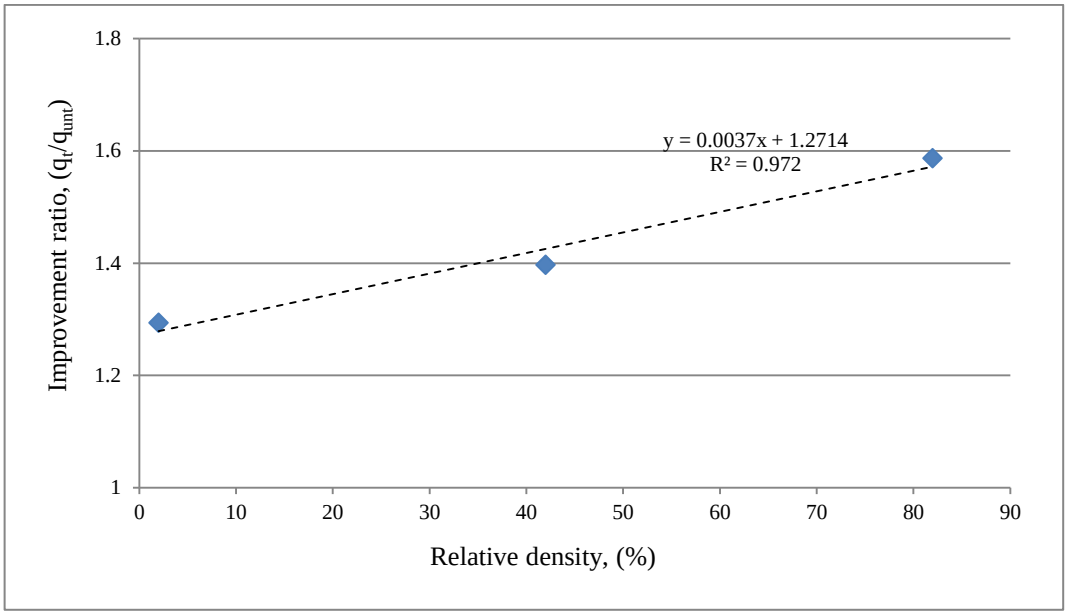

Figure 4.12 Improvement ratio versus the relative density

The pore pressure behaviour showed independency from the change in column density as can be seen in Figure 4.13 which shows the measurements of pore water pressures against the axial strain.

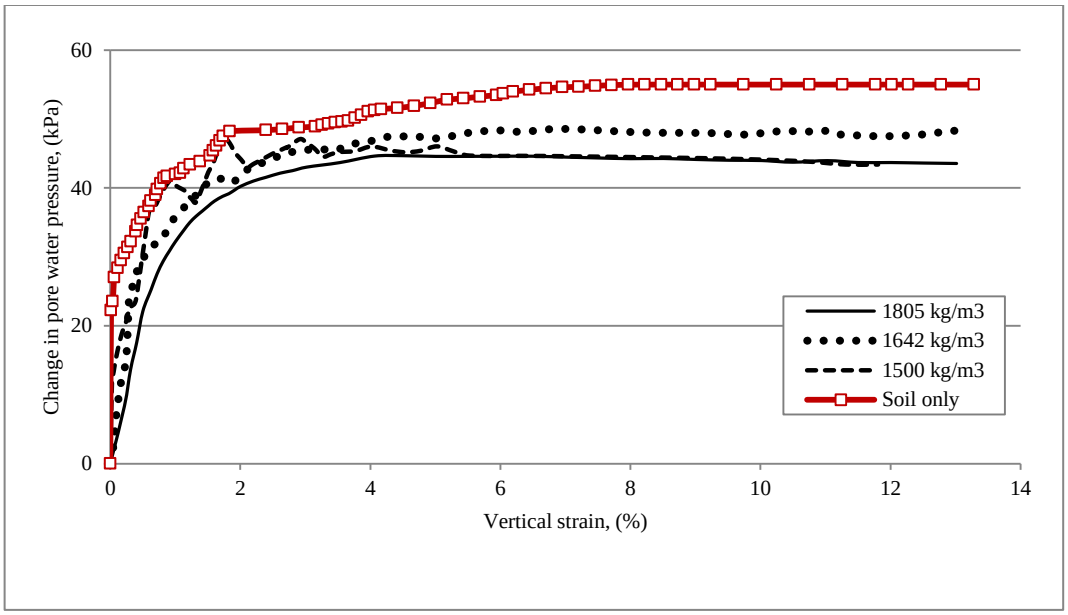

Figure 4.13 Change of pore pressure with column density

Results of this study together with these of other researchers are shown in Figure 4.14 in terms of maximum deviator stress to effective confining pressure ratio (q/σ_3'). Results show a general trend represented by the following equation:

$$\frac{q}{\sigma_3'} = 0.056\,(\gamma_d) + 0.0972 \qquad 4.8$$

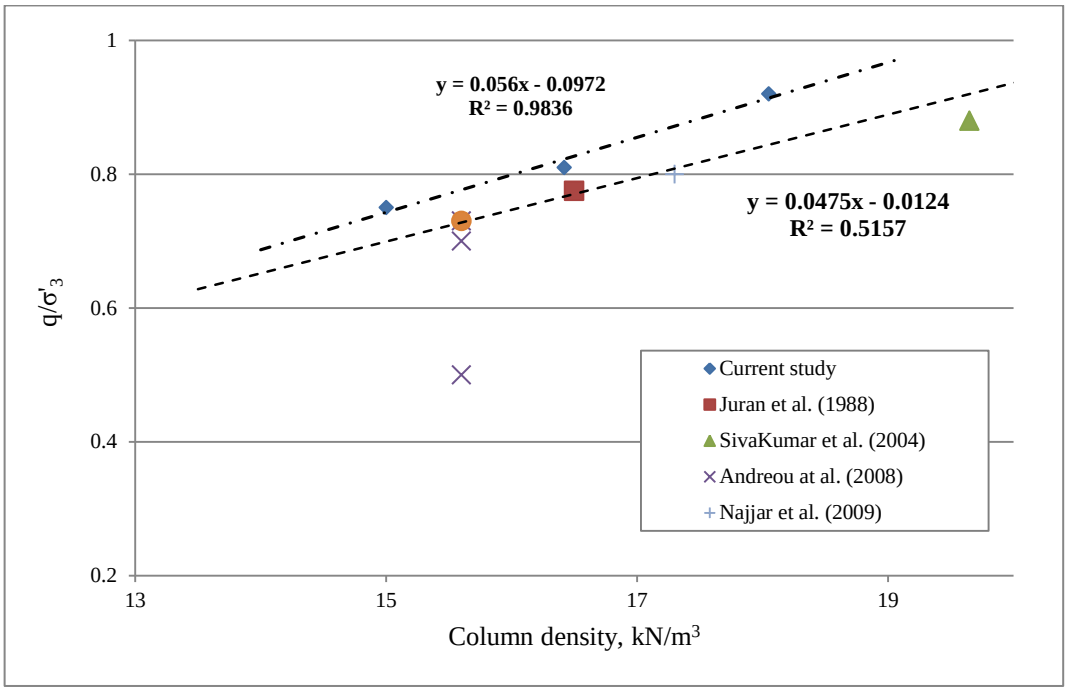

Figure 4.14 normalised deviator stress against column density

To conclude any reduction in relative density of the column leads to a reduction in the bearing capacity of about 14 % (midpoint of upper and lower bounds). This could be due to a reduction in the peak internal angle of friction of the column material and this might be related to the increase in the dilation angle of the column particle. Therefore, it might be ideal when designing stone columns to use the critical angle of friction which is function of both the peak shear angle and the angle of dilatancy.

4.3 Model II (Large Scale Test: Foundation Test)

Specimens were prepared and tested under the conditions explained in Sections 3.8.1 to 3.8.3. The specimens were tested under a confined pressure of 120 kPa which was maintained during the whole test procedure, aiming to simulate the surcharge on the ground in the field.

The model foundation was loaded at a constant strain rate of 0.03 mm/min, because It was concluded from the previous tests (i.e. triaxial model) that this rate was sufficient to allow excess pore water pressures to dissipate. The test was stopped when the footing displacement reached about 40 mm (15 % of deformation).

Three pore water pressures transducers placed in different locations at the base of the specimen as (see Section 3.5) monitored readings throughout.

The main aim of these large tests was to investigate the condition within which the lateral pressure distributed along the depth of the column (typically increase with the increase in depth (Bowles, 1996)). Thus the mode of failure is investigated in more detail than that in the triaxial condition.

4.3.1 Load - Displacement Relationship

Typical load-displacement relationship for both the reinforced and unreinforced soils are presented in Figure 4.15. The maximum load carrying capacity of soil (no column) specimen was found to be about 0.7 kN (equivalent to bearing pressure of 200 kPa). Penetration of 35 mm was required to achieve this. This bearing capacity was close to the predicted value of 171.6 kPa (16 % under estimated) based on the following relationship:

$$q_{ult} = c_u N_c + q N_q \qquad 4.9$$

Where c_u is the undrained shear strength of the soft soil (12 kPa), and N_c, N_q are the bearing capacity factor (value of 5.14 and 1 respectively for zero internal angle of friction ($\varphi = 0$)) and q is the surcharge pressure.

This value was approximately doubled when the 28 mm diameter column was installed beneath the foundation of 70 mm diameter. Bearing capacity of the stone column reinforced foundation was approximately 435 kPa (1.7 kN load capacity).

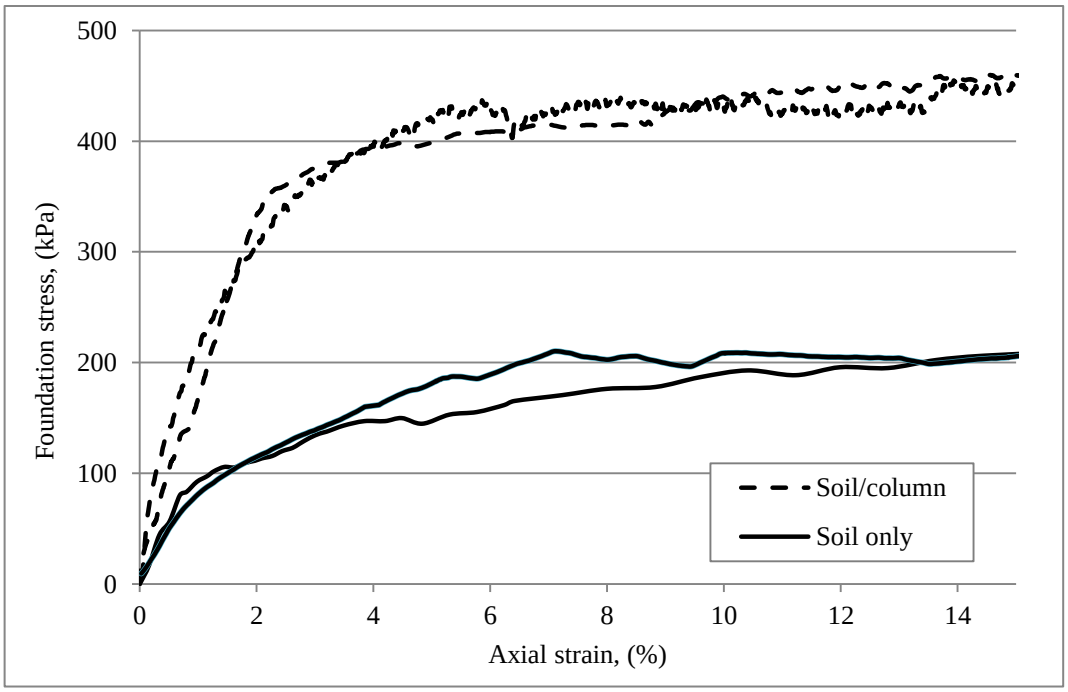

Figure 4.15 stress-strain relationship

Bearing capacity estimation

A reasonable agreement (within 13 %) between measured and predicted values was achieved, which using the expression proposed by (Hughes and Withers, 1974) (Equation 4.10). This was not surprising due to the fact that the empirical method considered only the influence of strength of the surrounding soil and the degree of the internal friction, but not the effect of

area replacement ratio and the column density as discussed in chapter two (sections 2.7.1.2-2.7.1.4).

$$\sigma_v = \left(\frac{1+\sin\emptyset'}{1-\sin\emptyset'}\right)\left(4c_u + \sigma_{r_0'}\right) \quad 4.10$$

Where $\emptyset'$ is the friction angle of the stone column material; $\sigma_{r_0'}$ is the effective in situ lateral stress and assumed to be $2c_u$; and c_u is the undrained shear strength of the soil and equals to 12 kPa. The predicted value was 485 kPa assuming a factor of safety of 1 to allow the comparison.

In addition to this, the degree of improvement was comparable with other researcher's results as can be noted in Table 4.5. The load bearing capacity ratios for before and after reinforcement over similar test conditions ranged between 2 and 4.

Results included laboratory, field, and numerical studies on the improvement provided by stone column are summarised in Table 4.5. Most of methods used to predict the bearing capacity of a stone column considered the soil shear strength and the angle of shearing resistance of the column material and ignoring the influence of column diameter (area replacement ratio).

This database was used to developed a simple linear model to predict the ultimate bearing capacity of reinforced soil as a function of c_u, A_s, and $\emptyset$. (more information available in Appendix D)

Figure 4.16 shows a scatter plot matrix between all variables. The bottom row of this scatter plot matrix gives the scatter plots of q_{ult} against each of the other three input variables. Additionally, the univariate relationship between our outcome variable q_{ult} and the input variables c_u, A_s, and $\emptyset$.

Table 4.5 Published database

Reference	c_u, (kP	Φ (o)	D_c mm	Sample size mm	A_S, (%)	$q_{untreated}$ (kPa)	$q_{treated}$ (kPa)	$q_{treated}/q_{untreated}$
Wood et al. (2000)	10.5	25	17.5	D= 300	30	84	105	1.25
Wood et al. (2000)	10	25	11	D= 300	24	84	90	1.07
Wood et al. (2000)	10	25	11	D= 300	10	84	86	1.02
Andereou et al. (2008)	20	32	20	D= 100, H= 200	4	55	62	1.13
Najjar et al. (2010)	20	33	20	D= 70.9, H= 141	7.9	62	75	1.21
Najjar et al. (2010)	20	33	30	D= 70.9, H= 141	17.8	67	100	1.49
Najjar et al. (2010)	20	33	20	D= 70.9, H= 141	7.9	84	101	1.20
Najjar et al. (2010)	20	33	30	D= 70.9, H= 141	17.8	84	148	1.76
Sivakumar et al. (2004)	25	35	32	D= 100, H= 200	10.2	60	83	1.38
Black et al. (2006)	25	35	25	D= 300, H= 400	17	1.25	2	1.60
Bergado et al. (1987)	20	35	300	Field Test	6.25	175	221	1.26
Hughes and Withers (1974)	19	35	38	225*160*150	40	171	418	2.44
Bergado et al. (1987)	20	37	300	Field Test	6.25	175	314	1.79
Juran and Guermazi (1988)	30	38	20	D= 100, H= 200	4	120	154	1.28
Ali et al. (2014)	7	38	30	D= 300, H= 550	25	25	70	2.80
Kim and Lee (2005)	4	38	22	250*100*250	30	30	75	2.50
Kim and Lee (2005)	4	38	22	250*100*250	40	45	135	3.00
Kim and Lee (2005)	4	38	22	250*100*250	50	45	155	3.44
Bergado et al. (1987)	20	39	300	Field Test	6.25	175	320	1.83
Bergado et al. (1987); st. Helens	30	42	600	Field Test	65	60	270	4.50
Bergado et al. (1987); Canvey	20	42	-	Field Test	28	95	240	2.53
Humber Bridge	25	42	-	Field Test	11	115	270	2.35
Black et al. (2011)	35	43	25	D= 300, H= 400	17	240	680	2.83
Black et al. (2011)	35	43	23	D= 300, H= 400	28	230	750	3.26
Black et al. (2011)	35	43	38	D= 300, H= 400	40	230	820	3.57
Bergado et al. (1987)	20	43	-	Field Test	6.25	175	370	2.11
Ambily and Gandhi (2007)	7	43	100	D= 830, H= 450	19	75	160	2.13
Ambily and Gandhi (2007)	14	43	100	D= 830, H= 450	19	88	350	3.98
Ambily and Gandhi (2007)	30	43	100	D= 830, H= 450	19	150	770	5.13
Ambily and Gandhi (2007)	30	43	100	D= 210, H= 450	5	150	600	4.00
Ambily and Gandhi (2007)	30	43	100	D= 420, H= 450	9	150	680	4.53
Ambily and Gandhi (2007)	30	43	100	D= 830, H= 450	19	150	770	5.13
Zahmatkesh and Choobbasti (2012)	5	43	800	F.E. PLAXIS	10	80	165	2.06
Zahmatkesh and Choobbasti (2012)	5	43	1000	F.E. PLAXIS	20	80	170	2.13
Zahmatkesh and Choobbasti (2012)	5	43	1200	F.E. PLAXIS	30	80	280	3.50
Watts et al. (2000)	40	45	600	Field Test	44	12	248	20.67
Current study (Model I)	12	48	28	D= 100, H= 200	5	55	90	1.63
Current study (Model II)	12	48	28	D= 300, H= 300	13	140	428	3.06
Kim and Lee (2005)	4	49	22	250*100*250	30	40	150	3.75
Kim and Lee (2005)	4	49	22	250*100*250	40	40	165	4.13
Kim and Lee (2005)	4	49	22	250*100*250	50	40	215	5.38

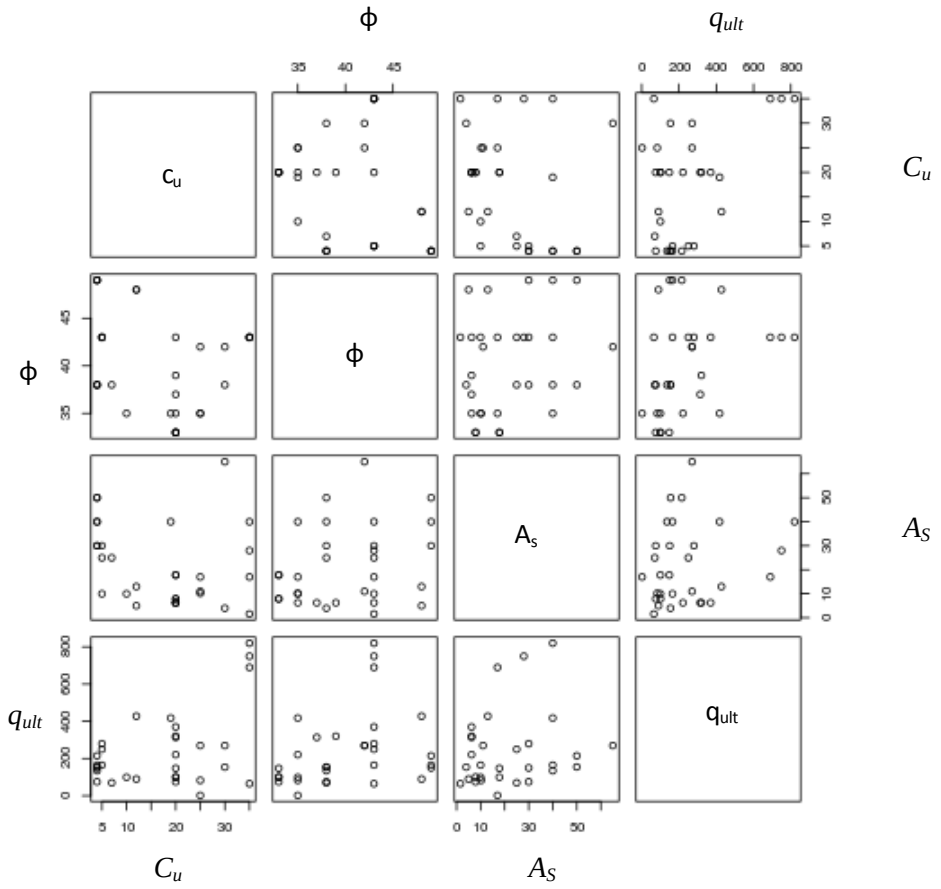

Figure 4.16 Scatter plot of all the variables

Regression analysis is a powerful technique that can be used to address various research questions. In this report, this was used to check how q levels are affected by A_s; c_u and ∅. In particular, the type of regression we are going to use is

Multiple linear regressions were used to process the data presented database, in order to determine the best-fitting line through the data points (this line is sometimes referred to as the regression line). Multiple means we have more than one input variable (also known as predictor); hence, we are trying to fit a plane or hyper-plane rather than a line (i.e. Combining all the input variables by conducting a coefficient multiplied by each variable, and then summing these variables). The idea was to use a linear combination of input variables to

model their relationship with an output variable (q_{ult}). After using R's lm() function, the model looks as follows:

$$q_{ult} = -609.893 + 11.313 * c_u + 3.167 * A_s + 14.629 * \emptyset \qquad 4.11$$

By examining equation 4.11, we observe that when fixing ∅ and A_S, an increase, or decrease, of c_u by one unit, causes an increase, or decrease, in q_{ult} by 11.313 units. Similarly, when fixing c_u and A_S, an increase, or decrease, of ∅ by one unit, causes an increase, or decrease, in q_{ult} by 14.629 units. Also, when fixing c_u and ∅, an increase, or decrease, of A_S by one unit, causes an increase, or decrease, in q_{ult} by 3.167 units.

Table 4.6 shows the values of four diagnostics that were used to examine the goodness of fit of a model. Namely, these were: Deviance, BIC, R^2, Adjusted R^2 and the Residuals (these factors were defined in Appendix D). As shown in this table the regression model has a coefficient of determination R^2 of 0.44, in other words 44% of the variation in the data can be explained using the best fitting represented by Equation 4.11.

Table 4.6 Deviance, BIC, R-Squared and Adjusted R^2 values

Deviance	BIC Value	R^2	Adj R^2
682279.8	415.1196	0.4448661	0.3831845

These data is also presented in Figure 4.17. The ultimate bearing capacity of the reinforced soil measurements were normalised by dividing it by the soils bearing capacity before reinforcement and plotted against the area replacement in terms of internal angle of friction of the column material creating a linear relationships between the bearing capacity ratio and the area replacement ratio at different internal angle of friction as presented in equations 4.12-4.15:

$$for\ \emptyset\ between\ (33^o - 35^o);\ q_{ratio} = 3.6 * A_s + 0.91 \quad 4.12$$

$$for\ \emptyset\ between\ (37^o - 39^o);\ q_{ratio} = 4.1 * A_s + 1.40 \quad 4.13$$

$$for\ \emptyset\ between\ (42^o - 45^o);\ q_{ratio} = 4.0 * A_s + 2.00 \quad 4.14$$

$$for\ \emptyset\ between\ (48^o - 49^o);\ q_{ratio} = 4.30 * A_s + 2.50 \quad 4.15$$

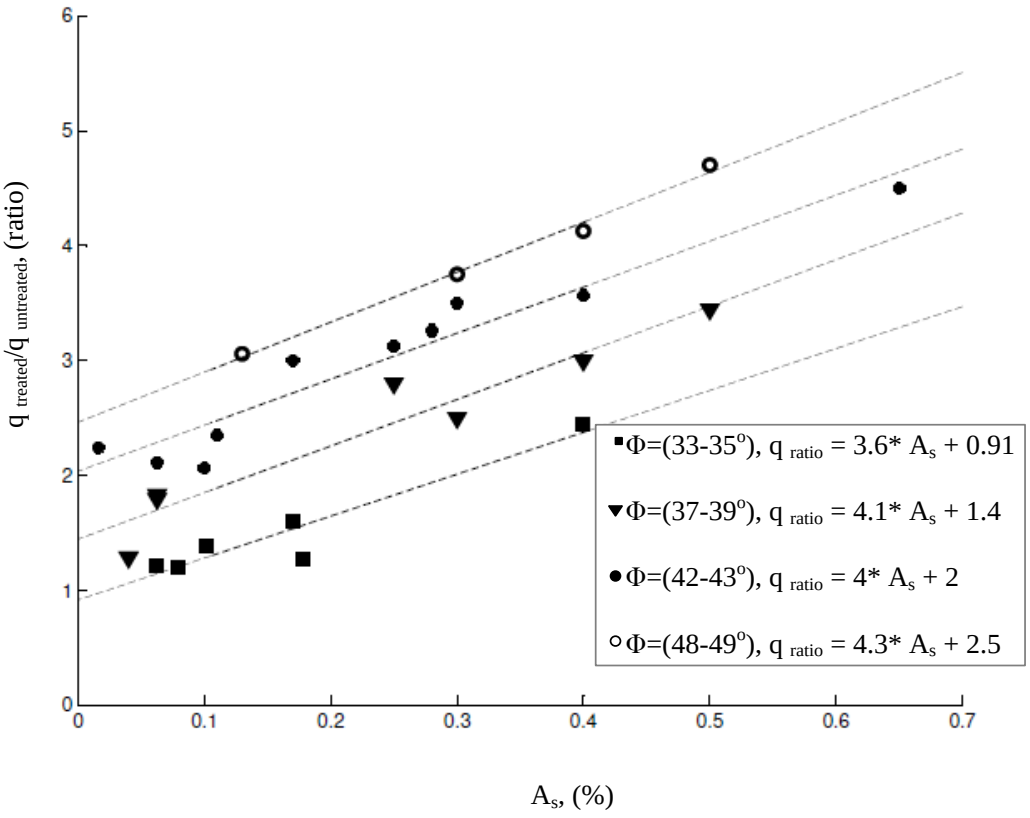

Figure 4.17 Relationship between q_{ratio} and A_s in terms of ∅

Settlement estimation:

Various design approaches used for estimating settlement of a stone column – soil system, as explained in the literature (section 2.6.2). They are based on the unit cell assumption. Priebe's method for settlement prediction is one of these approaches and considered to be the most

commonly used in practice. In order to compare test results, from this study firstly, one dimensional settlement for the soil only was calculated using the following formula:

$$S_0 = m_v \Delta\sigma_z H \qquad 4.16$$

Where m_v is the coefficient of volume compressibility of clay; $\Delta\sigma_z$ is the vertical stress at depth z due to the applied pressure at the surface and equals to (I_g P_0);(I_g is the Influence facto for the increase in vertical stress, P_0 is the imposed load) and H is the thickness of the soil layer.

Secondly, the settlement improvement factor was determined using the area replacement and angle of shearing resistance of column material relationship proposed in Priebe's method. As illustrated in chapter two (section 2.6.2.3). The internal angle of shearing resistance ranged between 35^o and 45^o, thus a value of 45^o was used to predict the improvement factor.

For example, based on the test conducted in this study, settlement estimation was based on Equation 4.16, where I_g = 0.64644, and P_0 = 100 kPa, leading to $\Delta\sigma_z$ = 64.64 kPa, also using m_v as 9.803* 10^{-4} m^2/kN (Section (3.3.6)). Settlement was estimated to be about 18 mm for the clay only; and then the settlement of the reinforced soil can be estimated by dividing the estimated settlement of the unreinforced soil by the improvement factor (n_0) of 2.8 (obtained from Priebe's charts, Figure 2.9) resulting in a value of 6.4 mm, which was about six times higher than the measured one. Although Priebe's method demonstrated an overestimation to the settlement of the reinforced soil, which confirmed the findings of Bouassida et al. (2003) and Ellouze et al. (2010), the measured improvement factor of 2.1 showed reasonable agreement with similar studies (Ambily and Gandhi, 2007; Black et al., 2011).

4.3.2 Change in Pore Water Pressure

Pore water pressure transducers PPT1,PPT2, and PPT3 were fitted at the centre of base, 50 mm from the centre and 100 mm from the centre respectively. Figures 4.18 and 4.19 show results during the foundation loading on the soil (only) and soil/ stone column composite specimens. When soils (no column) were tested, pore water pressure was seen to increase only at PPT1 (the midpoint) when loading the foundation to about 3 kPa, while in the other two (PPT2 and PPT3) transducers there were no observed change during the test.

On the other hand, when the column was installed, the PPT3 (close to the tank wall) did not show any change in pore water pressure measurements during the loading. There was gradual increase by about 5 kPa in pore water pressure at PPT2 (50 mm from the column); and beneath the column at the centre of the specimen (PPT1), the pore water pressure build-up rapidly after 20 mm (7 %) of footing settlement to approach approximately 20 kPa, then it started dissipating. This confirms that the column carried larger part of the load compared to the surrounding soil. Also when the pore water pressure stopped building up under the column and still increasing beneath the soil could indicate that the failure of the column had occurred.

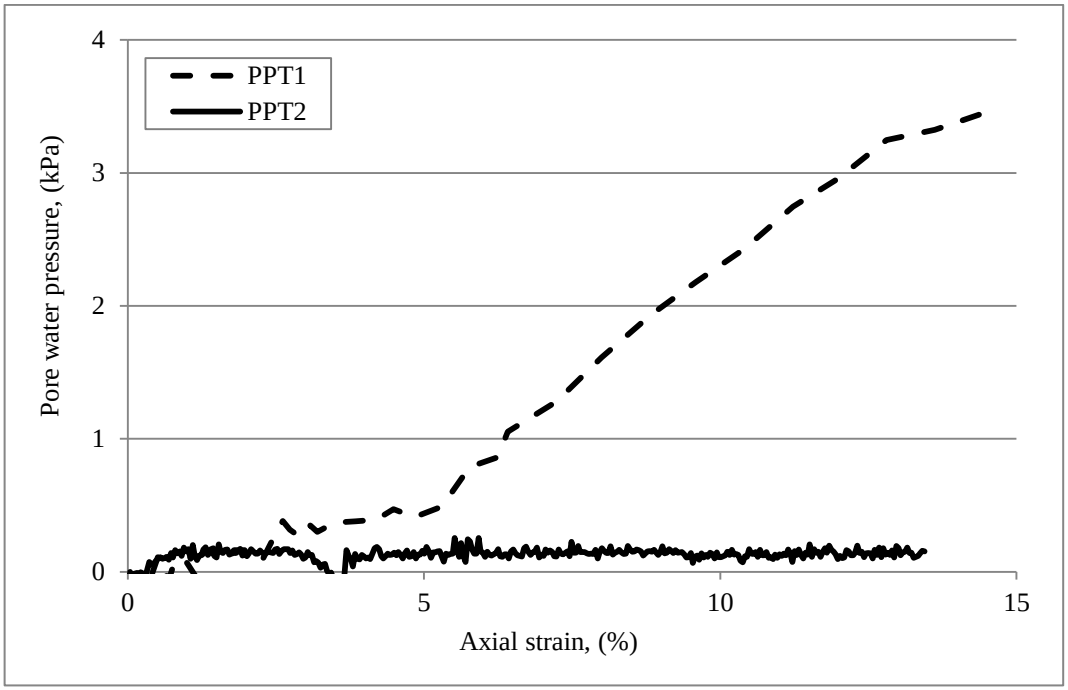

Figure 4.18 Typical results for changes in pore water pressure for soil (no column) specimens

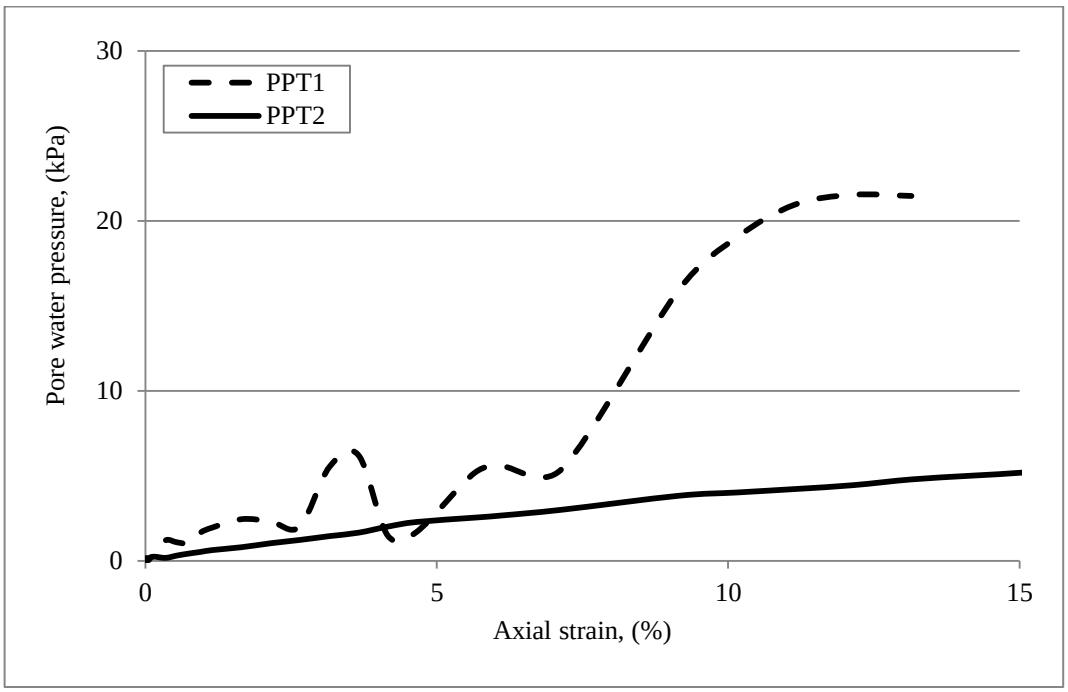

Figure 4.19 Typical results for changes in pore water pressure for soil/stone column specimens

4.3.3 Post Testing Investigation

In order to investigate the quality of the prepared clay bed, a series of shear vane tests were carried out at different positions to determine the undrained shear strength of the clay surrounding the column. Strength measurements are shown in Figure 4.20. The undrained shear strength was determined at (50, 100, 150, and 200 mm) depth and at four horizontal positions (around the midway between the column and the tank wall). In addition to this, water content measurements were made at the same levels as shown in Figure 4.21. Comparing both before and after testing for the shear vane results and water content, it can be observed that at the first 50 mm thickness of the soil there was an increase in the soil strength of about 12% this increase was accompanied by a reduction in water content of almost 1%.

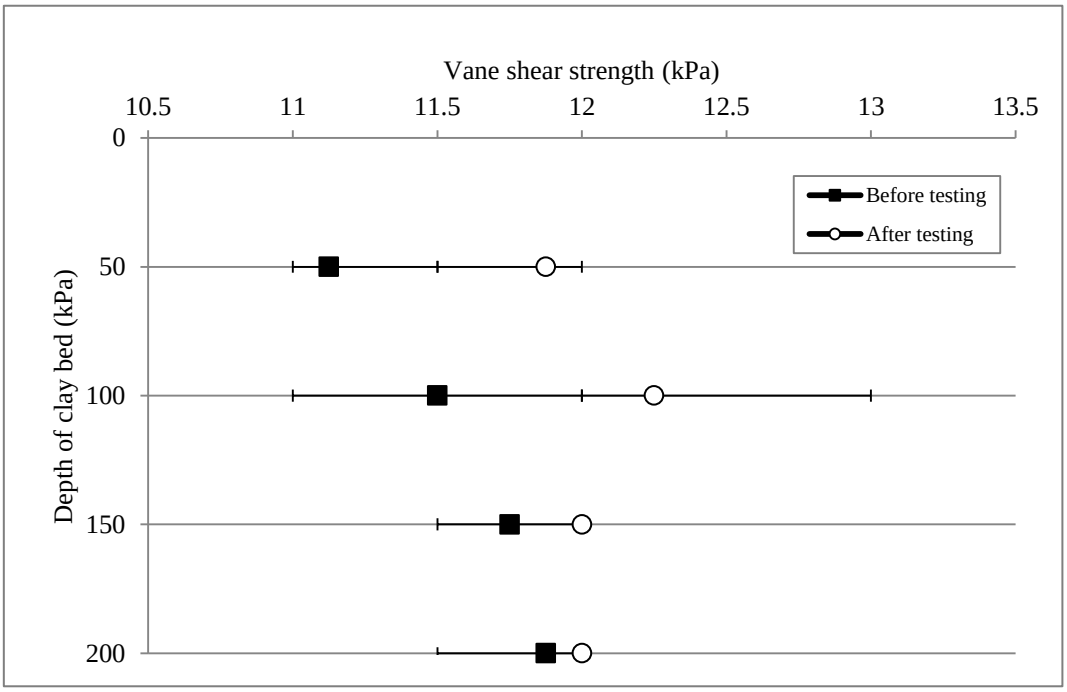

Figure 4.20 Hand vane shear test results before and after testing

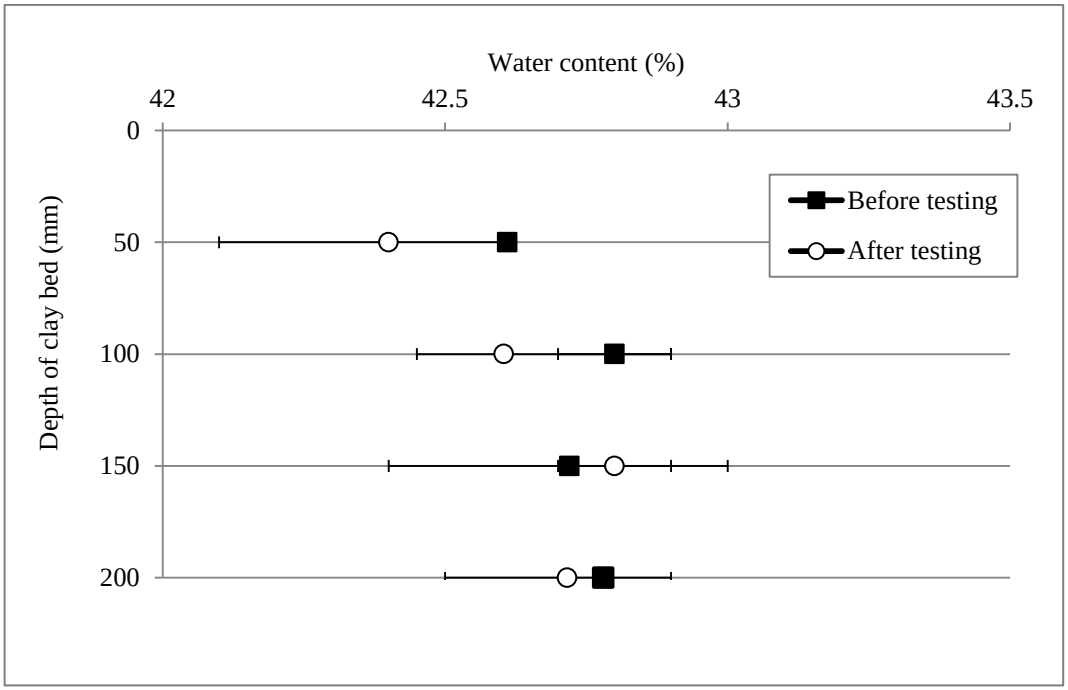

Figure 4.21 Water content variation before and after testing

After each test, the specimens were removed from the cell and split vertically along their diameter to examine the mode of failure. A typical example is shown in Figure 4.22. In most cases column bulge, took place at approximately at 120 mm below the surface, which is about 1.7 times the column diameter. This was very close to the expected value of 2 to 3 times the column diameter suggested by Hughes and Withers (1974).

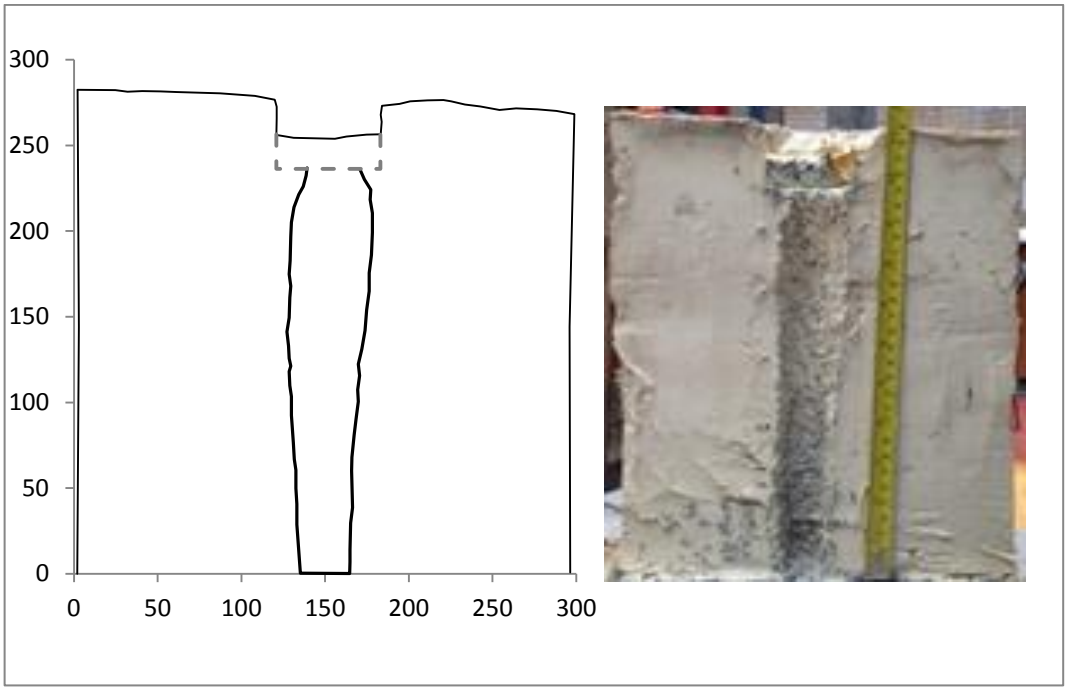

Figure 4.22 Deformation pattern

4.4 Concluding Remarks

A series of undrained triaxial and reduced scale foundation model tests were carried out in order to investigate the influence of strain rate and column material density on the behaviour and performance of soft clay deposits reinforced with a stone column.

Results showed that there was a considerable improvement in load carrying capacity and stiffness of soft clay when stone column was installed. For example, replacing a small part of soft soil (7 %) with granular materials that have a comparably a high angle of shear resistance (48^{o}) leads to an increase in bearing capacity and soil stiffness of approximately 30 % and reduces the settlement by about 80 % compared with the settlement of unreinforced soils.

Although results from this study showed reasonable agreement with empirical estimations and other published works in terms of load bearing capacity, observed settlement behaviour

showed a conservative figure not least when compared with the settlement estimated using Priebe's method.

Strain rate did not appear to have a significant influence on the level of improvements, where results show that there is a decrease of less than 10 % in deviator stress for second order of magnitude in change in rate of strain.

There was a strong indication suggests that the relative density of the column material may have a significant influence on column bearing capacity. For example, increasing the column density by about 25 % leads to an increase in soil/ stone column composite capacity of about 17 %.

CHAPTER 5

CYCLIC LOADING RESULTS AND DISCUSSION

5.1 Introduction

This chapter presents results of both the undrained cyclic triaxial tests (Model I) and cyclic foundation tests on large scale model (Model II) carried out on both soft clay and soft clay /stone column composite. Dynamic stress levels ranging between 50 to 70 kPa (equivalent to cyclic stress ratio (CSR) from 0.6 to 0.8) and frequencies ranging between 0.5 to 3Hz were used, as described in Sections 3.7.1 and 3.7.2. All tests were conducted at an effective confining pressure of 100 kPa. Comparison is made between the behaviour of the soft clay soils with and without stone column installation.

Change in pore water pressure and deformation with number of cycles were examined. The latter was used to identify threshold value of stress ratio. The variables examined during this stage of the study are shown in Table 5.1

Table 5.1 Summary varibles investigated using cyclic triaxial test

Soil type	Test	P_{max} (kN)	P_{min} (kN)	σ'_{cyclic} (kPa)	CSR	Loading frequency (*Hz*)
Stone column / soil system	**TRI-C.C-12**	0.8	0.2	70	0.8	0.5
	TRI-C.C-13	0.7	0.2	60	0.7	
	TRI-C.C-14	0.6	0.2	50	0.6	
	TRI-C.C-15	0.8	0.2	70	0.8	1.0
	TRI-C.C-16	0.7	0.2	60	0.7	
	TRI-C.C-17	0.6	0.2	50	0.6	
	TRI-C.C-18	0.8	0.2	70	0.8	3.0
	TRI-C.C-19	0.7	0.2	60	0.7	
	TRI-C.C-20	0.6	0.2	50	0.6	
Soil only	**TRI-C-21**	0.7	0.2	60	0.7	0.5
	TRI-C-22	0.6	0.2	50	0.6	
	TRI-C-23	0.7	0.2	60	0.7	1
	TRI-C-24	0.6	0.2	50	0.6	
	TRI-C-25	0.7	0.2	60	0.7	3
	TRI-C-26	0.6	0.2	50	0.6	

5.2 Model I (Triaxial Tests)

5.2.1 Permanent Strain during Cyclic Loading

Typical results of cyclic undrained triaxial tests are shown in Figures 5.1-5.3, which shows permanent axial strain against number of cycles. Results show the influence of cyclic stress levels (50, 60 and 70 kPa) at different loading frequency (0.5, 1 and 3 Hz) on the deformation pattern for soft soil specimens (no column) and soft soil/ stone column specimens. All specimens were subject to a number of cycles of 10000 cycles, apart from those whom failed before completing the test.

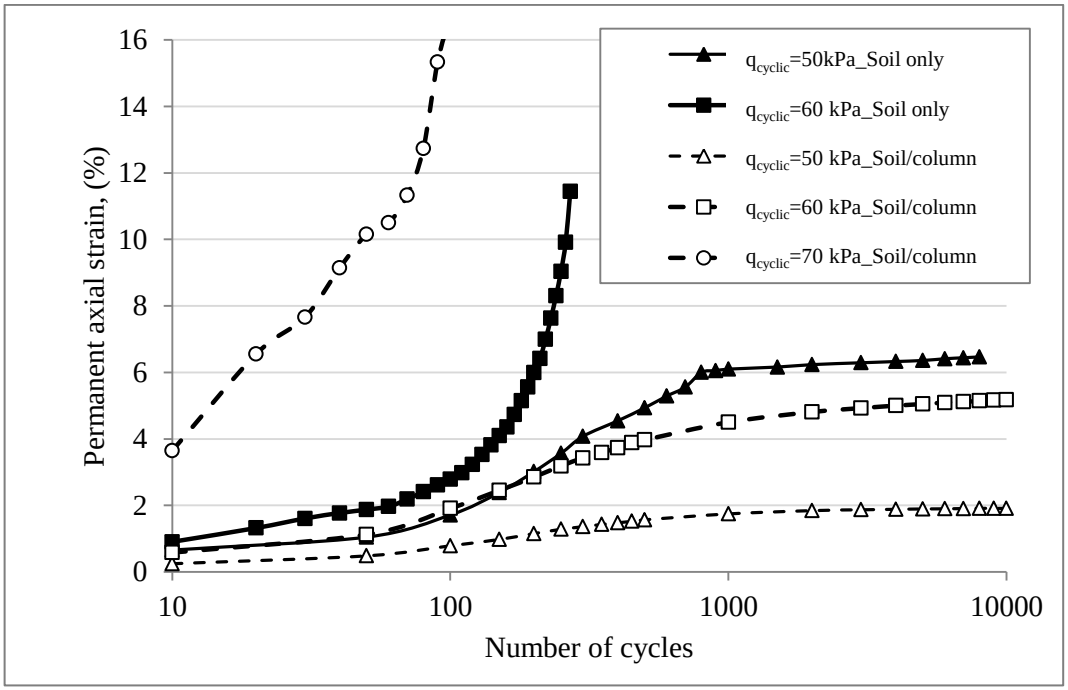

Figure 5.1 Pemanent axial strain and number of cycles relationship: at 0.5Hz loading frequency

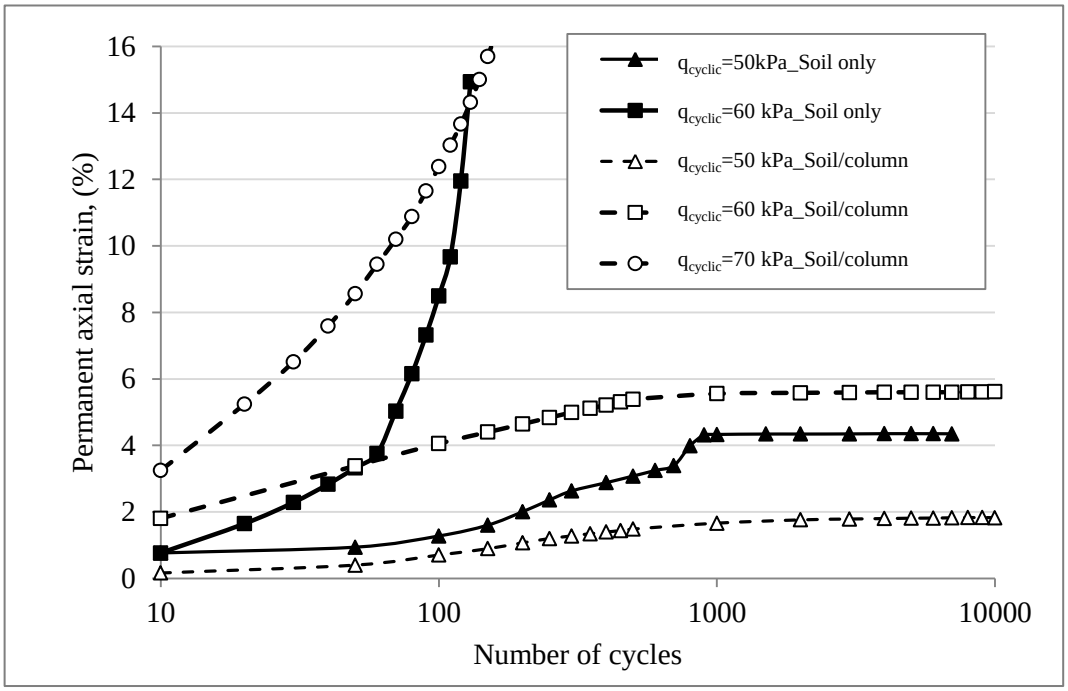

Figure 5.2 Pemanent axial strain and number of cycles relationship: at 1 Hz loading frequency

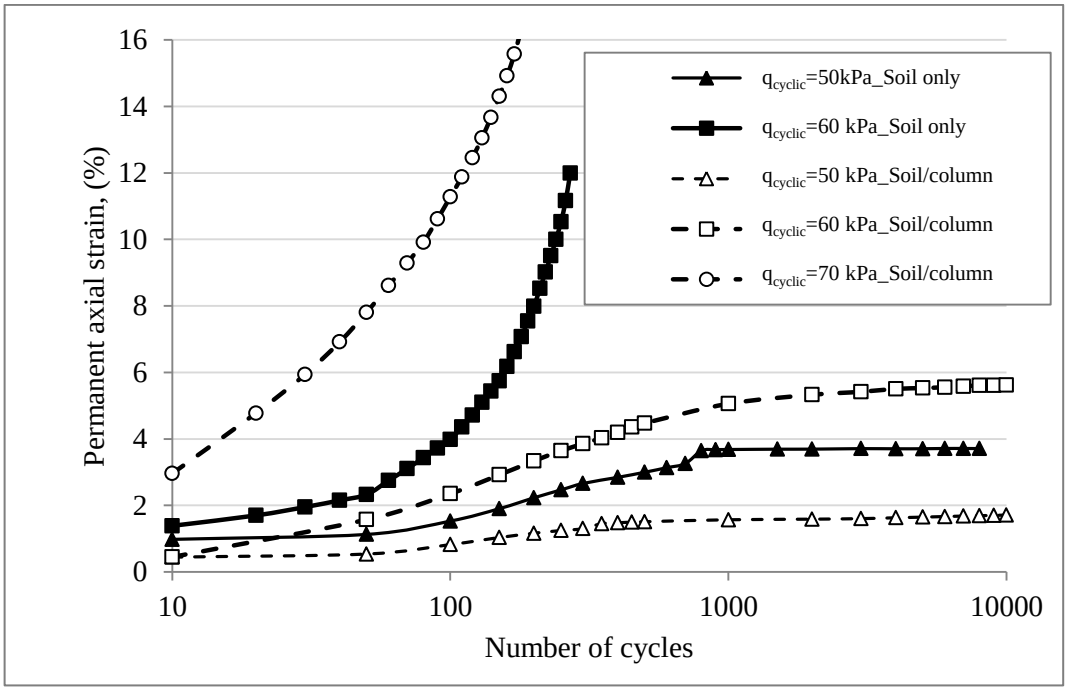

Figure 5.3 Pemanent axial strain and number of cycles relationship: at 3 Hz loading frequency

It can be noted that, for both soil (no column) and soil/ stone column composite, the progress of cumulative strain was highly influenced by increases in cyclic deviator stress applied hence CSR. However, in the range of the loading frequencies examined, soils (no column) specimens were more sensitive to the change of frequency than the soil/ stone column composite.

Results in Figures 5.1 to 5.3 showed that the permanent axial strains for soils specimens (no column) were larger at lower frequency (0.5 Hz) and decreases with the increase in loading frequency, for instance, when specimens were subjected to a cyclic stress of 50 kPa, the permanent axial strains after 10000 cycle were 6.3, 4.4 and 6.3 % for frequencies 0.5, 1 and 3 Hz respectively. However, in soil/stone column system specimens the effect of frequency on permanent axial strain was very small (at 50 kPa cyclic stress they were 1.9, 1.8 and 1.6 % for frequencies 0.5, 1 and 3 Hz respectively).

In addition, the effect of the cyclic stress on the development of permanent strain was significant for both types of specimens. For example, when tests were performed at loading frequency of 1 Hz, results (Figure 5.2) showed that soil specimens (no column) at an applied cyclic stress of 50 kPa stabilised after 900 cycles at a strain level of 4.4 %, when the cyclic stress was increased to 60 kPa a shear failure occurred at less than 100 cycles of load applications. On the other hand, when the stone column was installed and specimens tested under a 50 kPa cyclic stress application, the progress of the permanent strain stabilised after 1000 cycle at a value of 1.8 %. This value increases to reach 5.6 % by increasing the cyclic stress to 60 kPa, and when the test was performed at a cyclic stress of 70 kPa the specimen was failed in a shear failure after 30 cycles. Similar behaviour was shown when specimens tested under the condition of other loading frequencies (0.5 and 3 Hz).

These results indicate that there can be a threshold stresses of 50 kPa and 60 kPa for soil (no column) specimens and soil/ stone column composite specimens respectively above which the total permanent strain increased rapidly with repeat load application; and failure can occur during the first few cycles. Normalising these dynamic stresses in terms of static vertical stress at failure for both types of specimens (with and without column) leads to have a CSR of about 0.75. From literature this value varies from 0.4 to 0.8 and often is assumed to be 0.5. (Seed et al., 1955; Heath et al., 1972; Brown et al., 1975; Brown, 1996; Andersen, 2004; Jiang et al., 2010; Cai et al., 2013) This variation in the value of the threshold stress could be due to the difference in the soil types and their physical properties.

5.2.1.1 Effect of Cyclic Deviator Stress on Permanent Strain

Figure 5.4 shows the influence of cyclic deviator stress on the permanent strain of both soil only and soil/column composite specimens at load applications of 100 and 1000 cycle and loading frequency of 1 Hz. Results showed that below the threshold stress level in soil (no

column) specimens were more sensitive to number of loading application than the reinforced samples. For example, at 50 kPa cyclic stress, the permanent strain increased from 1.7 to 4.4 % by increasing number of cycles from 100 to 1000 cycle. On the other hand, the influence of number of cycles were much smaller in case of soil/column specimens, where difference in permanent strain between 100 and 1000 cycles at similar stress level was about 0.9 %. This is probably due to the fact that the column materials were compacted due to load application, increasing the density of the column leading to greater resistance with lower settlement.

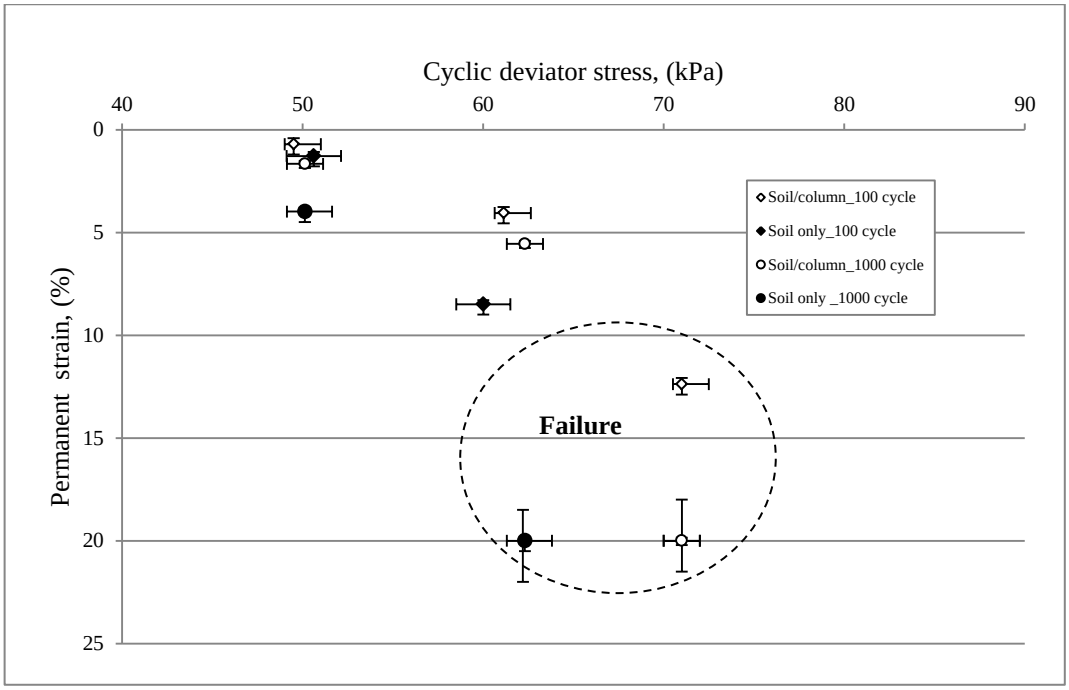

Figure 5.4 Effect of loading application and cyclic stress leve at frequency of 1 Hz

5.2.1.2 Effect of Loading Frequency on Permanent Strain

Frequency of cyclic load is believed to have an important influence on the dynamic properties of the saturated soft clay (Andersen et al., 1980), however, its effect is still attracting debate. Jian-hua Wang et al. (1998), Zhou and Gong (2001), and Jiang et al. (2010) indicated that

both accumulative permanent strain and pore water pressure induced by cyclic loading will increase with reduction in loading frequency. Whereas other published work indicated a different observation, where they reported that the change in frequency has little or no influence on the strength and deformation properties of soil (Ansal and Erken, 1989; Hyde et al., 1993).

In this current study, an increase in permanent deformation for the soil only specimens was observed with reduction in frequency of loading, as shown in Figure 5.5, for both soil specimens (with and without column) at load applications of 100, 1000 and 10000 cycles. All the test were undertaken at the same cyclic stress level (50 kPa) which was less than the threshold stress. For stone column reinforced specimens, the influence of loading frequency on the permanent stain was less pronounced compared with that for unreinforced specimens. Also the effect of number of cycles was negligible after 1000 cycle.

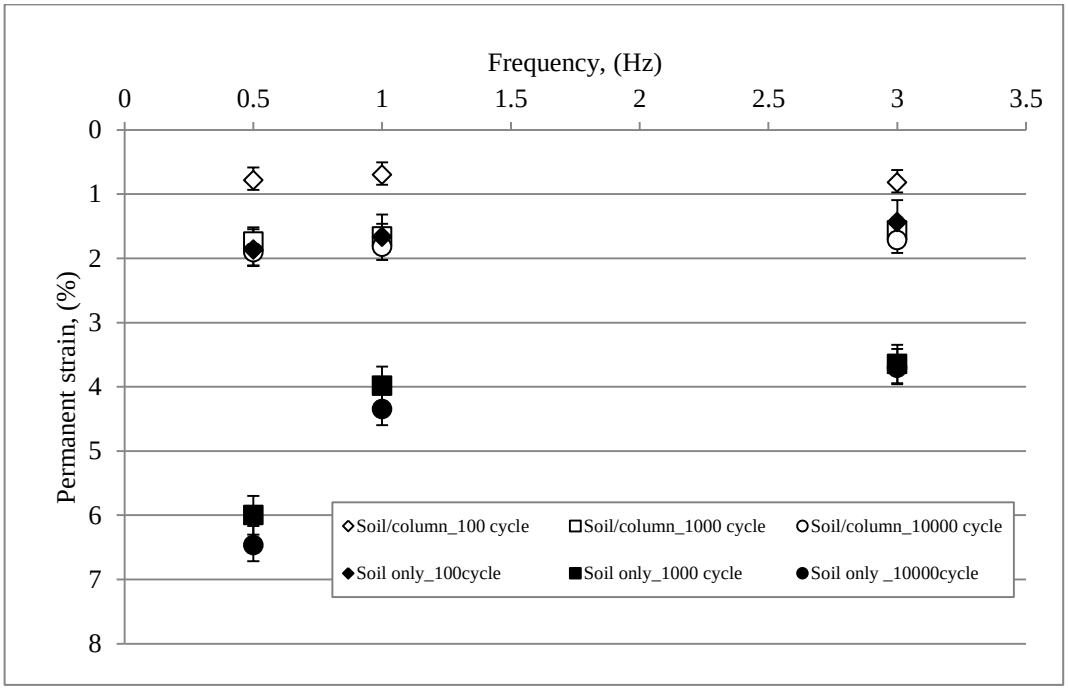

Figure 5.5 Effect of loading frequency and number of cycles under cyclic stress of 50 kPa.

5.2.1.3 Prediction of Permanent Strain

There are several models to predict permanent strain in soils subjected to cyclic loading conditions. The most commonly used is the power model which takes into account a number of factors such as number of loading cycles and both static and dynamic stresses (Li and Selig, 1996). This model is shown as follow:

$$\varepsilon_p = AN^b \qquad 5.1$$

Where ε_p is the permanent strain (cumulative strain) in %; *N* is the number of cycles; and *A* and b are material parameters (dependent in the soil properties and stress level). Li and Selig (1996), quantified the coefficient *A* by relating it to the physical state of the soil and the applied deviator stress, so it could be written as:

$$A = a(^{\sigma_d}/_{\sigma_s})^m \qquad 5.2$$

Where a and m are the correlation parameters; $\sigma_d \; and \; \sigma_s$ are the deviator stress and static strength respectively. Therefore, parameter (*A*) is highly dependent on the applied deviator stress and the maximum deviator stress that the soil can take at static test condition. Parameters *a*, *m*, and *b* can be determined from a cyclic triaxial tests.

Li and Selig (1996), recommend values for the above parameters for a number of soil types based upon back calculation from a number of different studies (Table 5.2). Values for the soft soils (no column) and the soil/ stone column composite parameters calculated in this study through regression analysis of cyclic triaxial results are included (see Appendix F for more information on regression analysis).

Table 5.2 Material parameters (after Li and Selig (1996))

Model parameters		Soil classification					
		ML	MH	CL	CH	Kaolin clay (test condition)	Kaolin/stone column (test condition)
a	Average	0.64	0.84	1.1	1.2	4.346	23.392
	Range	-	-	0.3-3.5	0.82-1.5	3.960-4.733	22.519-24.264
b	Average	0.1	0.13	0.16	0.18	0.096	0.019
	Range	0.06-0.17	0.08-0.19	0.08-0.34	0.12-0.27	0.085-0.107	0.015-0.024
m	Average	1.7	2.0	2.0	2.4	2.469	5.081
	Range	1.4-2.0	1.3-4.2	1.0-2.6	1.3-3.9	2.136-2.803	5.004-5.157

As explained by Li and Selig (1996), that exponent *b* reflects the accumulative strain rate under cyclic loading (i.e. that the higher the value of b the more the soil affected by number of cycles). Whereas exponents *a* and *m* are related to the deformation occurred at the first cycle and its relation to the cyclic stress ratio applied and also to the degree of softening of the deviator on the soil.

As can be seen in Table 5.2 the parameters value of the used soil (no column) is comparable with the CL values, the reason for this is that the kaolin clay considered as a clay soil with high plasticity. However, for soil/ stone column composite the exponent *b* showed a smaller value than other type of soils; this might indicate that the stone column reinforced soils are likely to be less sensitive to number of loading application. Whereas *a* value showed a higher level (23.39) than the other soils, which indicates that, the soil/ column system could have a higher degree of softening.

5.2.2 Cyclic Deformation

Figures 5.6 to 5.8 show the cyclic deformation behaviour for soil (no column) and soil/ stone column composite. The influence of loading frequency; dynamic stress level and number of loading application were included in these Figures.

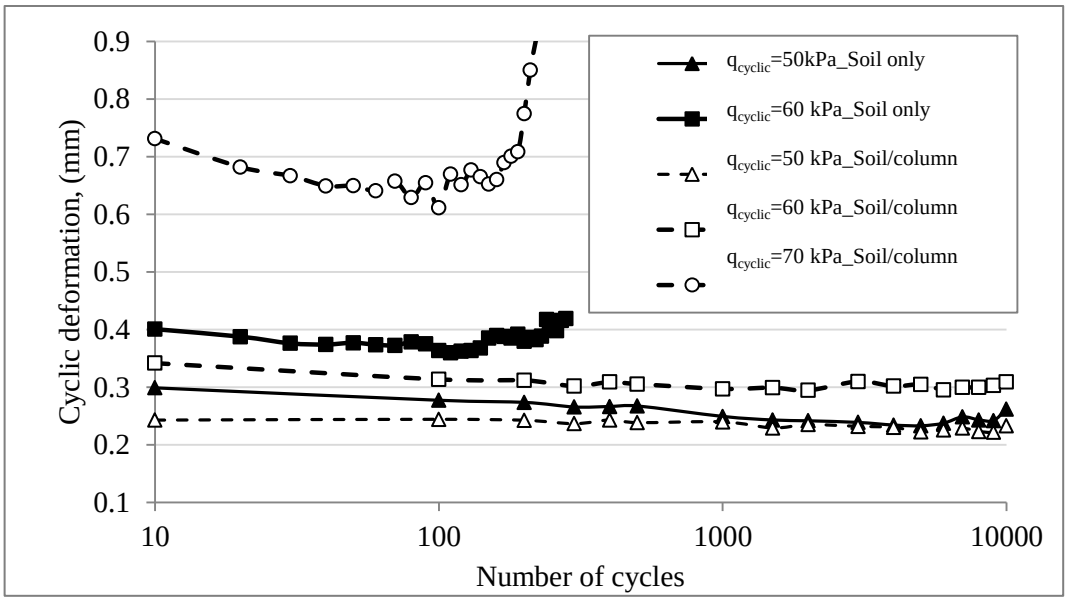

Figure 5.6 Cyclic deformation during cyclic triaxial test: at 0.5 Hz loading frequency

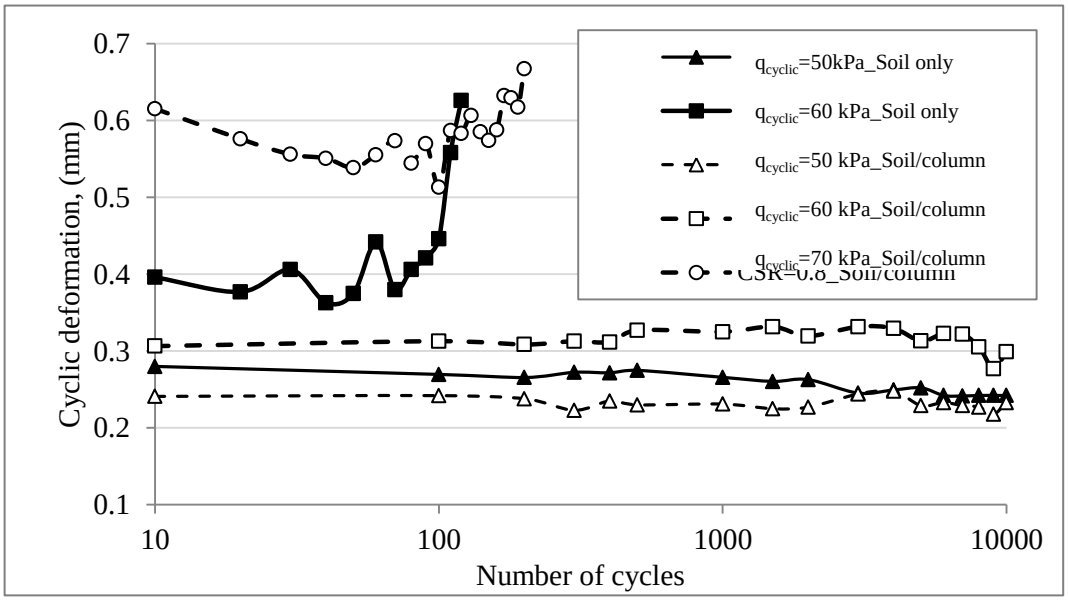

Figure 5.7 Cyclic deformation during cyclic triaxial test: at 1 Hz loading frequency

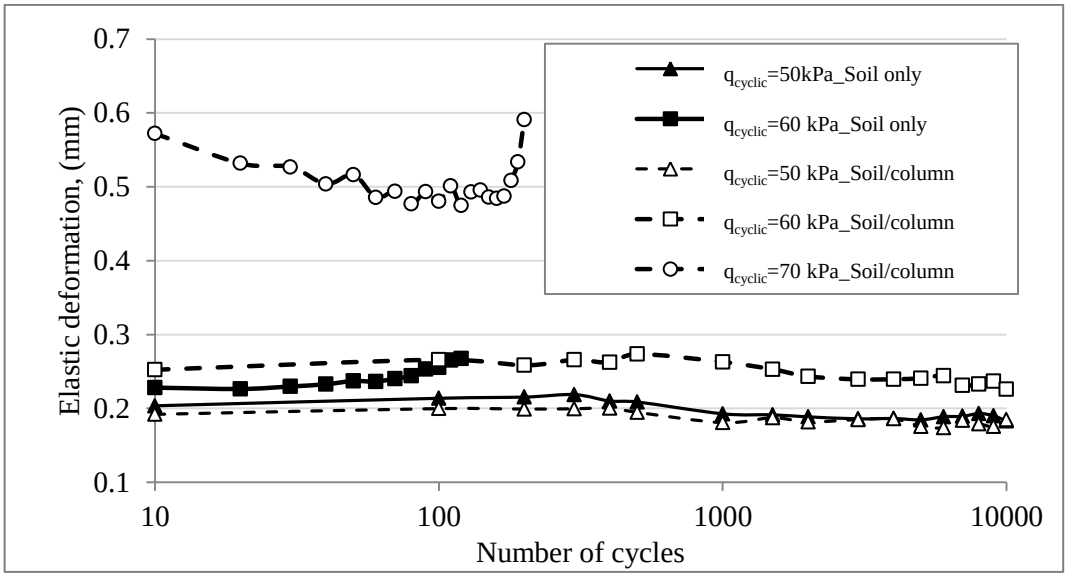

Figure 5.8 Cyclic deformation during cyclic triaxial test: at 3 Hz loading frequency

In all specimens tested, the cyclic deformation decreases as the number of cycles increases. This was due to hardening of soil specimens. This phenomenon occurs only at stresses below the threshold level (i.e. 50 kPa for soil (no column) and 60 kPa for soil/ stone column composite) above these stresses the cyclic strain sharply increases due to the shear failure occurred.

Figures 5.6 to 5.8 have also indicated that the cyclic strain in both soils (with and without stone column) are slightly influenced by the change in loading frequency as there was a small decrease in the cyclic deformation with the increase in the frequency.

For instance, when the specimens subjected to 50 kPa cyclic stress, the values of cyclic deformation for soil (no column) specimens after 10000 cycle were 0.24, 0.22 and 0.18 mm for frequencies 0.5, 1 and 3 Hz respectively. Whereas in the soil/ stone column specimens the cyclic deformations were 0.23, 0.22, and 0.17 mm for frequencies 0.5, 1 and 3 Hz respectively. This would indicate that there is a threshold elastic strain of 0.2 % for soil (no column) and about 0.1 % for soil/ stone column composite.

5.2.3 Resilient Modulus

Soil resilient modulus (M_r) can be defined as the ratio of the dynamic deviator stress (q_d) to the elastic (recoverable) strain (ε_r) (Brown et al., 1975; Selig and Waters, 1994; Brown, 1996).

$$M_r = \frac{q_d}{\varepsilon_r} \qquad 5.3$$

This parameter is considered to be one of the fundamental factors of understanding the elastic behaviour of soil foundations subjected to dynamic stresses. For instance, in railway track analysis, resilient modulus is important for determining stresses and settlement in the track foundation system (Loh and Nikraz, 2012).

Typical results of resilient modulus determination of both specimens type (soil (no column) and soil/ stone column composite) under dynamic stresses of 50 and 60 kPa at different loading frequencies (i.e. 0.5, 1 and 3.0 Hz) are shown in Figure 5.9 to 5.11 respectively.

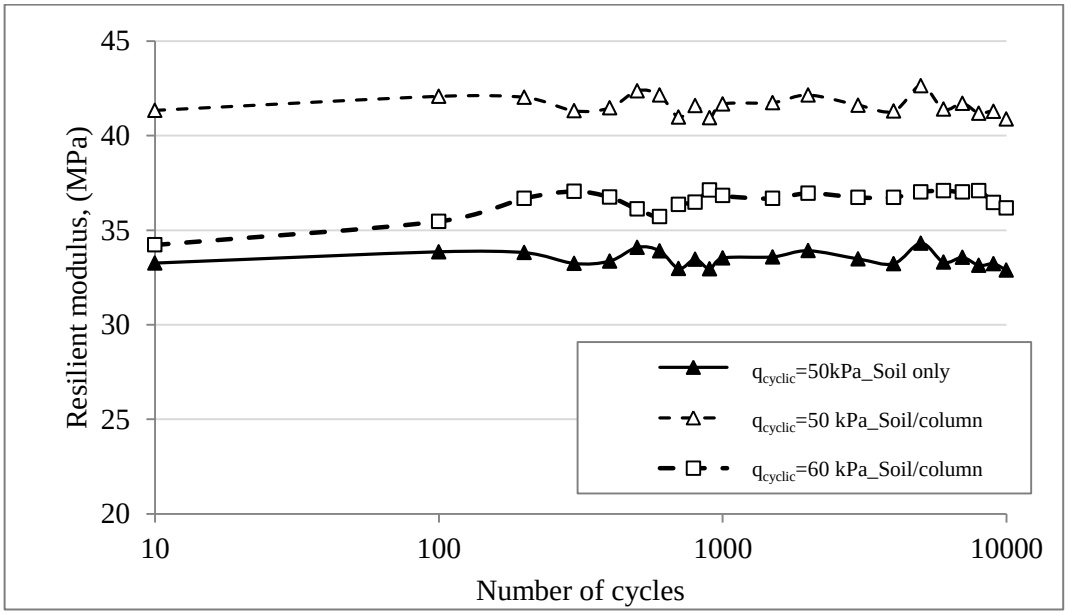

Figure 5.9 Variation of resilient modulus with number of cycles at loading frequncy of 0.5 Hz

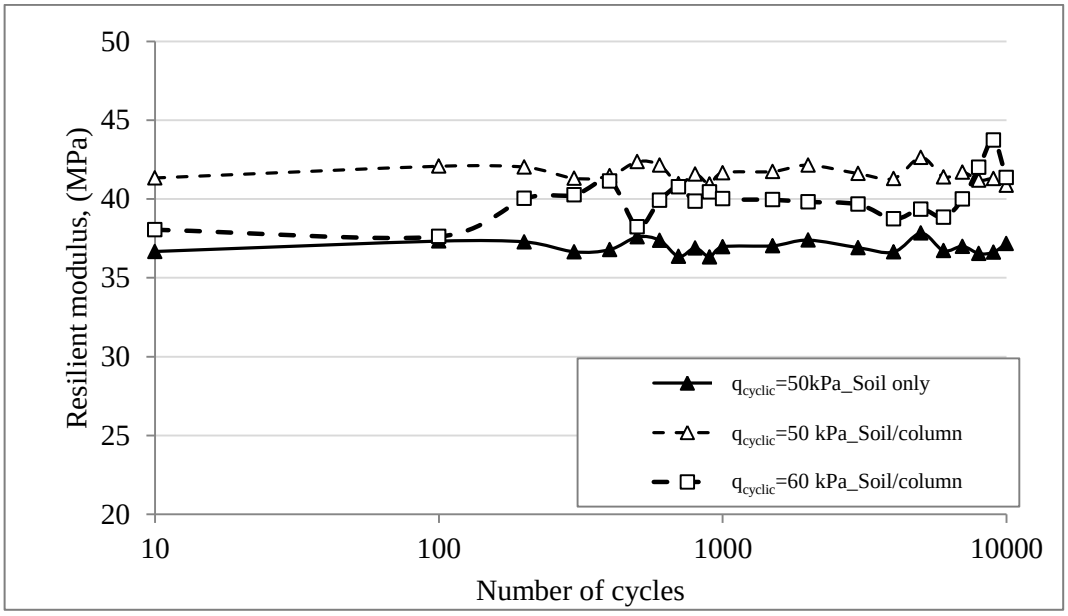

Figure 5.10 Variation of resilient modulus with number of cycles at loading frequncy of 1 Hz

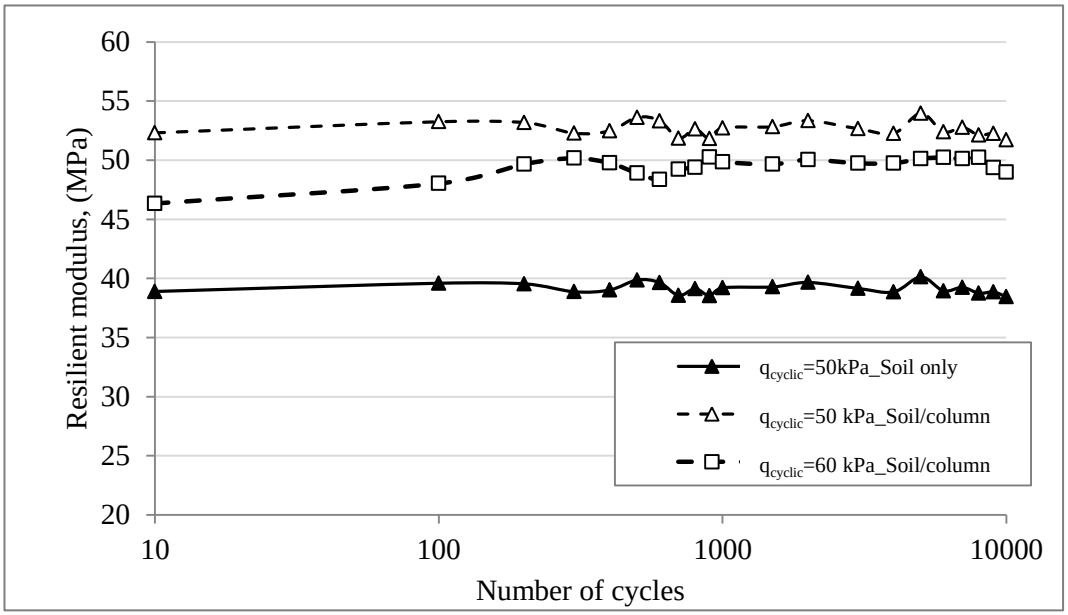

Figure 5.11 Variation of resilient modulus with number of cycles at loading frequncy of 3 Hz

Results indicated that the resilient modulus increased with frequency in both specimen types (20 % for soil/ stone column specimens and about 12 % for soil (no column) specimens). For example, during the application of 50 kPa dynamic stress, the increase was from 40.6 MPa to

49.4 MPa in case of soil/ stone column composite specimens, while it was from 33.5 MPa to 38 MPa in the soil specimens (no column).

In addition to this, Figure 5.12 shows that any increase in the dynamic deviator stress has a negative impact on resilient modulus, which decreases as dynamic stress increases. For soil/ stone column specimens, when the dynamic deviator stress was increased from 50 to 60 kPa, there was a general reduction in the amount of resilient modulus this reduction influenced by the change of frequency as well (i.e. the higher the frequency the smaller the reduction). For example, there was a reduction percentage in resilient modulus of 6.5, 7.6 and 13.3% when the tests were conducted at frequencies of 0.5, 1 and 3 Hz respectively.

Comparing the resilient modulus results with the secant modulus obtained from the static triaxial test in the previous chapter (Section 4.2.4.3), which was about 9.5 and 8 MPa for soil/column specimens and soil only specimens respectively; it was found that the resilient modulus could reach up to four times the secant modulus value when the cyclic deviator stress was 50 kPa.

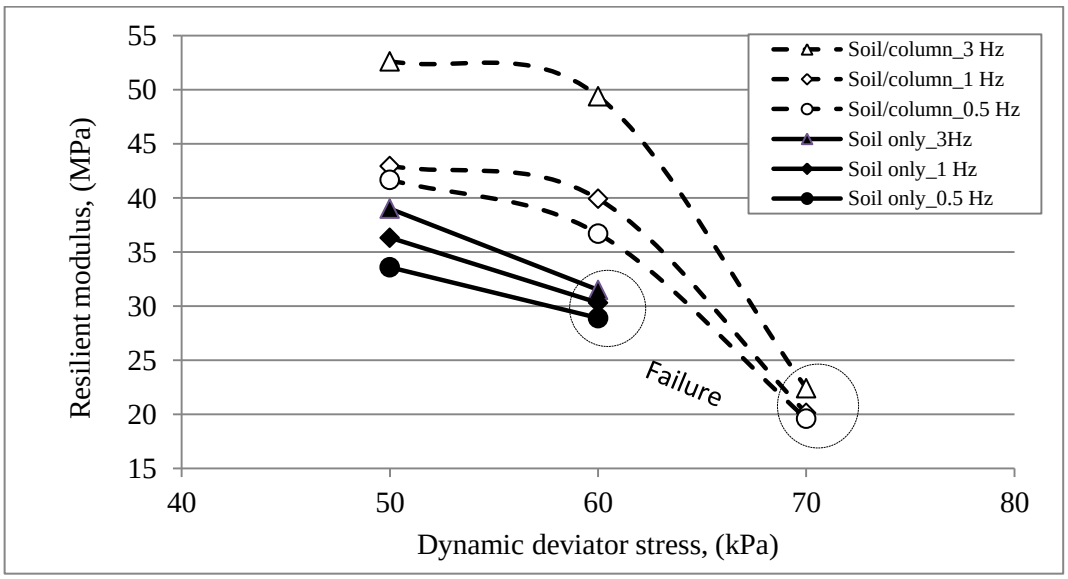

Figure 5.12 Variation of resilient modulus with respect to dynamic stress and loading frequency

5.2.4 Pore Water Pressure Response

Under continued application of cyclic loading, excess pore water pressure gradually built up over each cycle. Figures 5.13 to 5.15 show changes of pore water pressure corresponding to the cyclic deviator stress at the three loading frequencies for both soil (no column) and soil/ stone column composite specimens.

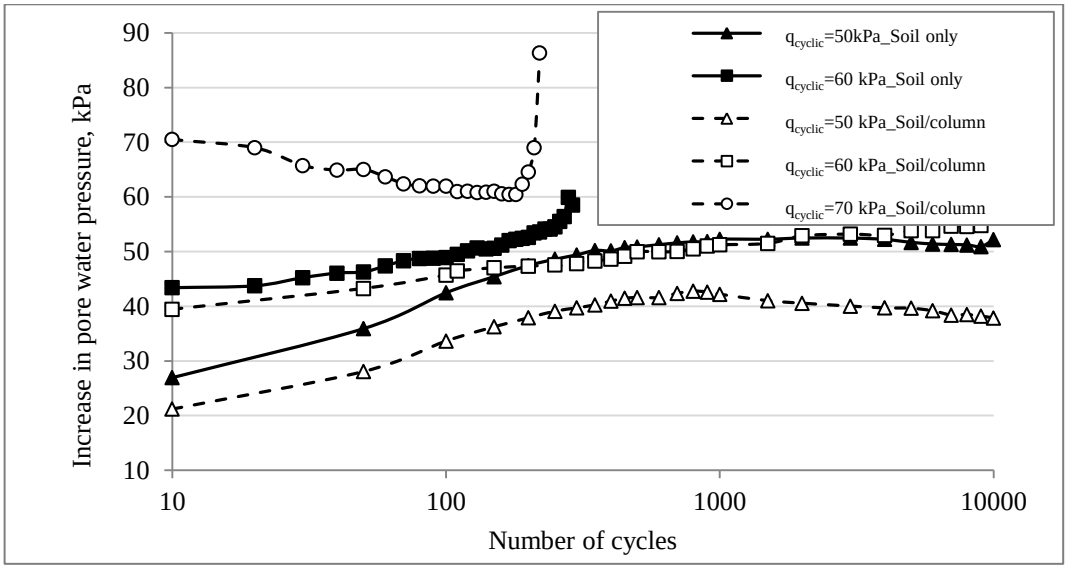

Figure 5.13 Accumulation of excess pore water pressure at loading frequency of 0.5 Hz

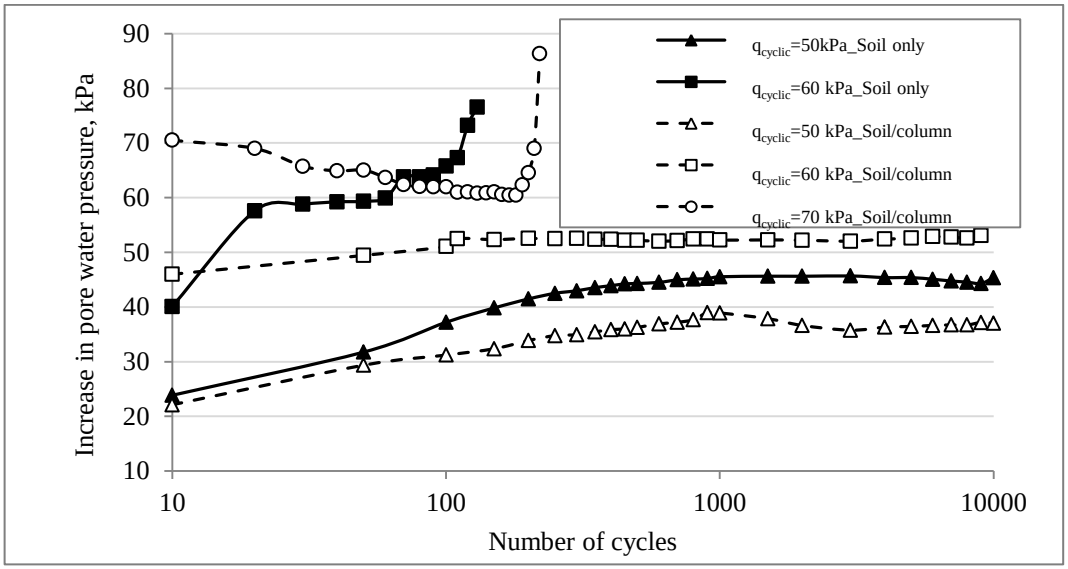

Figure 5.14 Accumulation of excess pore water pressure at loading frequency of 1Hz

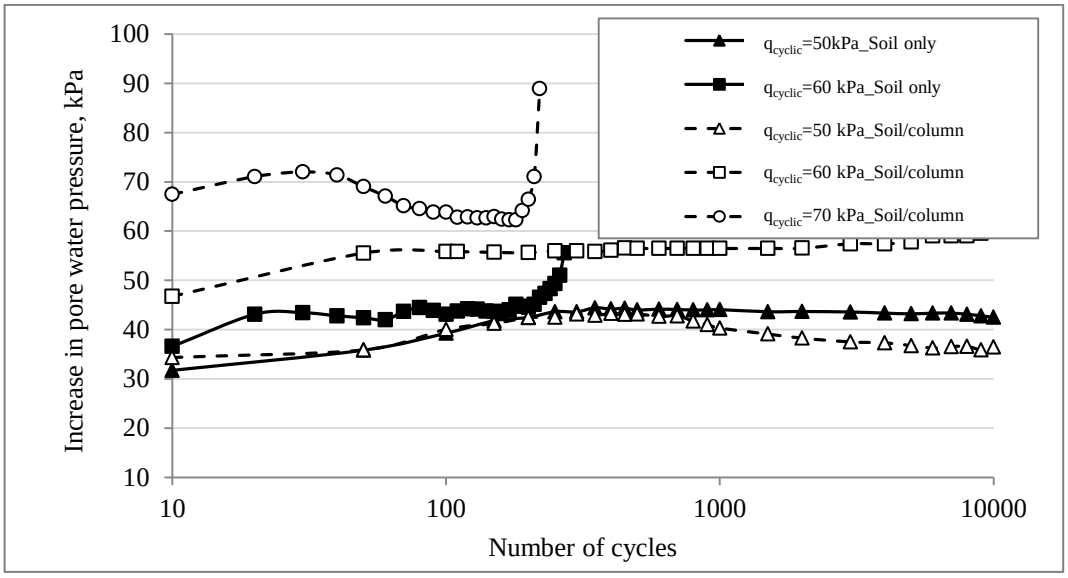

Figure 5.15 Accumulation of excess pore water pressure at loading frequency of 3Hz

As expected, the excess of pore water pressure increased with cyclic deviator stress at all loading frequencies examined. Results show that in the case of most specimens, the pore water pressure increased significantly at the initial stage of loading application (i.e. number of cycle less than 150) then there was a gradual increase up to 1000 cycle before it started to stabilise.

Figures 5.13 to 5.15 Also indicated that, the frequencies of loading did not show a noticeable influence on the excess of pore water pressure in the soil /column specimens. Tests carried out at 50 kPa cyclic stress the pore water pressures after 10000 cycles were 38, 37, and37 kPa for frequencies 0.5, 1 and 3 Hz. At higher cyclic stress level (70 kPa) the specimen failed before the pore water pressure could stabilise. Before failure it had increased rapidly to over than 75 kPa.

In contrast, for soil only samples results (Figures 5.13-5.15) showed that at a cyclic stress of 60 kPa, the excess pore water pressure increases rapidly to reach 70 kPa in few cycles leading to a rapid failure in the sample, however, there was a small effect on the soil only specimens,

where the build-up of pore water pressure decreased with increase in the loading frequency especially at the early stage of loading application (in the application of 50 kPa cyclic stress and after 10000 loading cycle, pore water pressures were 51, 45.4 and 42.5 kPa for frequencies 0.5, 1 and 3 Hz).

Generally, in most tests conducted below the threshold stress levels pore water pressure stabilises after 2000 cycles of loading applications. This behaviour is comparable with the general behaviour of soft clay under cyclic loading condition (Miller et al., 2000; Indraratna et al., 2009).

Figure 5.16, indicates that there was a critical excess of pore pressure and found at around 60 kPa for the soil specimens (no column) and about 70 kPa for the soil/column specimens (pore water pressure measurements at failure). These pore water pressure measures can be normalised in terms of effective confining pressure ($\sigma_3' = 100\ kPa$) leading to ratios of 0.6 for soil (no column) and 0.7 for soil/ stone column composite. This also indicates that the failure occurred when the pore water pressure approached the level of the dynamic stress.

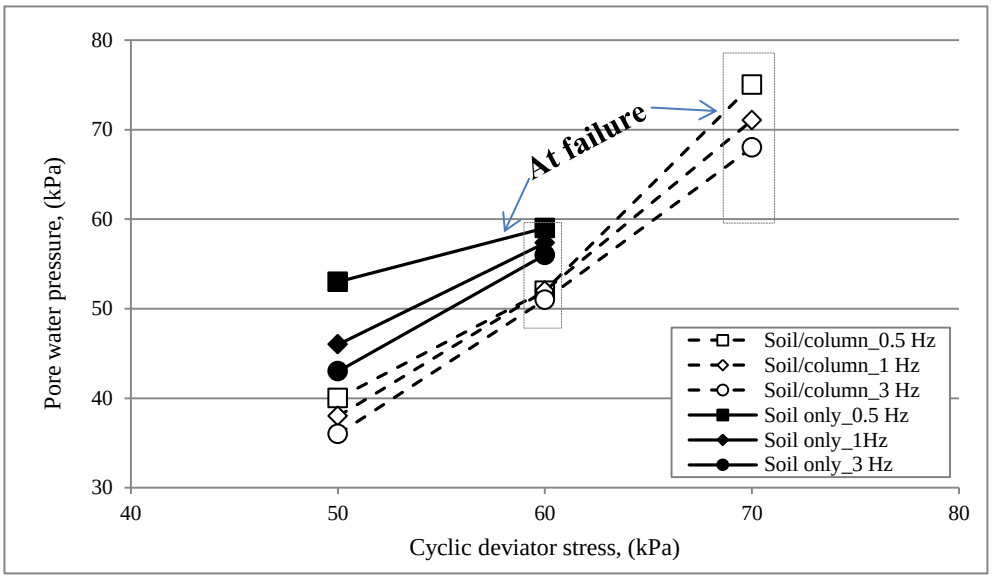

Figure 5.16 Effect of cyclic stress on pore water pressure

5.2.5 Deformation Pattern

Observation indicates that both soil specimens (no column) and soil/ stone column composite specimens fail in shear failure mode when subjected to cyclic stress above the threshold cyclic stress 50 kPa for soil and 60 kPa for soil/column specimens; this was irrespective of frequency of loading. Also below these stresses both specimens did not fail at the end of the test and behaved in a stable manner.

Figures 5.17 and 5.18 show the mode of failure for both reinforced and unreinforced specimens. Soil specimens (no column) specimens they failed within a range from 60 to 100 cycles of loading application (Figure 5.17) a slip surface was clear along weakest plan.

A combined mode of failure was observed in case of reinforced specimens (bulging and shear failure (Figure 5.18)). Due to the large strain happened bulging failure took place first and then by the increase in loading cycle shear failure accrued. The shear surface for the column was at approximately the bottom 50 mm resulting in L/D ratio of 5.4 which is close to the identified critical column length (L/D = 6).

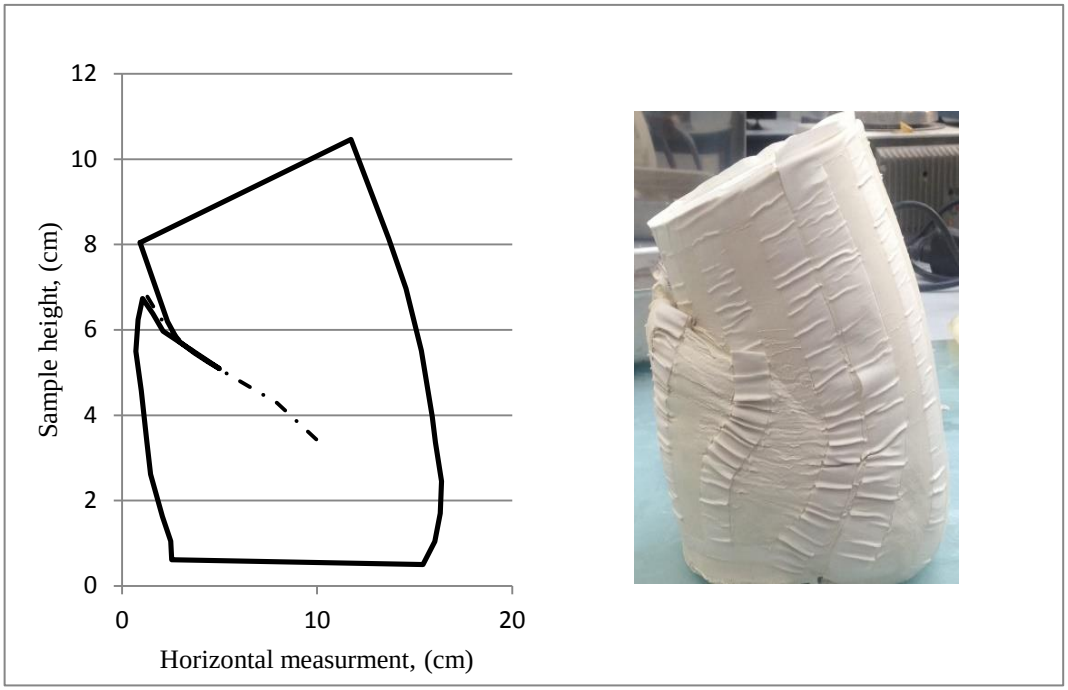

Figure 5.17 Deformed shape for soil only specimes

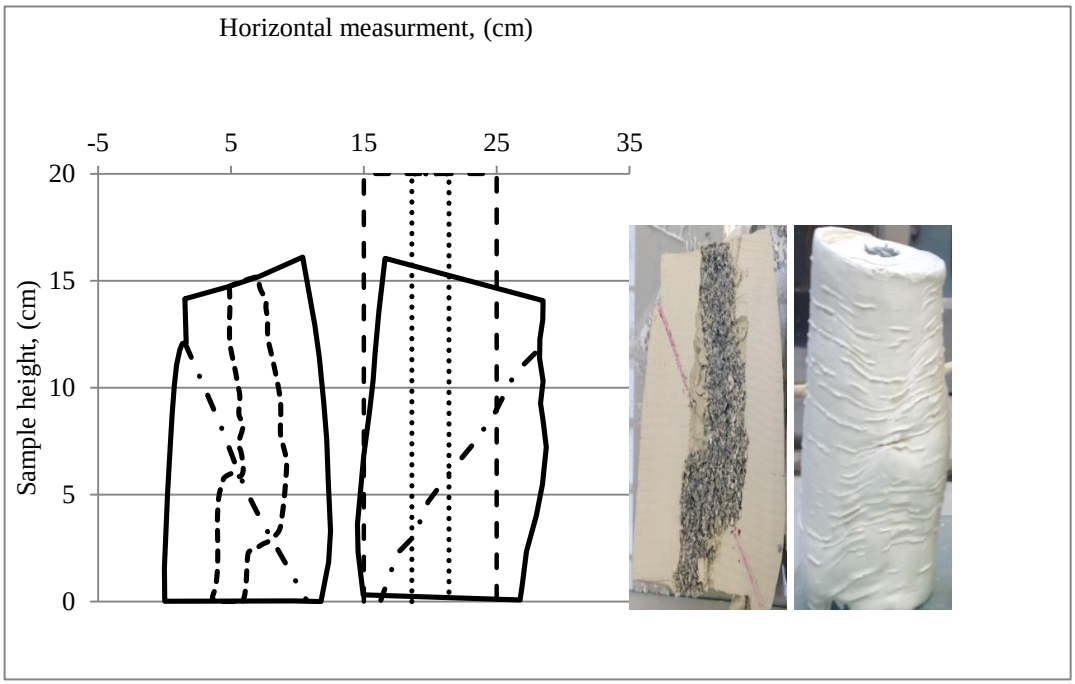

Figure 5.18 Deformed shape for the soil/column specimen

5.3 Model II Test Results (Large Scale Test: Foundation)

The procedure for undertaking these tests is described in Sections 3.6.7 and 4.3. As summarized in Table 5.3, the testing program included a series of cyclic zone load tests (Load applied to column and portion of the surrounding soil in case of soil/column test). These tests were conducted for both treated and untreated soils under two loading frequencies (1 and 3 Hz). Loading was applied in a sinusoidal wave form using two dynamic stress levels of 165 and 235 kPa, which were equivalent to cyclic stress ratios of 0.5 and 0.7 respectively.

The range of stress applied was based on the results of triaxial tests; particularly findings relating to the threshold value, which was 70 % of the reinforced soil strength at failure. Thus cyclic stress ratios of 0.5 and 0.7 were chosen for large scale test to evaluate this observation.

Table 5.3 Model II test program

Soil type	Test	P_{max} (kN)	P_{min} (kN)	σ_{max} (kPa)	σ_{min} (kPa)	Stress at failure (kPa)	CSR	Loading frequency (*f*)
Soil only	LM-C-05	0.8	0.2	210	45	200	-	1
	LM-C-06	0.8	0.2	210	45		-	3
Soil/column system	LM-C.C-07	0.8	0.2	210	45	410	0.5	1
	LM-C.C-08	0.8	0.2	210	45		0.5	3
	LM-C.C-09	1.05	0.2	280	45		0.7	1
	LM-C.C-10	1.05	0.2	280	45		0.7	3

5.3.1 Permanent Strain during Cyclic Loading

Investigating the behaviour of permanent deformation of the reinforced soil on large scale specimens indicated that the permanent stain was independent from the change in frequency of loading; also the permanent deformation is highly dependent on the amount of the dynamic

stress applied and its relation to monotonic stress at failure. This confirms to the results obtained from triaxial test described earlier in Section 5.2.

Figure 5.19 shows the effect of number of cycles; loading frequency, and cyclic stress ratio on the measured permanent strain for both soil (no column) and soil/ column composite specimens. It was observed when testing soil only specimens (no column) at a dynamic loading stress of 165 kPa and loading frequency of 1 and 3 Hz, that the soil failed after 20 cycles of loading application; this was the cases at both loading frequencies. This was expected as the loading stress was larger than the threshold ratio of the soil obtained in Section 5.2.2. (As discussed in the methodology chapter this load was chosen due to the limitation of the apparatus used in this study). On the other hand, soils/ stone columns composite showed increased resistance to load, and the permanent deformation did not go beyond 2 % at both loading frequencies. This increased to about 6 % when the dynamic stress load was increased from 165 to 235 kPa.

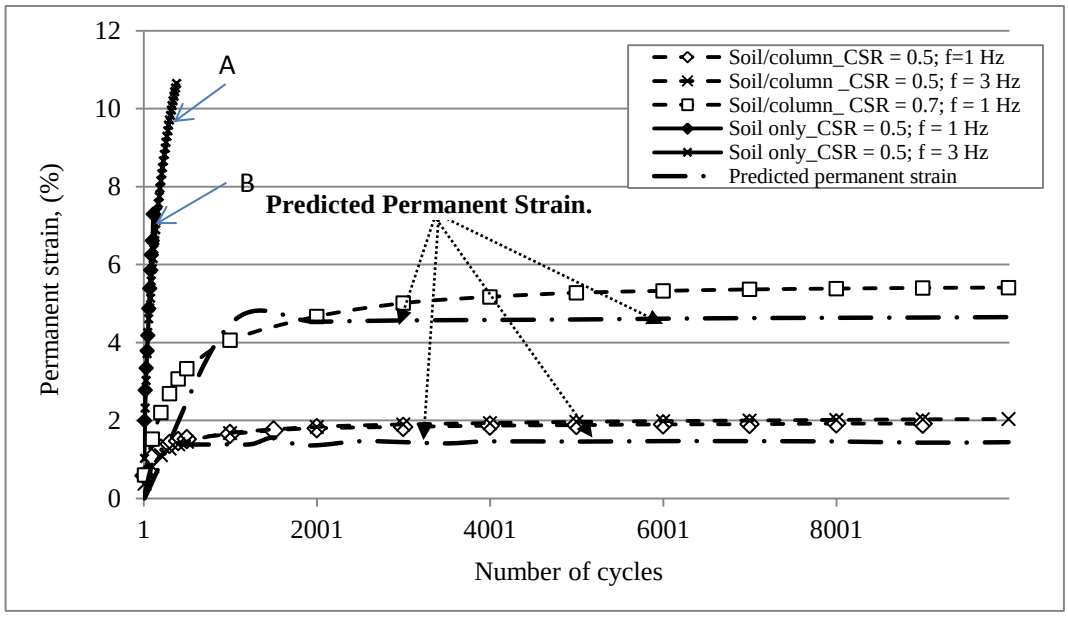

Figure 5.19 Permanent strain results/ number of cycles

Predicted values of permanent strain obtained from Equation 5.2 are also shown in Figure 5.19. Material parameters *a*, *b*, and *m*, determined from the trixial test and explained in Section 5.2.1, are used.

During the application of dynamic stress at 165 kPa, permanent strain was predicted to be increasing with the increase of number of applications reaching approximetly 1.6 % at 1500 cycles and then maintaining this level. Comparing this with the laboratory results, at the same stress level the permanent strain increased to 1.8% at 1500 cycles and then continued at that level to the end of the test (10000 cycles). A similar trend was observed when the stress level was increased to 235 kPa. The estimated permanent strain was supposed to reach a maximum of 4.6 % and stabilize after 1500 cycles, however, test results showed that the development of permanent strain reached a maximum of 5.3 % and stabilised at this level after 4000 cycles.

Although the predicted permanent strain was underestimated compared with the measured values, the difference seems to be considerable where it was within a range of 15 %. This variation could be due to the difference in test conditions, as the parameters used in the prediction were calculated from the triaxial test and for a limited CSR.

Figure 5.20 shows the deformation pattern after the cyclic loading application of 10000 cycles at a cyclic stress of 165 kPa and loading frequency of 3 Hz. Although it was expected that the columns will bulge at a depth of 2 to 3 times the column diameter as suggested by Hughes and Withers, (1974), it appears that the column bulging under dynamic loading was different from that of monotonic loading. In other words it was observed that the column bulge in two sections (double bulging). These bulges were at 20 and 60 mm depth from the top, this can expressed as 0.7 and 2 times the column diameter.

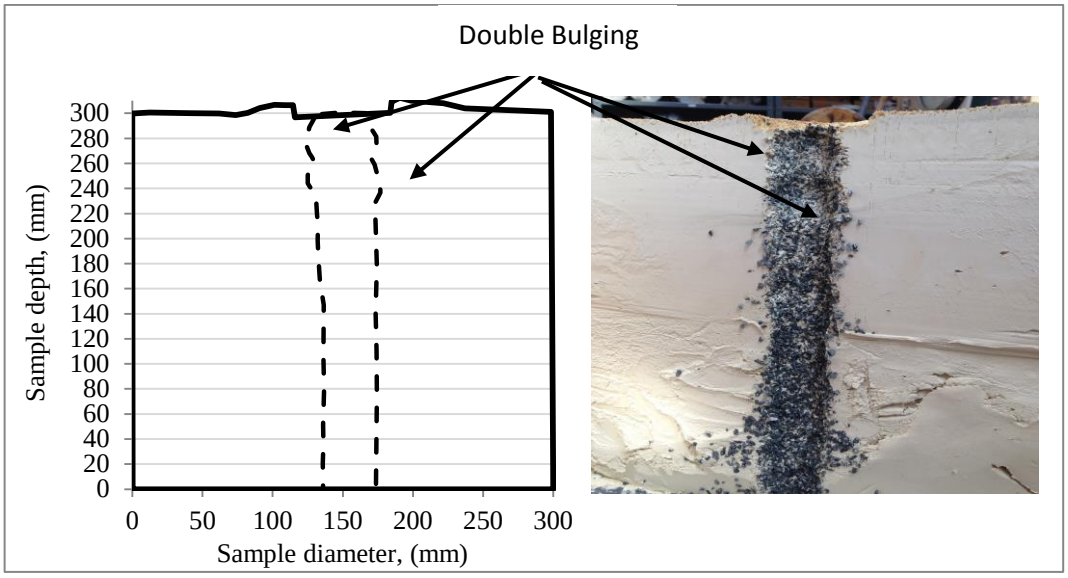

Figure 5.20 Deformation pattern after cyclic loading

5.3.2 Pore Water Pressure Changes

During cyclic loading pore water pressures were measured in two positions, at the centre (PPT1) of the specimen base and at a distance of 50 mm from the centre (PPT2). The pore water pressure measurements are illustrated in Figures 5.21 and 5.22; both show the pore pressure changes that occurred under peak cyclic loading on the foundation plate.

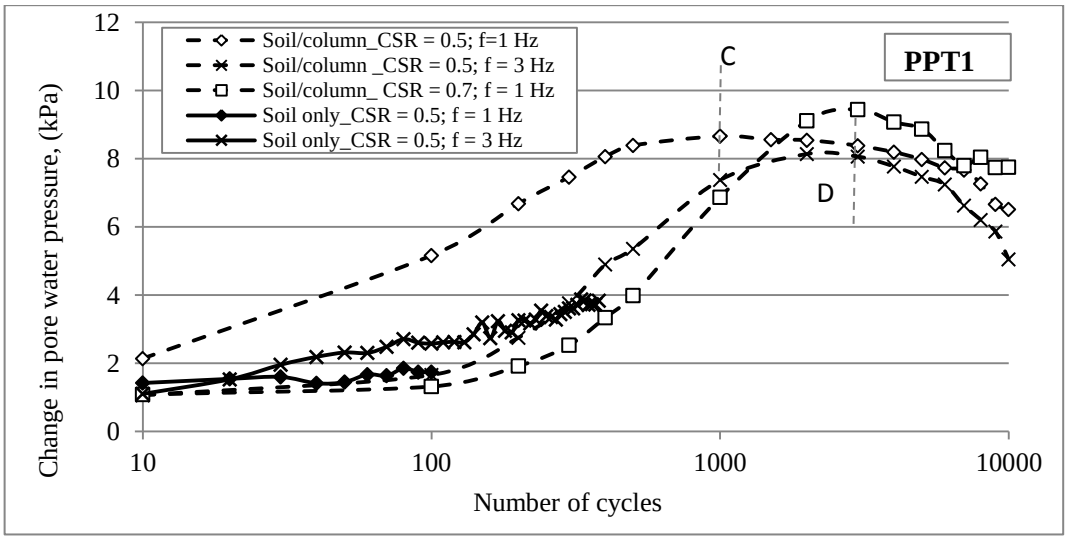

Figure 5.21 Pore water pressure measurment at the centre of the specime

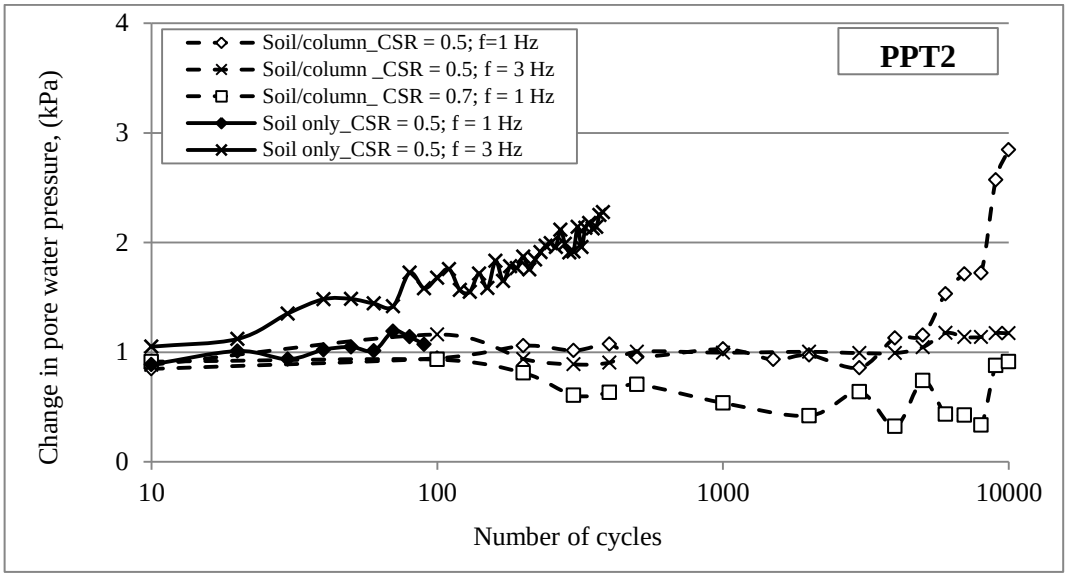

Figure 5.22 Pore water pressure measurment at 50 mm from the centre of the specime

As was the case for triaxial tests, under continues application of cyclic loading, excess pore water pressure was initially built up rapidly before it start to decrease (Figures 5.13 to 5.15).

Figure 5.21 shows the change in pore water pressure under the stone column at CSR of 0.5 was increased from about 1.5 kPa at the initial stage to about 8.7 kPa during the loading application of 1000 cycle, after this the pore water pressure start to decrease gradually. Similar behaviour was observed using CSR of 0.7 with larger magnitude of pore water pressure (about 10 kPa). However, this behaviour was different at the other position (PPT2); the change in pore water pressure was almost steady during the first 2000 cycle then started to rapidly increase.

5.3.3 Soil stiffness

Soil stiffness (**K**) is defined as the ratio of the dynamic applied load (P_d) on the foundation area to the recoverable displacement experienced.

Stiffness of the treated and untreated soil tested at CSR of 0.5 and 0.7 at loading frequencies of 1 and 3.0 Hz are shown in Figure 5.23 . Results show that after applying 10000 cycles the stiffness for soil/ stone column composite increased from 1770 to 2050 kN/m as frequency increased in from 1 Hz to 3 Hz (i.e. about 15 %).

Soil specimens (no column) at both frequencies 1 and 3 Hz showed low stiffness (745 and 960 kN/m respectively) before failure occurred after 100 and 330 cycles respectively. This was as a result of the high deformation occurred as shown before in Figure 5.19 (Points A and B).

In addition, it was noticeable that the stiffness at soil/ stone column composite, at CSR of 0.5, was decreased gradually (from1700 to 1630 kN/m at frequency of 3 Hz and from 1540 to 1450 kN/m at frequency of 1 Hz) during the first 100 cycles then increased by 20 % before it stabilised after 1500 cycles. This is likely due to the stiffening effect of stone column and its provision as a drainage path leading to reduction in pore water pressure (Figure 5.21 points C and D). As pore water pressures start decreasing from 8.7 to around 6 kPa after 1000 cycles for $f = 1\ Hz$ after 3000 cycle and at $f = 3\ Hz$.

This behaviour was different when the dynamic stresses was increased (CSR = 0.7), where the stiffness of the reinforced soil was almost constant during the first 100 cycles at 1320 kN/m then it started to decrease slowly to reach 1100 kN/m at the end of the test (10000 cycles). This could be due to softening of the composite system.

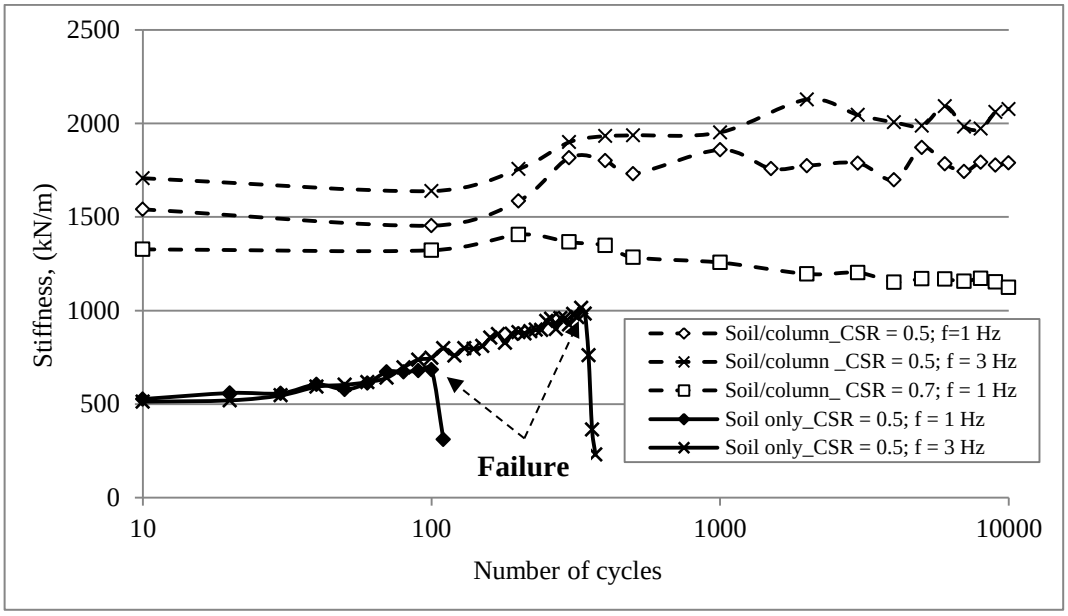

Figure 5.23 Stifness results

5.4 Implication for Stone Column Performance

The applied dynamic stress through the rail is transmitted through the ballast layer to the subgrade level, played the main role in controlling the amount of permanent deformation of the subgrade. Therefore, as suggested by Heath et al. (1972); Brown (1996) and Frost et al. (2004) identifying the threshold stress would help for determining the thickness of unbound layer.

From looking at literature and monotonic triaxal test results presented here it can be seen that the bearing capacity of soft clay subgrade soils can be improved by (15 to 40 %) if the soil was replaced by granular material having an angle of internal friction between 35 and 48^{o} formed in columns with an area replacement ratio between 5 and 15 %. However, in this current study using an angular crushed aggregate with an internal angle of friction and area replacement ratio of 7 % have led to improved the bearing capacity of the soil by 30 % under the monotonic loading (Figure 4.3).

This improvement in the bearing capacity under the monotonic loading showed an increase in the threshold cyclic stress (under the cyclic loading condition) of about 15 % and 70 % reduction in settlement; also showed an increase by 25 % in the resilient modulus of the soil. The threshold relation between reinforced and reinforced soils can be related to limiting the allowable stress applied on the soft subgrade via the relationship between the internal angle of friction, area replacement ration and the undrained shear strength of the soil (Section 4.3.1). This limit then can be applied in the design procedure of, for instance, railway tracks.

For example, this improvement in the soil properties could help to reduce the thickness of the ballast layer. As one of the important performing functions of this layer is to reduce stresses transferred through the sleepers from the train to the acceptable stress levels that the subgrade soils can carry. Thus for a 100 kN axel wheel load using Talbot's equation (Section 3.7.2), the ballast depth (h) can be reduced by 15 % from 500 mm to 425mm. This can save about 225m^3 of ballast per one kilometre of railway track which can cost around 2000 Pounds sterling per one kilometre. This can be considered as a cost effective impact.

Another impact is that, by simulating train movement with loading frequencies of 0.5, 1.0 and 3.0 Hz representing train speed of 35, 70 and 225 km/hr, stone columns reinforced subgrades showed stability and less pronounced influence toward both the change in loading frequency and long term loading application. This can increase the period of maintenance and provide the stability required to upgrade the track to higher speed level.

5.5 Concluding Remarks

A comparison between the behaviour of both reinforced and unreinforced soils under the application of cyclic loading was proposed in this chapter.

Results indicated that the presence of stone column enhanced the threshold cyclic stress of the soft soil by about 15 % and reduced the amount of permanent strain by more than double when testing the soils below their threshold cyclic stress. Stone columns also help reduce pore water pressure by providing a drainage path. This might be one of the reasons that allow the reinforced soil to tackle higher cyclic stress level.

Changes in frequencies had no significant influence on the total strain of reinforced soil, but these changes do affect the stiffness. Stiffness of the soil with the stone column was about 25% higher at 3.0 Hz compared to that at 0.5 Hz. Resilient modulus of the reinforced soil increased by 13 to 20 % depending on the frequency of loading where the resilient modulus tend to increase by the increase of the frequency.

CHAPTER 6

CONCLUSION

6.1 General

The vibro stone column technique is commonly used to improve bearing capacity and reduce settlement of soft soils. They have been used worldwide to provide economic, flexible (applicable to various types of week soils) and sustainable solution. More recently, stone columns have been used in the UK and Europe to improve soft subgrade soils subjected to cyclic loading such as railway track.

Performance and failure mechanisms of both isolated and grouped stone columns have been investigated under the application of monotonic loading but not under cyclic loading. This study was aimed to provide improved understanding of this behaviour.

This research focused on the load/deformation behaviour of single stone column subjected to monotonic and cyclic loading in both small scale models (triaxial specimen 100 mm diameter) and large scale models (300 mm diameter * 300 mm height). In both cases tests were performed on normally consolidated specimens of soft clay (undrained shear strength of ≈ 12 kPa) reinforced with 28 mm diameter stone columns. Effects of loading frequencies (0.5-3Hz) at a range of cyclic stress ratios (0.5-0.8) were examined. In addition to the influence of rate of strain on shear strength on both soils (no column) and soil/ stone column composite in the monotonic loading conditions (section 6.2) and cyclic loading conditions (Section 6.3). The following correlations were drawn from this study.

6.2 Monotonic Loading

6.2.1 General

Replacing 7 % of soft clay with granular materials, which had an internal of friction angle of 48^o, led to increase the bearing capacity and stiffness of the soil by a factor of 1.3. Compared to predicted values and previously reported results reasonable agreement was found in terms of bearing capacity, However, measured value for settlement were about 83 % lower than values predicted based on Priebe's method.

6.2.2 Effect of Strain Rate

- Both soils (no column) and soil/ stone column composite specimens showed a small influence from rate of strain; for soils (no column) there was an increase of about 10 % deviator stress associated with increasing the magnitude of rate of strain from 0.003 to 0.3 mm/minute. However, in the case of reinforced specimens the trend was reversed order where the deviator stress showed an increase of 8 % with the reduction of the strain rate (0.3 to 0.003).
- The presence of stone column helped reduce build-up of pore water pressure and there was limited influence from rate of strain on pore pressure as compared to soils (no column). The latter showed pore water pressure reduction with increase in strain rate.
- In case of soil/stone column composite, the secant modulus increased by about 30% compared to soil (no column). This improvement was higher between 1 and 3 % strain and for strains higher than about 4 % the secant modulus decreases and the degree of improvement in modulus decreased by about 17%.

- The secant modulus of soil was seen to be independent of strain across the range examined (0.3 to 0.003) for both soils (no column) and soil/ stone column composite specimens.
- In model I (Triaxial tests), the column bulging was found to be relatively uniform with the depth of the sample, this was probably due to the constant confining pressure along the depth. However, in model II (Large scale tests), bulging took place at approximately 120 mm below the surface, which was about 1.7 times the column diameter. This was very close to the expected value of 2 to 3 times the column diameter

6.2.3 Effect of Column Material Density

- A reduction in relative density of the column from 80 to 42 % decreases the bearing capacity of the soil/ stone column composite by about 14 %, this could be due to a reduction in the peak internal angle of friction of the column material and this might be related to the increase in the dilation angle of the column particle.
- A change in aggregate density of the column has showed negligible effect on pore pressure measurement.

6.3 Cyclic Loading

6.3.1 Effect of Stress Level

- Below the threshold stress level, reinforced soils were less sensitive to the number of loading application than soils (no column). This is likely due to compaction of the column materials that occurs during load application, leading to increase in density and resulting in greater resistance to deformation hence lower settlement.

- Presence of a stone column enhanced the threshold cyclic stress of the soil by about 15 % and reduced the amount of permanent strain by half relative to soil without column.
- Stone columns helped reduce pore water pressure by providing a drainage path. This may be one of the reasons that allows the reinforced soil to support higher cyclic stress level (since pore water pressure would also be reduced).
- Both reinforced and unreinforced soils failed in shear mode when subjected cyclic stress above the threshold cyclic stress. This failure mode was not affected by frequency of loading and below threshold stress both specimens did not fail throughout the load regime (10000 cycles).
- Large scale tests showed that the column bulging that forms under dynamic loading was different from that of monotonic loading. It was observed that the column bulge in two sections (double bulging) under cyclic loading. These bulges were at a depth of 0.7 and 2 times the column diameter below the surface of the samples.

6.3.2 Effect of Frequency

- In terms of permanent deformation, soil/ stone column composite showed little influence by the change in frequency of loading. However, in the case of soil (no column), larger permanent strains were measured at lower frequencies compared to those at higher frequency, about 55 % increase when frequency was changed from 3 to 0.5 Hz.
- Below the threshold stress, the resilient modulus of both reinforced and unreinforced soils increase with the increase of loading frequency. The value for soils/ stone column composite soils was twice that of soils (no column).

6.4 Recommendations for Future Research Works

Whilst this study has highlighted important aspects in the behaviour of stone column reinforced soil subjected to cyclic loading there are still important areas requiring further investigation. These are suggested below:

- Future work also needed to be carried out to investigate the effectiveness of stone columns under the condition of fluctuating ground water table associated with the application cyclic loading.
- It is anticipated that fines from surrounding soil may ingress into the stone column. Investigating the rate of movement of fine and their effect on durability of the stone column.
- Effect of embankment height on the general behaviour of the soil/ stone column composite soils.
- Study the influence of stone columns grid pattern and spacing on deformation of track due to cyclic loading.
- Relative density of the column has an influence on the bearing capacity of the soil/ stone composite soils. Therefore, it might be ideal to investigate the effect dilatancy of granular material on both settlement and bearing capacity.

REFERENCE

Aboshi, H., Ichimoto, E., Harada, K., et al. (1979) "The composer: A method to improve the characteristics of soft clays by inclusion of large diameter sand columns". **Proc., Int. Conf. on Soil Reinforcement., E.N.P.C.,**. Paris.

Adalier, K. and Elgamal, A. (2004) Mitigation of liquefaction and associated ground deformations by stone columns. **Engineering Geology**, 72: (3): 275-291.

Ahmadi, M. and Robertson, P. (2004) Calibration chamber size and boundary effect for CPT q (c) measurements. **Geotechnical and Geophysical Site Characterization. vols**, 1: 829-833.

Ali, K., Shahu, J.T. and Sharma, K.G. (2014) Model tests on single and groups of stone columns with different geosynthetic reinforcement arrangement. **Geosynthetics International**, 21: 103-118(115).

Ambily, A. and Gandhi, S. (2004) Experimental and theoretical evaluation of stone column in soft clay. **ICGGE-2004**, 201-206.

Ambily, A. and Gandhi, S. (2007) Behavior of Stone Columns Based on Experimental and FEM Analysis. **Journal of Geotechnical and Geoenvironmental Engineering**, 133: 405-415.

Andersen, K.H. (2004) "Cyclic clay data for foundation design of structures subjected to wave loading". **Proceedings of the International Conference on Cyclic Behaviour of Soils and Liquefaction Phenomena, CBS04, Bochum, Germany**.

Andersen, K.H., Rosenbrand, W.F., Brown, S.F., et al. (1980) Cyclic and static laboratory tests on Drammen clay. **Journal of the Geotechnical Engineering Division**, 106: (5): 499-529.

Anderson, W., Pyrah, I. and Fryer, S. (1991) A clay calibration chamber for testing field devices. **Geotechnical Testing Journal**, 14: (4).

Andreou, P., Frank, R., Frikha, W., et al. (2008) Experimental study on sand and gravel columns in clay. **Proceedings of the ICE - Ground Improvement**, 161: 189-198.

Ansal, A. and Erken, A. (1989) Undrained Behavior of Clay Under Cyclic Shear Stresses. **Journal of Geotechnical Engineering**, 115: 968-983.

Babu, M.D., Nayak, S. and Shivashankar, R. (2013) A critical review of construction, analysis and behaviour of stone columns. **Geotechnical and Geological Engineering**, 31: (1): 1-22.

Bae, W.-S., Shin, B.-W., An, B.-C., et al. (2002) "Behaviors of Foundation System Improved with Stone Columns". **The Twelfth International Offshore and Polar Engineering Conference**. Kitakyushu, Japan.

Balaam, N.P. and Booker, J.R. (1981) Analysis of rigid rafts supported by granular piles. **International Journal for Numerical and Analytical Methods in Geomechanics**, 5: (4): 379-403.

Balaam, N.P., Brown, P.T., Brown, H.G., et al. (1977) **Settlement Analysis of Soft Clays Reinforced with Granular Piles**. University of Sydney, School of Civil Engineering, Civil Engineering Laboratories.

Barksdale, R.D. and Bachus, R.C. (1983) "Design and construction of stone column ". Federal Highway Administration, RD-83/026.

Bell, A. (2004) The development and importance of construction technique in deep vibratory ground improvement. **Ground and Soil Improvement**, 103-111.

Bergado, D., Alfaro, M. and Chai, J. (1991) The granular pile: its present state and future prospects for improvement of soft Bangkok clay. **Geotechnical Engineering**, 22: 143-175.

Bergado, D., Huat, S.H. and Kalvade, S. (1987) "Improvement of soft Bangkok clay using granular piles in subsiding environment". **In: Proceedings, 5th international geotechnical seminar on case histories in soft clay**. Singapore.

Bergado, D. and Lam, F.L. (1987) Full scale load test of granular piles with different densities and different proportions of gravel and sand on soft Bangkok clay. **Soil Found**, 27: (1): 86-93.

Black, J., Sivakumar, V. and Bell, A. (2011) The settlement performance of stone column foundations. **Geotechnique**, 61: 909-922.

Black, J., Sivakumar, V., Madhav, M., et al. (2006) An Improved Experimental Test Set-up to Study the Performance of Granular Columns. **Geotechnical Testing Journal**, 29: 14195.

Bolton, M.D. (1991) **A guide to soil mechanics**. Universities Press.

Bouassida, M., Guetif, Z., De Buhan, P., et al. (2003) Variational approach for settlement estimation of a foundation on soil reinforced by columns. **Revue Française de Géotechnique**, 102: (1): 21-29.

Bowles, J.E. (1996) "Foundation analysis and design". Fifth ed., McGraw-Hill, New York.

Brough, M., Ghataora, G., Stirling, A., et al. (2003) Investigation of railway track subgrade. I: In-situ assessment. **Proceedings of the ICE-Transport**, 156: (3): 145-154.

Brown, S.F. (1996) Soil mechanics in pavement engineering. **Geotechnique**, 46: 383-426.

Brown, S.F. and Hyde, A. (1975) Significance of cyclic confining stress in repeated-load triaxial testing of granular material. **Transportation Research Record**, (537).

Brown, S.F., Lashine, A.K.F. and Hyde, A.F.L. (1975) Repeated load triaxial testing of a silty clay. 25: 95 - 114.

BSI, B.S.I. (2005) "Execution of special geotechnical works - Ground treatment by deep vibration". London, BS EN 14731:2005, BSI.

Cai, Y., Gu, C., Wang, J., et al. (2013) One-Way Cyclic Triaxial Behavior of Saturated Clay: Comparison between Constant and Variable Confining Pressure. **Journal of Geotechnical and Geoenvironmental Engineering**, 139: 797-809.

Cai, Y., Sun, Q., Guo, L., et al. (2015) Permanent deformation characteristics of saturated sand under cyclic loading. **Canadian Geotechnical Journal**, 52: (6): 1-13.

Charles, J. and Watts, K. (1983) "Compressibility of soft clay reinforced with granular columns". **Proceedings of the 8th European conference on soil mechanics and foundation Engineering, Helsinki**.

Chow, Y. (1996) Settlement Analysis of Sand Compaction Pile. **Soils and Foundations**, 36: (1): 111-113.

Ellouze, S., Bouassida, M., Hazzar, L., et al. (2010) On settlement of stone column foundation by Priebe's method. **Proceedings of the ICE-Ground Improvement**, 163: (2): 101-107.

Fatahi, B., Khabbaz, H. and Le, T.M. (2012) Improvement of rail track subgrade using stone columns combined with geosynthetics. **Advances in Transportation Geotechnics Ii**, 202-206.

Françaises, N. (2005) Recommendations for the design, calculation, installation and control of stone column foundations under buildings and structures sensitive to settlement. **Revue Française de Géotechnique**, 111: (2): 3-16.

Frikha, W., Bouassida, M. and Canou, J. (2014) Parametric Study of a Clayey Specimen Reinforced by a Granular Column. **International Journal of Geomechanics**.

Frost, M.W., Fleming, P.R. and Rogers, C.D. (2004) Cyclic triaxial tests on clay subgrades for analytical pavement design. **Journal of transportation Engineering**, 130: (3): 378-386.

Gniel, J. and Bouazza, A. (2007) "Methods used for the design of conventional and geosynthetic reinforced stone columns". **10th Australia New Zealand Conf. on Geomechanics (Australian Geomechanics Society and New Zealand Geomechanics Society 21/10/2007 to 24/10/2008)**. Geomechanics Society.

Gniel, J. and Bouazza, A. (2009) Improvement of soft soils using geogrid encased stone columns. **Geotextiles and Geomembranes**, 27: (3): 167-175.

Greenwood, D. (1970) "Mechanical improvement of soils below ground surface". **Proceedings, Ground Engineering Conference, Institution of Civil Engineers** London, UK.

Greenwood, D. (1991) Load tests on stone columns. **Deep Foundation Improvements: Design, Construction, and Testing**, 1089: 148.

Greenwood, D. and Kirsch, K. (1984) "Specialist ground treatment by vibratory and dynamic methods".

Gu, C., Wang, J., Cai, Y., et al. (2012) Undrained cyclic triaxial behavior of saturated clays under variable confining pressure. **Soil Dynamics and Earthquake Engineering**, 40: 118-128.

Han, J. (2015) Recent research and development of ground column technologies. **Proceedings of the Institution of Civil Engineers - Ground Improvement**, 168: (4): 246-264.

Hanna, A., Etezad, M. and Ayadat, T. (2013) Mode of failure of a group of stone columns in soft soil. **International Journal of Geomechanics**.

Head, K.H. (1996) **Manual of Soil Laboratory Testing, Permeability, Shear Strength and Compressibility Tests**. Wiley.

Head, K.H. (1998) **Manual of Soil Laboratory Testing, Effective Stress Tests**. Wiley.

Heath, D., Waters, J., Shenton, M., et al. (1972) "Design of conventional rail track foundations". **ICE Proceedings**. Thomas Telford.

Hu, W. (1995) **Physical modelling of group behaviour of stone column foundations**. University of Glasgow.

Hughes, J.M.O. and Withers, N.J. (1974) Reinforcing of soft cohesive soils with stone columns. **GROUND ENGINEERING**, 7.

Hughes, J.M.O., Withers, N.J. and Greenwood, D.A. (1976) A field trial of the reinforcing effect of a stone column in soil. **Ground treatment by deep compaction**.

Hyde, A., Yasuhara, K. and Hirao, K. (1993) Stability Criteria for Marine Clay under One-Way Cyclic Loading. **Journal of Geotechnical Engineering**, 119: 1771-1789.

ICE (1987) "Specification for Ground Treatment". Thomas Telford.

Indraratna, B., Attya, A. and Rujikiatkamjorn, C. (2009) Experimental Investigation on Effectiveness of a Vertical Drain under Cyclic Loads. **Journal of Geotechnical and Geoenvironmental Engineering**, 135: 835-839.

Jefferson, I., Gaterell, M., Thomas, A.M., et al. (2010) Emissions assessment related to vibro stone columns. **Proceedings of the ICE-Ground Improvement**, 163: (1): 71-77.

Jiang, M., Cai, Z., Cao, P., et al. (2010) "Effect of Cyclic Loading Frequency on Dynamic Properties of Marine Clay". **Soil Dynamics and Earthquake Engineering**. American Society of Civil Engineers 240-245.

Juran, I. and Guermazi, A. (1988) Settlement Response of Soft Soils Reinforced by Compacted Sand Columns. **Journal of Geotechnical Engineering**, 114: 930-943.

Killeen, M. (2012) **Numerical modelling of small groups of stone columns**. PhD, National University of Ireland, Galway.

Killeen, M. and McCabe, B.A. (2014) Settlement performance of pad footings on soft clay supported by stone columns: A numerical study. **Soils and Foundations**, 54: (4): 760-776.

Kim, B.-I. and Lee, S.-H. (2005) Comparison of bearing capacity characteristics of sand and gravel compaction pile treated ground. **KSCE Journal of Civil Engineering**, 9: (3): 197-203.

Kimura, T. and Saitoh, K. (1983) The influence of strain rate on pore pressures in consolidated undrained triaxial tests on cohesive soils. **Soils and Foundations**, 23: (1): 80-90.

Kolekar, Y.A., Mir, O.S. and Dasaka, S.M. (2011) " Behaviour of stone column reinforced marine clay under static and cyclic loading". **Proceedings of Indian Geotechnical Conference**. December 15-17, Kochi.

Lackenby, J., Indraratna, B., McDowell, G., et al. (2007) Effect of confining pressure on ballast degradation and deformation under cyclic triaxial loading. **Geotechnique**, 57: (6): 527-536.

Li, D. and Selig, E. (1996) Cumulative Plastic Deformation for Fine-Grained Subgrade Soils. **Journal of Geotechnical Engineering**, 122: 1006-1013.

Loh, R.B. and Nikraz, H.R. (2012) Compressibility and Strength of Clay Subgrade of Railroad Foundation in Highly Saturated Condition. **Journal of GeoEngineering**, 7: (2): 043-051.

Maakaroun, T., Najjar, S. and Sadek, S. (2009) "Effect of Sand Columns on the Load Response of Soft Clays". **Contemporary Topics in Ground Modification, Problem Soils, and Geo-Support**. American Society of Civil Engineers 217-224.

Madun, A. (2012) **Seismic evaluation of vibro-stone column**. PhD, University of Birmingham.

Madun, A., Jefferson, I., Foo, K., et al. (2012) Characterization and quality control of stone columns using surface wave testing. **Canadian Geotechnical Journal**, 49: (12): 1357-1368.

McCabe, B.A., Nimmons, G.J. and Egan, D. (2009) A review of field performance of stone columns in soft soils. **Proceedings of the Institution of Civil Engineers-Geotechnical engineering**, 162: 323–334.

McKelvey, D. (2002) **The performance of vibro stone column reinforced foundations in deep soft ground**. PhD, Queen's University of Belfast.

McKelvey, D. and Sivakumar, V. (2000) "A review of the performance of vibro stone column foundations". **Proceedings of the 3rd International Conference on Ground Improvement Techniques, Singapore**.

McKelvey, D., Sivakumar, V., Bell, A., et al. (2002) Shear strength of recycled construction materials intended for use in vibro ground improvement. **Proceedings of the ICE-Ground Improvement**, 6: (2): 59-68.

Miller, G.A., Teh, S.Y., Li, D., et al. (2000) Cyclic Shear Strength of Soft Railroad Subgrade. **Journal of Geotechnical and Geoenvironmental Engineering**, 126: 139-147.

Mitchell, J.M. and Jardine, F.M. (2002) **A Guide to Ground Treatment**. Construction Industry Research & Information Association.

Mohanty, P. and Samanta, M. (2015) Experimental and Numerical Studies on Response of the Stone Column in Layered Soil. **International Journal of Geosynthetics and Ground Engineering**, 1: (3): 1-14.

Moseley, M.P. and Kirsch, K. (2004) **Ground improvement**. London; New York: Spon Press.

Munfakh, G.A. (1984) "Soil Reinforcement by stone columns–varied case applications".

Munfakh, G.A. (1997) Ground improvement engineering–the state of the US practice: part 1. Methods. **Ground Improvement**, 1: 193–214.

Munfakh, G.A. (2003) Ground improvement in transportation projects: from old visions to innovative applications. **Proceedings of the ICE - Ground Improvement**, 7: 47-60.

Najjar, S. (2013) A State-of-the-Art Review of Stone/Sand-Column Reinforced Clay Systems. **Geotechnical and Geological Engineering**, 31: 355-386.

Najjar, S., Sadek, S. and Maakaroun, T. (2010) Effect of sand columns on the undrained load response of soft clays. **Journal of Geotechnical and Geoenvironmental Engineering**.

Nakase, A. and Kamei, T. (1986) Influence of strain rate on undrained shear characteristics of K0-consolidated cohesive soils. **Japanese Socity of Soil Mechanics and Foundation Engineering**, 26: (1): 85-95.

Ng, C., Zhou, C., Yuan, Q., et al. (2013) Resilient modulus of unsaturated subgrade soil: experimental and theoretical investigations. **Canadian Geotechnical Journal**, 50: (2): 223-232.

Peacock, W. and Bolton, S. (1968) Sand liquefaction under cyclic loading simple shear conditions. **Journal of Soil Mechanics & Foundations Div**.

Poorooshasb, H.B. and Meyerhof, G.G. (1997) Analysis of behavior of stone columns and lime columns. **Computers and Geotechnics**, 20: 47–70.

Powrie, W. (2013) **Soil mechanics: concepts and applications**. CRC Press.

Priebe, H.J. (1995) The design of vibro replacement. **GROUND ENGINEERING**, 28: 31–37.

Raju, V. (2003) "Ground Improvement Techniques for Railway Embankments". **Railtech Conference**.

Raju, V. and Sondermann, W. (2005) Ground improvement using deep vibro techniques. **Elsevier Geo-Engineering Book Series**, 3: 601-638.

Redgers, J.D., Moxhay, A.L., Ghataora, G.S., et al. (2008) Case Histories of Settlement Performance Comparisons on Ground Improvement Using Soil Stiffness Seismic Wave and Traditional Methods. **Proceedings of The International Conference On Case Histories In Geotechnical Engineering**.

Rollins, K., Price, B., Dibb, E., et al. (2006) Liquefaction mitigation of silty sands in Utah using stone columns with wick drains. **Ground Modification and Seismic Mitigation**, 343-348.

Rowe, P.W. and Barden, L. (1966) A New Consolidation Cell. **Geotechnique**, 16: (2): 162-&.

Rudolph, R., Serna, B. and Farrell, T. (2011) Mitigation of Liquefaction Potential Using Rammed Aggregate Piers. **Advances in Geotechnical Engineering**, 557-566.

Salahi, A., Niroumand, H. and Kassim, K.A. (2015) Evaluation of Stone Columns versus Liquefaction Phenomenon. **Electronic Journal of Geotechnical Engineering (EJGE)**, 20: (2).

Samadhiya, N., Maheswari, P., Basu, P., et al. (2008) Load-settlement characteristics of granular piles with randomly mixed fibres. **Indian Geotech. J**, 38: (3): 345-354.

Schanz, T., Vermeer, P. and Bonnier, P. (1999) The hardening soil model: formulation and verification. **Beyond 2000 in computational geotechnics**, 281-296.

Seed, H.B. and Booker, J.R. (1977) Stabilization of potentially liquefiable sand deposits using gravel drain systems. **ASCE Journal of Geotechnical Engineering**, 103: (7): 757-768.

Seed, H.B., Chan, C.K. and Monismith, C.L. (1955) "Effects of repeated loading on the strength and deformation of compacted clay". **Highway Research Board Proceedings**.

Sekine, E. (1996) **Bearing Capacity of Roadbed and its Reinforcement.** Department of Civil Engineering, Nagaoka University of Technology for the degree of Doctor.

Selig, E.T. and Waters, J.M. (1994) **Track geotechnology and substructure management**. Thomas Telford.

Serridge, C.J. (2005) Achieving sustainability in vibro stone column techniques. **Proceedings of the ICE-Engineering Sustainability**, 158: (4): 211-222.

Serridge, C.J. (2006) Some applications of ground improvement techniques in the urban environment. **Engineering Geology for Tomorrow's Cities, Geological Society, London, Engineering Geology Special Publications**, 22.

Sivakumar, V., Bell, A., McKelvey, D., et al. (2004a) Modelling vibrated stone columns in soft clay. **Proceedings of the ICE - Geotechnical Engineering**, 157: 137-149.

Sivakumar, V., Boyd, J.L., Black, J.A., et al. (2010) Effects of granular columns in compacted fills. **Proceedings of the ICE - Geotechnical Engineering**, 163: 189-196.

Sivakumar, V., Glynn, D., Black, J., et al. (2007) "A laboratory model study of the performance of vibrated stone columns in soft clay". **Proceedings of the 14th European Conference on Soil Mechanics and Geotechnical Engineering, Madrid, Spain**.

Sivakumar, V., McKelvey, D., Graham, J., et al. (2004b) Triaxial tests on model sand columns in clay. **Canadian Geotechnical Journal**, 41: 299-312.

Skempton, A. (1957) Discussion: Further data on the c/p ratio in normally consolidated clays. **Proceedings of the Institution of Civil Engineers**, 7: 305-307.

Slocombe, B., Bell, A. and Baez, J. (2000) The densification of granular soils using vibro methods. **Geotechnique**, 50: (6): 11.

Sun, X., Han, J., Wayne, M.H., et al. (2014) "Quantifying the Benefit of Triaxial Geogrid in Stabilizing Granular Bases over Soft Subgrade under Cyclic Loading at Different Intensities". **Geo-Congress 2014 Technical Papers at Geo-characterization and Modeling for Sustainability**. ASCE.

Unnikrishnan, N., Rajagopal, K. and Krishnaswamy, N.R. (2002) Behaviour of reinforced clay under monotonic and cyclic loading. **Geotextiles and Geomembranes**, 20: 117–133.

Valls-Marquez, M. (2009) **Evaluating the capabilities of some constitutive models in reproducing the experimental behaviour of stiff clay subjected to tunnelling stress paths**. The University of Birmingham.

Van Impe, W.F., De Cock, F., Van der Cruyssen, J.P., et al. (1997) Soil improvement experiences in Belgium: part II. Vibrocompaction and stone columns. **Proceedings of the ICE-Ground Improvement**, 1: 157–168.

Vardanega, P. and Haigh, S. (2014) The undrained strength–liquidity index relationship. **Canadian Geotechnical Journal**, 51: (9): 1073-1086.

Vekli, M., Aytekin, M., Ikizler, S.B., et al. (2012) Experimental and numerical investigation of slope stabilization by stone columns. **Natural hazards**, 64: (1): 797-820.

Wang, J.-h., Liu, Y.-f. and Xing, Y. (1998) Estimation of undrained bearing capacity for offshore soft foundations with cyclic load. **China Ocean Engineering**, 12: (2): 213-222.

Wang, J., Li, C. and Shi, M. (2006) Experimental study on cyclic mechanics characteristic of saturated soft clay strata. **Trans. Tianjin Univ.**, 12: (2).

Wang, L.-Z., Li, L.-L. and Dan, H.-B. (2011) Undrained behavior of natural marine clay under cyclic loading. **Ocean Engineering**, 38: 1792-1805.

Watts, F. (2000) Specifying vibro stone columns. **British Research Establishment (BRE) Report, Watford, UK**.

Wood, D.M., Hu, W. and Nash, D.F.T. (2000) Group effects in stone column foundations: model tests. **Geotechnique**, 50: 689–698.

Woodward, J. (2004) **An Introduction to Geotechnical Processes**. CRC Press.

Yasuhara, Hirao, K. and Hyde, A.F.L. (1992) Effects of cyclic loading on undrained strength and compressibility of clay. **Soils and Foundations**, 32: (1): 100-116.

Yasuhara, Yamanouchi, T. and Hirao, K. (1982) Cyclic strength and deformation of normally consolidated clay. **Soils and Foundations**.

Yoo, T. and Selig, E. (1979) Field observations of ballast and subgrade deformations in track. **Transportation Research Record**, (733).

Zahmatkesh, A. and Choobbasti, A.J. (2010) Settlement evaluation of soft clay reinforced with stone columns using the equivalent secant modulus. **Arabian Journal of Geosciences**.

Zhou, J. and Gong, X. (2001) Strain degradation of saturated clay under cyclic loading. **Canadian Geotechnical Journal**, 38: 208-212.

APPENDIX A

Material Properties

- Data of Sieve Analysis for Aggregate Used To Construct Stone Column

Sieve (mm)	Test (1)			Test (2)			Test (3)		
	Retain weight (g)	Retain (%)	Passing (%)	Retain weight (g)	Retain (%)	Passing (%)	Retain weight (g)	Retain (%)	Passing (%)
5	1.1	0.22	99.78	0.8	0.16	99.84	1.00	0.19	99.81
3.35	106.9	21.36	78.42	102.5	20.36	79.48	109.94	20.86	78.95
2.36	153	30.57	47.85	145	28.80	50.69	156.45	29.68	49.27
2	140	27.97	19.88	150	29.79	20.89	152.25	28.88	20.39
1.18	99.2	19.82	0.06	105	20.85	0.04	107.21	20.34	0.05
0.6	0.2	0.04	0.02	0.1	0.02	0.02	0.16	0.03	0.02
Pan	0.1	0.02	0.00	0.1	0.02	0.00	0.11	0.02	0.00
Total weight (g)	500.5			503.5			527.10		

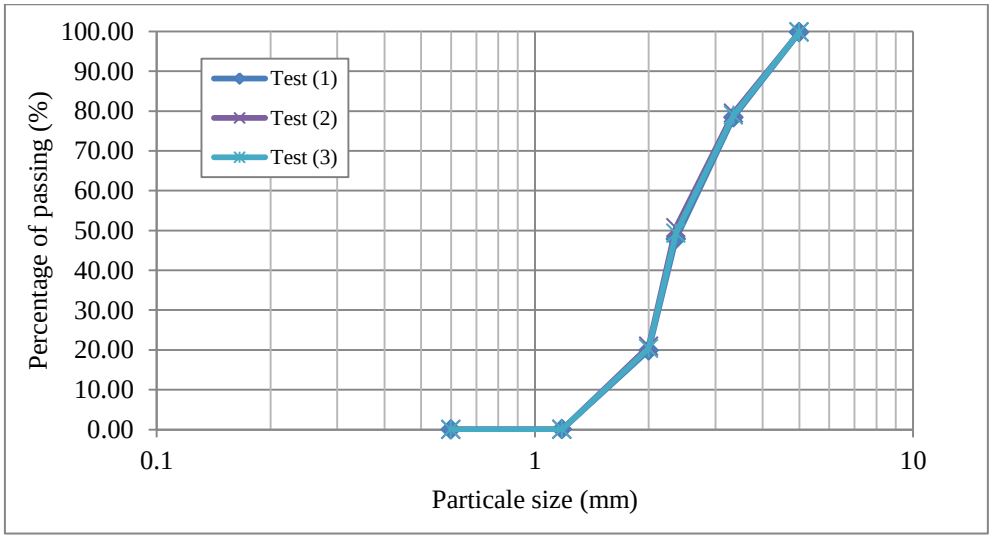

- China clay particle size distribution (hydrometer sedimentation)

Elapsed time, (min)	Temperature C°	Reading Rh'	Rh' + Cm =Rh	Effective depth Hr (mm)	Particle diameter D (mm)	Rh' - Ro' =Rd	Percentage finer (%)
0	25	25	25.5	97.07		24.5	
0.5	25	19	19.5	121.41	0.06	18.5	99.0
1	25	19	19.5	121.41	0.04	18.5	99.0
2	25	19	19.5	121.41	0.03	18.5	99.0
4	25	19	19.5	121.41	0.02	18.5	99.0
8	25	18.5	19	123.44	0.02	18	96.4
15	25	18	18.5	125.46	0.01	17.5	93.7
30	25	17.5	18	127.49	0.01	17	91.0
60	25	16	16.5	133.58	0.01	15.5	83.0
120	25	14	14.5	141.69	0.00	13.5	72.3
240	25	12.5	13	147.77	0.00	12	64.2
450	25	10.5	11	155.88	0.00	10	53.5
1420	25	8.5	9	164.00	0.00	8	42.8

Particle size **supplied by manufacturer *WBB***

size (micron)	**size (mm)**	**Percentage (%)**
1	**0.001**	**37**
2	**0.002**	**49**
5	**0.005**	**76**
10	**0.01**	**94**
20	**0.02**	**99**

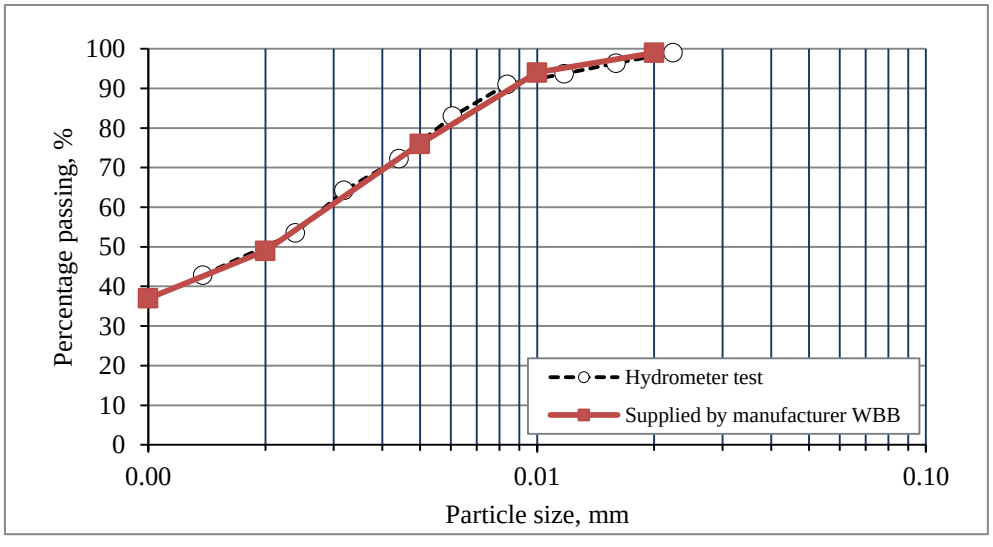

- Soil Index
- Liquid Limit

Test No.:	**(1)**			**(2)**			**(3)**			**(4)**		
dial gage reading	14.00	13.80	14.10	19.40	19.00	18.90	19.90	20.50	20.30	23.20	22.90	23.50
Average Penetration	13.97			19.10			20.23			23.20		
Container #	p6	pla3	y11	LLL	m45	120	E	342y	w17	8A	mc51	mc8
Mass of container g	3.15	3.99	3.19	7.84	5.49	4.41	3.34	3.39	4.72	4.73	4.76	5.40
Mass of container + Wet Soil (g)	16.31	19.24	23.67	21.59	26.45	20.52	17.11	18.34	25.51	20.64	28.46	26.06
Mass of container + Dry Soil (g)	11.75	13.95	16.56	16.70	19.00	14.79	12.17	12.98	18.06	14.83	19.80	18.51
Mass of Dry Soil (g)	8.60	9.96	13.37	8.86	13.51	10.38	8.83	9.59	13.34	10.10	15.04	13.11
Mass of Moisture (g)	4.56	5.29	7.11	4.89	7.45	5.73	4.94	5.36	7.45	5.81	8.66	7.55
Moisture content (%)	53.02	53.11	53.18	55.19	55.14	55.20	55.95	55.89	55.85	57.52	57.58	57.59
Ave. moisture content (%)	53.10			55.18			55.89			57.56		

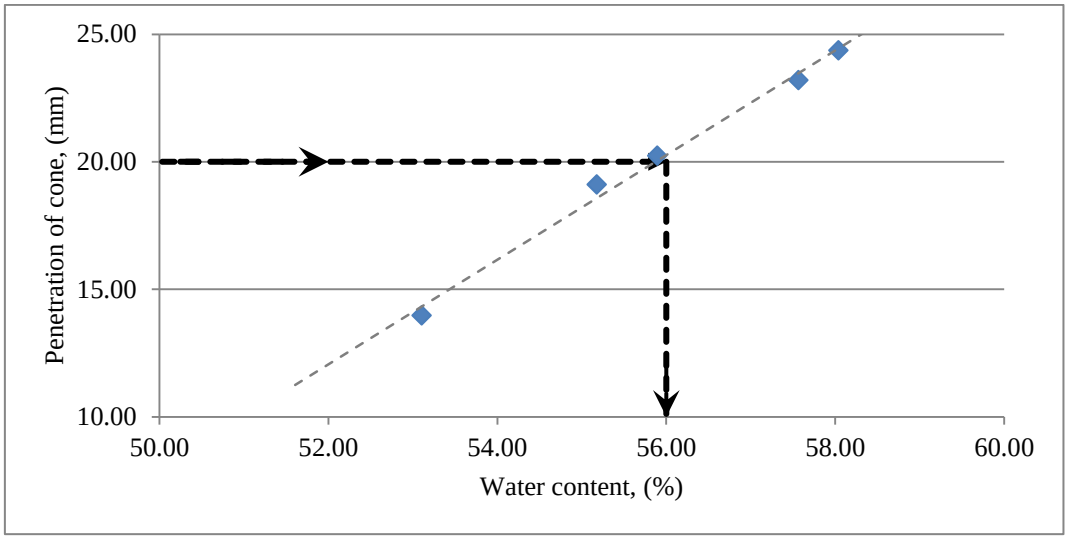

- Plastic Limit

Test No.:	**(1)**	**(2)**	**(3)**	**(4)**
Mass of container (g)	3.22	3.38	4.43	3.99
Mass of container + Wet Soil (g)	3.97	4.47	4.96	4.82
Mass of container + Dry Soil (g)	3.81	4.24	4.85	4.64
Mass of Dry Soil (g)	0.59	0.86	0.42	0.65
Mass of Moisture (g)	0.16	0.23	0.11	0.18
Moisture content (%)	27.12	27.09	27.14	27.08
Ave. water content (%)	**27.11**			

- Compaction Test Data

BS 1377:1990	Test NO.:	Location: Civil Engineering Lab
No. of layers: 3	Rammer: 2.5 kg	
Blow per layer : 25	Drop: 300mm	Soil description: English china clay
Compacted by:	Sample preparation:	Sample type:
Proctor cylinder NO.: 1	No. of separate batches:	

Density : Volume of cylinder "V": (Dia: 104.903mm, length : 115.470mm): 997.952mm^3

Test No.:	**(1)**			**(2)**			**(3)**		
Cylinder & soil, A (g)	6679			6785			6801		
Cylinder, B (g)	4978.5			4978.5			4978.5		
Wet soil, A-B (g)	1700.5			1806.5			1822.5		
Volume, cm^3	0.998			0.998			0.998		
Wet density, (Mg/m^3)	1.70			1.81			1.83		
Vane shear strength	over 120			over 120			53		
Moisture content									
Container No.:	f28t31	P12	66	S10	B22-8	212ms2	m9t2	T25	M7T
Wet soil & container, g	8.43	8.64	7.76	14.67	12.19	21.01	11.97	17.55	13.51
Dry soil & container, g	7.41	7.72	6.98	12.20	10.66	17.33	9.84	14.43	11.41
Container,(g)	3.17	3.92	3.67	3.39	5.32	4.22	3.36	4.70	4.78
Dry soil , (g)	4.24	3.80	3.31	8.81	5.34	13.11	6.48	9.73	6.63
Moisture loss, (g)	1.02	0.92	0.78	2.47	1.53	3.68	2.13	3.12	2.10
Moisture content,(%)	24.06	24.21	23.56	28.04	28.65	28.07	32.87	32.07	31.67
Average moisture, (%)	23.94			28.25			32.20		
Dry density, (Mg/m^3)	-			1.41			1.38		

Test NO.:	**4**	**5**	**6**
Cylinder & soil, A g	6738	6677	6593
Cylinder, B g	4978.5	4978.5	4979.3
Wet soil, A-B g	1759.5	1698.5	1613.7
Volume, cm3	0.998	0.998	0.998
Wet density, ρ Mg/m3	1.76	1.70	1.62
Vane shear strength	23	14	-

Moisture content									
Container No.:	f28t	39s	CL17	SA01	SA02	SA03	m90u	f28t31	39s
Wet soil & container, g	18.65	8.65	21.11	12.59	12.14	18.65	19.50	11.17	13.18
Dry soil & container, g	14.96	7.19	17.22	9.93	9.65	14.22	14.46	8.33	9.64
Container, g	4.77	3.18	6.54	3.29	3.50	3.19	5.32	3.18	3.18
Dry soil , g	10.19	4.01	10.68	6.64	6.15	11.03	9.14	5.15	6.46
Moisture loss, g	3.69	1.46	3.89	2.66	2.49	4.43	5.04	2.84	3.54
Moisture content, %	36.21	36.41	36.42	40.06	40.49	40.16	55.14	55.15	54.80
Average moisture, %	36.35			40.24			55.03		
Dry density ρd Mg/m3	1.29			1.21			1.04		

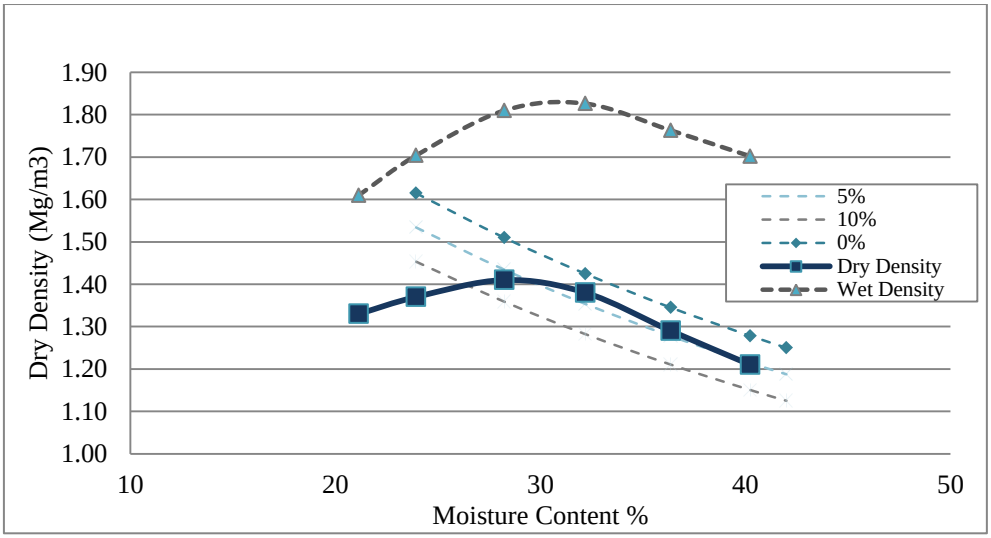

- Undrained Shear Strength for Kaolin Clay

- Hand Vane Shear Test

Test No.:	**Water content (%)**				**Shear strength (kPa)**			
	A	B	C	Average	A	B	C	Average
Test (1)	32.87	32.07	31.67	32.2	52	53	53	52.6
Test (2)	36.21	36.41	36.42	36.35	25	24	25	24.6
Test (3)	40.06	40.49	41.16	40.24	15	14	14	14.3
Test (4)	42.2	42.15	41.85	42.06	9	9	10	9.3
Test (5)	44.5	44.7	44.1	44.43	9	8	7	8
Test (6)	55.14	55.15	54.80	47.31	4	5	6	5

- Quick Undrained Triaxial Test

Test No.:	**Average water content (%)**	**Average deviator stress results**			**Shear strength (kPa)**
		σ_3= 50 kPa	σ_3= 100 kPa	σ_3= 150 kPa	
Test (1)	35	108	109	112	54.4
Test (2)	38	37	38	39	18.5
Test (3)	42.5	30	31	33	15.5
Test (4)	44	25.56	23.5	25.32	12.3

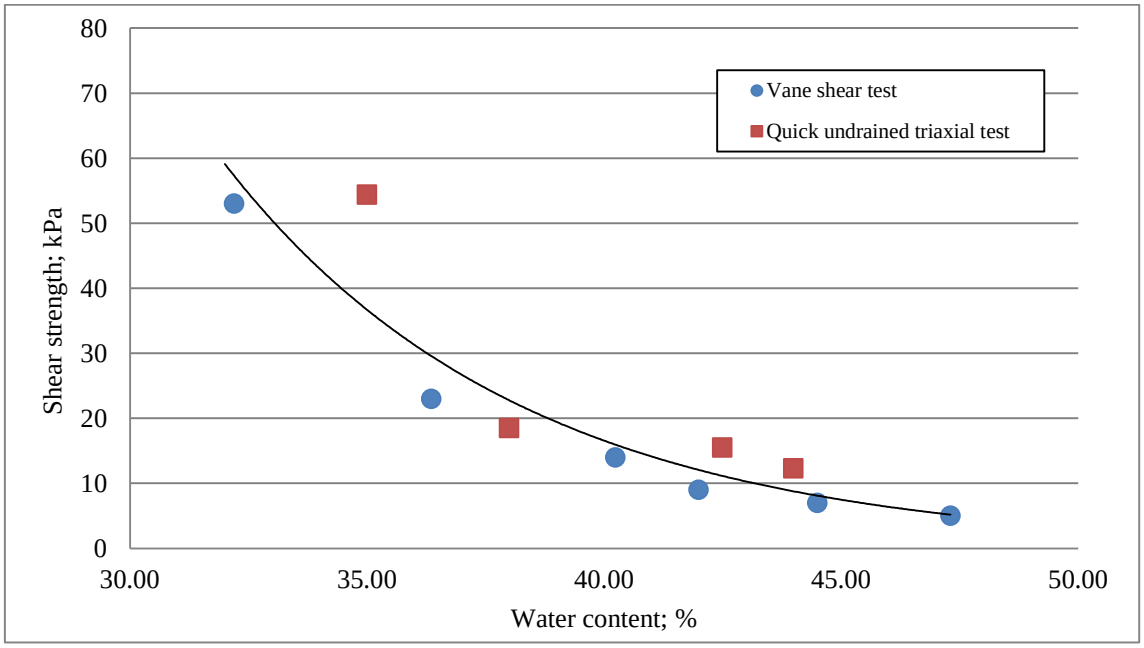

4.1 Shear Box Data Results for Column Material

Test No.:	**Shear stress results (wet condition)**				**Average internal angle of friction ∅ (^{o})**
	25 kPa	50 kPa	100 kPa	200 kPa	
Test (1)	37	64.13	121.63	217.66	48
Test (2)	38.20	63.21	120.1	210	

Test No.:	**Shear stress results (dry condition)**				**Average internal angle of friction ∅ (^{o})**
	25 kPa	50 kPa	100 kPa	200 kPa	
Test (1)	48	75.11	141.57	239.1	50
Test (2)	52.25	71.40	143.54	242.44	

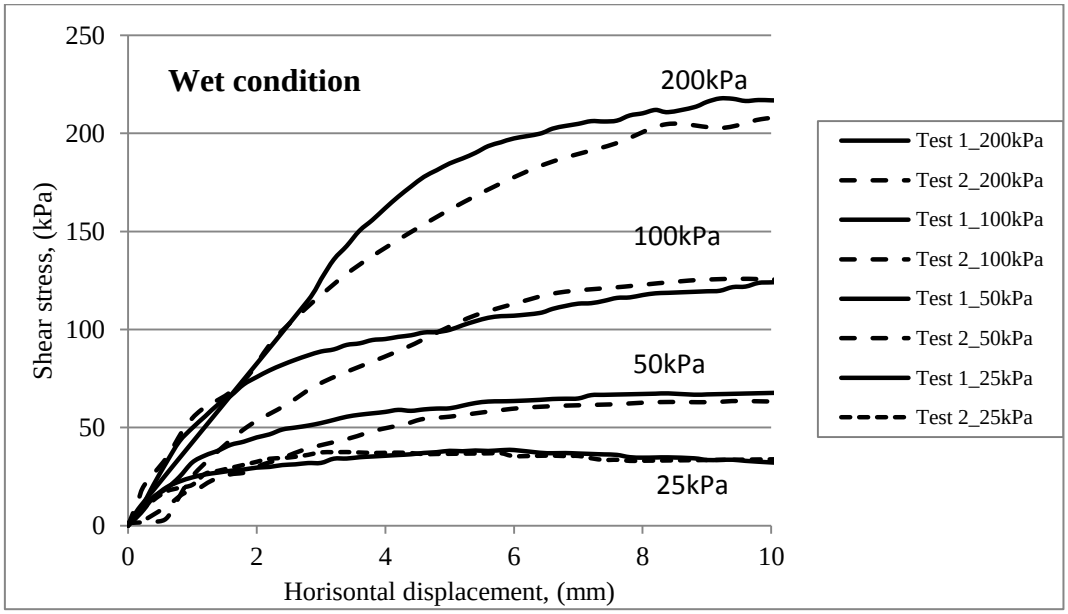

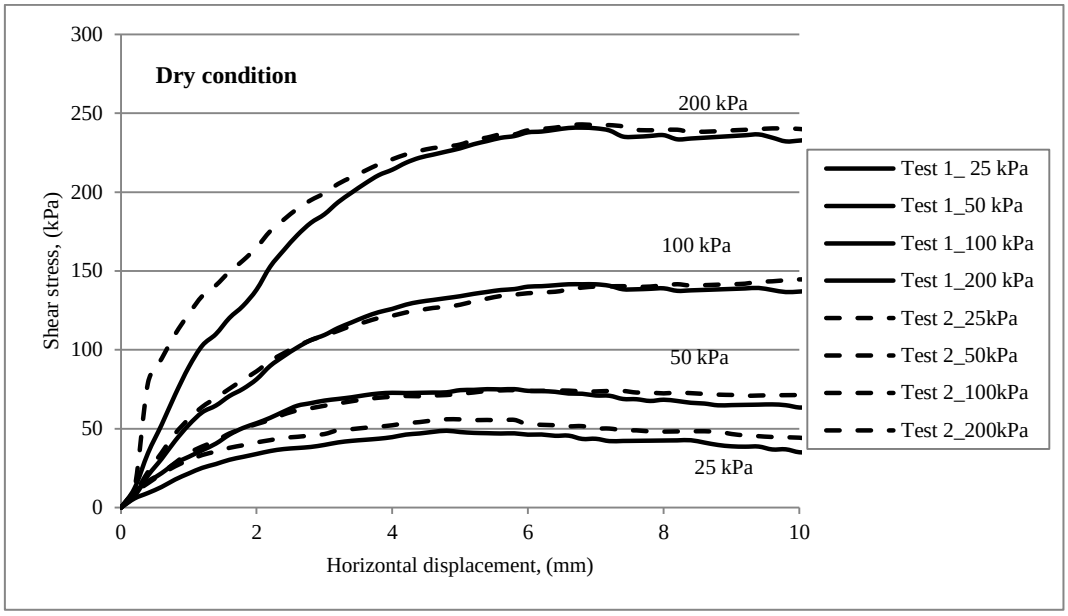
Dry condition
200 kPa
100 kPa
50 kPa
25 kPa
Shear stress, (kPa)
Horizontal displacement, (mm)
Test 1_ 25 kPa
Test 1_50 kPa
Test 1_100 kPa
Test 1_200 kPa
Test 2_25kPa
Test 2_50kPa
Test 2_100kPa
Test 2_200kPa

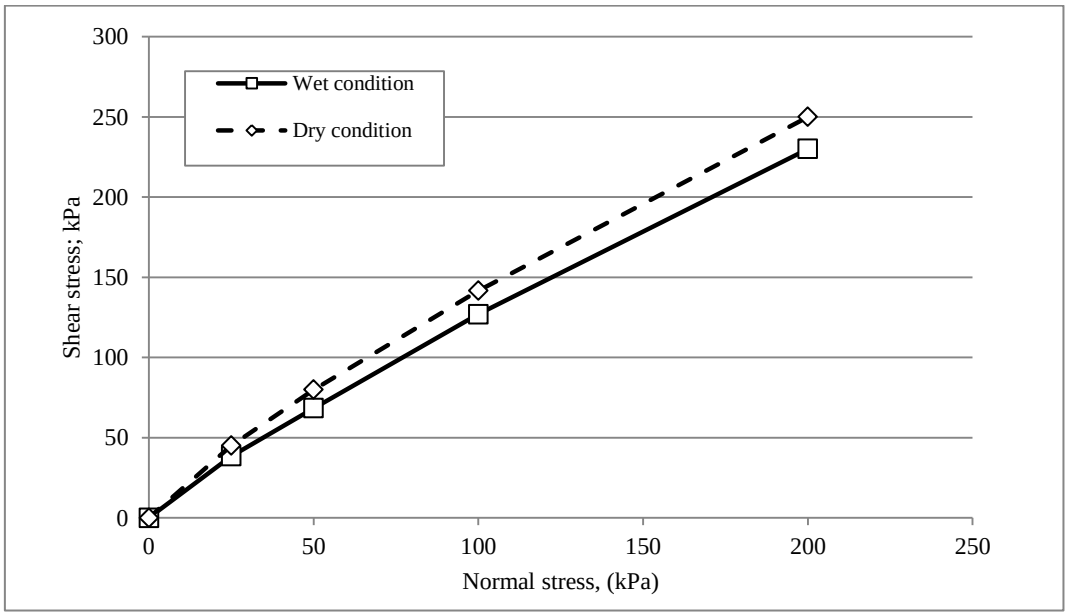
Wet condition
Dry condition
Shear stress; kPa
Normal stress, (kPa)

- Specific Gravity Test Data

- Specific Gravity for Kaolin Clay

Test No.:		**1**	**2**	**3**	**4**
Mass of bottle (g)	*m1*	48.16	46.88	49.48	48.57
Mass of bottle & soil (g)	*m2*	49.97	49.51	51.59	50.74
Mass of bottle water & soil (g)	*m3*	104.05	108.38	108.49	105.51
Mass of bottle full water (g)	*m4*	102.93	106.75	107.18	104.17
Specific gravity		2.62	2.64	2.64	2.61
average		2.63			

- Specific Gravity for Column Material

Test No.:		**1**	**2**	**3**	**4**
Mass of bottle (g)	*m1*	48.16	46.88	49.48	48.57
Mass of bottle & soil (g)	*m2*	60.98	61.03	59.62	58.94
Mass of bottle water & soil (g)	*m3*	110.97	115.72	113.60	110.67
Mass of bottle full water (g)	*m4*	102.90	106.78	107.19	104.15
Specific gravity		2.70	2.72	2.72	2.69
average		2.71			

- Clay Bed Consolidation

Pressure	**Test (1)**			**Test (2)**			**Test (3)**		
Consolidation pressure (6.45 kPa)	Time (minute)	Root Square Time	Deformation (mm)	Time (minute)	Root Square Time	Deformation (mm)	Time (minute)	Root Square Time	Deformation (mm)
	0	0.00	0.00	0	0.00	0.00	0	0.00	0.00
	1	1.00	0.15	1	1.00	0.19	1	1.00	0.20
	2	1.41	0.30	2	1.41	0.35	2	1.41	0.34
	4	2.00	0.55	4	2.00	0.63	4	2.00	0.40
	8	2.83	0.98	8	2.83	1.15	8	2.83	1.03
	15	3.87	1.60	15	3.87	1.95	20	4.47	2.14
	30	5.48	2.64	30	5.48	3.18	33	5.74	3.10
	60	7.75	4.30	60	7.75	5.25	60	7.75	4.80
	120	10.95	9.05	120	10.95	8.50	240	15.49	16.85
	240	15.49	14.82	240	15.49	17.00	1486	38.55	38.57

	480	21.91	22.30	432	20.78	23.00	1526	39.06	39.09
	1440	37.95	36.50	1476	38.42	39.95	2788	52.80	51.15
	2880	53.66	49.81	2827	53.17	45.95	2936	54.18	51.52
	3600	60.00	50.10						
Pressure	**Test (1)**			**Test (2)**			**Test (3)**		
Consolidation pressure (12 kPa)	Time (minute)	Root Square Time	Deformation (mm)	Time (minute)	Root Square Time	Deformation (mm)	Time (minute)	Root Square Time	Deformation (mm)
	0	0.00	0.00	0	0.00	0.00	0	0.00	0.00
	1	1.00	0.63	1	1.00	0.33	1	1.00	0.27
	2	1.41	0.81	2	1.41	0.62	2	1.41	0.33
	4	2.00	1.07	4	2.00	1.07	4	2.00	0.48
	8	2.83	1.45	8	2.83	1.50	8	2.83	0.70
	15	3.87	1.95	15	3.87	2.10	15	3.87	1.13
	30	5.48	2.75	30	5.48	2.67	30	5.48	1.70
	60	7.75	3.89	60	7.75	3.50	65	8.06	2.47
	120	10.95	4.84	120	10.95	4.68	115	10.72	3.50
	240	15.49	6.54	240	15.49	6.78	1322	36.36	12.84
	450	21.21	8.75	480	21.91	9.42	1460	38.21	13.25
	1329	36.46	10.90	1440	37.95	11.65			
	1440	37.95	11.00						
	1635	40.44	11.40						
Pressure	**Test (1)**			**Test (2)**			**Test (3)**		
Consolidation pressure (25 kPa)	Time (minute)	Root Square Time	Deformation (mm)	Time (minute)	Root Square Time	Deformation (mm)	Time (minute)	Root Square Time	Deformation (mm)
	0	0.00	0.00	0	0.00	0.00	0	0.00	0.00
	1	1.00	0.60	1	1.00	0.61	1	1.00	0.61
	2	1.41	0.79	2	1.41	0.76	2	1.41	0.76
	4	2.00	0.98	4	2.00	0.97	4	2.00	0.97
	9	3.00	1.35	9	3.00	1.25	9	3.00	1.25
	21	4.58	1.95	15	3.87	1.67	15	3.87	1.67
	30	5.48	2.32	30	5.48	2.29	30	5.48	2.29
	60	7.75	3.26	53	7.28	3.05	53	7.28	3.05
	120	10.95	4.55	116	10.77	4.45	116	10.77	4.45
	200	14.14	5.77	200	14.14	6.37	200	14.14	6.37
	462	21.49	7.95	456	21.35	8.16	456	21.35	8.16
	1448	38.05	8.95	1460	38.21	9.30	1460	38.21	9.30
Pressure	**Test (1)**			**Test (2)**			**Test (3)**		
Consolidation pressure (50 kPa)	Time (minute)	Root Square Time	Deformation (mm)	Time (minute)	Root Square Time	Deformation (mm)	Time (minute)	Root Square Time	Deformation (mm)
	0	0.00	0.00	0	0.00	0.00	0	0.00	0.00
	1	1.00	1.00	1	1.00	0.80	1	1.00	0.80
	2	1.41	1.20	2	1.41	0.97	2	1.41	0.97
	4	2.00	1.51	4	2.00	1.21	4	2.00	1.21
	8	2.83	1.97	8	2.83	1.58	8	2.83	1.58
	15	3.87	2.70	15	3.87	2.04	15	3.87	2.04
	30	5.48	3.40	30	5.48	2.84	30	5.48	2.84

	60	7.75	4.61	63	7.94	3.91	63	7.94	3.91
	120	10.95	6.33	123	11.09	5.60	123	11.09	5.90
	240	15.49	8.31	240	15.49	7.57	240	15.49	7.87
	480	21.91	9.65	360	18.97	8.55	360	18.97	8.85
	1440	37.95	10.02	440	20.98	8.86	420	20.49	9.06
				1440	37.95	9.42	1414	37.60	9.62
Pressure	**Test (1)**			**Test (2)**			**Test (3)**		
Consolidation pressure (100 kPa)	Time (minute)	Root Square Time	Deformation (mm)	Time (minute)	Root Square Time	Deformation (mm)	Time (minute)	Root Square Time	Deformation (mm)
	0	0.00	0.00	0	0.00	0.00	0	0.00	0.00
	1	1.00	0.35	1	1.00	0.35	1	1.00	0.35
	2	1.41	0.50	2	1.41	0.55	2	1.41	0.55
	4	2.00	0.82	4	2.00	0.88	4	2.00	0.88
	8	2.83	1.25	8	2.83	1.30	8	2.83	1.30
	15	3.87	1.87	15	3.87	1.90	15	3.87	1.70
	30	5.48	2.88	30	5.48	3.20	30	5.48	2.40
	60	7.75	4.25	60	7.75	5.10	60	7.75	4.10
	120	10.95	6.02	120	10.95	7.33	120	10.95	6.33
	240	15.49	7.50	240	15.49	9.25	240	15.49	8.25
	485	22.02	8.17	449	21.19	9.84	449	21.19	8.84
	1440	37.95	8.40	1380	37.15	10.14	1380	37.15	9.14

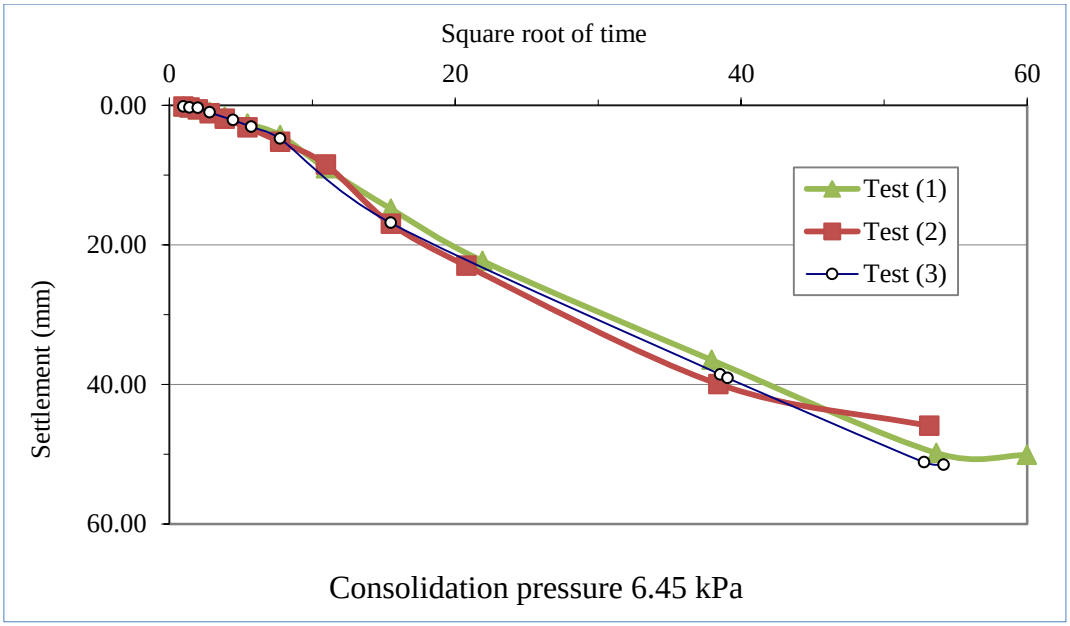

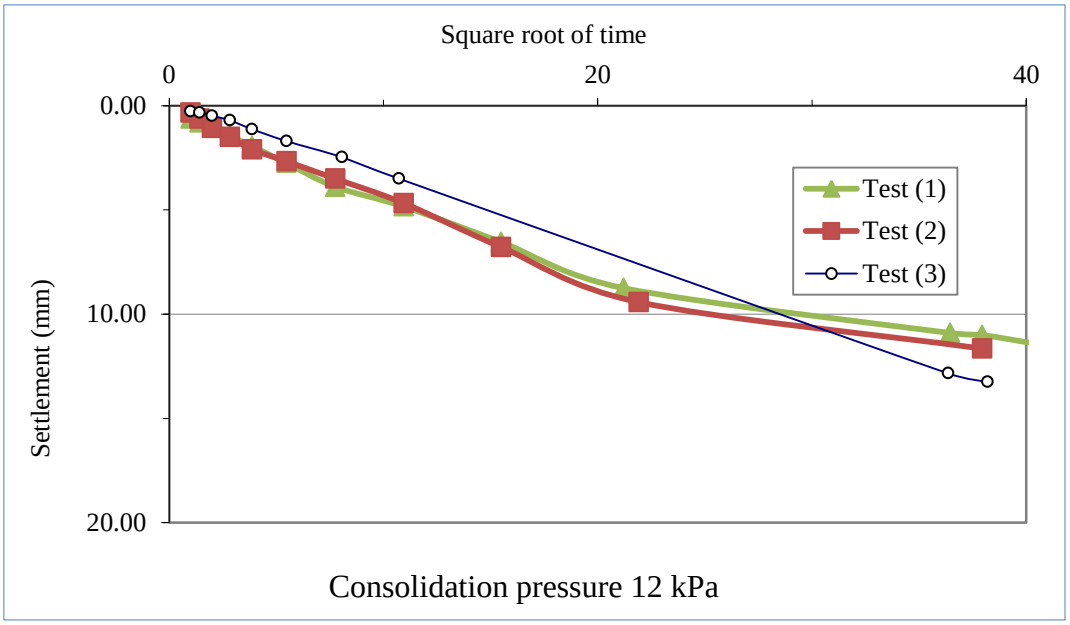

Consolidation pressure 12 kPa

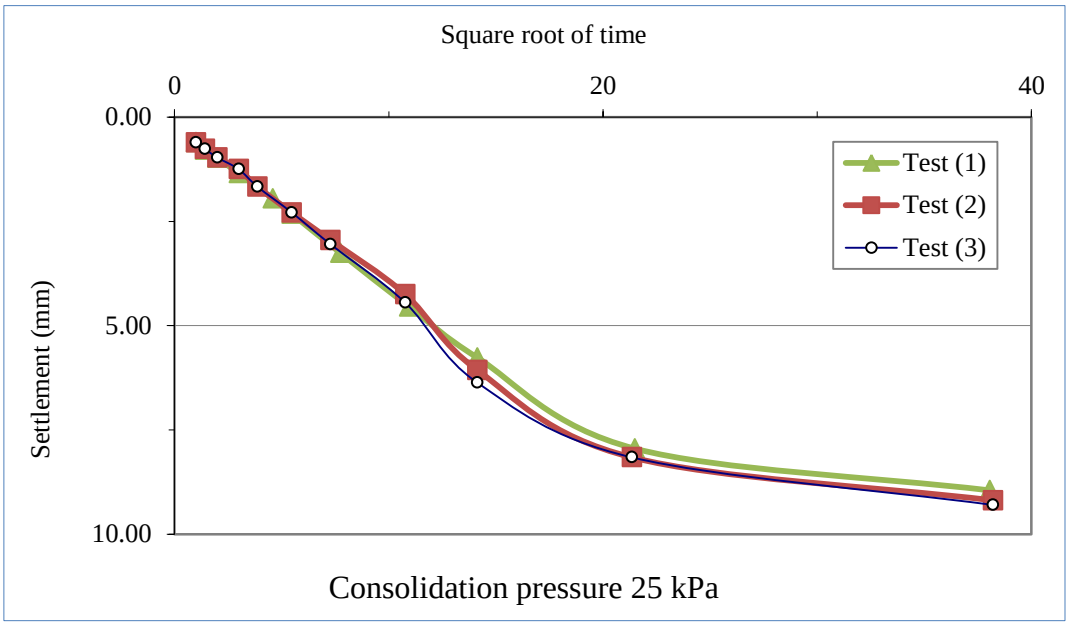

Consolidation pressure 25 kPa

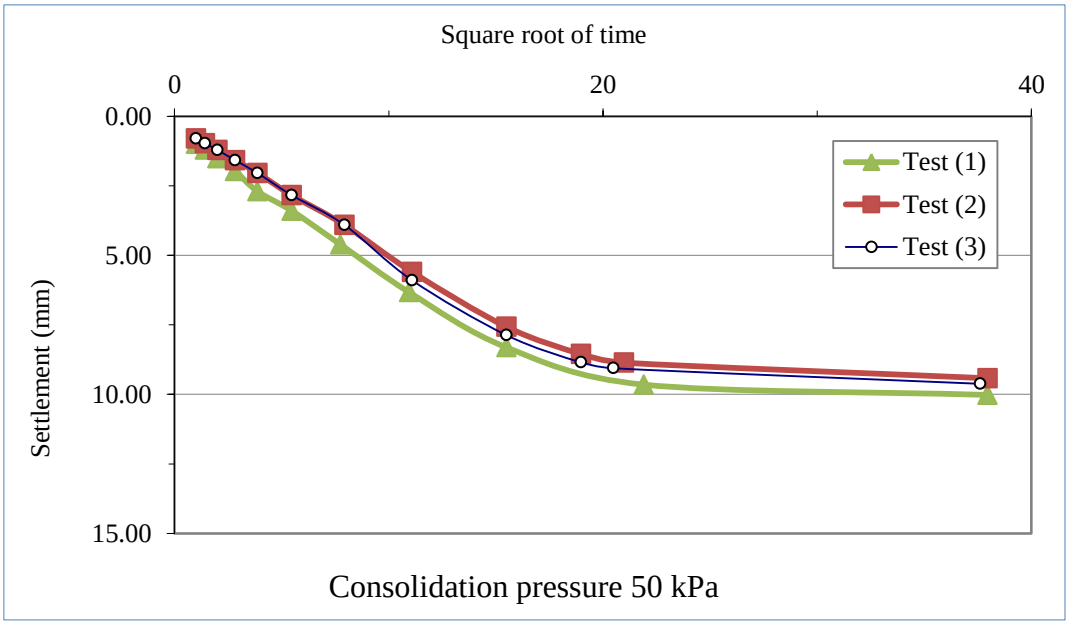

Consolidation pressure 50 kPa

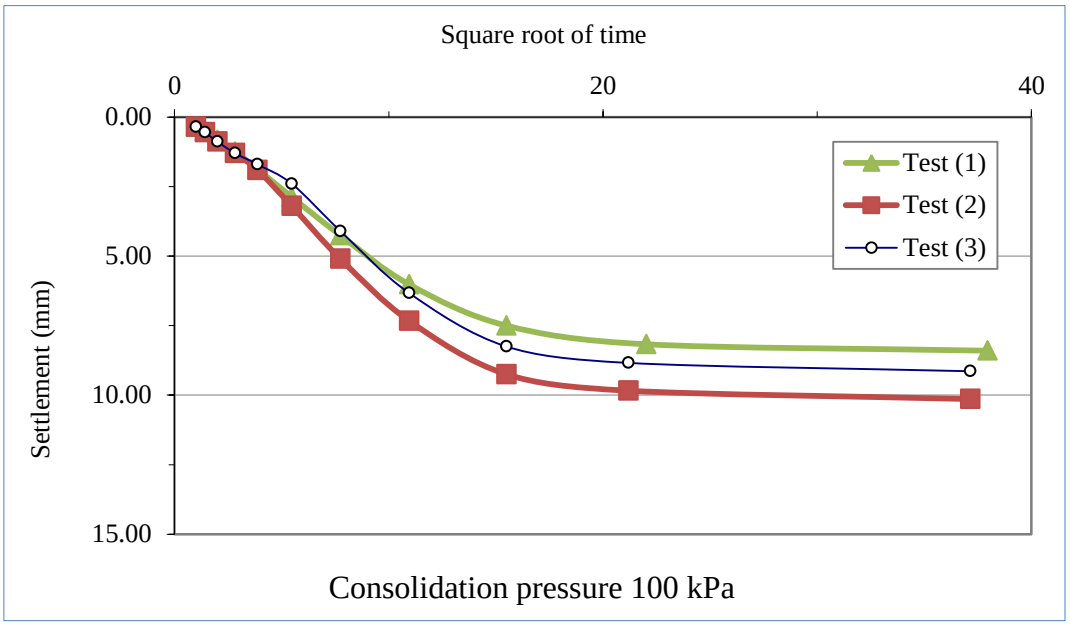

Consolidation pressure 100 kPa

APPENDIX B

1. Test Procedure

- Triaxial Test Procedure

- Consolidaing the sample

- Installing the stone colum

- Extroding the sample

- Placing the sample at the Mand Machine

- Large Scale Model Procedure

- Sample consolidation

- Stone colum Installation

- Positioning and placing the foundation

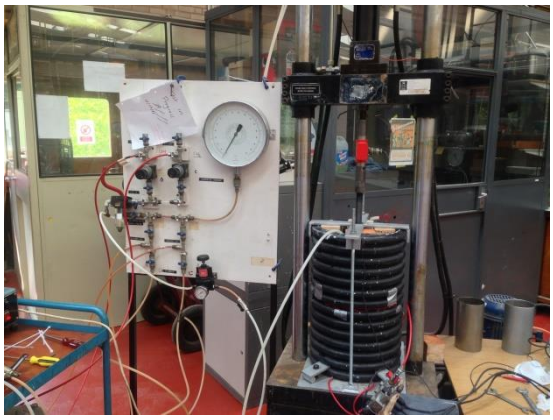

- Placing the sample at the Mand Machine

APPENDIX C

- Example of the data of the monotonic loading test on reinforce soil

Date	21/08/2013	Test Number	(5)
Time	08:30:00	Water content (%)	42.86
sample Dia.(mm)	101.00	Area of specimen (m^2)	0.01
sample Length (mm)	199.50		
Cell pressure (kPa)	400.67		
Back pressure (kPa)	295.00	Strain rate (mm/min)	0.03

Posn Pk	Load Pk (kN)	Stress (kPa)	stress corr. (kPa)	Disp. (mm)	Strain (%)	PWP (kPa)	Change PWP (kPa)	σ_3 (kPa)
-23.11	0.00	0.00	0.00	0.00	0.00	294.77	0	400.58
-23.05	0.04	4.46	4.45	0.38	0.18	295.15	0.54	400.67
-22.99	0.03	3.69	3.68	0.45	0.22	295.32	0.72	400.66
-22.92	0.02	2.67	2.67	0.52	0.25	295.54	0.93	400.69
-22.86	0.02	3.06	3.05	0.58	0.28	296.03	1.42	400.64
-22.79	0.09	10.95	10.92	0.65	0.31	297.80	3.20	400.77
-22.73	0.10	12.73	12.69	0.71	0.34	300.62	6.02	400.79
-22.67	0.16	19.74	19.66	0.77	0.37	302.96	8.36	400.53
-22.60	0.19	24.70	24.60	0.84	0.40	304.98	10.38	400.60
-22.54	0.19	24.70	24.59	0.91	0.44	306.82	12.22	400.56
-22.47	0.21	26.87	26.74	0.97	0.47	308.27	13.67	400.61
-22.40	0.24	31.07	30.91	1.04	0.50	309.80	15.20	400.85
-22.34	0.22	27.88	27.74	1.10	0.53	311.01	16.41	400.84
-22.27	0.25	32.21	32.03	1.17	0.56	312.15	17.54	400.49
-22.21	0.24	31.07	30.88	1.23	0.59	313.54	18.94	400.26
-22.14	0.29	37.31	37.07	1.30	0.62	314.67	20.07	400.63
-22.08	0.28	36.16	35.92	1.36	0.66	315.88	21.27	400.40
-22.01	0.32	40.74	40.46	1.43	0.69	316.77	22.17	400.81
-21.95	0.31	39.22	38.93	1.49	0.72	317.77	23.17	400.63
-21.88	0.30	38.45	38.16	1.56	0.75	318.45	23.84	400.57
-21.82	0.30	37.94	37.65	1.63	0.78	318.70	24.10	400.52
-21.75	0.34	43.29	42.94	1.69	0.81	319.69	25.09	400.40
-21.69	0.36	46.09	45.70	1.76	0.84	320.74	26.14	400.65
-21.62	0.38	47.75	47.33	1.82	0.87	321.64	27.03	400.67
-21.56	0.36	45.84	45.42	1.89	0.91	322.10	27.50	400.66
-21.49	0.41	52.71	52.22	1.95	0.94	322.87	28.27	400.82

-21.43	0.38	48.51	48.04	2.02	0.97	323.43	28.83	400.39
-21.36	0.38	48.26	47.77	2.08	1.00	323.92	29.32	400.46
-21.29	0.36	45.84	45.36	2.15	1.03	324.57	29.96	400.23
-21.23	0.39	49.27	48.75	2.21	1.06	325.14	30.54	400.59
-21.16	0.43	54.11	53.52	2.28	1.09	325.45	30.85	400.77
-21.10	0.41	52.08	51.49	2.35	1.13	325.98	31.38	400.18
-21.03	0.39	50.17	49.58	2.41	1.16	326.14	31.54	400.43
-20.97	0.41	51.57	50.95	2.47	1.19	326.99	32.39	400.26
-20.90	0.41	52.33	51.69	2.54	1.22	327.29	32.69	400.29
-20.83	0.42	53.73	53.06	2.61	1.25	327.80	33.19	400.51
-20.77	0.46	59.08	58.32	2.67	1.28	328.02	33.42	401.11
-20.70	0.46	58.82	58.05	2.74	1.32	328.46	33.85	400.64
-20.64	0.44	55.39	54.64	2.80	1.35	328.86	34.26	400.35
-20.57	0.47	59.59	58.77	2.87	1.38	329.18	34.58	400.65
-20.51	0.43	54.62	53.85	2.93	1.41	329.53	34.93	400.21
-20.44	0.46	58.82	57.98	3.00	1.44	330.00	35.40	400.63
-20.38	0.50	63.79	62.85	3.06	1.47	330.44	35.84	400.73
-20.31	0.42	53.86	53.05	3.13	1.50	330.28	35.68	399.96
-20.25	0.47	59.59	58.67	3.20	1.54	330.77	36.17	400.20
-20.18	0.47	59.21	58.28	3.26	1.57	330.94	36.34	400.61
-20.11	0.50	63.03	62.02	3.33	1.60	331.35	36.74	400.66
-20.05	0.47	60.35	59.37	3.39	1.63	331.42	36.82	400.51
-19.98	0.50	63.66	62.60	3.46	1.66	331.75	37.15	400.69
-19.92	0.48	60.61	59.58	3.52	1.69	332.01	37.41	400.24
-19.85	0.50	63.03	61.94	3.59	1.73	332.29	37.68	400.67
-19.79	0.54	69.01	67.80	3.65	1.76	332.46	37.86	400.74
-19.72	0.54	68.37	67.15	3.72	1.79	332.74	38.13	400.97
-19.65	0.52	66.72	65.50	3.78	1.82	332.95	38.35	400.79
-19.59	0.50	63.53	62.36	3.85	1.85	333.08	38.47	400.56
-19.52	0.51	64.94	63.71	3.92	1.88	333.40	38.79	400.46
-19.46	0.53	67.48	66.19	3.98	1.92	333.55	38.94	400.47
-19.39	0.41	52.71	51.69	4.05	1.95	333.20	38.60	400.29
-19.32	0.53	67.86	66.52	4.11	1.98	333.74	39.13	400.58
-19.26	0.49	62.64	61.38	4.18	2.01	333.63	39.03	400.21
-19.19	0.52	66.34	64.98	4.24	2.04	333.94	39.33	400.44
-19.13	0.56	70.92	69.45	4.31	2.07	334.34	39.74	400.60
-19.06	0.56	71.05	69.55	4.37	2.10	334.40	39.79	400.47
-19.00	0.47	59.33	58.07	4.44	2.14	334.34	39.74	399.87
-18.93	0.51	65.19	63.78	4.51	2.17	334.68	40.07	400.41
-18.87	0.54	68.63	67.12	4.57	2.20	334.90	40.30	400.48
-18.80	0.56	70.92	69.34	4.64	2.23	335.12	40.52	400.45
-18.74	0.55	70.03	68.44	4.70	2.26	335.31	40.70	400.30
-18.67	0.55	70.03	68.42	4.77	2.29	335.27	40.66	400.33

-18.61	0.59	74.74	73.00	4.84	2.33	335.53	40.92	400.65
-18.54	0.57	72.45	70.74	4.90	2.36	335.52	40.92	400.61
-18.47	0.56	70.79	69.10	4.97	2.39	335.57	40.97	400.37
-18.41	0.53	67.10	65.48	5.03	2.42	335.72	41.12	400.13
-18.34	0.56	71.68	69.93	5.10	2.45	335.73	41.13	400.06
-18.28	0.58	74.23	72.39	5.16	2.48	336.09	41.49	400.26
-18.21	0.54	68.88	67.15	5.23	2.52	335.85	41.25	400.28
-18.14	0.55	69.39	67.62	5.30	2.55	335.98	41.38	400.20
-18.08	0.61	77.41	75.42	5.36	2.58	336.20	41.59	400.63
-18.01	0.62	79.32	77.25	5.43	2.61	336.39	41.79	400.57
-17.95	0.56	71.68	69.79	5.49	2.64	336.29	41.68	400.20
-17.88	0.56	70.79	68.90	5.56	2.67	336.48	41.87	400.05
-17.82	0.58	73.21	71.23	5.62	2.70	336.66	42.06	400.24
-17.75	0.61	77.03	74.92	5.69	2.74	336.50	41.90	400.96
-17.68	0.58	74.10	72.05	5.75	2.77	336.70	42.10	400.39
-17.62	0.61	78.05	75.87	5.82	2.80	336.79	42.19	400.32
-17.55	0.60	76.14	73.98	5.89	2.83	336.82	42.21	400.46
-17.49	0.59	75.12	72.97	5.95	2.86	336.96	42.36	400.18
-17.42	0.61	77.03	74.80	6.02	2.89	336.81	42.20	400.61
-17.36	0.60	75.89	73.67	6.08	2.93	336.94	42.34	400.36
-17.29	0.56	70.92	68.82	6.15	2.96	336.99	42.39	399.93
-17.22	0.62	78.43	76.09	6.22	2.99	337.24	42.64	400.21
-17.16	0.59	75.63	73.35	6.28	3.02	337.29	42.69	400.13
-17.09	0.60	76.14	73.82	6.35	3.05	337.11	42.50	399.92
-17.03	0.61	78.18	75.77	6.41	3.08	337.56	42.96	400.46
-16.96	0.61	77.41	75.00	6.48	3.11	337.48	42.88	400.42
-16.90	0.61	78.18	75.72	6.54	3.15	337.54	42.93	400.45
-16.83	0.64	80.85	78.28	6.61	3.18	337.67	43.06	400.12
-16.76	0.60	75.76	73.33	6.68	3.21	337.61	43.01	400.15
-16.70	0.66	83.78	81.06	6.74	3.24	337.78	43.18	400.65
-16.63	0.57	72.32	69.95	6.80	3.27	337.57	42.97	400.02
-16.57	0.62	78.69	76.09	6.87	3.30	337.76	43.16	400.35
-16.50	0.64	81.61	78.89	6.94	3.33	337.66	43.06	400.36
-16.44	0.65	83.02	80.22	7.00	3.37	337.95	43.35	400.58
-16.37	0.66	83.52	80.69	7.07	3.40	338.01	43.41	400.55
-16.31	0.64	81.61	78.82	7.13	3.43	338.01	43.40	400.46
-16.24	0.61	78.18	75.47	7.20	3.46	337.90	43.30	400.37
-16.18	0.68	87.09	84.05	7.26	3.49	338.12	43.52	400.71
-16.11	0.61	77.16	74.44	7.33	3.52	338.11	43.50	400.20
-16.04	0.63	80.09	77.24	7.40	3.56	338.18	43.58	400.27
-15.98	0.66	83.40	80.41	7.46	3.59	338.25	43.65	400.66
-15.91	0.62	78.81	75.96	7.53	3.62	338.12	43.52	400.22
-15.85	0.61	78.05	75.20	7.59	3.65	338.17	43.56	400.21

-15.78	0.62	79.32	76.40	7.66	3.68	338.01	43.41	400.04
-15.72	0.65	82.63	79.56	7.72	3.71	338.14	43.54	400.48
-15.65	0.64	80.98	77.95	7.79	3.75	338.61	44.01	400.18
-15.58	0.65	82.63	79.51	7.86	3.78	338.47	43.87	400.69
-15.52	0.63	79.83	76.79	7.92	3.81	338.49	43.88	400.13
-15.46	0.67	84.67	81.42	7.99	3.84	338.57	43.97	400.72
-15.39	0.61	77.54	74.54	8.05	3.87	338.41	43.80	400.04
-15.32	0.66	83.65	80.39	8.12	3.90	338.52	43.92	400.37
-15.26	0.64	81.23	78.04	8.18	3.93	338.22	43.62	400.67
-15.19	0.64	80.85	77.64	8.25	3.97	338.67	44.07	400.53
-15.13	0.63	80.72	77.50	8.31	4.00	338.63	44.03	400.51
-15.06	0.69	87.73	84.19	8.38	4.03	338.82	44.21	400.72
-15.00	0.62	78.43	75.25	8.44	4.06	338.65	44.05	399.96
-14.93	0.63	80.34	77.05	8.51	4.09	338.75	44.15	399.96
-14.87	0.63	80.21	76.91	8.58	4.12	338.78	44.18	400.06
-14.80	0.66	84.16	80.67	8.64	4.15	338.77	44.16	400.58
-14.74	0.66	84.16	80.64	8.71	4.19	338.72	44.11	400.57
-14.67	0.63	80.34	76.95	8.77	4.22	338.27	43.66	400.17
-14.60	0.64	81.87	78.39	8.84	4.25	338.74	44.13	400.01
-14.54	0.69	87.22	83.48	8.90	4.28	338.85	44.24	400.46
-14.47	0.69	87.85	84.07	8.97	4.31	338.88	44.28	400.79
-14.41	0.68	86.71	82.94	9.03	4.34	339.11	44.50	400.46
-14.34	0.67	85.31	81.58	9.10	4.37	339.07	44.46	400.58
-14.28	0.62	78.43	74.98	9.17	4.41	339.01	44.41	399.95
-14.21	0.70	88.49	84.56	9.23	4.44	339.02	44.42	400.47
-14.14	0.61	77.54	74.07	9.30	4.47	338.76	44.15	399.88
-14.08	0.66	84.54	80.74	9.36	4.50	338.94	44.34	400.38
-14.01	0.68	86.96	83.02	9.43	4.53	339.10	44.50	400.56
-13.95	0.65	82.63	78.86	9.49	4.56	339.05	44.45	400.44
-13.88	0.67	85.56	81.63	9.56	4.60	339.04	44.43	400.23
-13.82	0.66	83.52	79.66	9.63	4.63	338.90	44.29	400.15
-13.75	0.74	93.84	89.47	9.69	4.66	339.11	44.51	400.72
-13.68	0.69	88.36	84.22	9.76	4.69	339.21	44.60	400.50
-13.62	0.69	87.34	83.22	9.82	4.72	339.19	44.59	400.41
-13.55	0.67	84.93	80.89	9.89	4.75	338.93	44.32	400.31
-13.49	0.68	85.94	81.83	9.95	4.78	339.02	44.42	400.44
-13.42	0.67	84.80	80.71	10.02	4.82	338.96	44.36	399.97
-13.36	0.70	89.00	84.69	10.08	4.85	339.00	44.40	400.28
-13.29	0.71	90.02	85.63	10.15	4.88	339.25	44.65	400.65
-13.23	0.67	85.56	81.36	10.21	4.91	339.09	44.49	400.31
-13.16	0.72	91.29	86.78	10.28	4.94	339.37	44.76	400.47
-13.10	0.65	82.76	78.64	10.35	4.97	339.12	44.52	400.06
-13.03	0.71	90.65	86.12	10.41	5.01	339.15	44.55	400.16

-12.96	0.69	87.47	83.07	10.48	5.04	339.26	44.66	400.12
-12.90	0.72	92.06	87.39	10.54	5.07	339.24	44.64	400.68
-12.83	0.66	84.54	80.23	10.61	5.10	339.23	44.63	400.28
-12.77	0.70	88.49	83.95	10.67	5.13	339.36	44.76	400.60
-12.70	0.71	89.76	85.13	10.74	5.16	339.35	44.74	400.36
-12.64	0.76	97.15	92.10	10.80	5.19	339.34	44.73	400.94
-12.57	0.76	96.38	91.35	10.87	5.23	339.28	44.68	400.63
-12.50	0.70	89.13	84.44	10.93	5.26	339.24	44.63	400.12
-12.44	0.68	87.09	82.48	11.00	5.29	339.24	44.64	400.35
-12.37	0.66	84.29	79.80	11.07	5.32	339.10	44.49	400.22
-12.31	0.71	89.89	85.08	11.13	5.35	339.16	44.56	400.13
-12.24	0.70	89.38	84.57	11.20	5.38	339.09	44.49	400.08
-12.18	0.77	98.17	92.85	11.26	5.41	339.47	44.87	400.54
-12.11	0.74	93.97	88.85	11.33	5.45	339.20	44.59	400.68
-12.04	0.78	99.06	93.63	11.39	5.48	339.22	44.62	400.77
-11.98	0.72	92.06	86.98	11.46	5.51	339.29	44.69	400.44
-11.91	0.67	85.05	80.34	11.53	5.54	339.25	44.64	399.58
-11.85	0.64	81.61	77.07	11.59	5.57	339.21	44.61	399.50
-11.78	0.70	89.51	84.49	11.66	5.60	339.23	44.63	399.99
-11.72	0.65	82.25	77.62	11.72	5.64	339.26	44.66	399.99
-11.65	0.73	92.95	87.68	11.79	5.67	339.23	44.62	400.57
-11.59	0.70	89.51	84.41	11.85	5.70	339.27	44.67	400.06
-11.52	0.74	94.35	88.94	11.92	5.73	339.17	44.57	400.40
-11.46	0.68	86.58	81.59	11.99	5.76	339.08	44.48	399.86
-11.39	0.66	83.78	78.93	12.05	5.79	339.22	44.61	399.74
-11.33	0.71	90.02	84.77	12.12	5.82	339.19	44.59	400.27
-11.26	0.75	94.86	89.30	12.18	5.86	339.34	44.73	400.53
-11.19	0.76	96.13	90.47	12.25	5.89	339.32	44.72	400.84
-11.13	0.73	93.33	87.80	12.31	5.92	339.25	44.64	400.28
-11.06	0.72	91.29	85.86	12.38	5.95	339.03	44.43	400.16
-11.00	0.70	88.62	83.32	12.45	5.98	339.13	44.53	400.00
-10.93	0.74	94.73	89.03	12.51	6.01	339.13	44.53	400.77
-10.86	0.73	92.95	87.33	12.57	6.05	339.39	44.78	400.35
-10.80	0.73	92.56	86.94	12.64	6.08	339.28	44.68	400.64
-10.73	0.66	83.91	78.78	12.71	6.11	338.80	44.20	399.84
-10.67	0.66	84.54	79.35	12.77	6.14	339.33	44.73	399.40
-10.60	0.73	92.31	86.61	12.84	6.17	339.31	44.71	400.10
-10.53	0.72	91.93	86.23	12.90	6.20	339.35	44.75	400.30
-10.47	0.72	91.55	85.84	12.97	6.23	339.21	44.61	400.50
-10.41	0.74	93.84	87.96	13.03	6.27	339.26	44.65	400.47
-10.34	0.71	90.40	84.71	13.10	6.30	339.24	44.64	399.90
-10.28	0.73	92.56	86.71	13.17	6.33	339.50	44.90	400.13
-10.21	0.71	90.65	84.89	13.23	6.36	339.36	44.75	400.18

-10.15	0.79	100.59	94.15	13.30	6.39	339.56	44.96	400.99
-10.08	0.66	84.16	78.75	13.36	6.42	338.92	44.31	399.36
-10.01	0.72	92.06	86.11	13.43	6.46	339.24	44.63	400.10
-9.95	0.75	95.37	89.18	13.49	6.49	339.49	44.88	400.14
-9.88	0.70	89.38	83.55	13.56	6.52	339.00	44.40	399.87
-9.82	0.72	91.29	85.31	13.63	6.55	339.32	44.71	399.94
-9.75	0.68	86.96	81.24	13.69	6.58	339.14	44.54	399.55
-9.68	0.71	90.78	84.78	13.75	6.61	339.33	44.73	399.77
-9.62	0.77	98.42	91.88	13.82	6.64	339.29	44.68	400.36
-9.55	0.74	94.35	88.05	13.89	6.68	339.34	44.73	400.01
-9.49	0.71	90.02	83.98	13.96	6.71	338.98	44.38	399.84
-9.42	0.78	99.57	92.86	14.02	6.74	339.42	44.81	400.70
-9.36	0.71	90.40	84.28	14.08	6.77	339.33	44.72	400.08
-9.29	0.71	90.91	84.73	14.15	6.80	339.02	44.42	399.83
-9.23	0.74	94.35	87.90	14.22	6.83	339.21	44.61	399.91
-9.16	0.78	99.06	92.26	14.28	6.87	339.12	44.52	400.16
-9.09	0.73	92.69	86.30	14.34	6.90	339.07	44.47	400.00
-9.03	0.67	85.82	79.87	14.41	6.93	338.87	44.27	399.75
-8.96	0.69	87.22	81.15	14.48	6.96	339.13	44.53	399.76
-8.90	0.74	93.84	87.28	14.54	6.99	339.29	44.68	399.70
-8.83	0.68	86.83	80.74	14.61	7.02	339.14	44.53	399.39
-8.77	0.80	102.24	95.03	14.67	7.05	339.60	44.99	400.54
-8.70	0.76	96.51	89.67	14.74	7.09	339.52	44.91	400.20
-8.64	0.79	100.97	93.78	14.80	7.12	339.44	44.83	400.43
-8.57	0.72	91.16	84.65	14.87	7.15	339.33	44.72	399.69
-8.51	0.80	101.35	94.07	14.93	7.18	339.40	44.79	400.27
-8.44	0.71	90.15	83.64	15.00	7.21	339.09	44.49	399.70
-8.37	0.74	93.97	87.16	15.07	7.24	339.35	44.74	399.94
-8.31	0.74	94.60	87.72	15.13	7.27	339.21	44.61	400.31
-8.24	0.74	94.60	87.69	15.20	7.31	339.31	44.70	400.23
-8.18	0.81	103.26	95.68	15.26	7.34	339.28	44.68	400.64
-8.11	0.71	89.76	83.15	15.33	7.37	339.13	44.53	399.73
-8.05	0.69	87.47	81.00	15.40	7.40	339.08	44.47	399.37
-7.98	0.77	97.66	90.40	15.46	7.43	339.26	44.66	399.72
-7.91	0.76	96.26	89.07	15.53	7.46	339.32	44.72	399.84
-7.85	0.73	93.46	86.45	15.59	7.50	339.18	44.58	400.37
-7.78	0.75	95.37	88.19	15.66	7.53	339.22	44.61	399.92
-7.72	0.76	96.26	88.98	15.72	7.56	339.27	44.66	399.88
-7.65	0.80	101.35	93.66	15.79	7.59	339.32	44.72	400.07
-7.58	0.75	95.62	88.33	15.85	7.62	339.12	44.52	399.67
-7.52	0.72	91.04	84.07	15.92	7.65	339.24	44.63	399.73
-7.46	0.76	96.64	89.21	15.99	7.69	339.28	44.68	399.96
-7.39	0.73	93.20	86.01	16.05	7.72	339.24	44.63	399.41

-7.32	0.74	93.71	86.45	16.11	7.75	339.07	44.47	399.57
-7.26	0.72	91.67	84.54	16.18	7.78	339.16	44.56	399.56
-7.19	0.78	99.06	91.32	16.25	7.81	339.33	44.72	400.15
-7.13	0.75	94.86	87.42	16.31	7.84	339.28	44.68	400.02
-7.06	0.75	95.11	87.62	16.38	7.87	339.20	44.60	399.99
-7.00	0.80	102.24	94.16	16.44	7.90	339.23	44.63	400.17
-6.93	0.77	97.53	89.79	16.51	7.94	339.17	44.56	399.87
-6.86	0.82	104.66	96.32	16.57	7.97	339.36	44.75	400.31
-6.80	0.74	93.71	86.21	16.64	8.00	338.93	44.32	399.87
-6.73	0.75	94.86	87.24	16.71	8.03	338.88	44.28	400.02
-6.67	0.76	96.51	88.73	16.77	8.06	339.05	44.45	399.84
-6.60	0.78	98.80	90.81	16.84	8.09	339.02	44.42	399.77
-6.54	0.70	88.49	81.30	16.90	8.13	338.84	44.24	399.14
-6.47	0.77	97.91	89.92	16.97	8.16	339.00	44.39	400.32
-6.41	0.70	89.64	82.29	17.04	8.19	339.00	44.40	399.42
-6.34	0.81	103.13	94.65	17.10	8.22	338.97	44.37	400.50
-6.27	0.77	97.78	89.72	17.16	8.25	339.06	44.46	400.04
-6.21	0.77	97.78	89.68	17.23	8.28	339.09	44.49	399.91
-6.14	0.76	96.77	88.72	17.30	8.31	339.10	44.49	399.55
-6.08	0.72	91.29	83.67	17.36	8.35	338.95	44.35	399.37
-6.01	0.78	99.31	90.99	17.43	8.38	338.96	44.35	399.93
-5.95	0.78	99.06	90.73	17.50	8.41	339.16	44.55	399.92
-5.88	0.76	96.26	88.13	17.56	8.44	339.05	44.44	399.64
-5.82	0.74	94.47	86.47	17.63	8.47	338.95	44.34	399.61
-5.75	0.77	98.04	89.70	17.69	8.51	338.97	44.37	399.63
-5.68	0.78	99.19	90.72	17.76	8.54	338.68	44.07	399.98
-5.62	0.71	90.53	82.77	17.82	8.57	338.78	44.17	399.36
-5.55	0.78	99.57	91.01	17.89	8.60	338.92	44.32	400.30
-5.49	0.77	98.55	90.04	17.95	8.63	338.97	44.36	399.75
-5.42	0.77	97.91	89.43	18.02	8.66	338.97	44.36	399.34
-5.35	0.79	99.95	91.26	18.08	8.69	338.94	44.34	399.85
-5.29	0.74	93.84	85.65	18.15	8.73	338.96	44.35	399.59
-5.22	0.73	92.82	84.69	18.22	8.76	339.03	44.43	399.27
-5.16	0.82	104.02	94.88	18.28	8.79	339.03	44.42	400.36
-5.09	0.80	102.11	93.11	18.35	8.82	338.99	44.38	399.99
-5.03	0.77	98.29	89.59	18.41	8.85	338.86	44.26	399.83
-4.96	0.76	96.51	87.94	18.48	8.88	338.85	44.24	399.59
-4.90	0.78	99.19	90.34	18.54	8.91	338.75	44.15	399.81
-4.83	0.73	92.56	84.28	18.61	8.95	338.72	44.11	399.46
-4.77	0.78	99.19	90.28	18.67	8.98	338.99	44.39	399.68
-4.70	0.80	101.35	92.22	18.74	9.01	338.94	44.34	399.65
-4.64	0.78	98.68	89.75	18.81	9.04	338.87	44.27	400.03
-4.57	0.75	95.37	86.71	18.87	9.07	338.73	44.13	399.60

-4.50	0.71	90.53	82.29	18.94	9.10	338.69	44.08	399.48
-4.44	0.77	98.04	89.08	19.00	9.13	338.73	44.12	399.68
-4.37	0.76	96.26	87.43	19.07	9.17	338.84	44.24	399.49
-4.31	0.77	97.53	88.56	19.13	9.20	338.88	44.27	399.72
-4.24	0.78	99.31	90.15	19.20	9.23	338.88	44.27	399.69
-4.18	0.80	101.22	91.85	19.27	9.26	338.74	44.14	399.58
-4.11	0.79	100.20	90.89	19.33	9.29	338.76	44.15	399.78
-4.05	0.86	109.88	99.63	19.40	9.33	338.92	44.31	400.41
-3.98	0.82	104.91	95.10	19.46	9.36	339.01	44.40	400.01
-3.91	0.78	99.19	89.87	19.53	9.39	338.78	44.17	399.67
-3.85	0.76	96.89	87.77	19.59	9.42	338.78	44.17	399.20
-3.78	0.80	101.60	92.00	19.66	9.45	338.96	44.36	399.62
-3.72	0.76	96.26	87.13	19.72	9.48	338.80	44.20	399.80
-3.65	0.77	98.55	89.17	19.79	9.51	338.80	44.19	399.89
-3.59	0.87	110.77	100.20	19.85	9.55	339.07	44.47	400.22
-3.52	0.82	104.02	94.06	19.92	9.58	338.83	44.22	399.74
-3.45	0.81	102.75	92.88	19.99	9.61	338.89	44.28	399.77
-3.39	0.74	94.22	85.14	20.05	9.64	338.60	44.00	399.38
-3.32	0.79	100.46	90.74	20.12	9.67	338.78	44.18	400.03
-3.26	0.83	105.42	95.20	20.18	9.70	338.67	44.06	400.36
-3.19	0.74	93.84	84.70	20.25	9.73	338.66	44.06	399.22
-3.13	0.83	105.30	95.01	20.31	9.77	338.77	44.17	399.75
-3.06	0.77	97.53	87.97	20.38	9.80	338.59	43.98	399.63
-2.99	0.82	103.90	93.68	20.45	9.83	338.82	44.22	399.93
-2.93	0.78	99.57	89.75	20.51	9.86	338.83	44.23	399.80
-2.87	0.76	97.28	87.65	20.57	9.89	338.60	43.99	399.79
-2.80	0.75	95.75	86.25	20.64	9.92	338.72	44.12	399.61
-2.73	0.76	97.28	87.59	20.71	9.96	338.79	44.18	399.46
-2.67	0.79	100.33	90.31	20.77	9.99	338.87	44.27	399.71
-2.60	0.81	102.75	92.46	20.84	10.02	338.94	44.34	400.10
-2.54	0.74	94.22	84.75	20.90	10.05	338.38	43.78	399.52
-2.47	0.82	103.77	93.31	20.97	10.08	339.04	44.43	399.84
-2.41	0.86	109.50	98.43	21.03	10.11	338.98	44.37	400.19
-2.34	0.74	94.35	84.78	21.10	10.14	338.80	44.20	399.28
-2.28	0.78	98.68	88.63	21.17	10.18	338.72	44.11	399.88
-2.21	0.79	100.33	90.09	21.23	10.21	338.55	43.94	399.89
-2.14	0.87	110.64	99.32	21.30	10.24	338.89	44.29	400.79
-2.08	0.81	103.01	92.43	21.36	10.27	338.76	44.16	399.81
-2.01	0.79	100.97	90.57	21.43	10.30	338.69	44.09	399.76
-1.95	0.83	106.06	95.10	21.49	10.33	338.75	44.14	400.02
-1.88	0.82	104.53	93.70	21.56	10.36	338.80	44.19	399.95
-1.82	0.76	96.89	86.82	21.63	10.40	338.77	44.17	399.66
-1.75	0.81	103.39	92.61	21.69	10.43	338.68	44.08	400.19

-1.68	0.76	96.89	86.76	21.76	10.46	338.71	44.10	399.27
-1.62	0.73	93.20	83.42	21.82	10.49	338.57	43.96	399.09
-1.55	0.84	107.33	96.04	21.89	10.52	338.62	44.02	400.25
-1.49	0.77	97.53	87.24	21.95	10.55	338.56	43.95	399.73
-1.42	0.73	93.07	83.22	22.02	10.59	338.58	43.97	399.21
-1.36	0.79	100.84	90.13	22.09	10.62	338.53	43.93	399.72
-1.29	0.75	94.98	84.87	22.15	10.65	338.47	43.87	399.20
-1.22	0.80	101.35	90.53	22.21	10.68	338.38	43.78	399.44
-1.16	0.79	100.46	89.70	22.28	10.71	338.69	44.08	399.84
-1.09	0.76	96.13	85.80	22.35	10.74	338.54	43.93	399.66
-1.03	0.79	99.95	89.18	22.41	10.77	338.62	44.02	399.63
-0.96	0.87	110.39	98.46	22.48	10.81	338.76	44.15	399.97
-0.90	0.87	110.14	98.20	22.54	10.84	338.85	44.24	399.97
-0.83	0.83	105.30	93.85	22.61	10.87	338.79	44.19	399.52
-0.76	0.87	110.77	98.70	22.67	10.90	338.87	44.27	400.04
-0.70	0.80	101.22	90.16	22.74	10.93	338.69	44.08	399.66
-0.63	0.86	108.86	96.93	22.80	10.96	338.72	44.11	400.16
-0.57	0.79	100.20	89.19	22.87	10.99	338.52	43.91	399.70
-0.51	0.84	107.21	95.38	22.94	11.03	338.65	44.05	399.56
-0.44	0.73	93.33	83.01	23.00	11.06	338.35	43.75	399.14
-0.37	0.80	102.37	91.01	23.07	11.09	338.60	44.00	399.74
-0.31	0.82	104.02	92.45	23.13	11.12	338.52	43.91	399.98
-0.24	0.81	103.01	91.52	23.20	11.15	338.68	44.07	399.70
-0.18	0.77	97.78	86.85	23.26	11.18	338.40	43.80	399.22
-0.11	0.77	98.17	87.16	23.33	11.22	338.46	43.85	399.42
-0.04	0.82	103.90	92.21	23.40	11.25	338.81	44.20	399.44
0.02	0.84	106.32	94.32	23.46	11.28	338.51	43.91	399.68
0.09	0.76	96.64	85.71	23.53	11.31	338.14	43.54	399.10
0.15	0.75	95.37	84.55	23.59	11.34	338.30	43.70	399.12
0.22	0.87	111.28	98.62	23.66	11.37	338.49	43.89	400.01
0.28	0.78	99.57	88.21	23.73	11.41	337.94	43.34	399.42
0.35	0.84	106.44	94.27	23.79	11.44	338.18	43.58	399.70
0.42	0.84	106.95	94.69	23.86	11.47	338.68	44.07	399.83
0.48	0.81	103.64	91.72	23.92	11.50	338.60	44.00	399.34
0.55	0.75	95.62	84.59	23.99	11.53	338.31	43.71	399.13
0.61	0.79	100.46	88.84	24.05	11.56	338.29	43.69	399.43
0.68	0.80	101.22	89.49	24.12	11.60	338.40	43.80	399.11
0.74	0.77	97.78	86.42	24.18	11.63	338.14	43.53	398.92
0.81	0.83	105.81	93.47	24.25	11.66	338.42	43.81	399.49
0.87	0.81	102.75	90.74	24.32	11.69	338.34	43.73	399.54
0.94	0.87	110.26	97.34	24.38	11.72	338.55	43.94	400.00
1.01	0.77	98.29	86.74	24.45	11.75	338.05	43.45	399.23
1.07	0.83	106.19	93.67	24.51	11.78	338.30	43.69	399.43

1.14	0.82	104.15	91.84	24.58	11.82	338.46	43.86	399.09
1.21	0.86	109.50	96.53	24.64	11.85	338.49	43.89	399.82
1.27	0.75	94.98	83.70	24.71	11.88	338.26	43.66	399.12
1.34	0.80	101.73	89.62	24.77	11.91	338.41	43.80	399.19
1.40	0.78	99.82	87.90	24.84	11.94	338.28	43.67	398.99
1.47	0.78	99.82	87.87	24.90	11.97	338.09	43.48	399.10
1.53	0.83	105.93	93.22	24.97	12.00	338.53	43.93	399.58
1.59	0.78	98.80	86.91	25.03	12.03	338.22	43.61	399.22
1.66	0.81	102.75	90.35	25.10	12.07	338.58	43.97	399.47
1.73	0.79	100.84	88.64	25.17	12.10	338.19	43.58	399.21
1.79	0.78	99.06	87.04	25.23	12.13	338.23	43.62	399.34
1.86	0.85	107.84	94.73	25.30	12.16	338.25	43.64	399.52
1.93	0.88	111.66	98.05	25.36	12.19	338.42	43.82	399.72
1.99	0.82	104.66	91.87	25.43	12.23	338.17	43.57	399.53
2.05	0.83	105.30	92.39	25.50	12.26	338.40	43.80	399.64
2.12	0.75	95.75	83.98	25.56	12.29	338.11	43.51	399.25
2.19	0.83	105.42	92.44	25.62	12.32	338.47	43.86	399.23
2.25	0.81	103.01	90.28	25.69	12.35	338.05	43.45	399.28
2.32	0.78	98.80	86.57	25.76	12.38	337.96	43.35	399.23
2.39	0.85	108.61	95.12	25.82	12.41	338.08	43.48	399.94
2.45	0.81	103.26	90.41	25.89	12.45	338.17	43.57	399.41
2.52	0.80	101.60	88.93	25.96	12.48	338.40	43.80	399.44
2.58	0.87	110.52	96.69	26.02	12.51	338.29	43.68	399.99
2.65	0.79	100.08	87.53	26.09	12.54	338.09	43.48	399.26
2.71	0.84	107.46	93.95	26.15	12.57	338.46	43.85	399.45
2.78	0.79	100.59	87.91	26.22	12.60	338.25	43.64	399.05
2.84	0.82	104.91	91.66	26.28	12.64	338.33	43.73	399.02
2.91	0.81	103.26	90.18	26.35	12.67	338.15	43.55	399.32
2.97	0.80	101.86	88.93	26.41	12.70	338.17	43.57	399.29
3.04	0.78	98.93	86.34	26.48	12.73	338.31	43.70	399.09
3.11	0.83	105.04	91.64	26.55	12.76	338.13	43.52	399.39
3.17	0.81	102.75	89.60	26.61	12.79	338.23	43.62	399.29
3.24	0.82	103.77	90.46	26.67	12.82	338.15	43.55	399.35
3.30	0.82	104.91	91.43	26.74	12.86	338.44	43.84	399.67
3.37	0.79	100.20	87.29	26.81	12.89	338.23	43.62	399.32
3.43	0.79	100.46	87.48	26.87	12.92	338.23	43.62	398.91
3.50	0.85	108.10	94.10	26.94	12.95	338.34	43.74	399.34
3.56	0.83	106.19	92.40	27.00	12.98	338.36	43.75	399.54
3.63	0.84	107.08	93.14	27.07	13.01	338.39	43.79	399.61
3.70	0.82	104.66	91.01	27.13	13.04	338.09	43.49	399.61
3.76	0.79	100.97	87.76	27.20	13.08	338.15	43.55	399.07
3.83	0.84	106.82	92.82	27.27	13.11	338.36	43.76	399.33
3.89	0.81	102.88	89.36	27.33	13.14	338.14	43.54	399.15

3.96	0.82	104.91	91.10	27.40	13.17	338.32	43.71	399.42
4.02	0.79	100.20	86.97	27.46	13.20	338.22	43.62	399.11
4.09	0.80	102.11	88.60	27.53	13.23	338.31	43.70	399.22
4.15	0.82	104.41	90.56	27.59	13.27	338.33	43.73	399.30
4.22	0.78	99.19	86.00	27.66	13.30	338.10	43.50	399.09
4.29	0.79	100.84	87.40	27.73	13.33	338.22	43.62	399.07
4.35	0.85	107.72	93.32	27.79	13.36	338.50	43.90	399.42
4.42	0.80	102.37	88.66	27.86	13.39	338.21	43.60	399.34
4.48	0.91	116.25	100.64	27.92	13.42	338.36	43.75	399.90
4.55	0.84	106.57	92.23	27.99	13.45	338.17	43.56	399.72
4.61	0.85	108.48	93.85	28.05	13.49	338.51	43.90	399.70
4.68	0.80	102.11	88.31	28.12	13.52	338.26	43.66	398.88
4.74	0.85	108.73	94.00	28.19	13.55	338.42	43.82	399.29
4.81	0.85	107.72	93.09	28.25	13.58	338.18	43.58	399.20
4.88	0.83	106.06	91.62	28.32	13.61	338.17	43.57	399.51
4.94	0.84	107.33	92.69	28.38	13.64	338.37	43.77	399.33
5.01	0.88	111.66	96.39	28.45	13.68	338.41	43.81	399.61
5.07	0.85	107.97	93.17	28.51	13.71	338.39	43.79	399.51
5.14	0.77	98.55	85.01	28.58	13.74	338.12	43.51	398.88
5.20	0.73	93.07	80.26	28.64	13.77	337.94	43.34	398.41
5.27	0.78	98.93	85.28	28.71	13.80	338.22	43.61	399.10
5.34	0.80	101.35	87.33	28.77	13.83	338.05	43.45	399.46
5.40	0.82	104.91	90.37	28.84	13.86	338.19	43.59	399.39
5.47	0.80	101.73	87.60	28.90	13.90	338.24	43.63	399.15
5.53	0.88	111.92	96.33	28.97	13.93	338.31	43.70	399.66
5.60	0.82	104.66	90.05	29.04	13.96	338.11	43.50	399.13
5.66	0.92	117.65	101.19	29.10	13.99	338.32	43.72	399.81
5.73	0.80	101.73	87.46	29.17	14.02	338.07	43.47	399.09
5.80	0.83	105.81	90.94	29.23	14.05	337.99	43.39	399.59
5.86	0.84	106.32	91.34	29.30	14.09	338.42	43.82	399.28
5.93	0.83	106.19	91.20	29.36	14.12	338.20	43.60	399.20
5.99	0.84	107.46	92.26	29.43	14.15	338.18	43.58	399.53
6.05	0.82	103.90	89.16	29.49	14.18	338.06	43.46	399.10
6.12	0.85	108.61	93.17	29.56	14.21	338.12	43.52	399.53
6.19	0.82	104.41	89.54	29.63	14.24	337.95	43.34	399.32
6.25	0.81	103.13	88.41	29.69	14.28	338.15	43.55	399.20
6.32	0.83	105.55	90.45	29.76	14.31	338.13	43.52	399.27
6.38	0.86	109.75	94.02	29.82	14.34	338.27	43.67	399.62
6.45	0.84	106.57	91.25	29.89	14.37	338.05	43.45	399.54
6.52	0.77	97.53	83.48	29.96	14.40	337.75	43.14	398.76
6.58	0.86	109.63	93.80	30.02	14.43	338.08	43.47	399.60
6.65	0.81	102.75	87.89	30.09	14.46	337.95	43.35	398.94
6.71	0.83	105.55	90.25	30.15	14.50	338.15	43.55	399.12

6.78	0.86	109.12	93.26	30.22	14.53	338.16	43.55	399.63
6.85	0.84	106.95	91.38	30.28	14.56	338.09	43.48	399.61
6.91	0.87	110.14	94.07	30.35	14.59	338.32	43.72	399.59
6.98	0.85	108.35	92.51	30.42	14.62	338.12	43.52	399.60
7.04	0.88	112.55	96.06	30.48	14.65	338.46	43.86	399.66
7.10	0.83	105.30	89.83	30.55	14.69	337.99	43.39	399.36
7.17	0.87	110.77	94.47	30.61	14.72	338.26	43.65	399.43
7.24	0.87	111.28	94.87	30.68	14.75	338.22	43.62	399.57
7.30	0.81	103.51	88.21	30.74	14.78	337.73	43.13	399.59
7.37	0.81	102.88	87.64	30.81	14.81	337.91	43.31	399.35
7.43	0.83	105.17	89.56	30.87	14.84	338.14	43.54	399.27
7.50	0.85	107.72	91.69	30.94	14.87	338.26	43.66	399.25
7.56	0.78	99.06	84.29	31.00	14.91	338.10	43.50	398.93
7.63	0.85	108.23	92.06	31.07	14.94	338.38	43.77	399.56
7.70	0.84	107.33	91.27	31.13	14.97	338.00	43.40	399.72
7.76	0.88	112.55	95.67	31.20	15.00	338.48	43.88	399.72
7.83	0.86	109.75	93.26	31.26	15.03	338.23	43.63	399.40
7.89	0.79	100.46	85.33	31.33	15.06	338.04	43.44	398.95
7.96	0.82	104.28	88.54	31.40	15.09	338.16	43.55	399.18
8.02	0.81	103.64	87.97	31.46	15.13	338.05	43.44	399.32
8.09	0.78	99.19	84.15	31.53	15.16	338.12	43.52	399.24
8.15	0.76	97.28	82.50	31.60	15.19	337.96	43.35	398.91
8.22	0.83	105.17	89.16	31.66	15.22	338.26	43.65	399.27
8.29	0.86	109.75	93.01	31.73	15.25	338.03	43.42	399.67
8.35	0.83	106.19	89.96	31.79	15.28	338.09	43.49	399.26
8.42	0.84	107.21	90.79	31.86	15.32	338.00	43.39	399.57
8.48	0.80	102.24	86.55	31.92	15.35	337.91	43.30	399.30
8.55	0.84	107.46	90.93	31.99	15.38	338.17	43.56	399.26
8.62	0.90	114.34	96.72	32.06	15.41	338.17	43.57	399.56
8.68	0.81	103.13	87.21	32.12	15.44	337.88	43.28	399.26
8.75	0.90	114.21	96.54	32.19	15.47	338.18	43.57	399.63
8.81	0.78	98.80	83.48	32.25	15.51	337.93	43.32	398.85
8.88	0.82	103.77	87.65	32.32	15.54	337.93	43.33	399.42
8.94	0.86	109.75	92.67	32.38	15.57	338.21	43.60	399.42
9.01	0.85	107.59	90.81	32.45	15.60	338.00	43.39	399.18
9.07	0.81	103.26	87.12	32.51	15.63	338.06	43.45	399.06
9.14	0.83	105.55	89.02	32.58	15.66	338.09	43.48	399.04
9.20	0.79	100.71	84.91	32.65	15.70	337.66	43.06	399.21
9.27	0.88	111.79	94.21	32.71	15.73	338.29	43.68	399.53
9.34	0.90	114.08	96.11	32.78	15.76	338.04	43.44	399.79
9.40	0.83	105.17	88.56	32.84	15.79	338.04	43.43	399.08
9.47	0.88	111.41	93.78	32.91	15.82	338.20	43.60	399.28
9.53	0.87	111.15	93.54	32.97	15.85	338.36	43.76	399.56

9.60	0.84	106.82	89.86	33.04	15.88	338.09	43.48	399.54
9.66	0.85	108.35	91.11	33.10	15.91	338.13	43.53	399.48
9.73	0.89	113.70	95.57	33.17	15.95	337.96	43.36	399.52
9.79	0.91	115.61	97.14	33.23	15.98	338.17	43.57	399.74
9.86	0.89	112.81	94.75	33.30	16.01	338.23	43.62	399.43
9.93	0.84	107.33	90.12	33.37	16.04	338.08	43.48	399.22
9.99	0.85	108.48	91.04	33.43	16.07	338.03	43.42	399.76
10.06	0.83	106.19	89.09	33.50	16.10	338.10	43.49	399.44
10.12	0.89	112.81	94.61	33.56	16.14	338.11	43.50	399.61
10.19	0.87	110.39	92.54	33.63	16.17	338.23	43.63	399.30
10.26	0.87	110.26	92.40	33.69	16.20	338.07	43.46	399.06
10.32	0.81	102.75	86.07	33.76	16.23	338.22	43.62	398.90
10.38	0.85	108.10	90.52	33.82	16.26	338.09	43.49	399.65
10.45	0.84	106.57	89.21	33.89	16.29	338.08	43.47	399.41
10.52	0.86	110.01	92.05	33.96	16.33	337.88	43.28	399.44
10.58	0.82	104.79	87.65	34.02	16.36	337.84	43.23	399.25
10.65	0.91	115.86	96.88	34.09	16.39	337.98	43.38	399.74
10.71	0.86	109.37	91.41	34.15	16.42	337.96	43.35	399.74
10.78	0.84	106.32	88.83	34.22	16.45	338.05	43.44	399.43
10.84	0.90	114.46	95.60	34.28	16.48	338.08	43.48	399.69
10.91	0.75	96.00	80.15	34.35	16.51	337.83	43.22	398.39
10.97	0.78	98.93	82.56	34.41	16.54	337.88	43.28	399.10
11.04	0.87	110.26	91.99	34.48	16.58	338.15	43.55	399.72
11.10	0.85	107.59	89.72	34.54	16.61	338.02	43.41	399.64
11.17	0.85	108.10	90.11	34.61	16.64	338.21	43.61	399.79
11.24	0.88	111.66	93.05	34.68	16.67	338.08	43.48	399.80
11.30	0.78	98.80	82.30	34.74	16.70	337.86	43.25	399.13
11.37	0.81	102.50	85.34	34.81	16.74	337.92	43.32	399.03
11.44	0.84	106.57	88.70	34.87	16.77	338.06	43.46	399.27
11.50	0.83	105.68	87.93	34.94	16.80	338.17	43.56	399.24
11.56	0.82	104.02	86.52	35.01	16.83	338.17	43.57	399.36
11.63	0.83	105.81	87.97	35.07	16.86	338.18	43.57	399.10
11.70	0.87	110.14	91.53	35.14	16.89	338.13	43.53	399.77
11.76	0.85	108.23	89.91	35.20	16.92	337.88	43.28	399.53
11.83	0.88	112.43	93.37	35.27	16.95	338.08	43.47	399.81
11.89	0.82	104.53	86.78	35.33	16.99	338.40	43.80	399.48
11.96	0.90	114.21	94.77	35.40	17.02	338.44	43.84	399.74
12.03	0.81	103.01	85.44	35.47	17.05	338.01	43.41	399.10
12.09	0.84	106.70	88.47	35.53	17.08	337.98	43.38	399.57
12.15	0.86	109.63	90.87	35.60	17.11	338.31	43.70	399.71
12.22	0.82	104.91	86.93	35.66	17.14	338.25	43.65	399.81
12.29	0.87	110.14	91.22	35.73	17.18	338.19	43.59	399.91
12.35	0.88	112.55	93.19	35.79	17.21	338.41	43.81	399.55

12.42	0.83	105.30	87.15	35.86	17.24	338.09	43.49	399.37
12.48	0.80	101.73	84.16	35.93	17.27	338.07	43.47	399.21
12.55	0.82	104.91	86.76	35.99	17.30	337.85	43.25	399.62
12.62	0.92	117.27	96.94	36.06	17.33	338.58	43.97	399.97
12.68	0.88	111.79	92.38	36.12	17.36	338.42	43.82	399.78
12.74	0.82	104.91	86.66	36.18	17.40	338.31	43.71	399.48
12.81	0.86	108.99	90.00	36.25	17.43	338.26	43.65	400.04
12.88	0.78	99.44	82.08	36.32	17.46	338.11	43.50	399.19
12.94	0.88	112.55	92.87	36.38	17.49	338.34	43.74	400.36
13.01	0.85	107.59	88.74	36.45	17.52	338.44	43.83	399.36
13.07	0.84	106.32	87.65	36.51	17.55	338.38	43.78	399.68
13.14	0.82	103.77	85.52	36.58	17.59	338.27	43.67	398.92
13.21	0.82	104.15	85.80	36.64	17.62	338.10	43.49	399.32
13.27	0.80	101.99	83.99	36.71	17.65	338.23	43.63	399.11
13.34	0.85	108.35	89.20	36.78	17.68	338.07	43.46	399.72
13.40	0.85	108.10	88.95	36.84	17.71	338.34	43.73	399.86
13.47	0.80	101.86	83.79	36.91	17.74	338.09	43.48	399.22
13.53	0.86	109.63	90.14	36.97	17.77	337.92	43.31	399.88
13.60	0.77	97.78	80.37	37.04	17.81	338.23	43.63	398.95
13.66	0.81	103.26	84.84	37.10	17.84	337.87	43.27	399.60
13.73	0.78	98.80	81.15	37.17	17.87	337.96	43.36	399.27
13.79	0.85	108.48	89.06	37.23	17.90	338.44	43.83	399.79
13.86	0.90	114.08	93.63	37.30	17.93	338.43	43.82	400.05
13.92	0.83	105.30	86.38	37.37	17.96	338.34	43.73	399.09
13.99	0.83	105.17	86.24	37.43	18.00	338.45	43.84	399.01
14.06	0.83	106.19	87.05	37.50	18.03	338.15	43.55	399.60
14.12	0.84	107.21	87.85	37.56	18.06	338.40	43.79	399.47
14.19	0.92	116.76	95.64	37.63	18.09	338.63	44.02	399.79
14.25	0.82	103.90	85.07	37.69	18.12	338.29	43.69	399.69
14.32	0.82	104.15	85.24	37.76	18.15	338.24	43.63	398.98
14.39	0.80	101.22	82.82	37.82	18.18	338.36	43.75	398.93
14.45	0.88	111.79	91.43	37.89	18.22	338.43	43.83	399.59
14.52	0.81	103.39	84.52	37.95	18.25	338.38	43.78	399.24
14.58	0.89	113.45	92.71	38.02	18.28	338.52	43.92	400.58
14.64	0.85	107.84	88.10	38.08	18.31	338.41	43.80	400.00
14.71	0.78	99.44	81.20	38.15	18.34	338.38	43.78	399.37
14.78	0.88	111.66	91.15	38.22	18.38	338.42	43.81	399.87
14.85	0.81	102.88	83.94	38.28	18.41	337.94	43.33	399.45
14.91	0.85	107.97	88.07	38.35	18.44	338.33	43.72	399.65
14.97	0.79	100.08	81.59	38.41	18.47	338.54	43.94	399.35
15.04	0.91	116.37	94.84	38.48	18.50	338.45	43.84	400.52

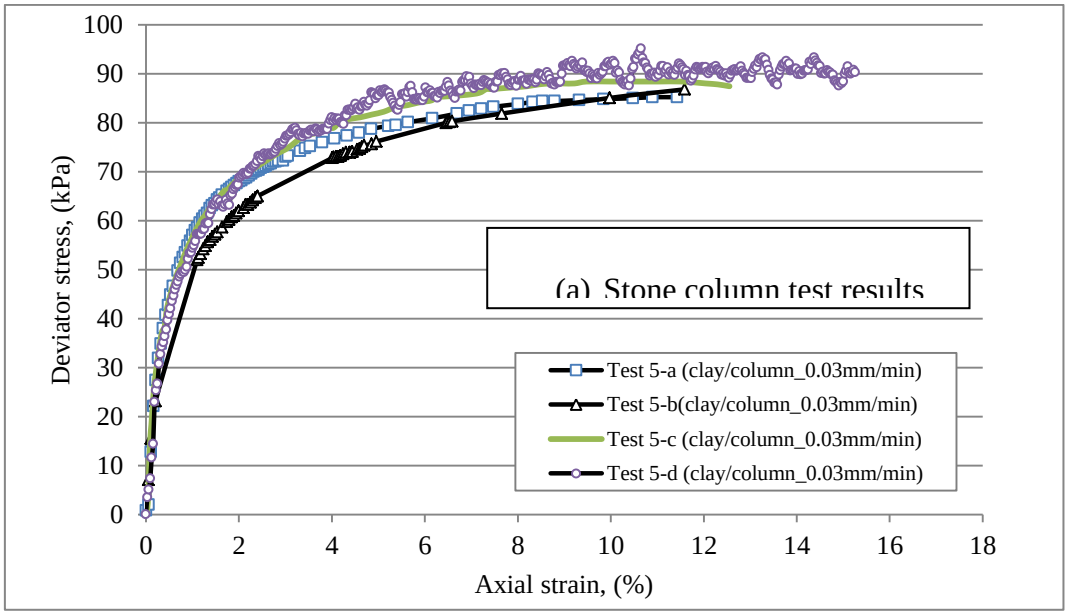
100
90
80
70
60
50
40
30
20
10
0
Deviator stress, (kPa)
0
2
4
6
8
10
12
14
16
18
Axial strain, (%)
(a) Stone column test results
Test 5-a (clay/column_0.03mm/min)
Test 5-b(clay/column_0.03mm/min)
Test 5-c (clay/column_0.03mm/min)
Test 5-d (clay/column_0.03mm/min)

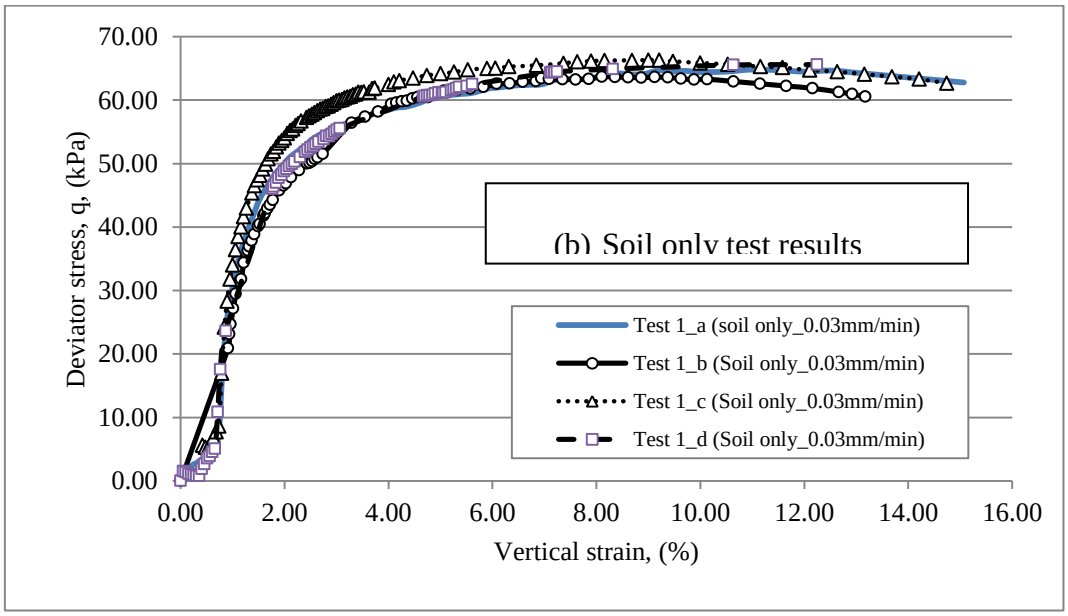
70.00
60.00
50.00
40.00
30.00
20.00
10.00
0.00
Deviator stress, q, (kPa)
0.00
2.00
4.00
6.00
8.00
10.00
12.00
14.00
16.00
Vertical strain, (%)
(b) Soil only test results
Test 1_a (soil only_0.03mm/min)
Test 1_b (Soil only_0.03mm/min)
Test 1_c (Soil only_0.03mm/min)
Test 1_d (Soil only_0.03mm/min)

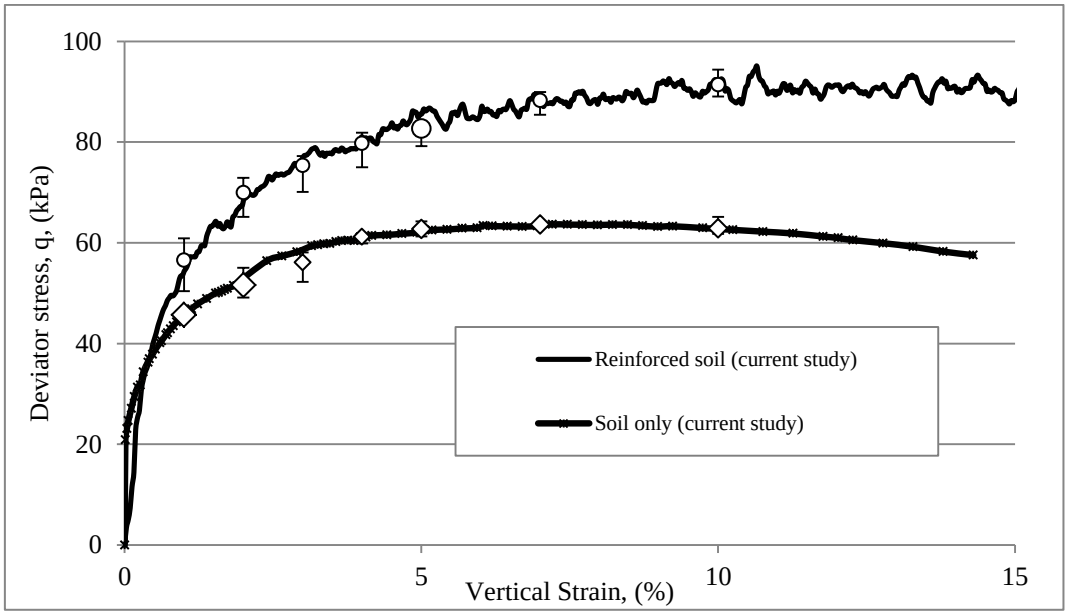
100
80
60
40
20
0
Deviator stress, q, (kPa)
0
5
10
15
Vertical Strain, (%)
Reinforced soil (current study)
Soil only (current study)

- Example of the data of the cyclic loading test on reinforce soil

Cycles	Load Pk (kN)	Load Tr. (kN)	Stress PK (kPa)	Stress Tr (kPa)	dP (PK-Trgh) (kN)	Posn Pk	Posn Trgh	Dis. Pk (mm)	Dis. Tr (mm)	Cyclic def. (mm)	stiffness	Strain PK %	Strain Trgh %	U Pk	Δ U pk	U Trgh	Δ U Trgh
1	0.35	0.35	44.69	44.69	0.00	-22.47	-22.47	0.86	0.86	0.241		0.40	0.40	328.54	20.54	328.54	20.54
10	0.47	0.15	59.87	19.52	0.32	-21.88	-22.13	0.59	0.35	0.23	1315.15	0.28	0.16	332.53	24.53	334.73	26.73
20	0.48	0.15	61.45	19.07	0.33	-21.65	-21.88	0.82	0.59	0.25	1446.96	0.38	0.28	336.18	28.18	338.46	30.46
30	0.47	0.15	60.36	18.89	0.33	-21.53	-21.78	0.95	0.70	0.256	1302.60	0.44	0.33	338.41	30.41	340.93	32.93
40	0.48	0.15	61.20	18.89	0.33	-21.43	-21.68	1.05	0.79	0.238	1298.05	0.49	0.37	340.06	32.06	342.42	34.42
50	0.48	0.15	61.57	18.98	0.33	-21.38	-21.62	1.09	0.86	0.229	1405.25	0.51	0.40	341.08	33.08	343.58	35.58
60	0.53	0.18	66.89	23.26	0.34	-21.15	-21.38	1.33	1.10	0.246	1496.29	0.62	0.51	343.42	35.42	345.82	37.82
70	0.53	0.17	67.13	22.18	0.35	-21.00	-21.24	1.48	1.23	0.25	1435.16	0.69	0.57	344.78	36.78	347.14	39.14
80	0.53	0.17	67.74	22.09	0.36	-20.87	-21.12	1.60	1.35	0.229	1433.88	0.75	0.63	345.73	37.73	348.31	40.31
90	0.53	0.18	67.13	22.35	0.35	-20.80	-21.03	1.67	1.44	0.242	1535.85	0.78	0.67	346.34	38.34	348.94	40.94
100	0.53	0.17	67.25	21.75	0.36	-20.73	-20.97	1.75	1.50	0.235	1476.65	0.82	0.70	347.31	39.31	349.69	41.69
110	0.55	0.19	69.91	24.48	0.36	-20.60	-20.84	1.87	1.64	0.254	1518.34	0.87	0.76	348.30	40.30	350.55	42.55
120	0.55	0.19	69.55	24.31	0.36	-20.50	-20.75	1.98	1.72	0.255	1398.82	0.92	0.80	348.93	40.93	350.97	42.97
130	0.55	0.20	69.67	24.91	0.35	-20.42	-20.68	2.05	1.80	0.236	1378.67	0.96	0.84	349.32	41.32	351.63	43.63
140	0.55	0.19	70.03	24.40	0.36	-20.38	-20.62	2.09	1.86	0.258	1518.77	0.98	0.87	349.88	41.88	352.06	44.06
150	0.55	0.19	69.91	24.31	0.36	-20.30	-20.56	2.17	1.91	0.256	1388.18	1.01	0.89	350.13	42.13	352.63	44.63
160	0.56	0.20	71.73	25.51	0.36	-20.22	-20.47	2.26	2.00	0.25	1418.05	1.05	0.93	350.92	42.92	353.25	45.25
170	0.57	0.20	72.45	25.25	0.37	-20.14	-20.39	2.34	2.09	0.234	1482.92	1.09	0.98	351.23	43.23	353.55	45.55
180	0.57	0.20	72.21	25.08	0.37	-20.07	-20.31	2.40	2.17	0.257	1581.92	1.12	1.01	351.51	43.51	353.75	45.75
190	0.57	0.20	72.09	24.91	0.37	-19.99	-20.25	2.48	2.23	0.238	1441.87	1.16	1.04	351.89	43.89	354.19	46.19

200	0.56	0.19	71.73	24.82	0.37	-19.95	-20.18	2.53	2.29	0.237	1547.82	1.18	1.07	352.07	44.07	354.47	46.47
210	0.57	0.20	73.06	25.59	0.37	-19.87	-20.11	2.60	2.36	0.235	1573.00	1.21	1.10	352.31	44.31	355.00	47.00
220	0.57	0.20	73.18	25.85	0.37	-19.83	-20.07	2.64	2.40	0.258	1581.87	1.23	1.12	352.34	44.34	354.85	46.85
230	0.58	0.20	73.30	25.51	0.38	-19.77	-20.03	2.70	2.45	0.246	1454.92	1.26	1.14	352.79	44.79	355.06	47.06
240	0.56	0.20	71.85	26.02	0.36	-19.72	-19.97	2.75	2.51	0.236	1463.21	1.29	1.17	352.94	44.94	355.38	47.38
250	0.58	0.20	73.30	25.76	0.37	-19.67	-19.91	2.80	2.56	0.239	1582.03	1.31	1.20	353.17	45.17	355.62	47.62
260	0.58	0.20	73.42	26.02	0.37	-19.64	-19.87	2.84	2.60	0.241	1557.74	1.33	1.21	353.56	45.56	355.87	47.87
270	0.58	0.21	73.54	26.27	0.37	-19.59	-19.83	2.89	2.64	0.227	1540.41	1.35	1.24	353.75	45.75	355.92	47.92
280	0.57	0.21	73.06	26.36	0.37	-19.55	-19.78	2.92	2.69	0.247	1615.73	1.36	1.26	353.61	45.61	356.14	48.14
290	0.57	0.20	72.09	26.02	0.36	-19.51	-19.76	2.96	2.72	0.223	1464.98	1.38	1.27	353.85	45.85	356.14	48.14
300	0.57	0.20	72.70	26.02	0.37	-19.52	-19.74	2.96	2.73	0.24	1643.95	1.38	1.28	353.92	45.92	356.15	48.15
310	0.58	0.21	73.54	26.53	0.37	-19.47	-19.71	3.00	2.76	0.247	1538.46	1.40	1.29	354.04	46.04	356.55	48.55
320	0.58	0.21	73.42	26.10	0.37	-19.44	-19.69	3.03	2.78	0.227	1504.57	1.42	1.30	353.99	45.99	356.42	48.42
330	0.58	0.20	74.03	26.02	0.38	-19.41	-19.64	3.06	2.84	0.247	1661.01	1.43	1.33	354.28	46.28	356.56	48.56
340	0.57	0.21	73.06	26.45	0.37	-19.39	-19.64	3.08	2.84	0.223	1482.19	1.44	1.32	354.29	46.29	356.64	48.64
350	0.58	0.21	73.42	26.19	0.37	-19.37	-19.60	3.10	2.88	0.237	1663.50	1.45	1.34	354.69	46.69	356.79	48.79
360	0.58	0.20	73.42	26.02	0.37	-19.34	-19.58	3.13	2.89	0.226	1570.89	1.46	1.35	354.57	46.57	357.07	49.07
370	0.58	0.21	73.42	26.19	0.37	-19.32	-19.54	3.16	2.93	0.255	1641.42	1.48	1.37	354.77	46.77	357.04	49.04
380	0.57	0.21	73.06	26.62	0.36	-19.28	-19.54	3.19	2.93	0.236	1430.43	1.49	1.37	354.77	46.77	357.13	49.13
390	0.58	0.21	73.91	26.62	0.37	-19.27	-19.51	3.20	2.97	0.235	1573.77	1.50	1.39	354.66	46.66	356.98	48.98
400	0.58	0.21	74.03	26.79	0.37	-19.25	-19.49	3.22	2.98	0.249	1578.81	1.50	1.39	354.61	46.61	357.19	49.19
410	0.57	0.21	73.06	26.27	0.37	-19.22	-19.47	3.25	3.01	0.258	1475.66	1.52	1.40	354.65	46.65	357.16	49.16
420	0.58	0.20	73.66	25.85	0.38	-19.19	-19.45	3.28	3.02	0.226	1455.58	1.53	1.41	354.73	46.73	357.27	49.27
430	0.58	0.21	73.78	26.27	0.37	-19.20	-19.43	3.27	3.04	0.248	1651.06	1.53	1.42	354.98	46.98	357.25	49.25
440	0.58	0.21	74.03	26.27	0.38	-19.17	-19.41	3.31	3.06	0.24	1512.26	1.55	1.43	355.18	47.18	357.28	49.28
450	0.57	0.21	72.94	26.10	0.37	-19.15	-19.39	3.32	3.08	0.236	1532.63	1.55	1.44	355.21	47.21	357.56	49.56
460	0.58	0.21	73.42	26.53	0.37	-19.14	-19.38	3.33	3.10	0.233	1560.51	1.56	1.45	355.36	47.36	357.57	49.57

470	0.58	0.21	73.66	26.36	0.37	-19.11	-19.35	3.36	3.13	0.245	1594.51	1.57	1.46	355.26	47.26	357.70	49.70
480	0.58	0.20	73.91	26.02	0.38	-19.10	-19.34	3.37	3.13	0.241	1535.10	1.58	1.46	355.21	47.21	357.69	49.69
490	0.57	0.21	73.18	26.10	0.37	-19.08	-19.32	3.39	3.15	0.23	1534.15	1.59	1.47	355.32	47.32	357.61	49.61
500	0.58	0.20	73.91	25.93	0.38	-19.07	-19.30	3.41	3.18	0.226	1638.13	1.59	1.48	355.32	47.32	357.64	49.64
510	0.58	0.21	73.42	26.53	0.37	-19.07	-19.29	3.41	3.18	0.249	1629.56	1.59	1.49	355.35	47.35	357.66	49.66
520	0.58	0.21	73.66	26.10	0.37	-19.04	-19.29	3.43	3.19	0.229	1500.12	1.60	1.49	355.50	47.50	357.82	49.82
530	0.58	0.21	73.30	26.36	0.37	-19.03	-19.26	3.45	3.22	0.259	1609.91	1.61	1.50	355.75	47.75	357.89	49.89
540	0.58	0.21	73.66	26.27	0.37	-19.01	-19.27	3.46	3.20	0.231	1437.03	1.62	1.50	355.71	47.71	357.85	49.85
550	0.58	0.21	73.30	26.45	0.37	-19.01	-19.24	3.46	3.23	0.25	1593.07	1.62	1.51	355.57	47.57	357.97	49.97
560	0.58	0.20	73.54	25.93	0.37	-18.99	-19.24	3.49	3.24	0.235	1495.68	1.63	1.51	355.69	47.69	358.12	50.12
570	0.58	0.21	73.78	26.27	0.37	-18.98	-19.21	3.49	3.26	0.234	1587.83	1.63	1.52	355.65	47.65	357.90	49.90
580	0.58	0.21	73.54	26.45	0.37	-18.98	-19.21	3.50	3.26	0.238	1580.77	1.63	1.53	355.59	47.59	357.92	49.92
590	0.58	0.21	73.66	26.27	0.37	-18.96	-19.20	3.51	3.27	0.227	1563.82	1.64	1.53	355.71	47.71	358.08	50.08
600	0.58	0.21	73.91	26.10	0.38	-18.95	-19.18	3.52	3.29	0.234	1653.88	1.64	1.54	355.70	47.70	357.87	49.87
610	0.57	0.21	72.94	26.53	0.36	-18.95	-19.18	3.53	3.29	0.236	1557.61	1.65	1.54	355.83	47.83	357.95	49.95
620	0.57	0.21	73.18	26.36	0.37	-18.92	-19.16	3.55	3.31	0.237	1558.14	1.66	1.55	355.82	47.82	358.05	50.05
630	0.58	0.21	74.03	26.53	0.37	-18.92	-19.16	3.55	3.31	0.247	1573.97	1.66	1.55	355.98	47.98	358.16	50.16
640	0.58	0.21	73.66	26.27	0.37	-18.91	-19.16	3.56	3.31	0.237	1506.84	1.66	1.55	355.86	47.86	358.24	50.24
650	0.58	0.21	74.03	26.27	0.38	-18.91	-19.15	3.56	3.33	0.221	1582.45	1.66	1.55	355.99	47.99	358.32	50.32
660	0.58	0.21	73.30	26.19	0.37	-18.89	-19.12	3.58	3.36	0.24	1674.25	1.67	1.57	355.94	47.94	358.47	50.47
670	0.59	0.21	74.51	26.62	0.38	-18.88	-19.12	3.59	3.35	0.235	1567.33	1.68	1.56	355.87	47.87	358.21	50.21
680	0.58	0.21	74.39	26.96	0.37	-18.89	-19.12	3.59	3.35	0.241	1585.23	1.68	1.57	355.96	47.96	358.28	50.28
690	0.58	0.21	73.91	26.70	0.37	-18.87	-19.11	3.61	3.36	0.242	1538.34	1.68	1.57	356.02	48.02	358.16	50.16
700	0.58	0.21	73.91	27.04	0.37	-18.86	-19.10	3.61	3.37	0.247	1520.91	1.69	1.57	356.02	48.02	358.39	50.39
710	0.58	0.21	73.54	26.27	0.37	-18.85	-19.09	3.63	3.38	0.237	1503.00	1.70	1.58	356.08	48.08	358.41	50.41
720	0.59	0.21	74.75	26.45	0.38	-18.84	-19.08	3.63	3.40	0.243	1600.84	1.70	1.59	356.04	48.04	358.56	50.56
730	0.58	0.21	74.15	26.27	0.38	-18.84	-19.08	3.64	3.40	0.225	1547.28	1.70	1.59	356.05	48.05	358.40	50.40

740	0.58	0.21	74.15	26.27	0.38	-18.83	-19.06	3.64	3.41	0.218	1671.07	1.70	1.60	356.14	48.14	358.47	50.47
750	0.58	0.21	74.15	26.19	0.38	-18.83	-19.05	3.64	3.43	0.255	1727.80	1.70	1.60	356.19	48.19	358.62	50.62
760	0.58	0.21	73.54	26.53	0.37	-18.81	-19.07	3.66	3.41	0.236	1447.96	1.71	1.59	356.23	48.23	358.41	50.41
770	0.58	0.21	73.78	26.19	0.37	-18.82	-19.06	3.65	3.42	0.232	1583.94	1.71	1.60	356.09	48.09	358.35	50.35
780	0.58	0.21	73.42	26.36	0.37	-18.80	-19.03	3.67	3.44	0.237	1593.19	1.72	1.61	356.08	48.08	358.40	50.40
790	0.57	0.21	73.18	26.19	0.37	-18.80	-19.03	3.68	3.44	0.229	1557.22	1.72	1.61	356.07	48.07	358.48	50.48
800	0.58	0.21	73.42	26.19	0.37	-18.79	-19.02	3.68	3.45	0.245	1619.91	1.72	1.61	356.19	48.19	358.55	50.55
810	0.57	0.21	73.18	26.79	0.36	-18.79	-19.03	3.69	3.44	0.245	1487.22	1.72	1.61	356.23	48.23	358.82	50.82
820	0.58	0.21	74.15	26.87	0.37	-18.77	-19.02	3.70	3.46	0.247	1515.51	1.73	1.61	356.31	48.31	358.96	50.96
830	0.58	0.21	74.15	26.19	0.38	-18.76	-19.01	3.71	3.46	0.234	1524.94	1.73	1.62	356.34	48.34	358.67	50.67
840	0.58	0.21	73.91	27.04	0.37	-18.76	-19.00	3.71	3.48	0.23	1572.91	1.73	1.62	356.32	48.32	358.68	50.68
850	0.58	0.21	73.78	26.19	0.37	-18.76	-18.99	3.71	3.48	0.247	1625.26	1.73	1.63	356.41	48.41	358.66	50.66
860	0.58	0.21	73.54	26.45	0.37	-18.75	-19.00	3.72	3.48	0.223	1497.57	1.74	1.62	356.30	48.30	358.61	50.61
870	0.58	0.21	73.66	27.04	0.37	-18.75	-18.98	3.72	3.50	0.242	1641.97	1.74	1.63	356.23	48.23	358.56	50.56
880	0.57	0.21	73.06	26.53	0.37	-18.74	-18.98	3.74	3.49	0.255	1510.04	1.75	1.63	356.35	48.35	358.69	50.69
890	0.58	0.21	74.27	26.53	0.37	-18.72	-18.98	3.75	3.50	0.23	1470.31	1.75	1.63	356.31	48.31	358.87	50.87
900	0.58	0.21	73.54	26.79	0.37	-18.73	-18.96	3.74	3.51	0.232	1596.61	1.75	1.64	356.24	48.24	358.65	50.65
910	0.58	0.20	73.66	26.02	0.37	-18.72	-18.96	3.75	3.52	0.235	1612.93	1.75	1.64	356.37	48.37	358.79	50.79
920	0.58	0.21	74.27	26.36	0.38	-18.73	-18.96	3.75	3.51	0.236	1601.15	1.75	1.64	356.51	48.51	358.87	50.87
930	0.57	0.21	72.94	26.36	0.37	-18.72	-18.95	3.76	3.52	0.238	1550.08	1.76	1.65	356.73	48.73	358.99	50.99
940	0.58	0.21	74.15	26.27	0.38	-18.71	-18.95	3.76	3.52	0.251	1579.79	1.76	1.65	356.37	48.37	358.91	50.91
950	0.58	0.21	73.42	26.10	0.37	-18.70	-18.95	3.77	3.52	0.232	1480.60	1.76	1.65	356.57	48.57	358.70	50.70
960	0.58	0.21	74.03	26.62	0.37	-18.69	-18.92	3.79	3.55	0.246	1605.00	1.77	1.66	356.30	48.30	358.65	50.65
970	0.58	0.21	73.78	26.45	0.37	-18.70	-18.95	3.77	3.53	0.245	1511.38	1.76	1.65	356.43	48.43	358.72	50.72
980	0.58	0.21	74.15	26.36	0.38	-18.69	-18.94	3.78	3.54	0.221	1531.92	1.77	1.65	356.41	48.41	358.76	50.76
990	0.58	0.21	73.78	26.10	0.37	-18.70	-18.92	3.78	3.56	0.231	1694.48	1.76	1.66	356.53	48.53	358.66	50.66
1000	0.58	0.21	74.15	26.62	0.37	-18.69	-18.92	3.79	3.56	0.241	1616.06	1.77	1.66	356.65	48.65	359.02	51.02

APPENDIX D

1 Linear Regression Analysis

1.1 Introduction

Regression analysis is a powerful technique that can be used to address various research questions. In this report, we are going to use it to check how q_{ult} levels are affected by c_u and φ.

In particular, the type of regression we are going to use is ”Multiple Linear Regression”. Linear regression is the process of finding the best-fitting straight line through data points (this line is sometimes referred to as the regression line). Multiple means we have more than one input variable (also known as predictor), hence, we are trying to fit a plane or hyper-plane rather than a line. The input variables in our case are cu, phi and as. Linear means that we are trying to find a combination of the input variables such that each variable is multiplied by a coefficient and then we sum the products. The idea is to use this linear combination of input variables to model their relationship with an output variable (in our case, this is q_{ult}).

1.2 The Modelling Tool

In order to fit models, we are going to use R [ ] which is a powerful and easy to use tool for statistical computing and graphics. R makes it easy to manipulate data and perform calculations as well as display information graphically. It also facilitates modelling (linear and nonlinear) and other statistical processes.

1.3 Diagnostics for Examining a Fit

There are several diagnostics that can be used to explore the goodness of fit of a model. The following are going to be used:

- R-squared

This value calculates the percentage of variation of the output explained by the input variables in the model. This means the higher the value of R-squared the better the model.

- R-squared adjusted

This value is similar to R-squared but it accounts for the number of input variables in the model, hence, it is sometimes preferred to R-squared.

- Residuals

A residual is the difference between the actual value and predicted value for each point (or record) in the data. Histograms are often used to check the distribution of residuals. Also, they are plotted against each input variable. If a model fits well, the residuals will be small and will be no pattern of their distribution around zero (i.e. they should be evenly spread around zero).

- Deviance

The deviance is a statistic that is used to determine the quality of fit for a model. It is a measure of how much better a model with more parameters fits the data. It is used to compare nested models. A nested model is a model which is a subset of another model. For example, if we have two models, the first describes the relationship between one input variable x and an output variable y and the second describes the relationship between two input variables x and z and an output variable y, then the first model is nested within the second.

- Bayesian Information Criterion (BIC)

When there are a limited number of models, the BIC is often used for model selection. Often, the model with the smallest BIC is preferred. The BIC is a penalised version of the deviance where the penalty is relevant to the number of input variables.

- P-values

It is common to provide p-values when conducting statistical analysis. P-values are propabilities (i.e. their values always lie between zero to 1) and they show how likely certain situations are. P-values which are close to zero (usually <= 0.05) are more likely to occur if the study has shown something positive. It is said that the result is significant if the p-value is close to zero. On the other hand, the result is said to be non-significant if the p-value is away from zero (usually > 0.05).

- Confidence Intervals

It is known that in statistics we use the sample data at hand to draw inferences about the entire population (i.e. all the data) and make an estimate of the value(s) we are trying to measure or predict. It is very important to present such estimate with a measure of precision. This measure of precision depends on the sample size and normally takes the form of a 95% Confidence Interval or a standard error value (the former is calculated from the latter). The 95% confidence interval gives the range of poulation parameters that the sample leads us to believe are possible. The 95% confidence interval is presented as a range of two values (a, b) and is interpreted as: we can be 95% confident that the result/effect we are trying to measure what will happen by an overage of at least a and maybe as much as b

Data base

Reference	c_u,	Φ,	A_S,	$q_{untreated}$,	$q_{treated}$,	$q_{treated}/q$
Wood et al. (2000)	10.5	25	30	84	105	1.25
Wood et al. (2000)	10	25	24	84	90	1.07
Wood et al. (2000)	10	25	10	84	86	1.02
Andereou et al. (2008)	20	32	4	55	62	1.13
Najjar et al. (2010)	20	33	7.9	62	75	1.21
Najjar et al. (2010)	20	33	17.8	67	100	1.49
Najjar et al. (2010)	20	33	7.9	84	101	1.20
Najjar et al. (2010)	20	33	17.8	84	148	1.76
Sivakumar et al. (2004)	25	35	10.2	60	83	1.38
Black et al. (2006)	25	35	17	1.25	2	1.60
Bergado et al. (1987)	20	35	6.25	175	221	1.26
Hughes and Withers	19	35	40	171	418	2.44
Bergado et al. (1987)	20	37	6.25	175	314	1.79
Juran and Guermazi	30	38	4	120	154	1.28
Ali et al. (2014)	7	38	25	25	70	2.80
Kim and Lee (2005)	4	38	30	30	75	2.50
Kim and Lee (2005)	4	38	40	45	135	3.00
Kim and Lee (2005)	4	38	50	45	155	3.44
Bergado et al. (1987)	20	39	6.25	175	320	1.83
Bergado et al. (1987); st.	30	42	65	60	270	4.50
Bergado et al. (1987);	20	42	28	95	240	2.53
Humber Bridge	25	42	11	115	270	2.35
Black et al. (2011)	35	43	17	240	680	2.83
Black et al. (2011)	35	43	28	230	750	3.26
Black et al. (2011)	35	43	40	230	820	3.57
Black et al. (2011)	35	43	1.6	29	65	2.24
Bergado et al. (1987)	20	43	6.25	175	370	2.11
Ambily and Gandhi	7	43	19	75	160	2.13
Ambily and Gandhi	14	43	19	88	350	3.98
Ambily and Gandhi	30	43	19	150	770	5.13
Ambily and Gandhi	30	43	5	150	600	4.00
Ambily and Gandhi	30	43	9	150	680	4.53
Ambily and Gandhi	30	43	19	150	770	5.13
Zahmatkesh and	5	43	10	80	165	2.06
Zahmatkesh and	5	43	20	80	170	2.13
Zahmatkesh and	5	43	25	80	250	3.13
Zahmatkesh and	5	43	30	80	280	3.50
Watts et al. (2000)	40	45	44	12	248	20.67
Current study	12	48	5	55	100	1.82
Current study	12	48	13	140	428	3.06
Kim and Lee (2005)	4	49	30	40	150	3.75
Kim and Lee (2005)	4	49	40	40	165	4.13
Kim and Lee (2005)	4	49	50	40	215	5.38

1.4 Examining the Variables

As there are three numerical input variables, it is appropriate to examine their statistical summaries. This is what we show in table 1.

Table 1: Statistical Summaries of the Variables with 95% Confidence Interval for the Mean values

Property	c_u	∅	A_s	q_{ult}
Valid	31	31	31	31
Missing	-	-	-	-
Mean	17.23	40.31	21.55	240.3
Median	20.00	39.00	17.00	165.0
Std. deviation	10.87101	5.168765	16.41788	202.4052
Minimum	4.00	33.00	1.60	2.0
Maximum	35.00	49.00	65.00	820.00

By examining the table, we observe that we have data for all the points (i.e. no missing values). Also, we notice that there is no big deference between the mean and median values of each variable, hence outliers are unlikely (outliers usually have a big influence on the deference between the mean and the median). Another values that can analyse from the table are the minimum and maximum values for each input variable. They appear to be within possible ranges for all of the three input variables. Finally, as standard deviation is an indicator of how spread out the data is, we can check the validity of our data by going 2 standard deviations on each side of the mean for the outcome variable Q. We notice that more than 95% of all values of this variable lie within that range.

1.5 Histograms of the Variables

Histograms of the three input variables and the output variable are displayed in Figure 1. A close look at these histograms indicate some "bunching" around multiples of 5 for the c_u input variable (Figure 1a) and around multiples of 10 for the A_S variable (Figure 1c).

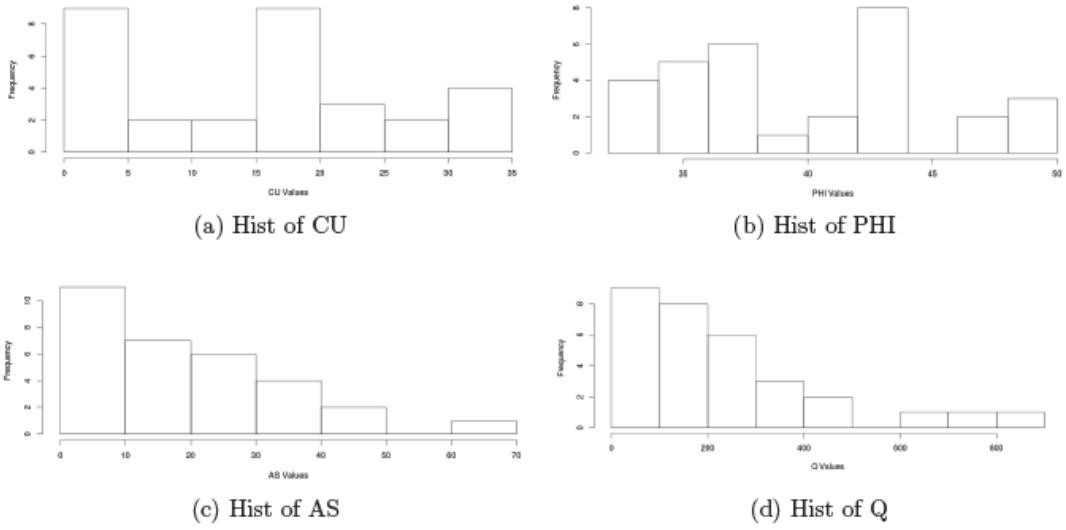

(a) Hist of CU (b) Hist of PHI

(c) Hist of AS (d) Hist of Q

Figure 1: Histograms of the Variables

1.6 Relationships between the Variables

A scatter plot matrix between all variables in is shown Figure 2. The top row of this scatter plot matrix gives the scatter plots of q_{ult} against each of the other three input variables. Additionally, we show the univariate relationship between our outcome variable q_{ult} and the input variables in Table 2. From this table, we can notice that the correlation between c_u and q_{ult} and between φ and q_{ult} is significant at the $p < 0.05$ level.

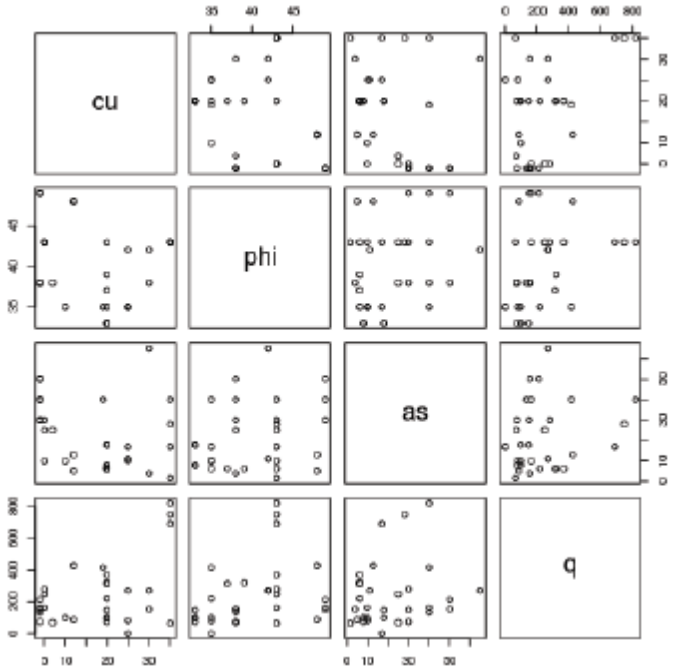

Figure 2: Scatter plot of all the variables

Table 2: Correlations between the Input Variables and q_{ult}

Influence factor	**Correlation (p-value) with q_{ult}**	
	Pearson	**Spearman**
c_u	0.4595897 (0.009293)	0.1952728 (0.2925)
A_s	0.1964417 (0.2895)	0.2026105 (0.2743)
∅	0.3082577 (0.09158)	0.3982587 (0.02649)

Information also are provided about the correlations between our input variables in table 3. From this table we can observe that none of the correlations between the input variables is significant at the $p < 0.05$ level

Table 3 correlation between input variables

(a) Pearson correlation

	A_s	c_u	∅
A_s	1	-0.2596521 (0.1584)	0.2605386 (0.1569)
c_u	-0.2596521 (0.1584)	1	-0.2176558 (0.2395)
∅	0.2605386 (0.1569)	-0.2176558 (0.2395)	1

(b) Spearman correlation

	A_s	c_u	∅
A_s	1	-0.3944457 (0.0281)	0.204013 (0.271)
c_u	-0.3944457 (0.0281)	1	-0.2161602 (0.2428)
∅	0.204013 (0.271)	-0.2161602 (0.2428)	1

1.7 Fitting the Models

As the aim is to determine the relation between VARIABLE(s) and q_{ult}. Therefore, it would seem reasonable to model CONFOUNDER FIRST and then enter c_u into the model and see whether it is associated with q_{ult}. We can do this in the opposite way by entering c_u into the model first and then follow it by φ and A_S in turn to see what impact each of them would have on the model.

1.7.1 Modelling the Relationship between c_u and $\mathbf{q_{ult}}$ (Model 1)

In this section, a simple linear regression model is built using just c_u as input and q_{ult} as output. After using R's lm() function, the model looks as follows:

$$q_{ult} = 92.890 + 8.557 * c_u \quad (1)$$

By examining Equation 1, we observe that an increase, or decrease, of c_u by one unit, causes an increase, or decrease, in q_{ult} by 8.557 units

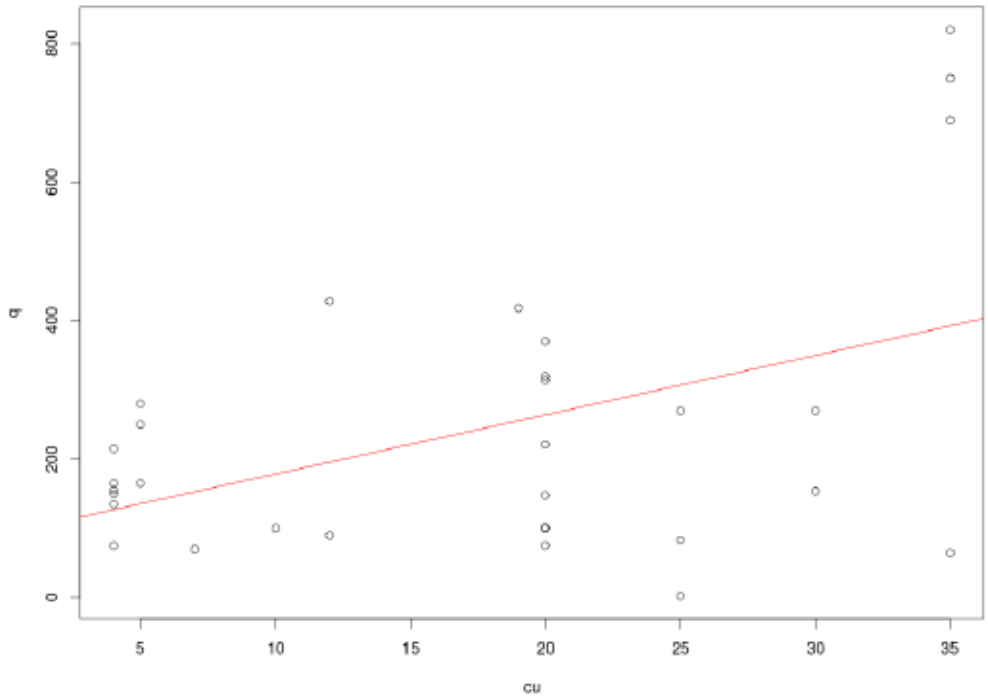

Figure 3: The Relationship between c_u and q_{ult}

Now after building the model that describes the relationship between c_u and q_{ult}, let us plot the input variable c_u against the residuals. As Figure 4 shows, the residual values do not seem to have a particular pattern and they are randomly scattered around zero.

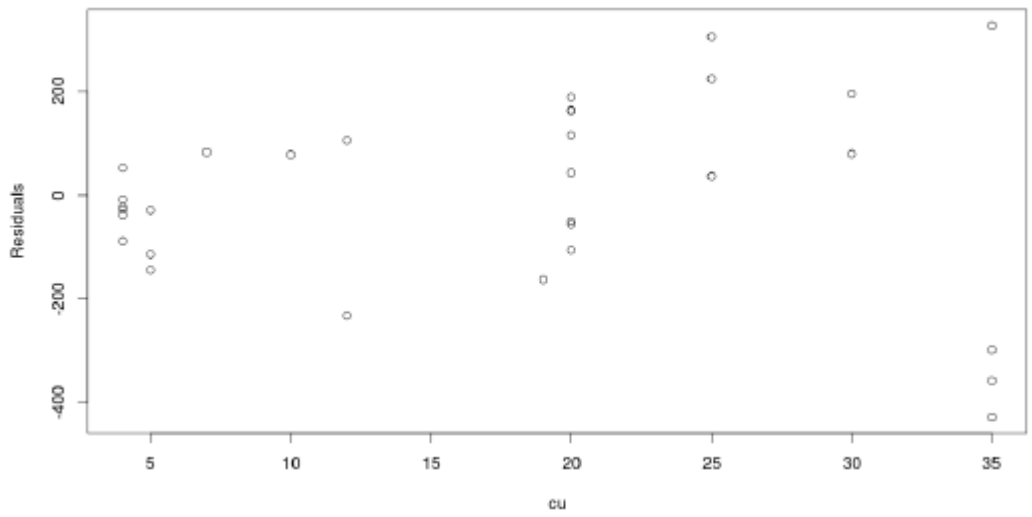

Figure 4: c_u vs Residuals for Model 1

1.7.2 Modelling the Relationship between AS and qult (Model 2)

In this section, we are going to build a simple linear regression model using just AS as input and Q as output. After using R's lm() function, the model looks as follows:

$$q_{ult} = 188.089 + 2.422 * A_s \qquad (2)$$

By examining equation 2, we observe that an increase, or decrease, of A_S by one unit, causes an increase, or decrease, in q_{ult} by 2.422 units

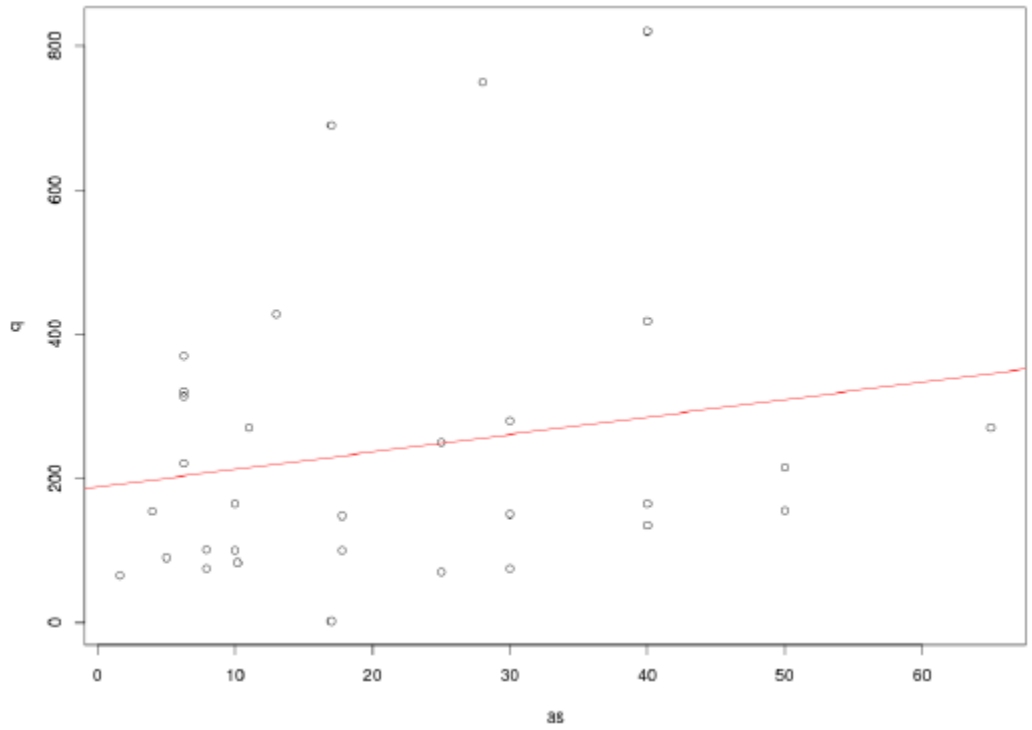

Figure 5: The Relationship between A_S and q_{ult}

Now after building the model that describes the relationship between A_S and q_{ult}, let us plot the input variable AS against the residuals. As Figure 6 shows, the residual values do not seem to have a particular pattern and they are randomly scattered around zero (as we stated in Section 4.3).

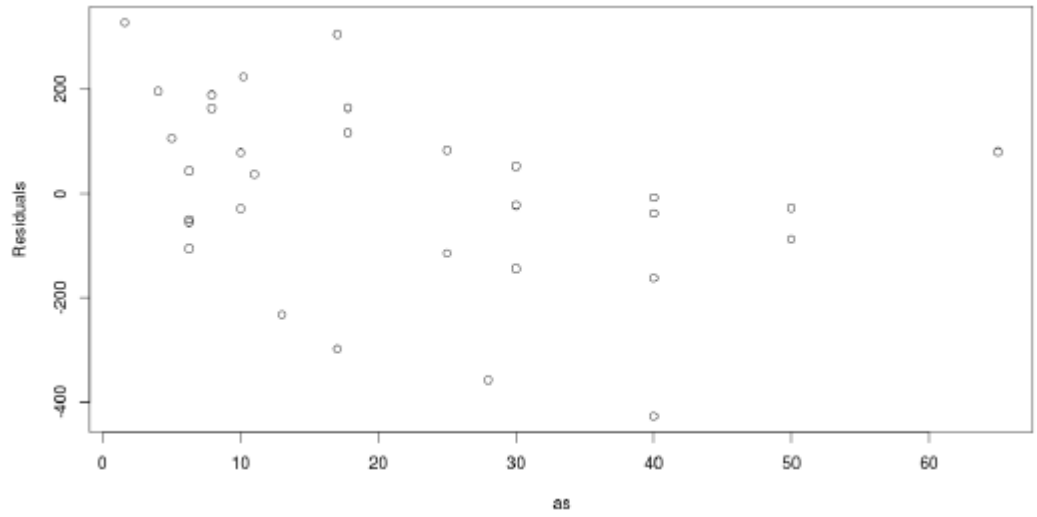

Figure 6: AS vs Residuals for Model 2

1.7.3 Modelling the Relationship between φ and $\mathbf{q_{ult}}$ (Model 3)

In this section, a simple linear regression model was built using just φ as input and q_{ult} as output. After using R's lm() function, the model looks as follows:

$$q_{ult} = -244.11 + 12.07 * \emptyset \qquad (3)$$

By examining equation 3, we observe that an increase, or decrease, of PHI by one unit, causes an increase, or decrease, in Q by 12.07 units

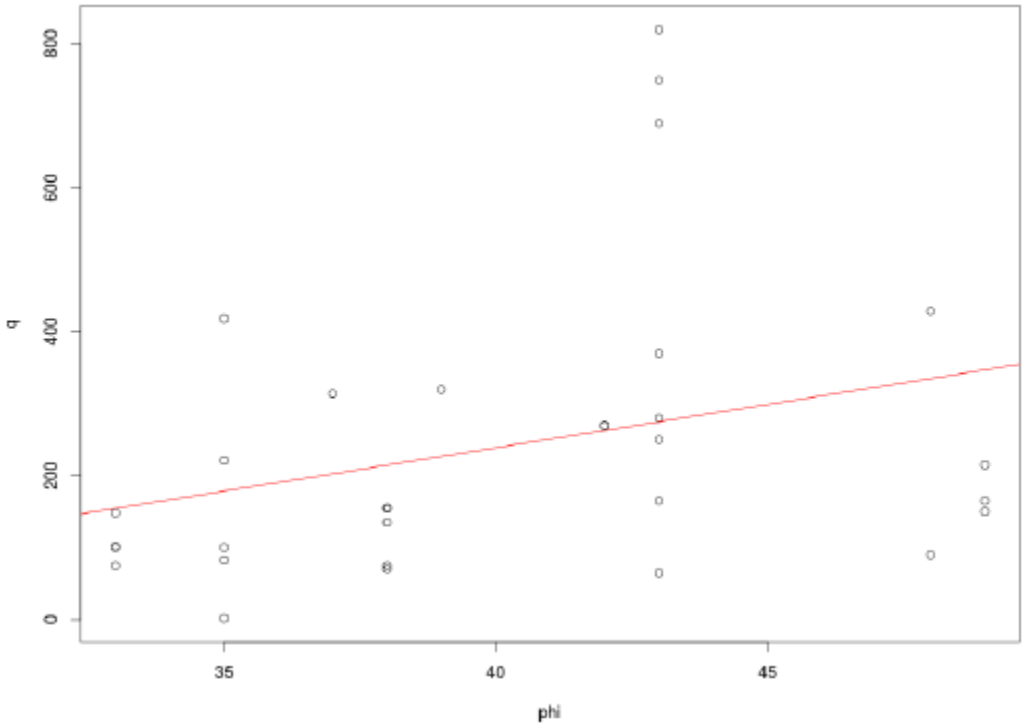

Figure 7: The Relationship between φ and q_{ult}

Now after building the model that describes the relationship between φ and q_{ult}, let us plot the input variable PHI against the residuals. As Figure 8 shows, the residual values do not seem to have a particular pattern and they are randomly scattered around zero.

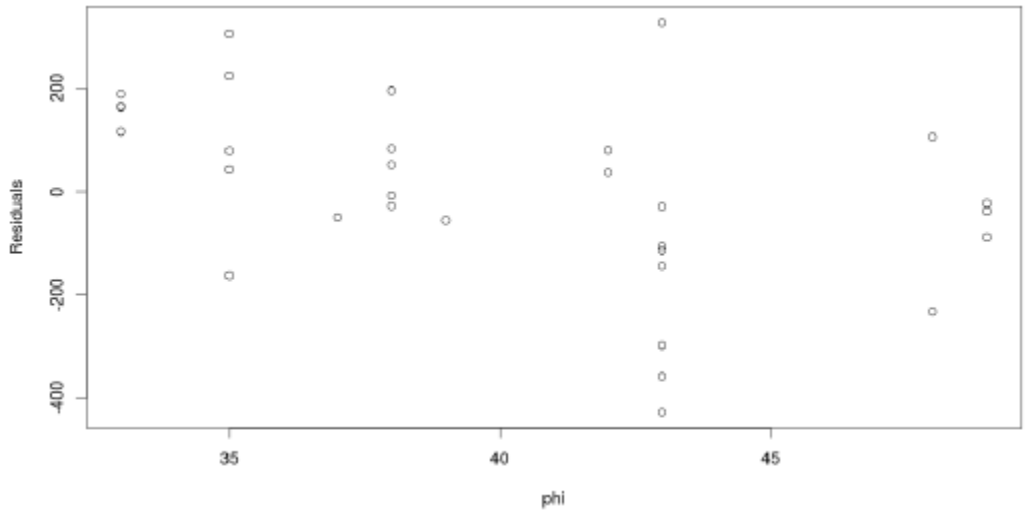

Figure 8: PHI vs Residuals for Model 3

1.7.4 Modelling the Relationship between cu, AS and qult (Model 4)

In this section, we are going to build a simple linear regression model using CU and AS as inputs and Q as output. After using R's lm() function, the model looks as follows:

$$q_{ult} = -25.286 + 10.194 * c_u + 4.174 * A_s \qquad (4)$$

By examining Equation 4, we observe that when fixing A_S, an increase, or decrease, of c_u by one unit, causes an increase, or decrease, in q_{ult} by 10.194 units. Similarly, when fixing c_u, an increase, or decrease, of A_S by one unit, causes an increase, or decrease, in q_{ult} by 4.174 units.

Now after building the model that describes the relationship between c_u, A_S and q_{ult}, let us plot the input variables c_u and A_S against the residuals. As Figure 9 shows, the residual values do not seem to have a particular pattern and they are randomly scattered around zero.

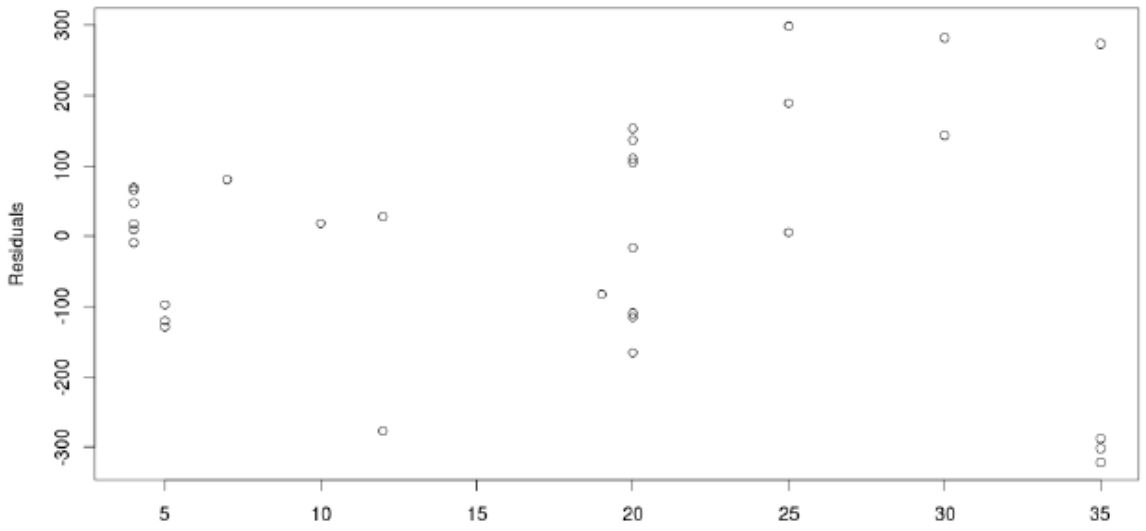

(a) c_u vs Residuals for Model 4

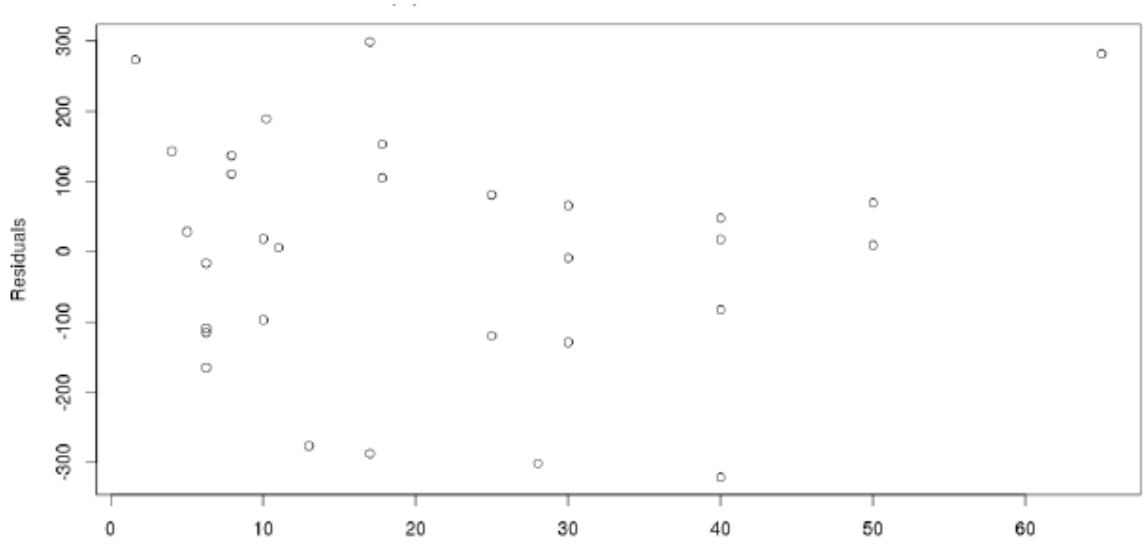

(b) A_S vs Residuals for Model 4

Figure 9: Input Variables vs Residuals for Model 4

1.7.5 Modelling the Relationship between cu, φ and qult (Model 5)

In this section, we are going to build a simple linear regression model using c_u and φ as inputs and q_{ult} as output. After using R's lm() function, the model looks as follows:

$$q_{ult} = -610.53 + 10.29 * c_u + 16.78 * \emptyset \quad (5)$$

By examining equation 5, we observe that when fixing φ, an increase, or decrease, of c_u by one unit, causes an increase, or decrease, in q_{ult} by 10.29 units. Similarly, when fixing CU, an increase, or decrease, of φ by one unit, causes an increase, or decrease, in q_{ult} by 16.78 units. Now after building the model that describes the relationship between c_u, PHI and q_{ult}, let us plot the input variables c_u and φ against the residuals. As Figure 10 shows, the residual values do not seem to have a particular pattern and they are randomly scattered around zero.

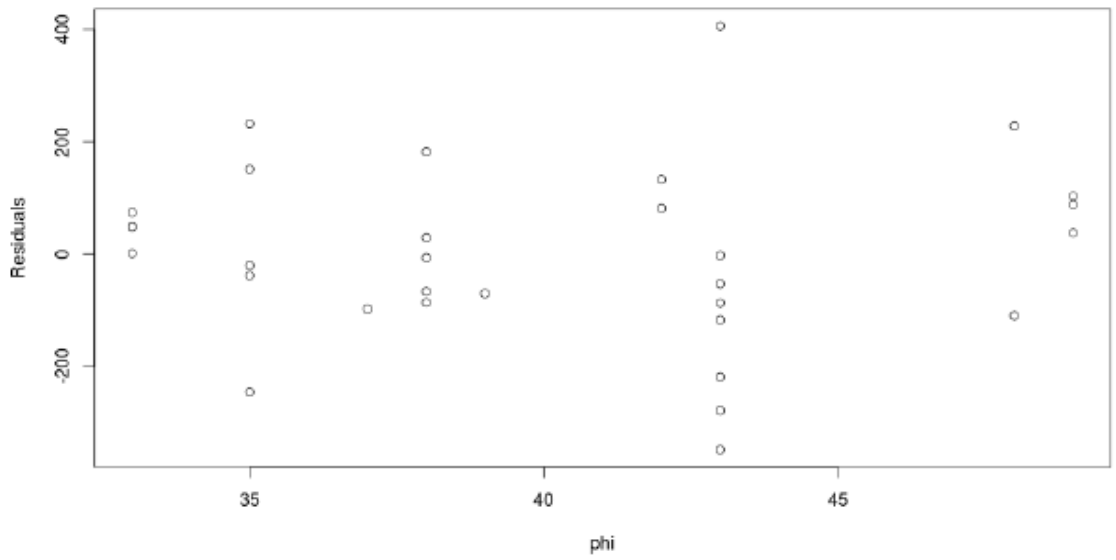

(a) c_u vs Residuals for Model 5

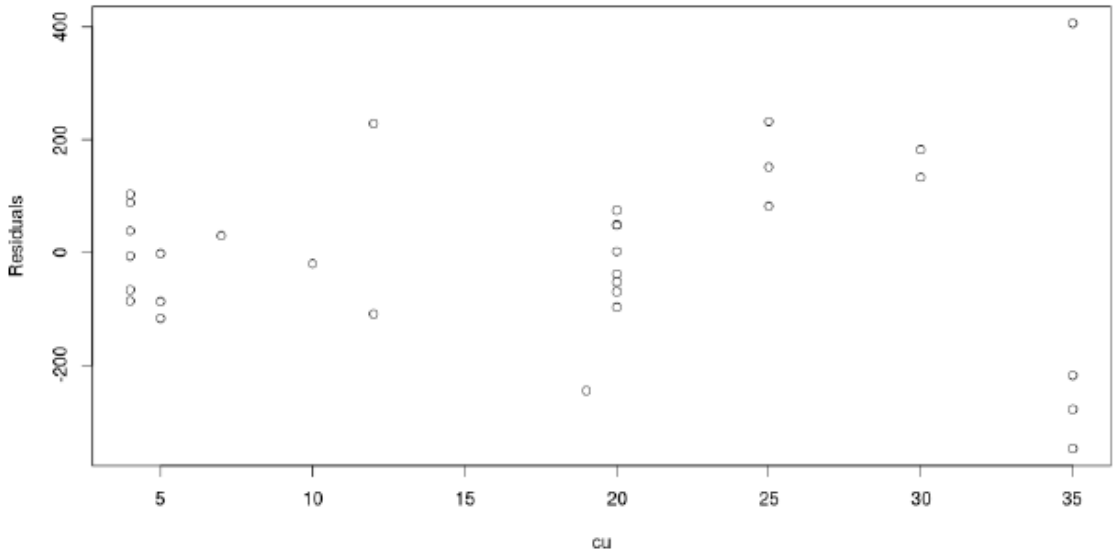

(b) φ vs Residuals for Model 5

Figure 10: Input Variables vs Residuals for Model 5

1.7.6 Modelling the Relationship between AS, φ and qult (Model 6)

In this section, we are going to build a simple linear regression model using A_S and φ as inputs and q_{ult} as output. After using R's lm() function, the model looks as follows:

$$q_{ult} = -226.213 + 1.536 * A_s + 10.8 * \emptyset \qquad (6)$$

By examining equation 6, we observe that when fixing φ, an increase, or decrease, of A_S by one unit, causes an increase, or decrease, in q_{ult} by 1.536 units. Similarly, when fixing A_S, an increase, or decrease, of φ by one unit, causes an increase, or decrease, in q_{ult} by 10.8 units. Now after building the model that describes the relationship between A_S, φ and q_{ult}, let us plot the input variables A_S and φ against the residuals. As Figure 11 shows, the residual values do not seem to have a particular pattern and they are randomly scattered around zero.

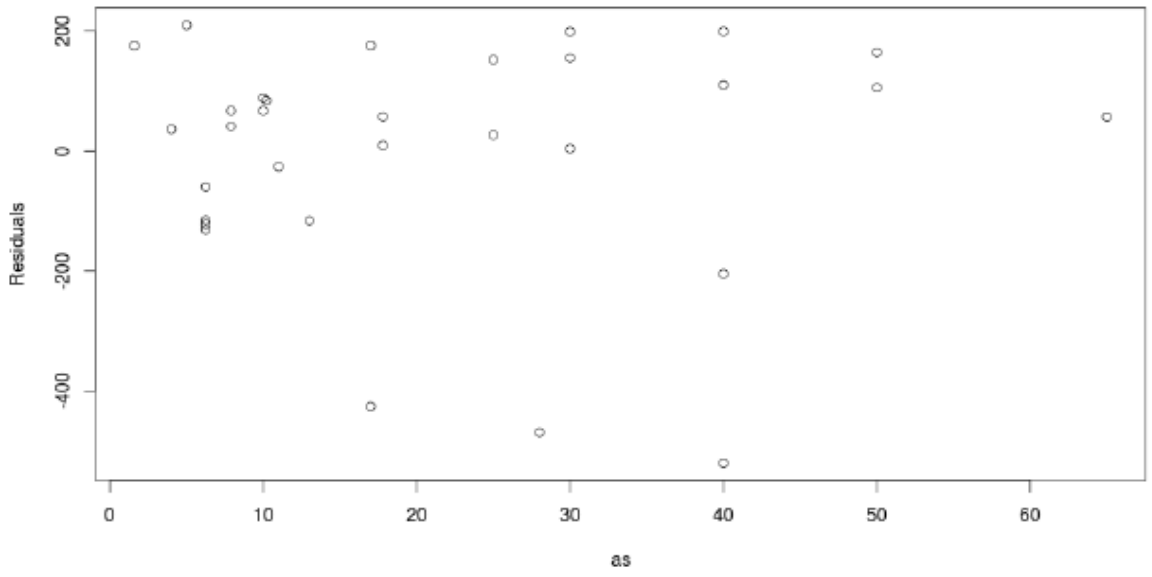

(a) A_S vs Residuals for Model 6

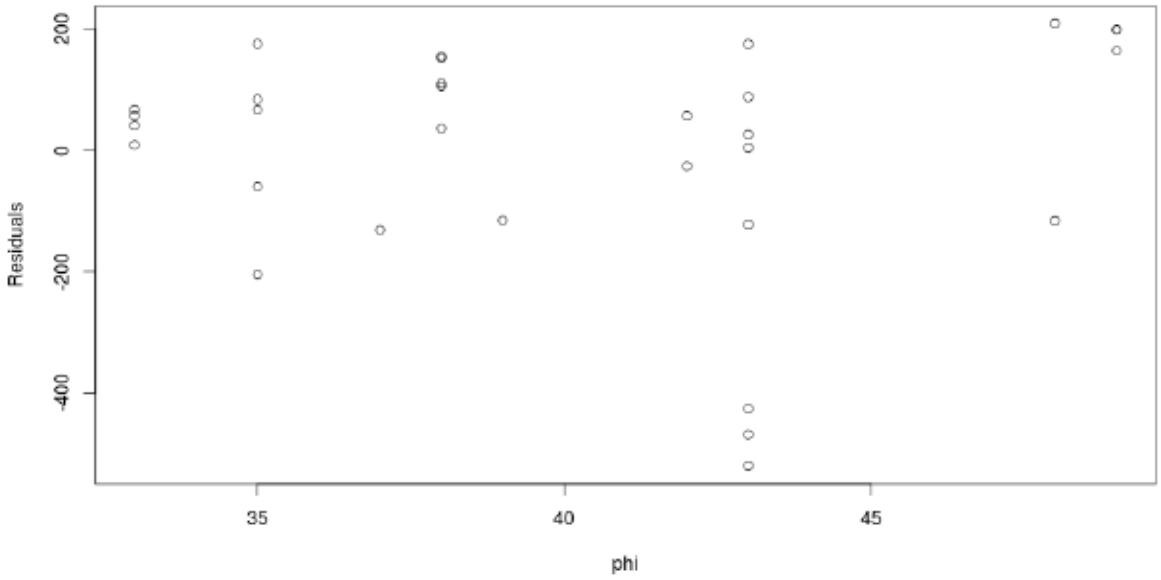

(b) φvs Residuals for Model 6

Figure 11: Input Variables vs Residuals for Model 6

1.7.7 Modelling the Relationship between cu, AS, φ and qult (Model 7)

In this section, we are going to build a simple linear regression model using CU, AS and PHI as inputs and Q as output (recall this is the purpose of this study). After using R's lm() function, the model looks as follows:

$$q_{ult} = -609.893 + 11.313 * c_u + 3.167 * A_s + 14.629 * \emptyset \qquad (7)$$

By examining Equation 7, we observe that when fixing φ and A_S, an increase, or decrease, of c_u by one unit, causes an increase, or decrease, in q_{ult} by 11.313 units. Similarly, when fixing c_u and A_S, an increase, or decrease, of φ by one unit, causes an increase, or decrease, in q_{ult} by 14.629 units. Also, when fixing c_u and φ, an increase, or decrease, of A_S by one unit, causes an increase, or decrease, in q_{ult} by 3.167 units.

Now after building the model that describes the relationship between c_u, A_S, φ and q_{ult}, let us plot the input variables cu, A_S and φ against the residuals. As Figure 12 shows, the residual values do not seem to have a particular pattern and they are randomly scattered around zero.

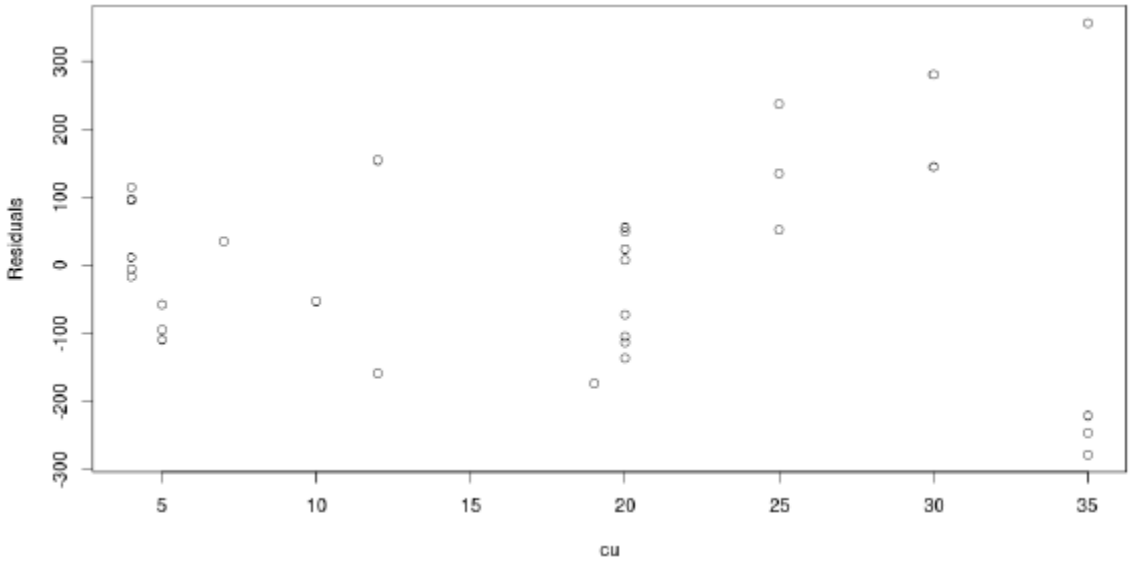

(a) c_u vs Residuals for Model 7

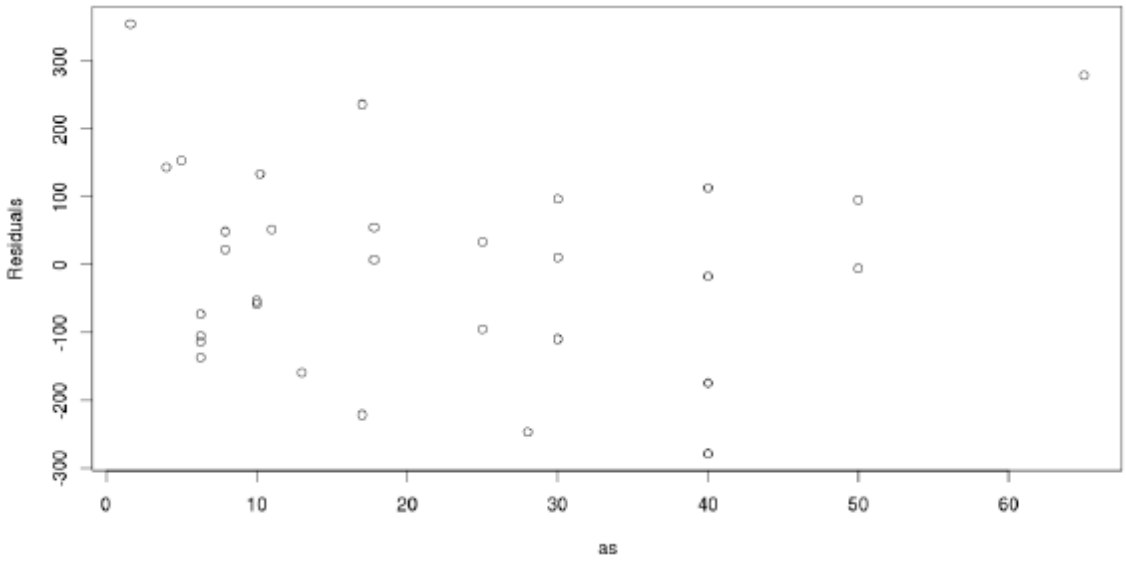

(b) A_S vs Residuals for Model 7

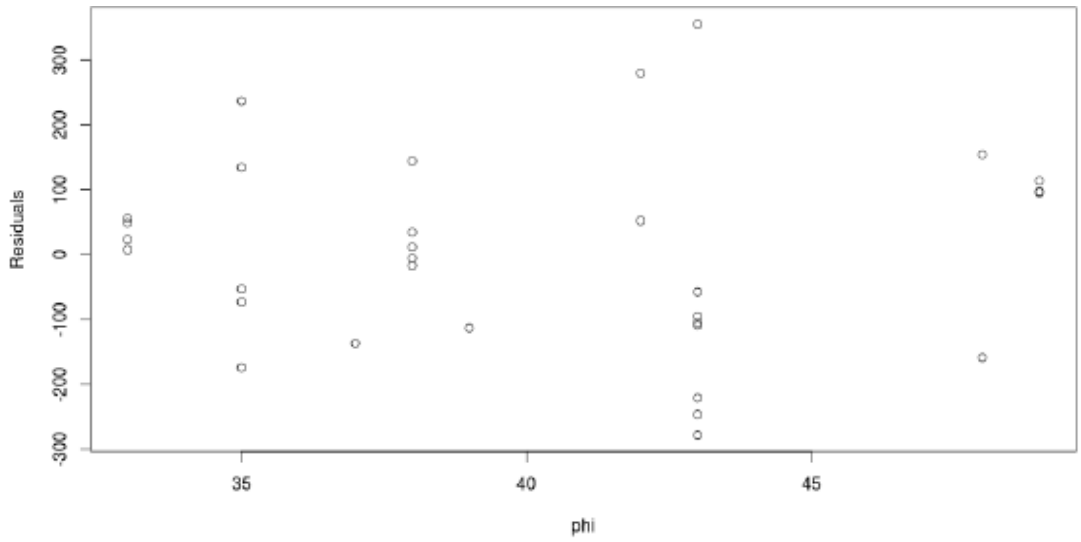

φ vs Residuals for Model 7

Figure 12: Input Variables vs Residuals for Model 7

1.7.8 Checking the Model Fit

Five diagnostics that can be used to examine the goodness of fit of a model were mentioned In Section 1.3. Namely, these were: Deviance, BIC, R-Squared, Adjusted R-Squared and the Residuals. Table 4 shows the values of the remaining four diagnostics for the seven models.

Table 4: Deviance, BIC, R-Squared and Adjusted R-Squared of the Seven models

Model	Deviance	BIC Value	R-Squared	Adj R-Squared
Model (1)	969436	419.1411	0.2112227	0.1840235
Model (2)	1181609	425.2766	0.03858933	0.005437238
Model (3)	1112250	423.4013	0.09502283	0.06381672
Model (4)	838024.3	418.0594	0.3181453	0.2694414
Model (5)	754365.9	414.7992	0.3862136	0.3423717
Model (6)	1094468	426.3357	0.1094908	0.04588297
Model (7)	682279.8	415.1196	0.4448661	0.3831845

As we mentioned before, lower BIC indicates a better fitting model. By analysing table 4 we observe that Model 5 has the lowest BIC with Model 7 in second. Howerver, when we examine the value of R-Squared, we realise that Model 7 has the highest R-Squared amongst all the models (see Section 4.1). This gives us confidence that from amongst the seven models that we created using various combinations of the input variables, Model 7 is the best model that describes the relationship between the input variables CU, AS and PHI and the output variable Q.

APPENDIX F

Nonlinear Regression Analysis

- Nonlinear Regression Analysis_ soil only

Iteration History[b]

Iteration Number[a]	Residual Sum of Squares	Parameter		
		a	b	m
1.0	71288.417	.000	.000	.000
1.1	29769.136	1.807	.000	.000
2.0	29769.136	1.807	.000	.000
2.1	23243.121	3.354	.202	3.196
3.0	23243.121	3.354	.202	3.196
3.1	4830.984	3.625	.145	2.993
4.0	4830.984	3.625	.145	2.993
4.1	4333.676	4.377	.091	2.411
5.0	4333.676	4.377	.091	2.411
5.1	4316.993	4.332	.097	2.477
6.0	4316.993	4.332	.097	2.477
6.1	4316.966	4.348	.096	2.468
7.0	4316.966	4.348	.096	2.468
7.1	4316.965	4.346	.096	2.470
8.0	4316.965	4.346	.096	2.470
8.1	4316.965	4.346	.096	2.469

Derivatives are calculated numerically.

a. Major iteration number is displayed to the left of the decimal, and minor iteration number is to the right of the decimal.

b. Run stopped after 16 model evaluations and 8 derivative evaluations because the relative reduction between successive residual sums of squares is at most SSCON = 1.000E-8.

Parameter Estimates

Parameter	Estimate	Std. Error	95% Confidence Interval	
			Lower Bound	Upper Bound
a	4.346	.197	3.960	4.733
b	.096	.005	.085	.107
m	2.469	.170	2.136	2.803

Correlations of Parameter Estimates

	a	b	m
a	1.000	-.400	.550
b	-.400	1.000	.540
m	.550	.540	1.000

ANOVA[a]

Source	Sum of Squares	df	Mean Squares
Regression	66971.451	3	22323.817
Residual	4316.965	3058	1.412
Uncorrected Total	71288.417	3061	
Corrected Total	4932.510	3060	

Dependent variable: VAR00005

a. R squared = 1 - (Residual Sum of Squares) / (Corrected Sum of Squares) = .125.

- Nonlinear Regression Analysis_ soil/stone column

Iteration History[b]

Iteration Number[a]	Residual Sum of Squares	Parameter		
		a	b	m
1.0	105048.595	.000	.000	.000
1.1	59039.952	1.285	.000	.000
2.0	59039.952	1.285	.000	.000
2.1	14058.800	3.055	.145	2.207
3.0	14058.800	3.055	.145	2.207
3.1	15227.522	6.360	.098	4.206
3.2	9802.091	4.171	.146	3.403
4.0	9802.091	4.171	.146	3.403
4.1	10647.892	7.604	.105	4.544
4.2	8249.791	5.485	.145	4.075
5.0	8249.791	5.485	.145	4.075
5.1	7672.376	8.405	.108	4.564
6.0	7672.376	8.405	.108	4.564
6.1	6139.380	11.429	.082	4.654
7.0	6139.380	11.429	.082	4.654
7.1	6122.613	17.495	.034	4.895
8.0	6122.613	17.495	.034	4.895
8.1	5059.439	20.596	.030	4.991
9.0	5059.439	20.596	.030	4.991
9.1	5023.065	23.229	.019	5.066
10.0	5023.065	23.229	.019	5.066
10.1	5017.609	23.381	.019	5.082
11.0	5017.609	23.381	.019	5.082
11.1	5017.607	23.393	.019	5.080
12.0	5017.607	23.393	.019	5.080
12.1	5017.607	23.392	.019	5.081

Derivatives are calculated numerically.

a. Major iteration number is displayed to the left of the decimal, and minor iteration number is to the right of the decimal.

b. Run stopped after 26 model evaluations and 12 derivative evaluations because the relative reduction between successive residual sums of squares is at most SSCON = 1.000E-8.

Parameter Estimates

Parameter	Estimate	Std. Error	95% Confidence Interval	
			Lower Bound	Upper Bound
a	23.392	.445	22.519	24.264
b	.019	.002	.015	.024
m	5.081	.039	5.004	5.157

Correlations of Parameter Estimates

	a	b	m
a	1.000	-.751	.335
b	-.751	1.000	.355
m	.335	.355	1.000

ANOVA[a]

Source	Sum of Squares	df	Mean Squares
Regression	100030.989	3	33343.663
Residual	5017.607	6050	.829
Uncorrected Total	105048.595	6053	
Corrected Total	26624.392	6052	

Dependent variable: permanent deformation

a. R squared = 1 - (Residual Sum of Squares) / (Corrected Sum of Squares) = .812.

APPENDIX G

Subgrade Stress Investigation

A large scale test at the University of Birmingham (unpublished work) included application of 125 kN wheel load on rail across three sleepers as shown in Figure 1a. The cross section of the setup is shown in Figure 1b. Load was applied at 2 Hz for 2 million cycles. Transducer positioned at top of subgrade under the central sleeper (where load was applied) in order to monitor the stresses. Figure 2 showed that the dynamic stresses at the subgrade level were approximately 80 kPa showing good agreement with Yoo and Selig (1979) study.

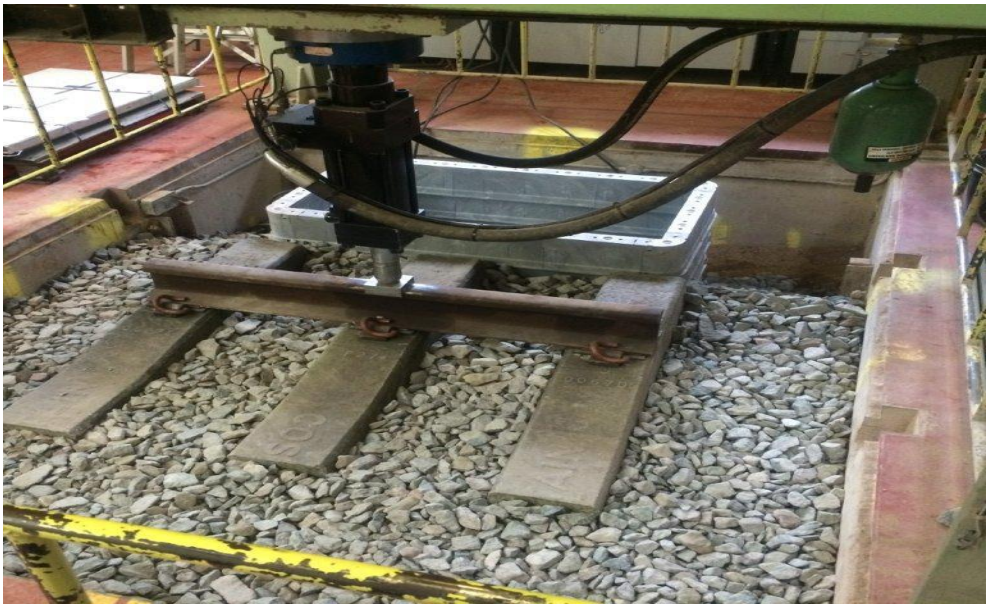

a. Cyclic load application

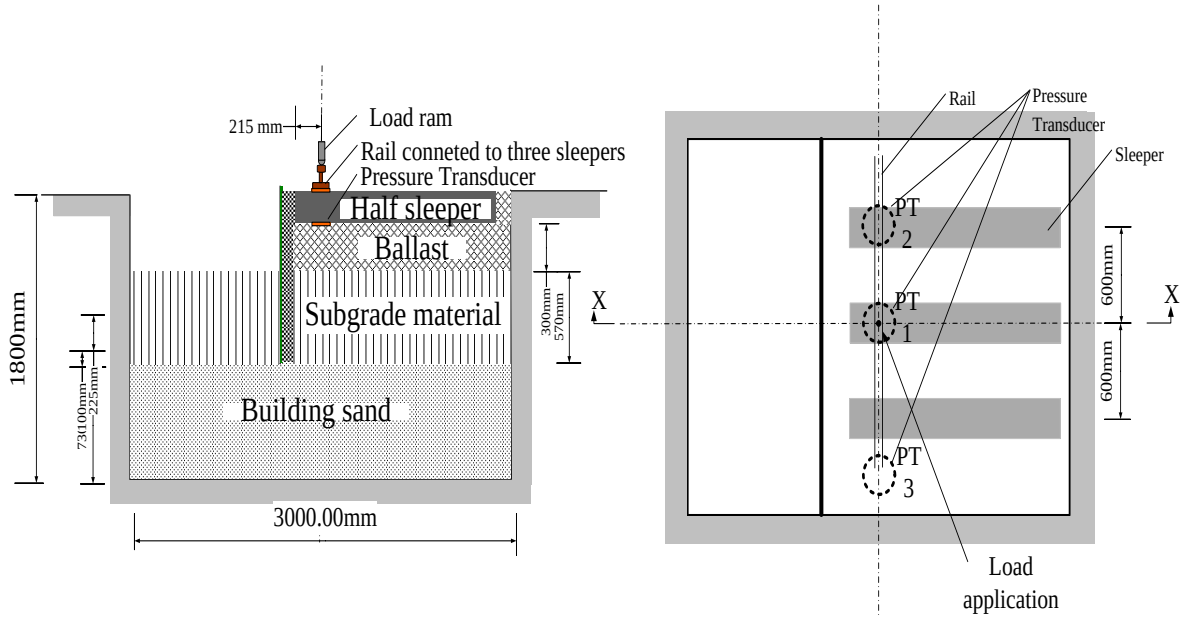

b. Test cross section layout

Figure 1 Large scale test set up

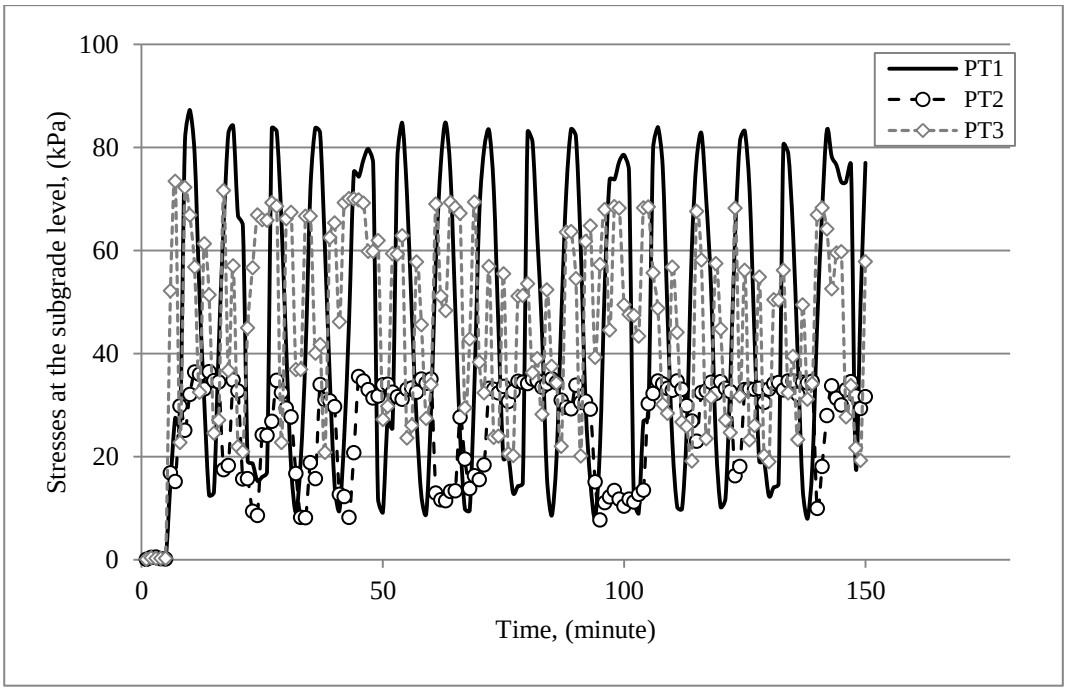

Figure 2 Dynamic stresses measurements at subgrade level (under 300mm of ballast)

Based on the above, cyclic stresses of 50 kPa, 60 kPa and 70 kPa were used in this study. These values are equivalent to a cyclic stress ratio (CSR) of 0.6, 0.7 and 0.8 (CSR = the cyclic deviator stress (q_{cyclic})/ the static deviator stress of reinforced soil at failure ($q_{failure}$)).

Surcharge Pressure

Surcharge pressure, equivalent to the weight of the track component (see Figure 3) was applied as the lowest pressure level during cyclic loading. this could be ranged between 10 and 25 kPa depending on the rail and sleeper types and the depth of the used ballast layer (Selig and Waters, 1994; Brough et al., 2003). Using ballast thickness of 300 mm with a density of 19 kN/m^3, rail weight of 60 kg/m, and a concrete sleeper of 300 kg with typical dimensions of 285 mm X 2420 ($l_{sleeper}$) mm laying in distance ($S_{sleeper}$) of 600 mm centre to centre, the surcharge pressure should be equivalent to 9.4 kPa. However, due to limitation of the test apparatus minimum of 20 kPa only could be applied

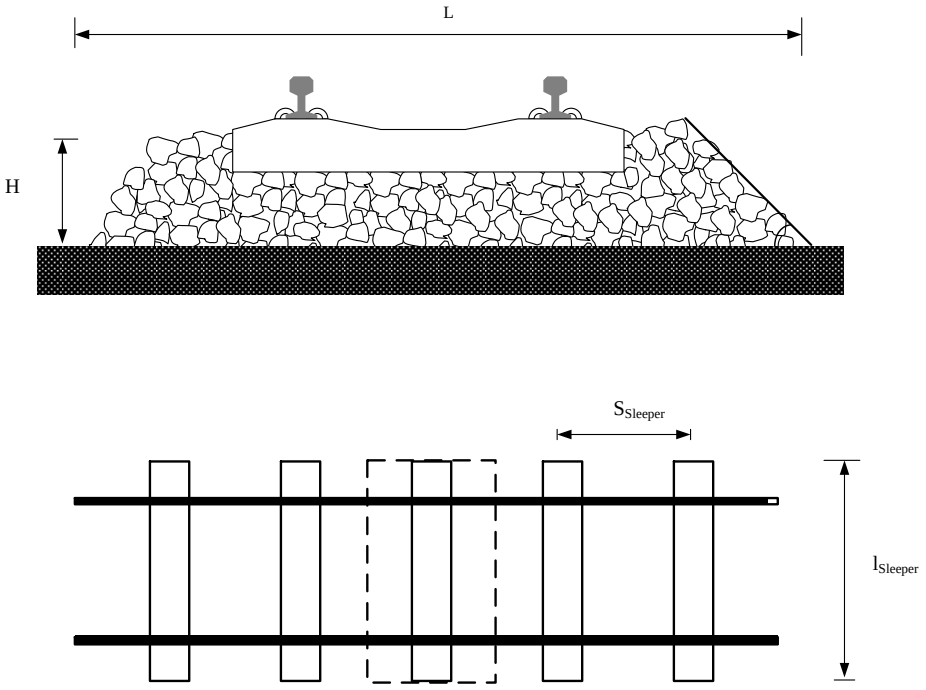

Figure 3 Structure of a rail track system used to calculate the surcharge pressure.